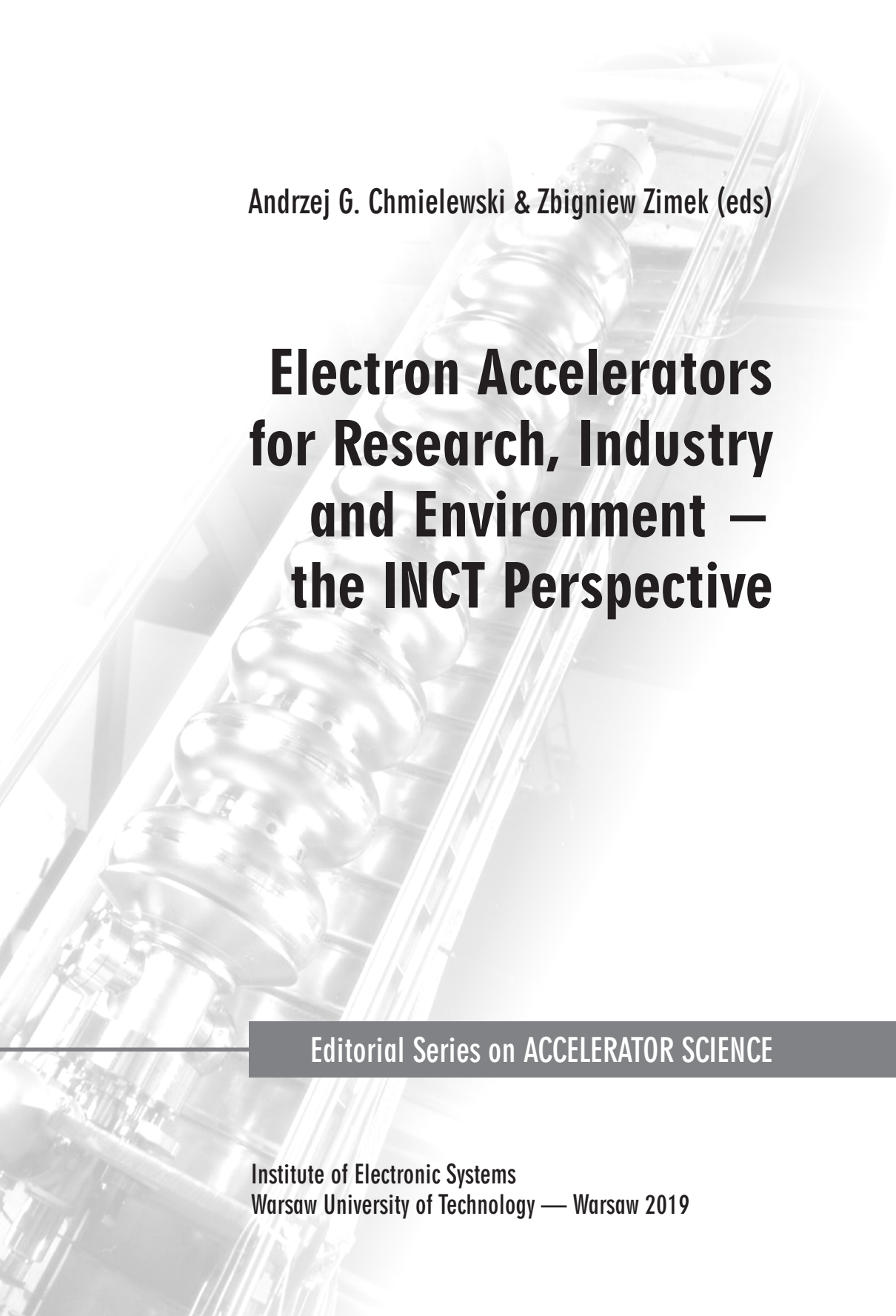

Andrzej G. Chmielewski & Zbigniew Zimek (eds)

# Electron Accelerators for Research, Industry and Environment — the INCT Perspective

Editorial Series on ACCELERATOR SCIENCE

Institute of Electronic Systems
Warsaw University of Technology — Warsaw 2019

The work is vol. LII in the Editorial Series on Accelerator Science and Technology.
The series is associated with the EU H2020 ARIES Project – Accelerator Research and Innovation for European Science and Society.
The H2020 ARIES Project is coordinated by CERN. Additional information about the Editorial Series on Accelerator Science and Technology can be found at CERN ARIES web site: https://aries.web.cern.ch/ (Results, Publications) and at the web site of the Warsaw University of Technology Publishing House: http://www.wydawnictwopw.pl.
Previous volumes in the series were published with the EU FP7 Project EuCARD2 – Enhanced European Coordination for European Research and Development: http://eucard2.web.cern.ch/science/monographs.

Series Editors:

*Ryszard S. Romaniuk,* Warsaw University of Technology
*Maurizio Vretenar,* CERN, Geneve

Reviewers:

*Ryszard S. Romaniuk,* Warsaw University of Technology
*Mirosław Dors,* The Szewalski Institute of Fluid-Flow Machinery, Polish Academy of Sciences

Cover design

*Danuta Czudek-Puchalska*

The cover photo shows view of the INCT laboratory installation for electron beam flue gas purification



**ISBN 978-83-7814-798-5**

Internet bookshop of the Warsaw University of Technology Publishing House (OWPW):
http://www.wydawnictwopw.pl; e-mail: oficyna@pw.edu.pl
phone 48 22-234-75-03; fax 48 22-234-70-60

Printed and bound by OWPW,
ul. Polna 50, 00-644 Warszawa, Poland, phone 48 22-234-70-30, 1st edition, order no 210/2019

## CONTENTS

**Chapter 1**

# INTRODUCTION

The Institute of Nuclear Chemistry and Technology (INCT) was established in 1983 (www.ichtj.waw.pl). It had been formerly operating since 1955 as the Chemistry Division of the Institute of Nuclear Research. The Institute has an interdisciplinary character. The activities of the INCT include basic research, development and applications as well as various services related to the profile of its activities. The results of the INCT works have been implemented in various branches of national economy, particularly in industry, medicine, environmental protection and agriculture. Since the early sixties, the Institute has played a leading role in developing and implementing nuclear and radiation technologies, methods and instruments in the country. Nowadays, the Institute is one of the most advanced centers in the field of radiation chemistry and technology, application of nuclear methods in material and process engineering, design and production of instruments based on nuclear techniques, radioanalytical techniques, environmental research. Basic research is focused on radiochemistry, chemistry of isotopes, physical chemistry of separation processes, cellular radiobiology and radiation chemistry, particularly that based on pulse radiolysis method. The activities of the Institute concern different aspects of nuclear energy: fuel precursors synthesis and fuel reprocessing, radioactive waste reprocessing, radiobiological methods of radiological protection, material radiation damage, nuclear electronics. Nowadays, with its seven electron accelerators in operation and with the staff experienced in the field of electron beam application, the Institute is one of the most advanced centers of science and technology in this domain. The Institute has four pilot plants equipped with five electron accelerators: for radiation sterilization of medical devices and transplantation grafts, for radiation modification of polymers, for removal of $SO_2$ and $NO_x$ from flue gases, for food hygienization. The Institute is composed of three centers: Centre for Radiation Research and Technology, Centre for Radiochemistry and Nuclear Chemistry, Centre for Radiobiology and Biological Dosimetry, and seven laboratories: Accredited Laboratory for Measurements of Technological Doses, Accredited Laboratory for Detection of Irradiated Food, Laboratory of Nuclear Control Systems and Methods, Stable Isotope Laboratory, Laboratory for Nuclear Analytical Methods, Laboratory of Material Research, and Pollution Control Technologies Laboratory, a library and an information center. The Institute is editor of the scientific journal *Nukleonika* (journal with IF), *Postępy Techniki Jądrowej* (Advances in Nuclear Technology), *INCT Reports* and *Annual Report*.

The Institute conducts doctoral studies in chemistry and is holder of Erasmus chart. The project "Joint innovative training and teaching/learning program in enhancing development and transfer knowledge of application of ionizing radiation in materials processing" has filled up the gap of education quality between different regions of EU countries. Seven partners from five EU countries and one associate member state (Poland, France, Italy, Lithuania, Romania and Turkey) were involved in this project (http://tl-irmp.eu/en/).

The Institute is a member of the International Irradiation Association. In May 2010, the Institute was nominated by the International Atomic Energy Agency (IAEA) a Collaborating Centre for Radiation Processing and Industrial Dosimetry. In 2016, this nomination was prolonged till 2020. According to announcement on the webpage of Division of Physical and Chemical Sciences "The new Collaborating Centre RAPID" (from Radiation Processing and Industrial Dosimetry) is an important addition to the IAEA's resources in further serving Member States in feasibility assessment of emerging applications of radiation processing to facilitate adoption and industrial dosimetry intercomparison exercise, vital for effective and efficient application of the technology (http://www-naweb.iaea.org/NA/ccentres.html). The Centre organizes quite a few meetings and workshops, accepts fellows and supports the Agency by other means. This is a good synergy between the IAEA and EU programs, such as ARIES.

Chapter 2

# THE INCT ELECTRON ACCELERATOR RESEARCH FACILITIES

**Zbigniew Zimek**

## 2.1. NANOSECOND PULSE RADIOLYSIS

Pulse radiolysis is a unique research method allowing to obtain, with the required time resolution, various information on transient processes. The subject of the research is chemical reactions taking place in a sample subjected to the impact of a short pulse of accelerated electrons. One of the basic parameters of the pulse radiolysis system is its time resolution. In the first period, optical measurements with microsecond resolution predominated. Currently, measurements with nanosecond resolution are most often carried out. Recently developed methods of forming accelerated electron pulses of duration measured in femtoseconds enable the construction of a new generation of devices designed to conduct experiments using pulse radiolysis. However, the obstacle lies not only in technical difficulties and costs, but primarily in the desirability of building such installations. For such short times, we are talking rather about physical aspects than chemical processes taking place, and one of the most important factors is the lack of influence of diffusion on the course of chemical reactions in this time scale.

The measuring apparatus used in pulse radiolysis is usually built to meet the requirements of the test program. It is not possible to use all the latest achievements in one set due to the sometimes precluded assumptions. This is the source of a favorable tendency towards specialization of individual impulse radiolysis systems and conducting scientific cooperation enabling the use of apparatus built in other centers.

The activities undertaken in cooperation with domestic and foreign units were adopted as the basis for the proposed basic research carried out at the Centre for Radiation Research and Technology of the Institute of Nuclear Chemistry and Technology (INCT). The basic direction of research is to determine the importance of free radical processes in biological systems. Understanding the mechanisms of radical reactions initiated by ionizing radiation in systems of compounds of biological importance from the perspective of using the obtained results in the development of specific pharmaceuticals, raising the quality of life through learning the mechanisms of aging processes, learning the pathology of many disease states.

Electron accelerators are integral parts of technological installations used in radiation processing and they are the basic devices in experimental sets used in research in the field of radiation chemistry. Particle accelerators have been developed and built for the needs of nuclear physics since the early 1930s. Apart from reactors, these devices belong to the largest technical undertakings in nuclear research, and are responsible in a significant degree for the progress in many branches of science and technology. While in physical studies the basic direction of development is the work on increasing the energy of accelerated particles, in the accelerators used in chemistry basic study electron pulse duration plays an important role.

Currently built accelerators for radiation chemistry and radiation technology are characterized by relatively low energy of electrons (0.15-15 MeV). The lower energy range determines too little electron penetration and high beam power losses in output devices equipped with metal foils as a window for electrons. The upper energy range is limited by the radioactivity induced in the irradiated material. In industrial applications, an important parameter is the adequately high average power of the beam, which ensures the required process productivity, minimizes costs and allows to fulfill required production demands. The time structure of the electron beam is less important. On the other hand, the time char-

acteristics of accelerated electrons are fundamentally important in the study of radiation chemistry performed by pulse radiolysis method.

Practical activities in the field of radiation chemistry and radiation technology based on the use of accelerators started in Poland when the first accelerator of electrons with energy of 5-13 MeV and beam power of 9 kW [1] was put into operation at the Institute of Nuclear Research (currently Institute of Nuclear Chemistry and Technology). 17 January 1971 is the date when the beam of accelerated electrons was introduced for the first time. For many years LAE 13/9 accelerator was the only large source of ionizing radiation in the form of accelerated electron beam available in Poland. This device was designed for multi-purpose work, which, in addition to basic and applied scientific research, allowed to carry out radiation treatment on a mass scale. The microsecond pulse radiolysis system was constructed and used for basic study [2]. This was ensured not only by the unique design of the accelerator equipped with two independent electron beam extraction systems, but also by appropriately adapted rooms and installed auxiliary equipment.

Development of scientific research in the field of radiation chemistry required the expansion of the accelerator base to perform basic experimental work. This is due not only to the limited access to the LAE 13/9 accelerator, which was intensively used in applications, but also to certain parameters of the electron beam that do not meet the requirements, especially in the dynamically developing fast kinetic research studies. Therefore, a decision was made to build a research installation equipped with an LAE 10 accelerator to conduct kinetic study in nanosecond time scale using the pulse radiolysis method.

The linear electron accelerator LAE 10 was designed and constructed at the INCT for research in the field of radiation chemistry with the use of pulse measurement techniques. The basic experimental set-up of pulse radiolysis with nanosecond time resolution operates in single pulse mode with high intensity of accelerated electrons. According to the assumptions, the LAE 10 accelerator is an independent research facility, installed in a specially built shielded room. The essential parameters of the LAE 10 accelerator are presented in Table 2.1.

Table 2.1. Basic parameters of the LAE 10 electron accelerator

| Parameter | Value |
|---|---|
| Pulse duration | 10 ns, 100 ns |
| Pulse beam current | 0.5-1 A |
| Pulse repetition rate (max.) | 50 Hz |
| Single pulse operation mode | |
| Average beam current (max.) | 50 μA |
| Average beam power (max.) | 500 W |
| Frequency | 1818 MHz |

The LAE 10 accelerator was built and commissioned at the Department of Chemistry and Radiation Technology (currently Centre for Radiation Research and Technology) of the INCT in accordance with formulated assumptions in 2000 [3]. This device was designed to conduct scientific research in the field of radiation chemistry with the use of pulse radiolysis method. An automatic recording system of single kinetic courses with a nanosecond time resolution is available. This research, especially in connection with the tracking of transition processes in biologically important compounds is currently carried out by many world laboratories. Thus, the LAE 10 accelerator together with the measurement system is an important complement to the existing radiation installations located in the INCT. It is worth mentioning that accelerators with similar parameters are not typical devices, and the purchase of a ready-made accelerator would be associated with high costs. The choice of a specific frequency of accelerating section resulting from the availability and cost of microwave

devices. Majority of untypical components have been designed at the INCT. Mechanical works related to untypical devices and subassemblies have been carried out outside the Institute. In addition to the typical equipment purchased predominantly in Poland, the acceleration section and some elements of the waveguide route were purchased from the D.V. Efremov Institute of Electrophysical Apparatus, Saint Petersburg, Russia. The assembly and commissioning of the accelerator were carried out by the employees of the INCT, in addition to the duties related to the operation of the other accelerators.

The principle on which the operation of accelerators is based is the phenomenon of accelerating electrons (generally charged particles) under the influence of an electric field. Microwave energy is provided to accelerating section with multi-cavity construction. During accelerating process the electric component of the electromagnetic wave is used to increase electron energy in microwave linear accelerator. The process of accelerating electrons takes place in a vacuum in which the cathode emitting electrons is placed. The length of the electron pulse being most often determined by the parameters of pulses supplying the electron gun. The energy of electrons at the level of 10 MeV assumed a structural solution in the form of a linear accelerator with a traveling or standing wave.

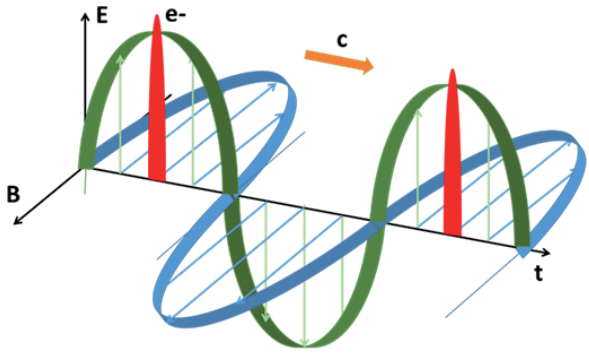


Fig. 2.1. The principle of microwave linac operation in traveling wave mode

The operation of the LAE 10 accelerator is based on the traveling wave mechanism. The accelerating electrons are moving in a compatible phase together with the electric field constituting the component of the electromagnetic wave along the axis of the accelerating section (Figs. 2.1 and 2.2).

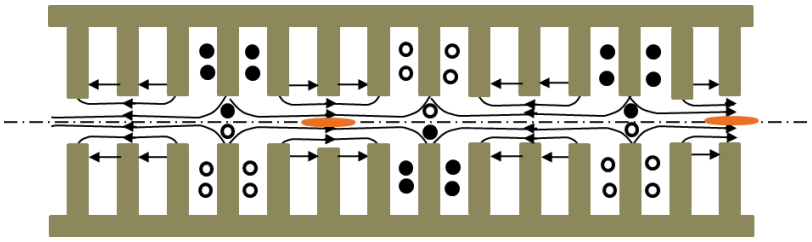

Fig. 2.2. Accelerating section of microwave linac with traveling wave composed as cylindrical diaphragmatic waveguide

The accelerating section of the LAE 10 linac was built as a cylindrical diaphragmatic waveguide with $2\pi/3$ modes with a prebunching part. Acceleration is preceded in the first part of the acceleration phase of the phase grouping process of electron intensity. Changing the geometry of the section along the symmetry axis provides the optimal phase between the densities and the electromagnetic field moving along the section in the form of a current wave.

The initial speed of the electrons is determined by the parameters of the electron gun and in the adopted solution is half the speed of light. The speed of electrons after obtaining 3 MeV energy is close to the speed of light and changes slightly in the further acceleration process. The intensity of the electric field in the acceleration section is of the order of 100 kV/cm, and the synchronous movement of electrons in such a field enables the increase in energy determined by the length of the acceleration section. It is worth noting that the acceleration section used in the LAE 10 accelerator ensures, with pulses of electrons in the microsecond range and beam current in the impulse below 1 A, acceleration of electrons to the energy up to 10 MeV.

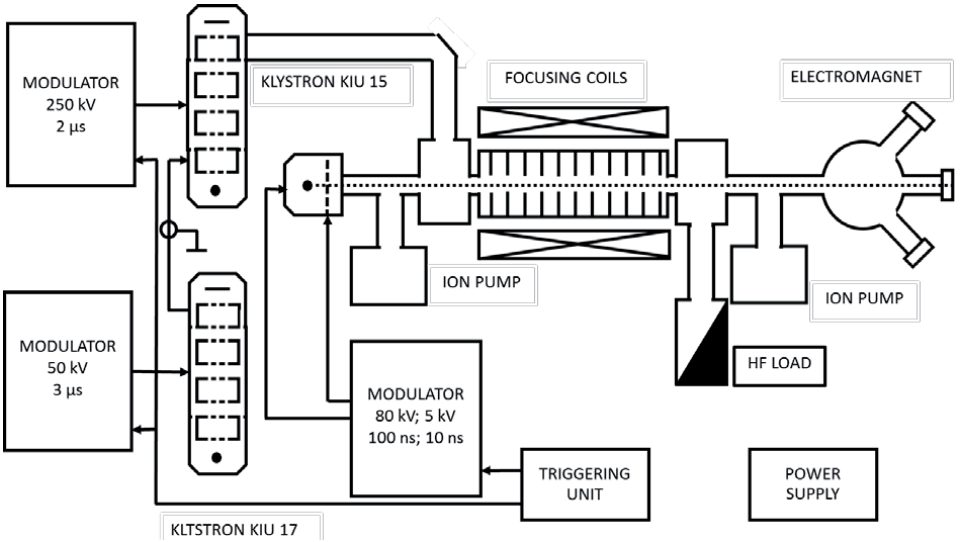


Fig. 2.3. Block diagram of the LAE 10 accelerator with the main devices

Figure 2.3 shows a block diagram of the LAE 10 accelerator with the main devices. The electrons emitted from the guns are directed through the focusing system to the entrance of the accelerating section. The accelerating section built as a waveguide with diaphragms with axial symmetry is excited by an electromagnetic wave from a high frequency generator based on klystron KIU 15.

Accelerator LAE 10 consists of a number of devices and installations:

I. Electron acceleration trajectory devices:
– triode electron gun (80 kV, 5 kV);
– traveling wave acceleration section with focusing coils, and coils dedicated for correcting the position of the beam;
– deflection electromagnet with three electron beam exits.

II. Pulse operating devices:
– electron gun pulse anode modulator (pulse amplitude and duration: 80 kV, 200 ns),
– electron gun grid modulator (pulse amplitude and duration: 5 kV, 10 ns),
– klystron KIU 15 modulator (pulse amplitude and duration: 50 kV, 3 μs),
– klystron KIU 17 modulator (pulse amplitude and duration: 250 kV, 2 μs).

III. High frequency devices:
– microwave generator (frequency and average power: 1818 MHz, 100 mW),
– microwave semiconductor amplifier,
– klystron KIU 17 (frequency and pulse power: 1818 MHz, 100 kW),
– klystron KIU 15 (frequency and pulse power: 1818 MHz, 20 MW),
– waveguide transmission lines with measuring elements and security systems.

IV. 220/380 V power supply.
V. Control and interlock systems.
VI. Cooling installations:
– cooling water installation with distilled water (flow: 80 l/min),
– installation of thermostatic water (36°C, flow: 60 l/min).
VII. Vacuum installations:
– pre-vacuum installation,
– high vacuum installation (two ion pumps and two 7 kV power supplies).

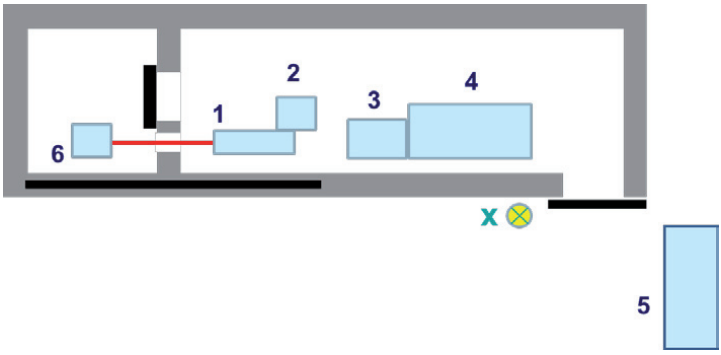


Fig. 2.4. Layout of the LAE 10 accelerator: 1 – accelerating section, 2 – gun modulator, 3 – klystron, 4 – modulators of KIU 15 and KIU 17 klystrons, 5 – control room, 6 – pulse radiolysis equipment, X – safety signaling lamp

In accordance with the assumptions, the LAE 10 accelerator was installed in a specially built premises with an area of 220 $m^2$. Figure 2.4 shows the location of the most important accelerator devices. The separated room was designated for the installation of output devices (deflection electromagnet) and devices for conducting experiments. The room with an area of 15 $m^2$ has been additionally shielded and equipped with an independent grounding to protect the measuring apparatus and to reduce the level of electromagnetic interference. The main parts of accelerator together with the modulators and microwave systems are located in a separate room, unavailable during the operation of the accelerator due to the increased level of ionizing radiation. The installation channel for conducting electrical, water and vacuum installations leads from the LAE 10 accelerator room to the control devices located behind the shielding wall. Heat exchangers with water pumps for distilled and thermostatic water circuits are located in a separate room together with similar LAE 13/9 accelerator devices. Similarly, electrical switchboards for both devices are located in one room.

The original nanosecond triode electron gun with porous tungsten cathode has been developed and used as a source of electrons. It was designed and tested on its own [4]. The gun is equipped with an indirectly heated cathode with a diameter of 14 mm. It can be operated with two different pulses of electrons: 100 ns or 10 ns. In the first case, the formation of the electron beam is determined only by the voltage pulse applied between the anode and the cathode with an amplitude of 50-80 kV and a duration of 200 ns. Working with short pulses requires additionally polarity of the grid up to 3 kV and application of a pulse applied to the grid works with an amplitude of 2-4 kV and a duration of 10 ns. The construction of the electron gun is shown in Fig. 2.5. The nanosecond grid modulator has been designed and built. Good quality R and C components were used to improve time performances of the modulator. Ultra-fast transistor on and off switch HTS 80-12-UF type was applied. The rise and fall times not higher than 3 ns have been obtained. Simplified diagram of high voltage modulators for electron gun is presented in Fig. 2.6. Electron gun is located at entrance of accelerating section in close distance from metal box containing 10 ns, 5 kV pulse modulator (Fig. 2.7).

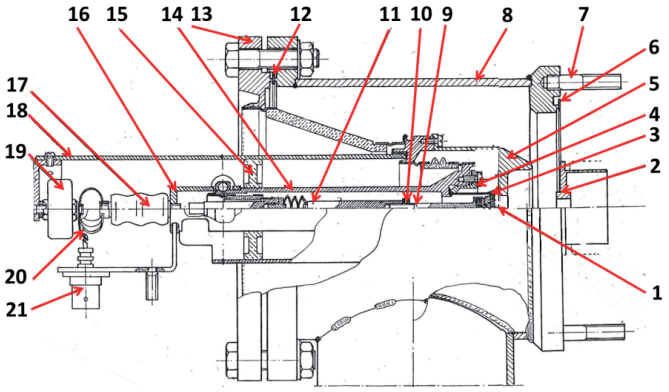


Fig. 2.5. Cross-section of nanosecond electron gun: 1 – cathode, 2 – grid, 3 – duct to vacuum pump, 4 – electrical connection of cathode heater, 5 – concentric line to provide grid driving pulses, 6 – isolator, 7 – external envelope

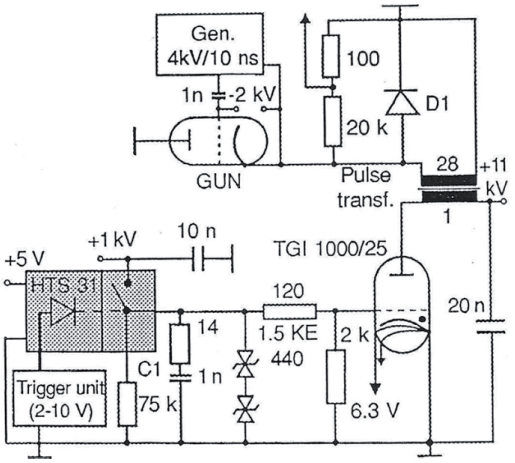


Fig. 2.6. Simplified diagram of high voltage modulators for electron gun

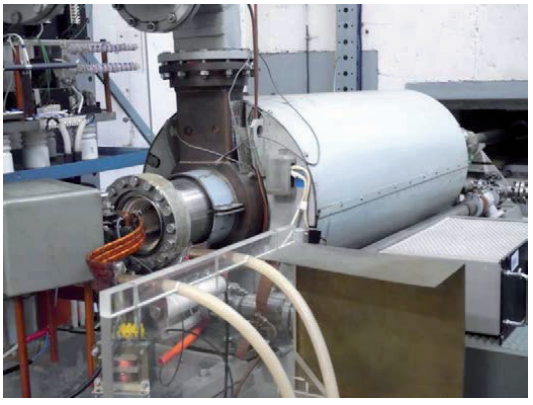

Fig. 2.7. Nanosecond electron gun located at entrance of accelerating section in close distance from metal box containing 10 ns, 5 kV pulse modulator

The accelerating section is built in the form of a waveguide with diaphragms and axial symmetry (length: 1270 mm). Focusing and position correcting coils of the beam are placed outside of the section. The magnetic field along the coil's axis is constant and amounts to approximately 800 Oe. The sectioned coil winding was made of copper foil separated by water-cooled disks. To maintain the stability of the acceleration section parameters for its cooling, water from the thermostatic circulation at 36ºC is used. Figure 2.8 presents the general view of the acceleration section together with the elements of the electronic circuit, the vacuum system and the waveguide line. On the right side of the picture pressure vessel with nitrogen can be seen. The nitrogen with pressure 0.4-0.5 MPa is used to fill waveguides to prevent electrical breakdowns.

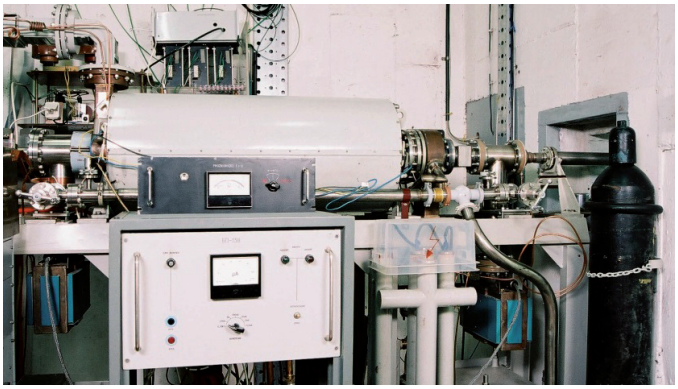

Fig. 2.8. Genereal view of the acceleration section and beam line structure

The electron gun and klystrons modulators are providing the pulses with required specific amplitude and duration. Table 2.2 includes basic parameters of pulse operating devices of LAE 10 accelerator.

Table 2.2. Parameters of pulse operating devices

| Parameter | Units | Type of equipment | | | |
|---|---|---|---|---|---|
| | | Klystron KIU 15 modulator | Klystron KIU 17 modulator | Gun modulator | |
| | | | | Anode | Grid |
| Pulse amplitude | kV | 250 | 50 | 80 | 5 |
| Pulse duration | Ms | 2 | 3 | 0.2 | 0.01 |
| Pulse current | A | 200 | 90 | 20 | 2 |
| Average power | kW | 10 | 1 | 1 | < 0.1 |
| DC voltage | kV | 20 | 25 | 20 | 5 |

The simplified schematic diagram of the modulator of KIU 15 is shown in Fig. 2.9. The impulse triggering the TGI 2500/50 thyratron is formed by a thyristor system. After the thyratron key is triggered, an output pulse is formed with a duration defined by the parameters of the forming line and the amplitude determined by the supply voltage and transformer gears.

Figure 2.10A shows the klystron KIU 17 with focusing coil and coupler located on its top. Figure 2.10B shows pulse transformer of modulator and KIU 15 klystron together with the

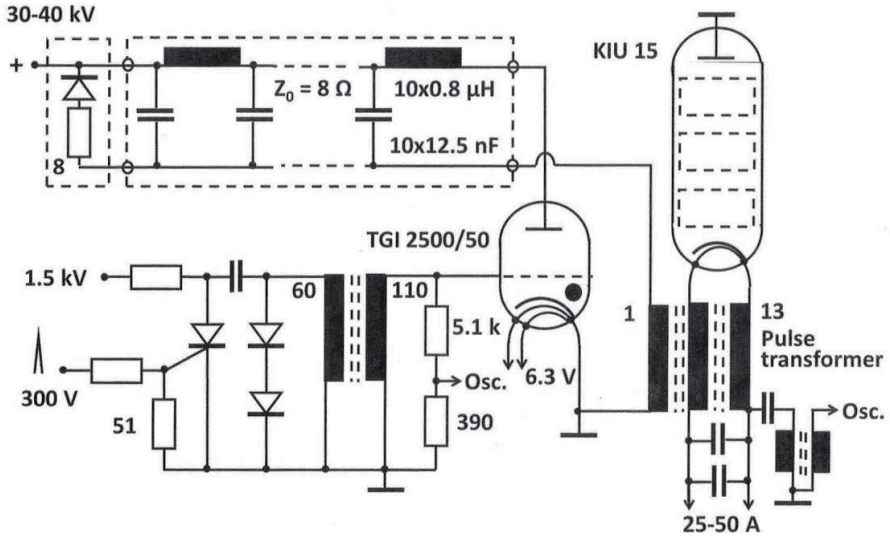


Fig. 2.9. Simplified diagram of KIU 15 klystron pulse modulator

elements of the focusing coil. The KIU 17 modulator has a similar schematic diagram but a correspondingly lower supply voltage. In this system, the TGI 1000/25 thyratron was used as a switch. Table 2.3 includes main parameters of KIU 15 and KIU 17 klystrons.

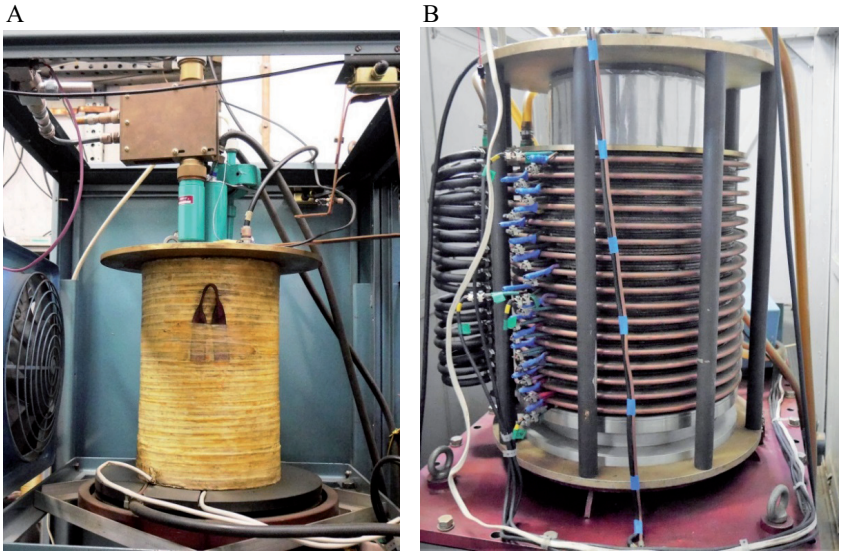


Fig. 2.10. Focusing coils of klystron KIU 17 (A) and klystron KIU 15 (B)

The following devices are included to high frequency track (Fig. 2.11):

- HF generator (1818 MHz, 1 mW),
- semiconductor amplifier (1818 MHz, 100 mW),
- klystron KIU 17 (1818 MHz, power in 100 kW impulse),
- klystron KIU 15 (1818 MHz, power in 20 MW impulse),
- waveguide transmission lines with measuring elements and security systems.

Table 2.3. Main parameters of KIU 15 and KIU 17 klystrons

| Parameter | Unit | Klystron KIU 15 | Klystron KIU 17 |
|---|---|---|---|
| Heater voltage | V | 12 | 3.15 |
| Heater current | A | 50 | 26.5 |
| Anode voltage | kV | max. 280 | max. 50 |
| Ion pump voltage | kV | 3.2 | 3 |
| Standing wave coefficient | - | max. 1.25 | max. 1.25 |
| Input power | kW | max. 6 | 0.15 |
| Focusing current | A | 30/30 | 10 |
| Pulse duration | μs | max. 6 | max. 8 |
| Frequency | MHz | 1818 | 1818 |
| Frequency band (0.8) | MHz | ±9 | ±9 |
| Output pulse power | MW | 20 | 0.112 |
| Efficiency | % | 35 | 44 |
| Amplification | dB | 35 | 69 |
| Average output power | kW | 18 | 0.175 |
| Cooling water | l/min | 60 | 2 |

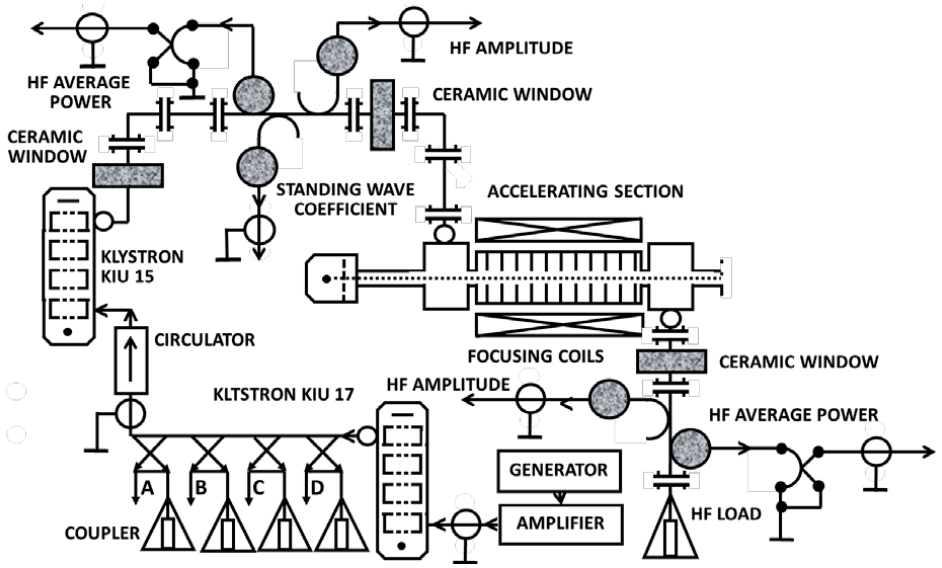


Fig. 2.11. Main components of microwave system of LAE 10 accelerator: A and B – signals for automatic control for microwave power, C – signal for HF amplitude control, D – signal for frequency measurements

The source of the working frequency in the LAE 10 accelerator is the G4-79 generator, which generates a signal at a power level < 1 mW. The next amplifying stages (semiconductor amplifier, KIU 17, KIU 15) allow to achieve the output pulse power of 20 MW. HF pulses amplified by the KIU 15 klystron are sent to the acceleration section by means of a nitrogen-filled rectangular waveguide 120 mm × 57 mm in cross-section, with a pressure of 0.4-0.5 MPa to increase the electrical strength. At the entrance and exit of the accelerating section, ceramic windows separating the vacuum part of the accelerator from waveguides filled with nitrogen under pressure were used. Second ceramic window is located after accelerating section. The not used portion of microwave energy is taken away by water cooled HF load. Standing wave coefficient (SWC) of accelerating section vs. frequency of microwave power was measured (Fig. 2.12). As can be noticed for frequency operating level 1817.9-1818.0 MHz, SWC is far below accepted value for klystrons operation (1.25) according to technical specification (Table 2.3).

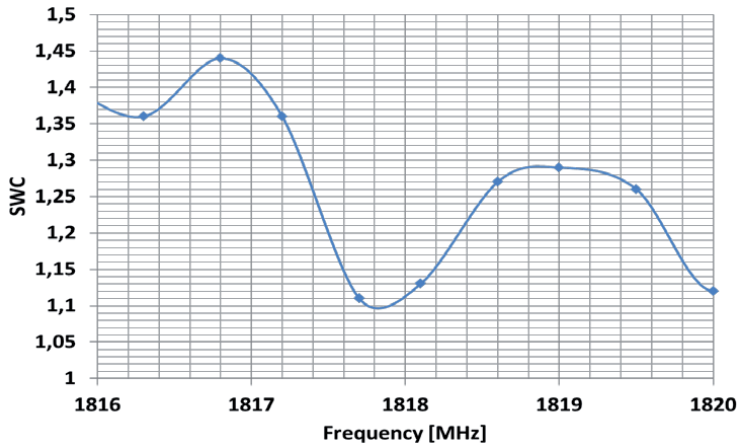


Fig. 2.12. Standing wave coefficient of accelerating section vs. frequency of microwave power

In order to protect the proper operating conditions of klystrons, a number of circuits protecting against the effects of damages resulting from non-catalog operating conditions were used. Table 2.4 presents the list of controlled parameters and the levels beyond which the

Table 2.4. Systems protecting the proper operation of klystrons KIU 17 and KIU 15

| Parameter | Threshold for the operation of the safety devices | |
|---|---|---|
| | Klystron KIU 17 | Klystron KIU 15 |
| Klystron breakdown | 60% higher anode current | 60% higher anode current |
| Anode voltage | 10% higher level | 10% higher level |
| SWC | 1.5 | 1.5 |
| Focusing current | drop 50% | < 25 A |
| Cooling water temperature | 60°C | 60°C |
| Heater voltage | - | ±0.3 V |
| Heater current | ±0.5 A | - |
| Nitrogen pressure | - | 0.37 < P < 0.55 |

triggering of klystron modulators is immediately switched off. Activation of a single blockade is a sufficient reason to block the operation of both modulators and thus the entire accelerator.

The most important auxiliary systems installed in the LAE 10 accelerator are:

- 220/380 V power supply;
- control, control and blocking systems;
- cooling installations:
  - installation with distilled water (flow: 80 l/min),
  - installation with thermostatic water (36ºC, flow: 60 l/min);
- vacuum installations:
  - pre-vacuum installation,
  - high vacuum installation.

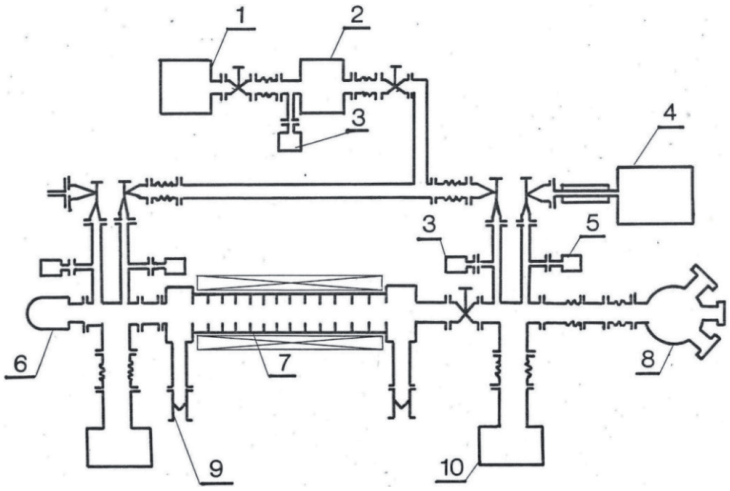


Fig. 2.13. Block diagram of vacuum system of LAE 10 electron accelerator: 1 – fore-vacuum system, 2-6 – electron gun, 7 – accelerating section, 8 – bending electromagnet, 9 – ceramic window, 10 – ion pump

Figure 2.13 presents the block diagram of vacuum system of LAE 10 electron accelerator. Two-stage vacuum system includes an oil mechanical pump together with a nitrogen trap of oil vapor for preliminary pumping and two ion pumps with pumping speed 100 l/s supplied with 7 kV capable to provide high vacuum conditions necessary for electron accelerating process. The system can be divided into two parts by vacuum valve located after accelerating section. A low and high vacuum measurement systems have been installed.

To ensure a constant working temperature of the accelerating section, a separate closed thermostat water circuit was installed. The temperature is automatically maintained at the level of 36 ±0.5ºC at a capacity of 60 l/min. Stable temperature of the accelerating section stabilizes dimension of accelerating structure what means optimal operating frequency and stable conditions for electron accelerating process.

Selected systems of LAE 10 accelerator are powered from a stabilized network to improve the stability of the accelerator operation. The control systems provide remote control of variable accelerator parameters such as the working voltage of the klystrons or the focusing currents of the klystron coils and the accelerating section. The control of impulse devices is carried out by means of fiber optic connectors. The timing system is determined by the synchronization system equipped with adjustable delays of specific triggering signals dedicated for pulse operated devices. Control rack of LAE 10 accelerator is presented in Fig. 2.14.

One of the important stages of work on the construction of the LAE 10 accelerator was the design and testing up synchronization systems based on fiber-optic connections. The main

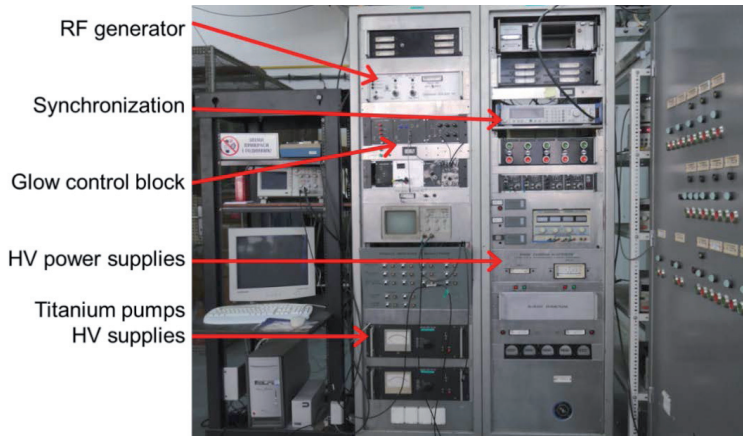


Fig. 2.14. Control rack of LAE 10 accelerator

function of that system is providing adjustable time sequence of high voltage pulse from KIU 15 klystron modulator, high voltage pulse from KIU 17 klystron modulator, high voltage pulse (anode) at the output of the modulator of the electron gun, and nanosecond grid of the gun modulator.

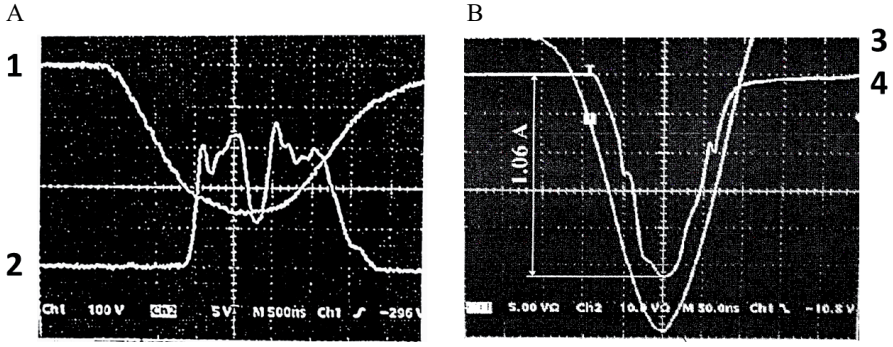


Fig. 2.15. Oscillograms: (A – 500 ns/div) 1 – high voltage pulse with 220 kV amplitude for klystron KIU 15, 2 – envelope of HF pulse measured after accelerating section with electron beam presence; (B – 50 ns/div) 3 – high voltage pulse with 80 kV amplitude for electron gun, 4 – pulse of electron beam current measured by Faraday cup

Figure 2.15A shows oscillograms of high voltage pulse with 220 kV amplitude for klystron KIU 15 (1) and related to it an envelope of HF pulse measured after accelerating section with electron beam presence (2). The characteristic amplitude drop in the middle of that pulse is related to absorption of HF power by accelerated electrons in 100 ns long pulses. Figure 2.15B shows high voltage pulse with 80 kV amplitude for supplying electron gun (3). Pulse of electron beam current was measured by Faraday cup (4). Grid modulator is triggered in nanosecond mode accelerator operation. Figure 2.16 shows results of beam shape measurements when Faraday cup with coaxial 50 Ω structure was located directly after accelerator exit window (A). Pulse of accelerated electrons is shown in Fig. 2.16B where both gun anode voltage amplitude (1) and pulse shape of accelerated electrons (2) are displayed. Exact results are as follows: beam pulse current amplitude ($I_{eb}$) – 0.78 A, rise time at the level of 0.1-0.9 – 2.7 ns, falling time at the level of 0.9-0.1 – 3.3 ns, pulse duration at the level of 0.5 – 8.7 ns.

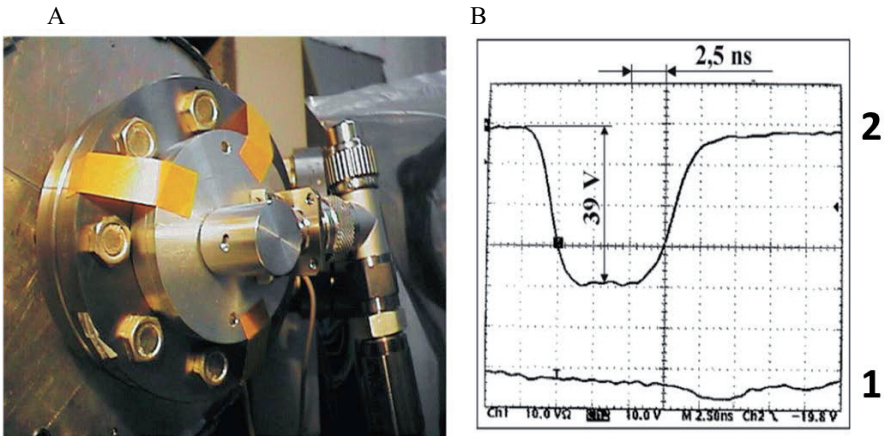


Fig. 2.16. Faraday cup located directly at accelerator exit window (A); measured pulse characteristics (B), where: 1 – amplitude of gun anode voltage, 2 – shape of the beam current (2.5 ns/div)

The spot of electron beam in nanosecond mode was measured with PVC foil dosimeter. It is shown in Fig. 2.17 where foil was exposed on 7000 pulses of accelerated electrons.

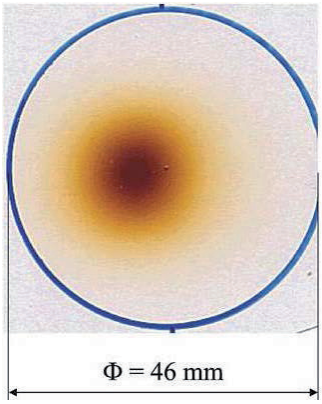


Fig. 2.17. Spot on PVC dosimetric foil after 7000 beam pulse shots

Depth dose distribution in water is displayed in Fig. 2.18. The calculation was made with application of computer program based on Monte Carlo method for pencil type electron beam with electron energy 10 MeV. A non-destructive beam-charge monitor was designed to measure the charge within single pulse of accelerated electrons in range 1-15 nC and pulse duration 1-1500 ns [5]. The measuring error does not exceed 6% and the linearity in one week is within the limit ±1%. The calibration of the charge monitor was verified by measurements performed with Faraday cup.

The LAE 10 accelerator is solely dedicated for conducting scientific research in the field of radiation chemistry by pulse radiolysis method with automatic recording of individual kinetic runs and nanosecond time resolution. Thus, the LAE 10 accelerator together with the measuring system being built is a necessary complement to the radiation installations at the INCT. The pulse radiolysis set-up contains digital storage oscilloscope (bandwidth DC to 500 MHz), programmable via GPIB and RS-232C. The separation between successive points is 0.5 ns. Resolve time constants vary from a few nanoseconds to hundreds of microseconds. Measured transients are detected by UV/VIS absorption spectroscopy using two kind of xenon

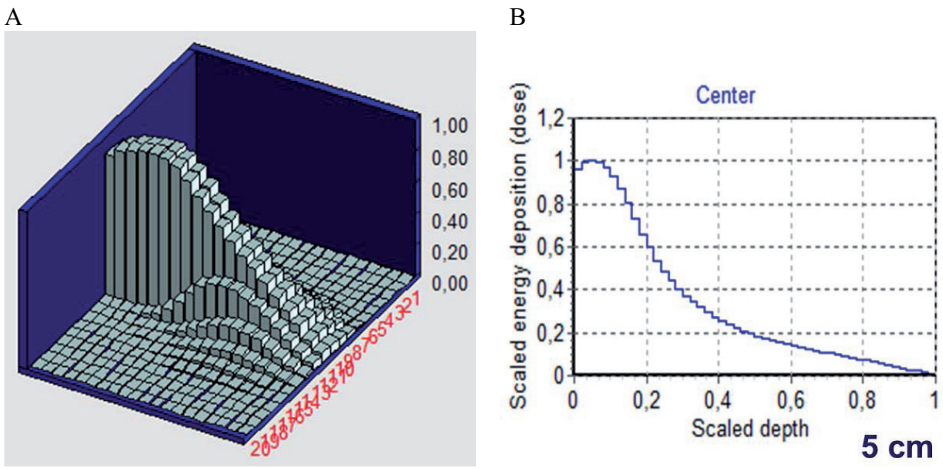


Fig. 2.18. Depth dose deposition in water absorber calculated by computer program based on Monte Carlo method: A – initiated by pencil type electron beam, B – dose deposition along beam axis

lamps as sources of analytical light. The data-acquisition subsystem includes a mono-chromator, photomultiplier tube with spectral response 160-900 nm and detecting diode array to detect in single shot not only time related but also spectral response related signals. The program controls the peripherals over GPIB and RS-232 and RS-485 lines. Figure 2.19 shows pulse radiolysis equipment located at front of electron beam exit.

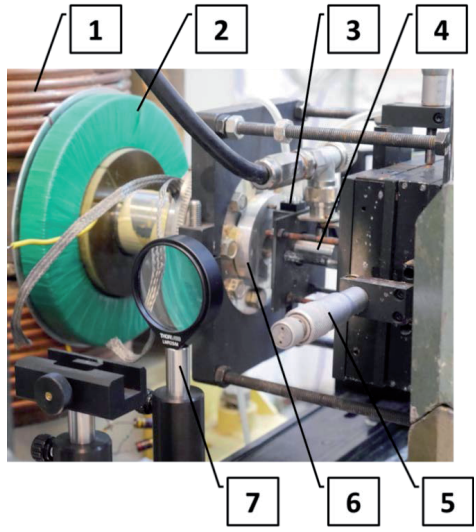


Fig. 2.19. Pulse radiolysis equipment located at front of electron beam exit: 1 – bending magnet, 2 – single pulse charge monitor, 3 – reaction vessel, 4 – Faraday cup coaxial cable, 5 – reaction vessel positioning system, 6 – beam exit window; 7 – analytical light focusing lens

Pulse radiolysis control system is located in a separate room, where optical signal (analytical light) is transferred to monochromator and detector from beam exit room through specially constructed optical channel, to avoid scattered radiation. Figure 2.20 shows two-channel monochromator and computer monitor screens of data acquisition system, which

A B

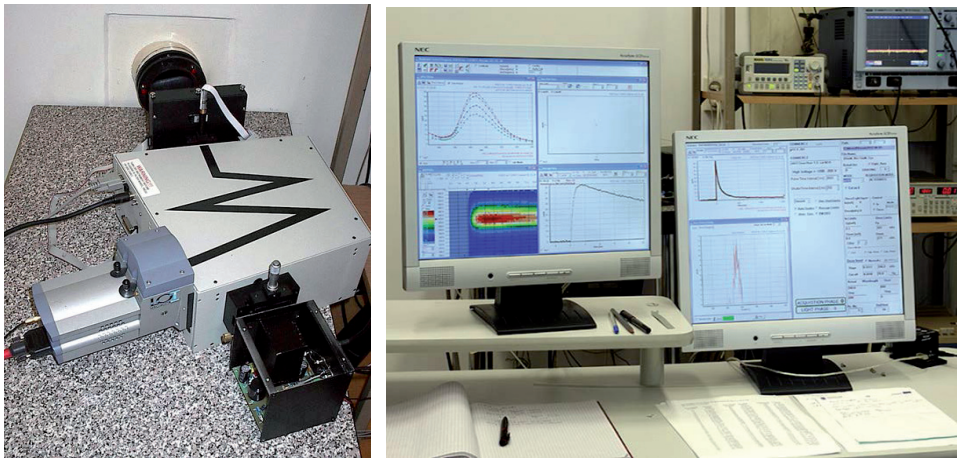

Fig. 2.20. Two-channel monochromator (A) and computer monitor screens (B) of data acquisition system

are used to change experiment conditions, processing the data (averaging, sensitivity, dose, time scale) and displaying time and wavelength related characteristics. An ICCD camera was installed as an additional detector at the facility for nanosecond pulsed radiolysis, equipped with a two-channel monochromator, allowing registration of transient absorption spectra after a single pulse of accelerated electrons. Table 2.5 shows main functions of pulse radiolysis equipment.

Table 2.5. Pulse radiolysis experimental set-up characteristics

| Electron beam characteristics | | |
|---|---|---|
| Electron energy: 10 MeV, beam current: 1 A | Pulse duration: 4-10 ns, 100 ns | Repetition rate: 1, 12,5, 25 Hz; single mode operation |
| Pulse radiolysis set-up characteristics | | |
| Optical detection: PM (260-900 nm), ICCD camera | Samples: liquid and solids; flowing system for liquid samples | Observation: 10 ns-10 ms, single shot spectral characteristic |

The design and construction of this specialized facility was possible because of the presence at the INCT of various types of accelerators with different technical parameters and applications. This will allow to make modifications of the accelerator and measuring set-up to perform scientific work programs in the future.

## 2.2. VAN DE GRAAFF ACCELERATOR

The first electrostatic accelerator was constructed and demonstrated by Robert J. Van de Graaff in the early 1930s. High voltage in such accelerators is obtained by mechanical transfer of electrical charge from the ground level up to high voltage electrode, then the voltage difference is formed which can be used for particle acceleration. In 1956, an electrostatic

electron accelerator with 2 MeV electron energy and 0.5 kW average beam power was used in the first commercial facility to perform radiation sterilization process. Since then more than three thousands of electron accelerators based on different principles constructing and operating offer much higher beam power (up to 700 kW) and frequently with higher energy (up to 10 MeV). They have been successfully applied in the different fields of radiation chemistry and radiation processing. The current capacity of the electrostatic accelerator is limited by the width of the transmission belt, acceptable surface charge density (type of material) and linear speed of the belt. The beam current usually does not exceed 2 mA, which limits the beam's power to several kilowatts. Due to significant limit in beam power level currently accelerators based on electrostatic conception are practically apply only as research facilities mainly in nuclear and solid state physics.

An AS-2000 electron electrostatic accelerator manufactured by HVEC, Netherland, was installed at the Radiation Physics Laboratory of the Institute of Nuclear Research (currently the National Centre for Nuclear Research) in Świerk in relation with radiation damage studies in solids. The investment was sponsored by the International Atomic Energy Agency (IAEA). The accelerator was assembled in 1965, and equipped with convertible pulsed/DC operation mode [6]. It was extensively used for investigations in solid state physics with main application to study properties of radiation defects in semiconductors. In 1985, the accelerator was disassembled following the decision of the National Atomic Energy Agency and relocated to the Institute of Nuclear Chemistry and Technology [7].

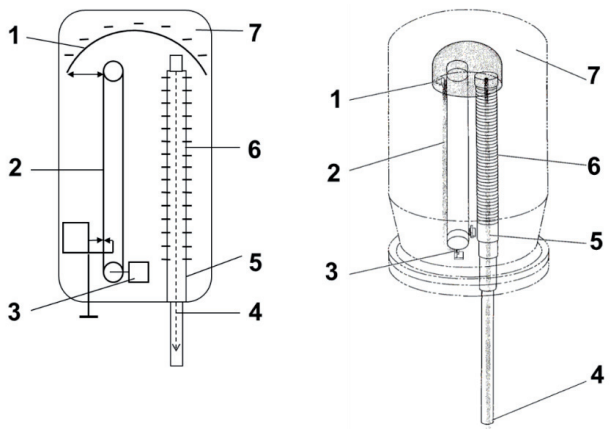


Fig. 2.21. The principle of electrostatic accelerator operation: 1 – HV electrode, 2 – belt, 3 – engine, 4 – beam exit, 5 – anode, 6 – accelerating section, 7 – gas insulation

The accelerator AS-2000 nominal parameters according to the manufacturer specification gives the possibility of electron beam irradiation with energy in the range 0.1-2.0 MeV, and nominal beam current up to 100 μA. Currently the accelerator works in a continuous beam mode. The beam current densities used do not exceed 1 $\mu A/cm^2$ for a beam of 50 mm diameter or 30 $\mu A/cm^2$ for a focused beam. Practical electron energy range is 0.2-1.7 MeV, what can be afforded on regular voltage conditioning basis. Figure 2.21 illustrates the principle of electrostatic accelerator operation. Moving belt transmits electrical charge provided by power supply located at bottom part of pressure vessel to the electrode, where high voltage potential is formed. The sharp edge acting as the emitter is connected to the power supply and placed near the belt. The presence of high voltage in the gas medium causes the ionization of the gas near the blade. If the negative potential is connected to the edge electrode, the negative ions are repelled and settled on the surface of the belt. The negative charge is transmitted by belt towards the high voltage electrode equipped with the charge collector. Thanks to this, the electrode achieves a high negative potential, which allows the acceleration of electrons. HV

negatively charged electrode is loaded by accelerating section equipped with the electron gun. The accelerating section is located inside of pressure tank. The pressure vessel is filled with a mixture of gaseous nitrogen and carbon dioxide, maintained at high pressure up to 2.5 MPa to insulate the high voltage terminal from the ground and to avoid the breakdowns. The gas $N_2$ and $CO_2$ mixture is used with proportion $N_2$:$CO_2$ in the range varied from 3:1 to 4:1.

Power supply located inside pressure vessel is providing charging voltage in 30-40 kV range. The voltage level between HV electrode and ground depends on its capacitance (C) to the ground and deposited charge (Q) according to formula:

$$U = Q/C$$

MV level voltage can be obtained relatively easily when capacitance is not too high and loading current due to insulation quality, voltage divider and beam current load is sufficiently low to compare with charge transfer capability. Long-time stability of accelerating voltage was found to be ±10 kV and is supported by automatic control. High voltage ripple is at the level ±2 kV. Various experiments require information related to exact electron energy level. The generating voltmeter is used to measure output voltage. This voltage is directly related to electron energy level. Necessary calibration can be done at suitable intervals using the gamma-neutron reaction of beryllium as a reference target material. The electron beam from the accelerator is used to create X-rays and, if they have sufficient energy (at least 1.66 MeV), the fifth neutron is separated from the nucleus of 4Be. These neutrons 4Be make a silver target radioactive. A sudden increase in the radioactivity of the silver sample provides the calibration point for the voltmeter at E = 1.66 MeV.

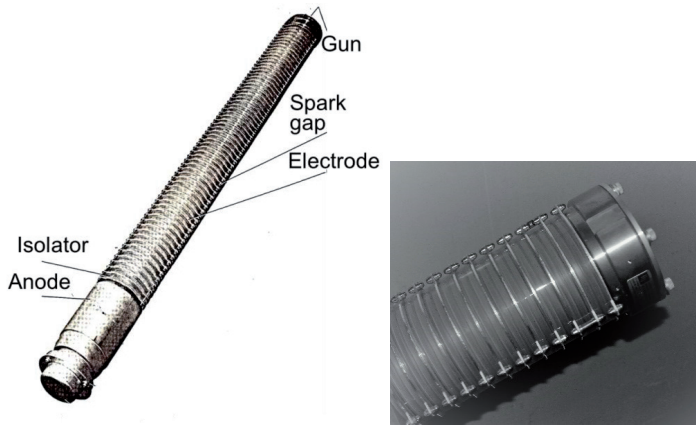


Fig. 2.22. Accelerating section

Accelerating section (Fig. 2.22) is composed of metal electrodes and glass insulators sealed together. The electron gun is located on top part and grounded anode on other side of accelerating section. The electron gun is composed of directly heated tungsten cathode supplied by emission control unit. Acceleration process takes place in high vacuum ($10^{-4}$ Pa). High vacuum installation includes pump, vacuum measuring gauge on vacuum valves. Grounded anode of accelerating section, with central hole, is connected to metal tube which evacuates the beam outside of pressure vessel. Replacement of old fashion diffusion vacuum pump on modern turbo-molecular pump has been done according to accelerator upgrading program.

The electron beam is transported into open air through thin titanium window. Figure 2.23 shows high voltage structure of the electrostatic accelerator with open pressure tank (open high pressure vessel and direct view of HV electrode). Figure 2.24 shows location of certain components inside the pressure vessel (belt charge power supply, belt engine, energy adjustment circuit).

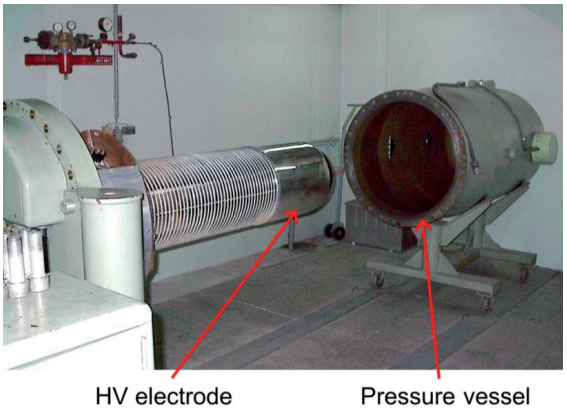


Fig. 2.23. High voltage structure with open pressure tank

Open pressure vessel is displayed in Fig. 2.25. A routine accelerator review should be performed in time interval according to national safety regulation. The following steps are recommended:

- opening the tank, the high-voltage head dismantle and the cathode system and cathode itself remove;
- review of accelerator elements (drive unit, accelerator tube, column elements);
- all elements should be cleaned and washed;
- emission tests should be carried out.

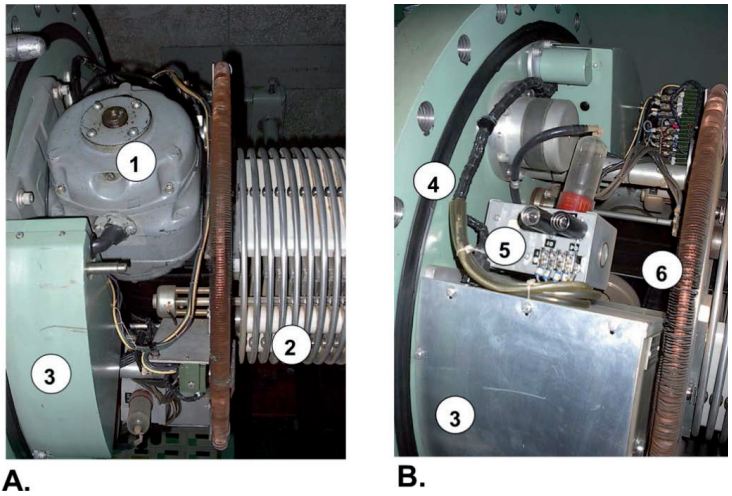


Fig. 2.24. Location of components inside the pressure vessel: 1 – engine, 2 – equipotential rings, 3 – belt charge power supply, 4 – rubber gasket, 5 – energy adjustment circuit, 6 – element of cooling system

After accelerator tank closing procedure a mixture of $CO_2$ and $N_2$ gases to a working pressure of 2.5 MPa should be pumped to pressure vessel. Required vacuum should be obtained ($10^{-4}$ Pa) in accelerating section using fore-vacuum and turbomolecular pumps (Fig. 2.26). Voltage conditioning the accelerator at high energies 1-1.7 MeV is required before starting regular work.

Fig. 2.25. View of the open pressure vessel

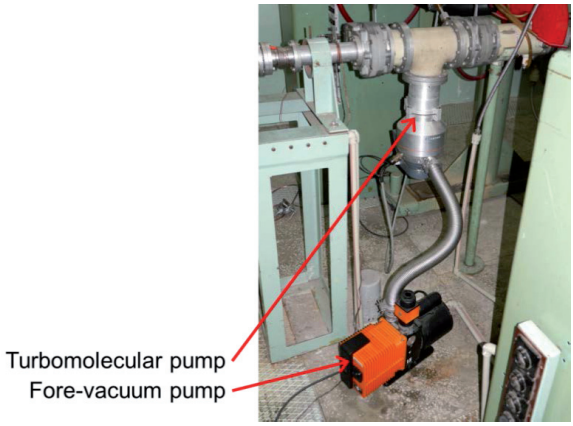


Fig. 2.26. Fore-vacuum and turbomolecular pump location

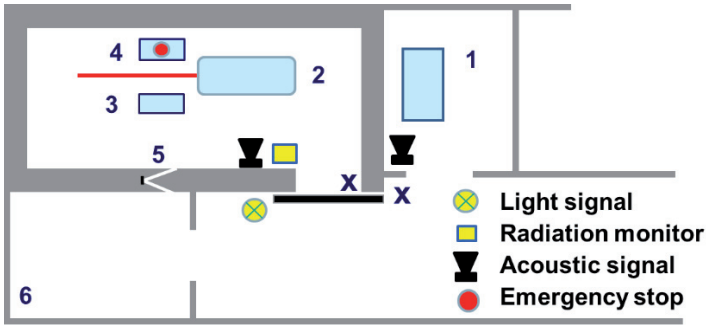


Fig. 2.27. Layout of AS-2000 electrostatic accelerator facility: 1 – control room, 2 – accelerator, 3 – cooling water panel, 4 – distribution panel, 5 – optical channel, 6 – experimental room, X – interlock system

During the review, the accelerator system must be inspected by the Office of Technical Inspection. A positive evaluation and admission to work of the accelerator system should be provided. Accelerator aging problems are mainly related to spare parts availability including vacuum tubes and belt.

The layout of AS-2000 accelerator compartments is shown in Fig. 2.27. This part of the building is an annex to the existing building of the Centre for Radiation Research and Technology of the INCT [8].

The basic physical program directed towards better understanding of the nature of radiation defects and their influence on macroscopic properties of semiconductors comprises knowledge of defects formation, their electronic structure and physical properties. The following experimental equipment has been used:

- high temperature target for study defect annealing phenomena against the ionizing radiation provided by electron beam,
- photo- and cathode-luminescence,
- deep level transient spectroscopy (DLTS) for characterization traps in semiconductors,
- variable temperature liquid nitrogen cryostat enabling conducting irradiations at temperatures from 110 K to 450 K.

A

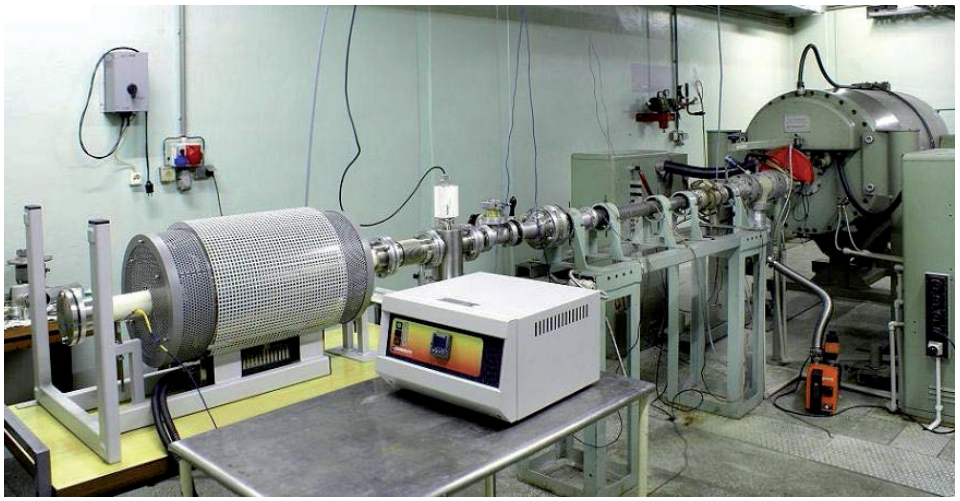

B

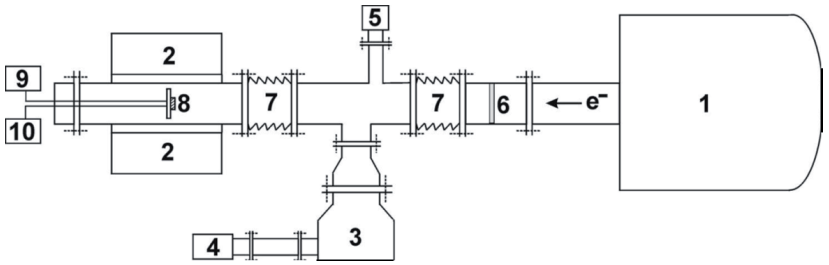


Fig. 2.28. (A) Stand with the AS-2000 accelerator for high temperature irradiation (resistance furnace Carbolite, 1700 K). (B) Block diagram: 1 – high pressure vessel of accelerator, 2 – high temperature oven, 3 – turbo-molecular vacuum pump, 4 – fore-vacuum pump, 5 – vacuum meter, 6 – Ti window, 7 – elastic joint, 8 – sample, 9 – thermocouple, 10 – beam current monitor

The accelerator is mainly used for the irradiation of crystalline semiconductor materials. Radiation defects in semiconductor crystals are characterized by a certain thermal stability, i.e. a temperature range in which they are subject to transformation or disappearance. These processes cause changes in physical properties related to the presence of defects and thus have great practical significance. Determination of thermal stability of defects is therefore an important element in the identification of defects. Such tests impose specific requirements on the measuring apparatus and, above all, on the sample irradiation process, which must be kept in a controlled temperature.

The accelerator installed at the INCT is equipped with, apart from the target for irradiation at room temperature, a stand for irradiation at elevated temperatures with the possibility of conducting the process in a vacuum or protective atmosphere. The stand, apart from the accelerator, consists of a heating device, a vacuum system and a power supply system enabling programing and control of the desired temperature waveforms. As a heating device, a vacuum resistance furnace with a maximum operating temperature of 1850 K is equipped with a programmable power supply. The furnace provides a constant temperature in the zone with a length of 180 mm and a diameter of 50 mm. The built-in system enables high temperature irradiations, i.e. at the maximum temperature of approximately 1700 K, and the management of annealing in this temperature (Fig. 2.28). The above equipment was built as part of the research project ordered PBZ-MEiN-6/2/2006 in cooperation with the Institute of Electronic Materials Technology, Warszawa, Poland. The accelerator is also equipped with a variable temperature liquid nitrogen cryostat enabling conducting irradiations at temperatures from 110 K to 450 K with the possibility of conducting measurements of electrical properties directly after irradiation without heating the sample to room temperature.

Electron irradiation of samples of laser materials was carried out for the Institute of Physics of the Polish Academy of Sciences, Warszawa, Poland. Results of the influence of ionizing radiation on these materials are included in the publications on optical observation of the recharging of crystals under radiation and thermal treatment [9, 10].

Quantitative measurements of hydrogen generated in the radiation/catalytic process using a Shimadzu GC-2010 chromatograph with a helium-ionization detector were performed.

$$Z_r + 2H_2O \rightarrow 2H_2 + Z_rO_2$$

Hydrogen emission rates are the following:

– 0.97 mol/cm$^2$ for temperature 600ºC,
– 4.1 mol/cm$^2$ for temperature 1000ºC.

## 2.3. $e^-$/X TEST FACILITIES

Installation of a target for conversion of accelerated electrons to X-rays extends technological abilities of electron accelerators due to better penetration of X photons inside the irradiated material.

A converter of electron beam to bremsstrahlung radiation with tantalum as target material has been built and tested. Figure 2.29 shows the overall view of electron beam–X-rays converter with tantalum plate – 0.5 mm, cooling water layer – 20 mm, and steel plate – 0.8 mm [11]. The results of the experimental work performed with the ILU 6 accelerator are shown in Table 2.6.

Another test concerned application of conversion target at Elektronika 10/10 and testing of a tantalum target with 5 MeV electron beam was performed. An operational test with high density food samples has proved the applicability of the target to food processing. Scheme of target is presented in Fig. 2.30. The average efficiency of conversion was 5.9% [12].

Fig. 2.29. Electron beam–X-rays converter (tantalum – 0.5 mm, $H_2O$ – 20 mm, steel – 0.8 mm)

Table 2.6. Basic data of X-ray tantalum target, tested at the ILU 6 electron accelerator

| Parameter | Value |
|---|---|
| Electron energy | 2 MeV |
| Average beam power | 20 kW |
| Photon transmission | 1.7% |
| $^{60}$Co source equivalent | 25 kCi |
| Mass throughput | 600 kGy kg/h |
| Unit cost of irradiation | 10 kGy kg/USD |

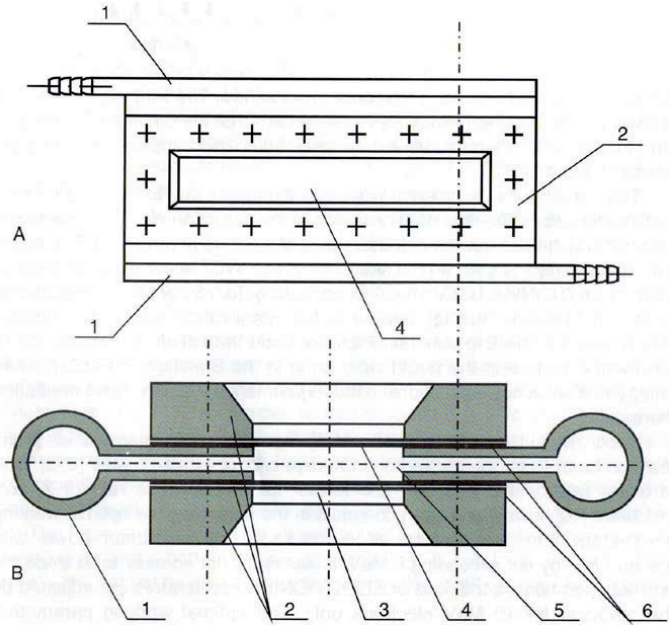


Fig. 2.30. Scheme of $e^-$/X target developed for food processing (1,3,5,6 – water cooling system; 2 – steel plate; 4 – tantalum plate) [12]

## References


[1]. Zimek, Z., Kołyga, S., Lewin, W., Nikołajew, W., Rumiancew, W., & Fomin, L. (1971). Linejnyj uskoritel' elektronov Instituta Jadernych Issledovanij (The linear accelerator of electrons of the Institute of Nuclear Research). *Nukleonika*, *XVII*, 1-2, 75-85.

[2]. Zagórski, Z.P., Grodkowski, J., Zimek, Z., & Roszczynko, W. (1975). *Stanowisko nr 1 dla radiolizy impulsowej przy akceleratorze liniowym elektronów LAE 13/9 Żerań* (Stand No 1 for pulse radiolysis at Linear electron accelerator LAE 13/9). Warszawa: Instytut Badań Jądrowych. Raport INR-1564/XVII/C/B.

[3]. Zimek, Z. (1990). A new electron linac for pulse radiolysis experiments at the Institute of Nuclear Chemistry and Technology, Poland. *Radiat. Phys. Chem.*, *36*, 2, 81-83.

[4]. Dźwigalski, Z., & Zimek, Z. (1997). The electron gun of LAE 10 linear electron accelerator. *Electron Technol.*, *30*, 4, 331-334.

[5]. Dźwigalski, Z.,& Zimek, Z. (2002). LAE 10 electron accelerator charge monitor. In *Proceedings of EPAC 2002, Paris, France* (pp. 1979-1881).

[6]. Sawicki, A., Orzechowski, T., Hentszel, A., Rzewuski, H., Werner, Z., & Merski K. (1967). Pulsed electron beam Van de Graaff accelerator. *Nukleonika*, *XII*, 441-450.

[7]. Rzewuski H., & Zięborak J. (1986). *Konsultacje i nadzór w trakcie budowy i wyposażenia komory akceleratora Van de Graffa*. Warszawa: Instytut Chemii i Techniki Jądrowej.. Opracowanie wewnętrzne nr 130/VII/86.

[8]. Zięborak, J., Warchoł, S., Rzewuski, H., & Krynicki, J. (1993). The mesurement system for radiation enhaced annealing experiments with a Van de Graaff electron accelerator. *Nukleonika*, *38*, 1, 5-22.

[9]. Zhydachevskii, Ya., Suchocki, A., Sugak, D., Luchechko, A., Berkowski, M., Warchol, S., & Jakieła, R. (2006). Optical observation of the recharging processes of manganese ions in $YAlO_3$:Mn crystals under radiation and thermal treatment. *J. Phys. Condens. Mat.*, *18*, 5389-5403.

[10]. Zhydachevskii, Ya., Durygin, A., Suchocki, A., Matkovskii, A., Sugak, D., Bilski, P., & Warchol, S. (2005). Mn-doped $YalO_3$ crystal: a new potential TLD phosphor. *Nucl. Instrum. Meth. Phys. Res. B*, *227*, 545-550.

[11]. Zimek, Z., Woźniak, A. (1995). *Konwerter wiązki elektronów* (X-ray converter). Polish Patent No. 168057.

[12]. Migdal, W., Malec-Czechowska, K., & Owczarczyk, B. (1996). Study on application of e/X conversion for radiation processing. *Nukleonika*, *41*, 3, 57-66.

Chapter 3

# ELECTRON ACCELERATOR PLANTS CONSTRUCTED AND OPERATED BY THE INCT

**Zbigniew Zimek, Andrzej Rafalski, Wojciech Migdał, Urszula Gryczka**

## 3.1. ELECTRON ACCELERATOR CONSTRUCTED BY THE INCT

The main reason for undertaking work on the construction of the LAE 10/15 accelerator at the Insitute of Nuclear Chemistry and Technology (INCT) was the need to maintain the continuity of the Radiation Sterilization Station activity. The Station operates a linear electron accelerator type Elektronika 10/10 of Russian production, providing the process of radiation sterilization on a mass scale [1]. Lack of the possibility of regular supplying of spare parts of Russian production created problem in maintaining the continuity of the work of this accelerator. Higher technical and economical effectiveness and better operational characteristics suitable for radiation processing were also included to assumptions of new accelerator construction. Accelerator LAE 10/15 is equipped with an accelerating section of standing wave type, supplied by klystron as a source of microwave energy [2-4]. The block diagram of this device is shown in Fig. 3.1.

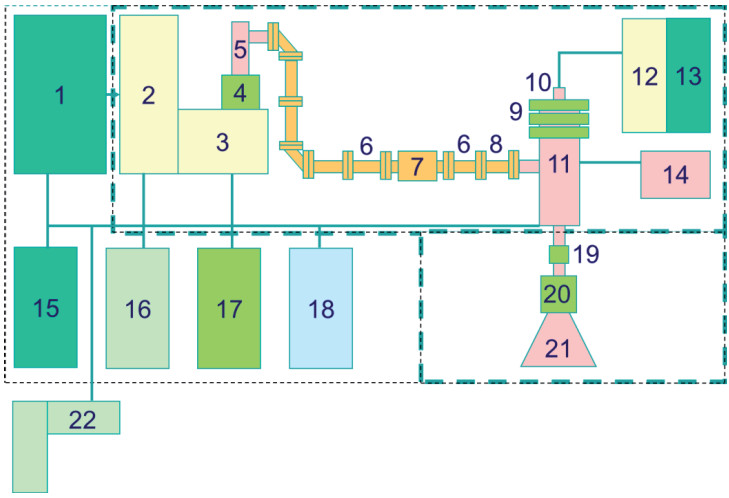


Fig. 3.1. Block diagram of an electron accelerator LAE 10/15: 1 – power supply 13 kV, 2 – modulator, 3 – pulse transformer 135 kV, 4 – focusing coil, 5 – klystron, 6 – coupler, 7 – circulator, 8 – HF window, 9 – focusing coil, 10 – electron gun, 11 – accelerating section, 12 – modulator 15 kV, 13 – HV power supply, 14 – fore-vacuum pump, 15 – AC distribution panel, 16 – microprocessor, 17 – auxiliary equipment, 18 – water cooling system, 19 – collimator, 20 – electromagnet, 21 – scanner, 22 – control desk

The AC power line supply of the Radiation Sterilization Station was made according to the design of the Bureau of Studies and Designs of Nuclear Techniques PROATOM "PT electrical installations – technological power" and supplemented in accordance with the as-built documentation presented in the project "PT electrical installations – main switching low voltage station". The project includes: power supply installations, control installations, interlocks and

signaling devices, work and protective grounding, lightning protection installation. Protection against electric shock provides zeroing for low voltage circuits, and grounding for accelerator devices. A part of the control circuits is based on a 24 V installation. The AC power line 220/380 V of LAE 10/15 accelerator provides electrical energy for the following circuits:

- high voltage power supply: 3 × 380 V, 50 kW;
- auxiliary equipment and control systems: 220/380 V, 35 kW;
- stabilized network for selected units: 220 V, 5 kW.

The total power consumption of the devices included in the LAE 10/15 accelerator is ~90 kW with the overall accelerator electrical efficiency 15%.

LAE 10/15 accelerator water cooling system consists of three close loop subsystems [5], as can be seen in Fig. 3.2. Outside cooling loop filled up with ordinary water consists of fan cooler, compensation vessel, heat exchanger and two water pumps. Fan cooler is located on the roof of the accelerator building.

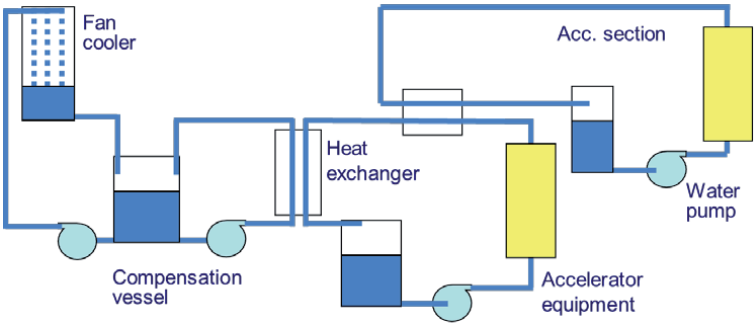


Fig. 3.2. LAE 10/15 accelerator water cooling systems

The inside secondary cooling loop consists of heat exchanger, compensation vessel and all accelerator equipment required to be cooled down. Figure 3.3 shows part of the secondary water cooling system with water flow meters and cupper tubes for water distribution between certain accelerator components.

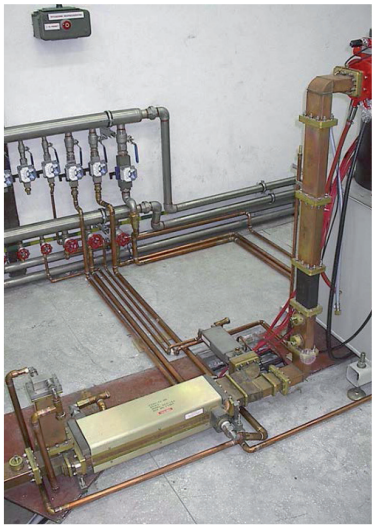

Fig. 3.3. Part of the secondary water cooling system with water flow meters and cupper tubes for water distribution between accelerator components

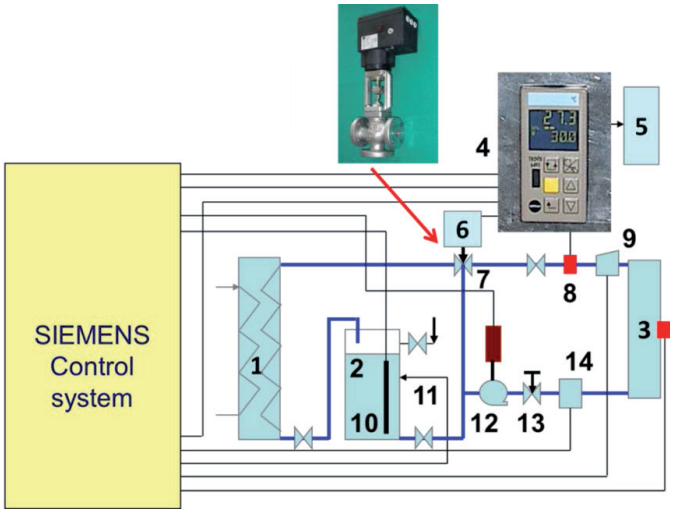


Fig. 3.4. The configuration of water loop with temperature stabilization: 1 – heat exchanger, 2 – compensation vessel, 3 – accelerating section, 4 – microprocessor, 5 – control signal, 6 – driver, 7 – three-fold valve, 8 – temperature sensor, 9 – flow rate sensor, 10 – heater, 11 – level sensor, 12 – water pump, 13 – valve, 14 – pressure sensor

The third loop system is filled up with distillated water, and consists of heat exchanger, compensation vessel, water pump and accelerating section. The primary task of that system is stabilization of the accelerator section temperature on certain level. It can be obtained by the application of three-way valve operated by dedicated microprocessor. The configuration of water loop with temperature stabilization is shown in Fig. 3.4.

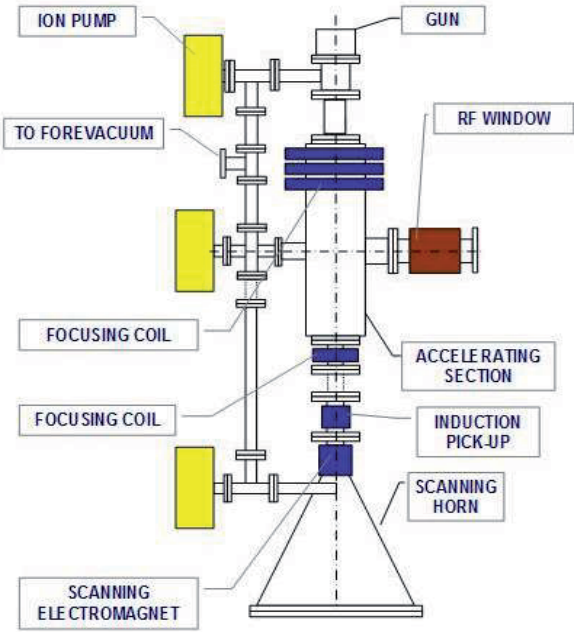


Fig. 3.5. The block diagram of accelerator LAE 10/10 vacuum system

The accelerator LAE 10/10 vacuum system consists of three ion vacuum pump type HMDI-0,063 (pumping velocity: 60 l/s) with power supply (Fig. 3.5). Turbomolecular pump is used to start ion pumps at certain vacuum level. The main characteristics of vacuum system operation are shown in Fig. 3.6.

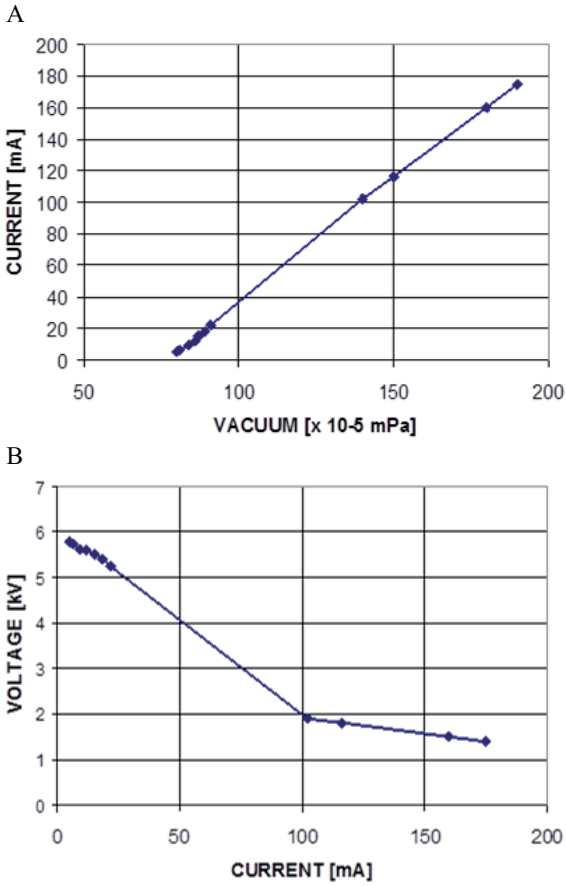


Fig. 3.6. Operational characteristics of accelerator vacuum system: A – power supply current vs. vacuum level, B – power supply voltage vs. loading current

Accelerator section is the important part of any accelerator. Two basic types of accelerating section construction were taken into account: traveling wave and standing wave mode of operation. The basic features each of them are given in Table 3.1.

Table 3.1. The basic features of accelerating section with traveling wave and standing wave mode of operation

| Traveling wave structure | Standing wave structure |
|---|---|
| Frequency: ≈3 GHz | Frequency: 100 MHz-3 GHz |
| Pulsed: up to 20 μs | Continuous operation possible |
| Gradient: 10-50 MV/m. | Gradients: 10 MV/m |
| | Linear and circular accelerators |

The principle of accelerating section with standing wave mode is presented in Fig. 3.7. The phase distribution of electrical field along accelerating section is constant, whereas amplitude of electrical field is being changed in certain part of the section. The electron bunches are being formed at the beginning of accelerating section and traveling along the axis. The same time their energy is increased.

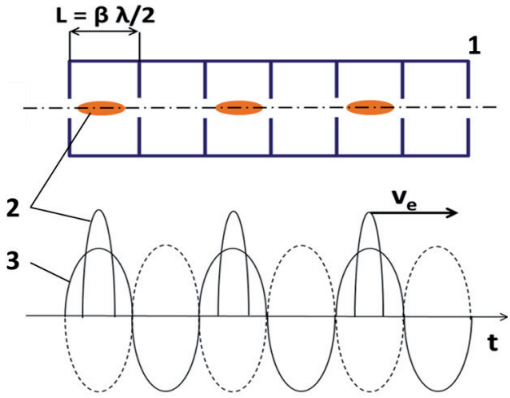


Fig. 3.7. Principle of accelerating section with standing wave mode: 1 – accelerating structure, 2 – bunches of accelerated electrons, 3 – distribution of electrical field along accelerating section axis

Accelerating section of LAE 10/15 accelerator (Fig. 3.8) was designed and built at the D.V. Efremov Institute of Electrophysical Apparatus, Saint Petersburg, Russia. This section enables the acceleration of electrons to 10 MeV at a beam average power of 10-15 kW [6]. The electrical field distribution along accelerating section axis (A) and electron energy spectrum (B) are shown in Fig. 3.9. The electron accelerating section is powered by micro-wave energy at 2856 MHz coming from the microwave energy source included in the accelerator installation (klystron TH-2158). The technical characteristics of the acceleration section are the following:

- electron energy: 10 MeV,
- energy distribution: ±2%,
- electron beam power (average): 10-15 kW,
- microwave energy in impulse: 5 MW,
- operating frequency: 2856 MHz,
- beam diameter at half height: 1.2 mm.

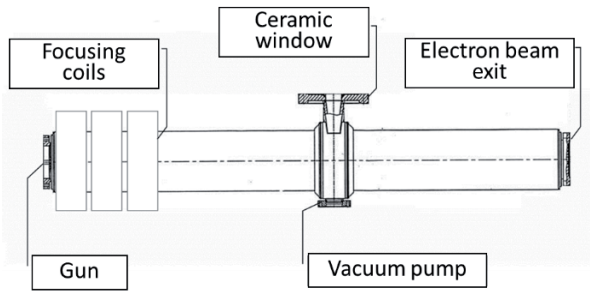


Fig. 3.8. Accelerating section with standing wave equipped with vacuum flange connections for connecting: electron gun, RF window, vacuum pump and electron beam scanning system

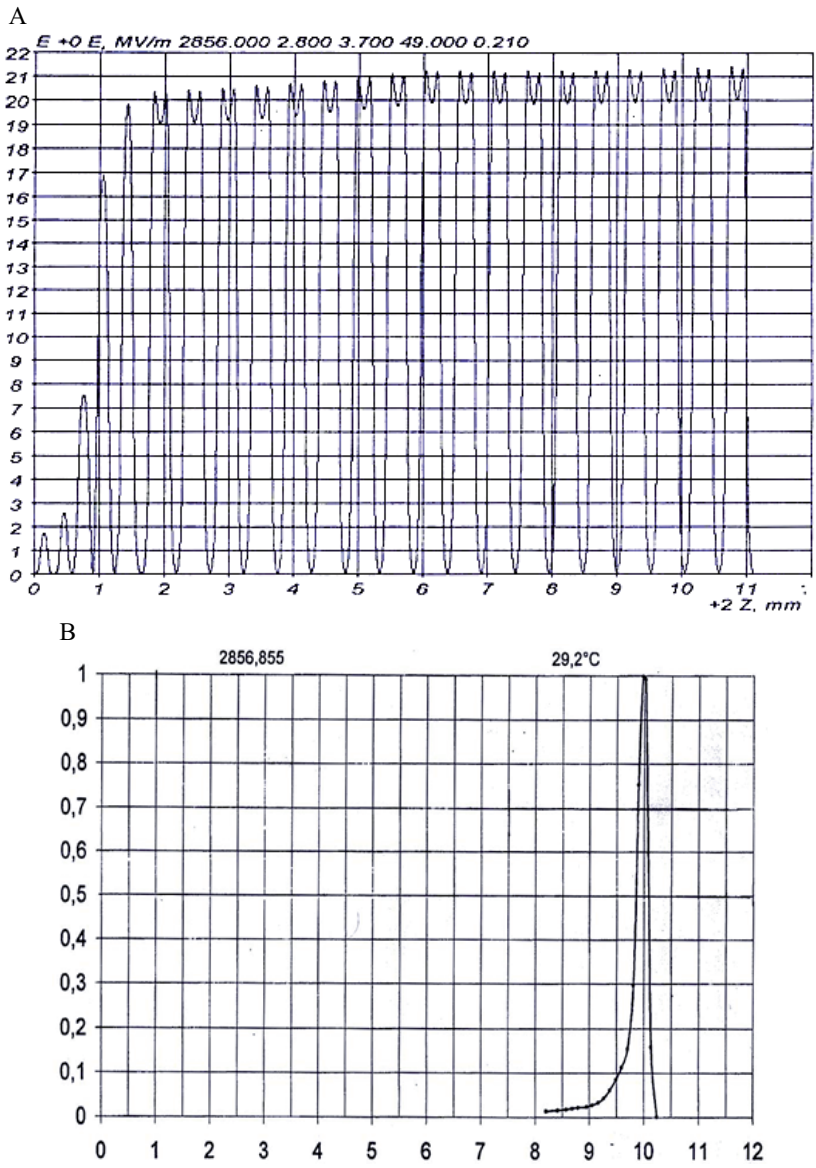


Fig. 3.9. Performances of accelerating section: A – electrical field distribution along accelerating section axis, B – electron energy spectrum ±1.5%

The electron gun parameters (pulse current, voltage) should be compatible with electrical specification of the accelerating structure. The triode electron gun with spherical impregnated cathode (manufacturer: NPO Toriy, Russia) is used as a source of electrons in accelerator LAE 10/15. Electron gun as can be seen in Fig. 3.10 meets requirements of standing wave structure applied in accelerator and provides desirable parameters of the electron beam which are presented in Table 3.2. The following computer gun optimization was performed to meet requirements of standing wave structure applied in accelerator: distance between cathode and grid, distance between grid and anode, beam focusing to obtain proper beam dimensions.

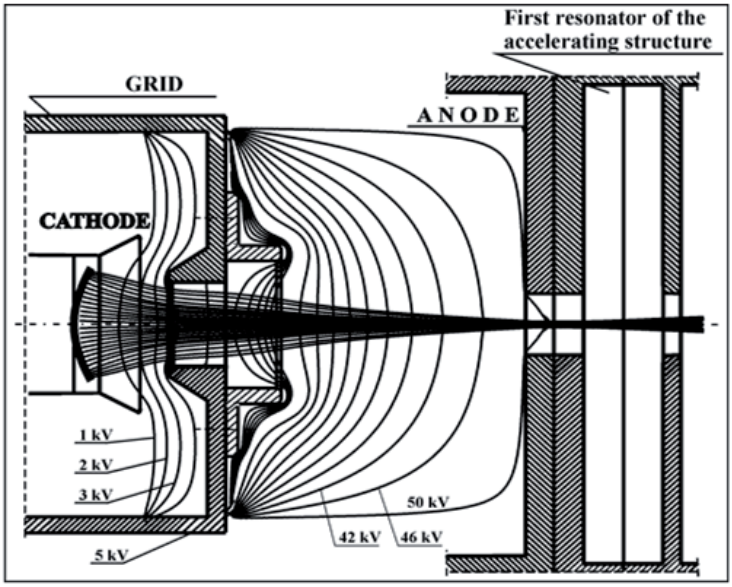


Fig. 3.10. Electron gun with voltage equipotential lines and electron trajectories

Table 3.2. Electron beam parameters provided by electron gun

| Accelerating section | Electron beam parameters | | | |
|---|---|---|---|---|
| | Energy [keV] | Diameter [mm] | Pick current [A] | Pulse [μs] |
| Standing wave accelerating structure operated at a frequency 2856 MHz | 50 | 2.5-3 | ~0.3 | 20 |

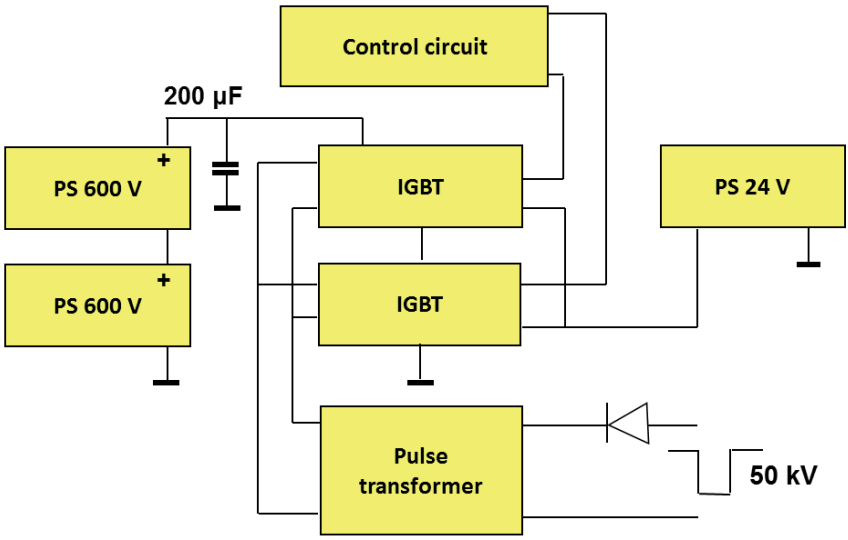


Fig. 3.11. Block diagram of electron gun modulator unit

Table 3.3. Selected technical parameters of TH-2158 klystron No. 158011

| Parameter | Value |
|---|---|
| Heater voltage | 9 V |
| Heater current | 31.1 A |
| Heater power | 280 W |
| Pulse duration | 27.7 μs |
| Anode voltage amplitude | 126 kV |
| Pulse RF inlet power | 64 W |
| Current of focusing coils No. 1, No. 2, No. 3 | 26.7, 30, 30 A |
| Ion pump current | < 1 μA |
| Ion pump voltage | 5 ± 0.5 kV |
| Water pressure drop in klystron body and ceramic window: 8 $dm^3$/min | 2.5 |
| Water pressure drop in klystron collector: 120 $dm^3$/min | 1 |

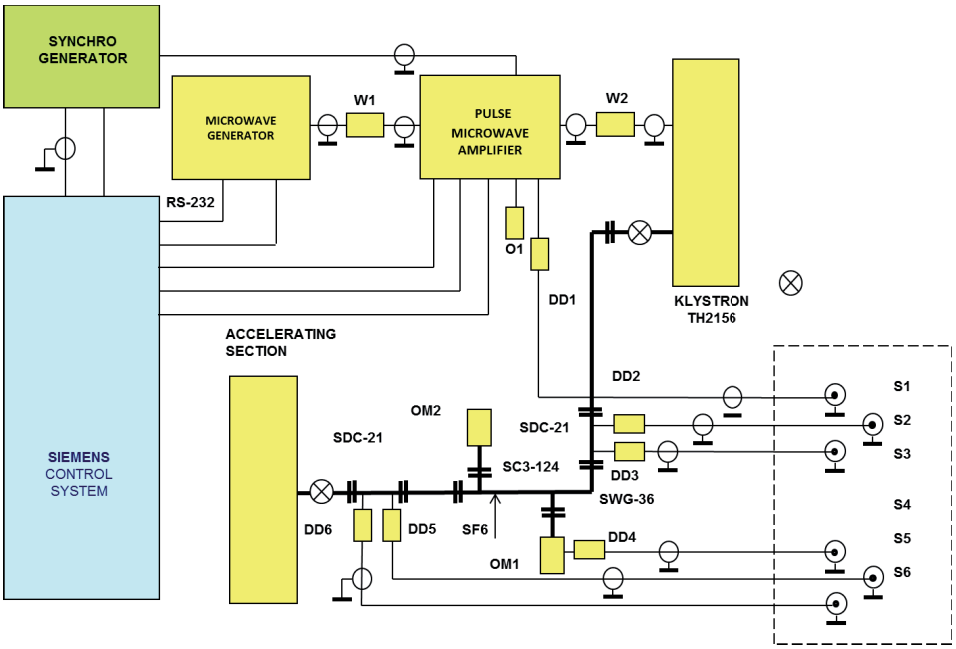


Fig. 3.12. The block diagram of accelerator LAE 10/10 microwave system: O1 – 50 Ω load, OM1-OM2 – microwave load, DD1-DD6 – diode, SDC-21 – directional coupler, SWG-36 – E plane bend, SC3-124 – isolator, S1-S6 – measured signals, RS-232 – data transfer, W1-W2 – low power isolator, SF6 – gas insulation

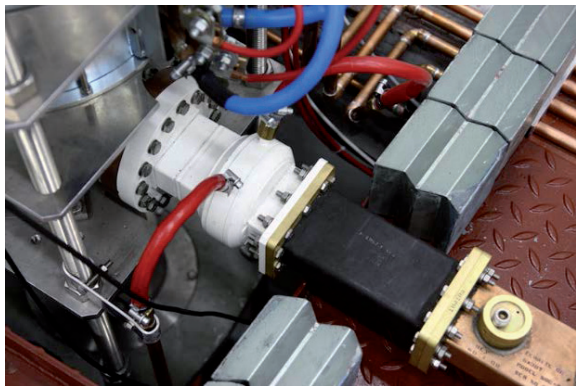

Fig. 3.13. Ceramic RF window at the entrance of accelerating section

Table 3.4. Selected parameters of semiconductor switch type HTS 181-160 FI

| Parameter | Value |
|---|---|
| Break down voltage | 18 kV |
| Maximum reverse voltage | 540 V |
| Input pulse amplitude | 5 V |
| Maximum pulse current | 1600 A |
| Maximum repetition rate | 500 Hz |
| Delay switching time | ~130 ns |
| Typical rise time | 80 (0.1 $I_{ampl}$) ns<br>180 (1 $I_{ampl}$) ns |
| Typical drop time | ~1 μs |

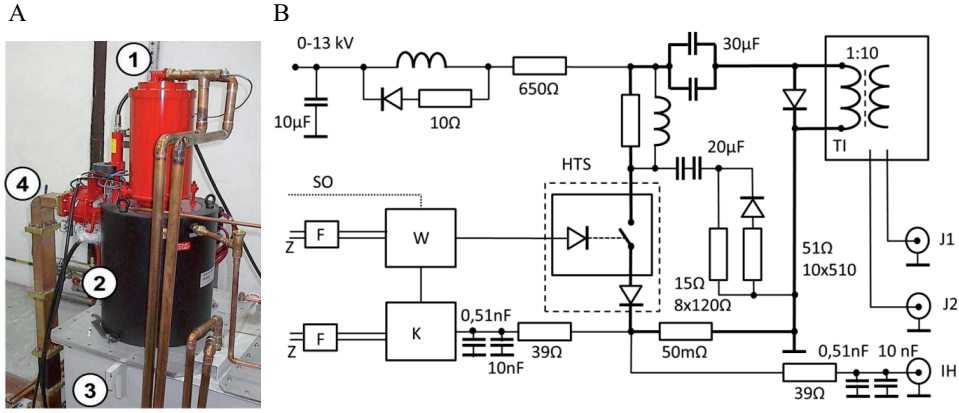


Fig. 3.14. Klystron modulator: A – klystron stand (1 – klystron TH-2158, 2 – focusing coil, 3 – HV pulse transformer, 4 – waveguide), B – modulator principal diagram

The electron gun modulator unit which block diagram is presented in Fig. 3.11 provides pulses with amplitude 50 kV and duration up to 20 μs. The modulator can be operated with the following parameters: frequency – 330 Hz, average current – 2 mA, maximum pulse current – 1.3 A.

The TH-2158 klystron was applied as a powerful source of microwave energy in the construction of LAE 10/15 accelerators. According technical specification its guaranteed lifetime amounts 4000 h. The actual lifetime of this device even comes to 10 000 h. The use of klystron as a microwave energy source provides the possibility of obtaining stable conditions for the sterilization process. In addition, it will allow to extend the life of the high frequency energy source several times, which in turn will reduce the operating costs of the installation. After reaching the nominal parameters of the electron beam (energy: 10 MeV, beam power: 10-15 kW), accelerator LAE 10/15 will provide the desired quality of radiation treatment and will achieve failure-free operation at the level necessary to perform services for the needs of health care. Table 3.3 contains the more specific parameters TH-2158 with manufacturer serial number 158011.

The main microwave system of the accelerator is composed of klystron TH-2158, waveguides and accelerator section in addition to microwave generator and pulse amplifier which are used to provide necessary microwave signal on klystron input [7]. Pulse microwave amplifier type AM82-2,85S-43-53R provides microwave signal with frequency 2856 MHz ±10 MHz, output pulse power 53 dBm, amplification factor 43 dBm. The block diagram of accelerator LAE 10/10 microwave system is shown in Fig. 3.12. Ceramic RF window at the entrance of accelerating section is displayed in Fig. 3.13.

High voltage, pulse modulator was designed and constructed to provide pulses with amplitude up to 135 kV, duration 20 μs and repetition rate up to 330 Hz. The partly discharged capacitor bank is applied and semiconductor switch is used to form certain pulse time structure. The klystron TH-2158 (modulator load device) is supplied by HV pulse through pulse transformer. Klystron modulator is based on semiconductor switch HTS 181-160 FI (acceptable current load 1600 A, with voltage up to 18 kV – Table 3.4). The modulator is equipped with safety shutdown circuit for protection against current overload which may appear. The klystron and principal diagram of modulator are presented in Fig. 3.14.

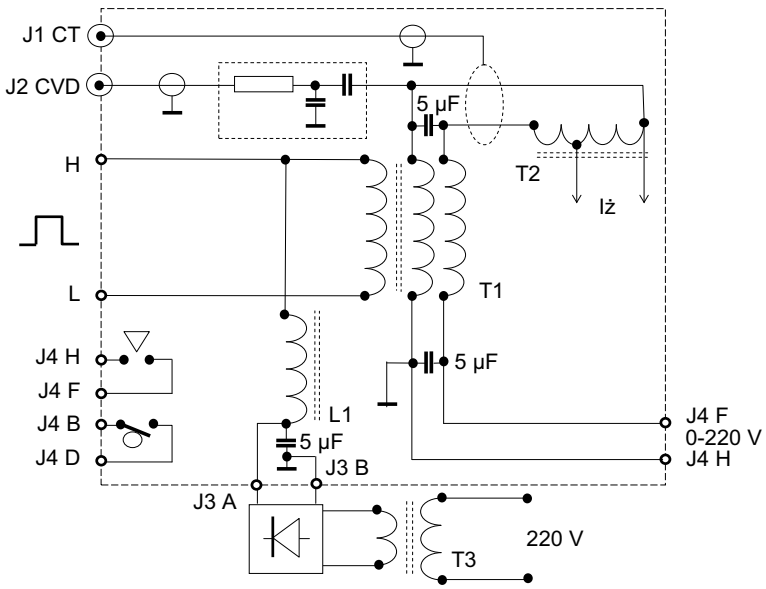


Fig. 3.15. Electrical circuit of klystron TH-2158 pulse transformer

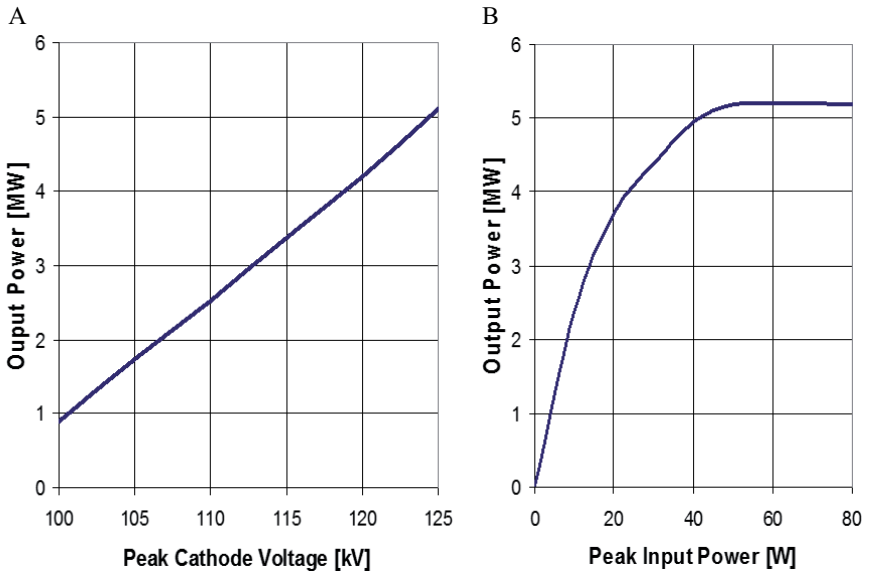


Fig. 3.16. Loading characteristics of TH-2158 klystron: A – output pulse power vs. peak cathode voltage, B – output pulse power vs. peak input power

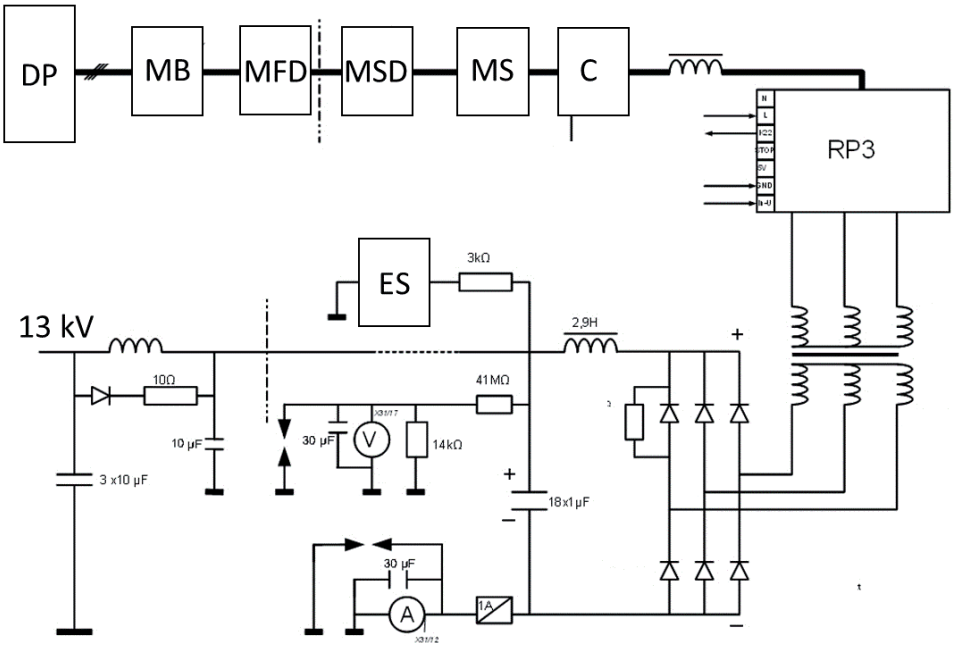


Fig. 3.17. Klystron modulator DC power supply electrical circuit: DP – low voltage distributive panel, MB – manual breaker, MFD – manual fuse disconnector, MSD – manual safety disconnector, MS – manual switch, C – contactor, RP3 – thyristor voltage regulator, ES – grounding switch

Figure 3.15 shows electrical circuit of pulse transformer unit. Transformer step up ratio amounts 1:10. Calibrated measuring loops for pulse current J1 and pulse voltage are installed. Electrical contacts are installed to indicate high or low oil level. Figure 3.16 shows relation between output pulse power and cathode voltage (A), and peak input power (B).

The largest receiver of AC electric energy built as a part of the LAE 10/15 accelerator is the modulator of the TH-2158 klystron. The direct receiver of electricity from the AC power line station is a high voltage power supply (Fig. 3.17). The HV power supply is supplied from a four-wire network (three phases and a neutral) 3 × 380/220 V ±5%, 50 Hz. The modulator system is supplied with a constant DC voltage of maximum 13 kV. The required average power supply of the klystron modulator is 50 kW.

An important task of the RP3 thyristor controller is the ability to smoothly adjust the voltage amplitude as a function of a continuous signal. The intended effect is achieved when the phase angle of switching the receiver current is controlled by an analog signal from microprocessor control system. The voltage control system of the HV power supply is connected to the microprocessor system responsible for the operation of the entire accelerator. One of many functions of this system is the high voltage regulation realized with the use of a touch panel. Other tasks include switching the power supply unit on and off, controlling and stabilizing the voltage level, supervising the fulfillment of specific health and safety requirements (e.g. door switches) and automatic reaction to emergency situations.

The HV power supply is equipped with a grounding bar, dielectric mats and a switch grounding the capacitor banks when the power supply is turned off. In the upper part of the power supply casing, a button that indicates the opening of the door is located. The power supply housing has been connected to a safety ground. Inspection and repair work may only be carried out after disconnecting the power line. It is forbidden to work with open doors of individual panels as well as with faulty blocking and grounding circuits. After switching off the power supply and opening the door, the capacitors in the HV filter should be grounded using the rod. Pressing any of the emergency buttons (including the HV power supply button) immediately disables individual devices included in the accelerator and transporter. Similarly, the opening of doors equipped with interlocks while working with the electron beam causes the accelerator and transporter to be switched off immediately. An exit control button was installed at the accelerator chamber to provide information that all persons should left the room. After starting the button, the acoustic signal is automatically turned on for the duration of the procedure of closing the rooms.

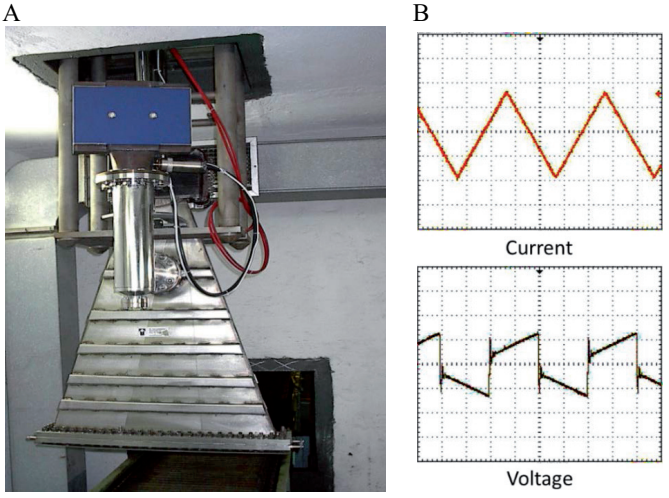


Fig. 3.18. Accelerator LAE 10/15 output beam scanning device: A – scanning chamber with exit foil, B – shape of the scanning current and voltage

In addition to the functions connected with the work of the LAE 10/15 accelerator, the high voltage power supply has local protections resulting in the disconnection of this device from the power supply network. These include protection of the thyristor controller, fan operation, position of the jumper, position of the contacts of the manual switch, protection against smoke, door locks. The normal operation of the fans is indicated by the "ventilation" lamp. The power supply is equipped with safeguards to protect personnel against electric shock. Power supply cabinets are earthed at the point marked with the mass symbol. On the door and side shields, symbols indicating high voltage are painted. The filter capacitors are automatically grounded through the appropriate contacts of the safety switch, which is equipped with contacts with a visible gap.

Accelerator LAE 10/15 output device consists of output scanner chamber with titanium foil 50 μm thick, vacuum pump and scanning electromagnet (Fig. 3.18).

Accelerator control system is located in control panel unit (Fig. 3.19). It is equipped with Siemens microprocessors and modules type Simatic S7-300, with communication channel Profibus and SCADA (supervisory control and data acquisition) tool WinCC. The structure of control system consists of PS – power supply, CPU – microprocessor, IM – interface module, SM – analog and digital input/output modules, FM – functional counter module, ET 200 S – extension unit to RS232 interfaces, MP 370 – touch panel.

Fig. 3.19. Control panel with fuse and breaker unit, connection unit, and microprocessor and interface module units

Control system is responsible of switching on and off all independent units, safety interlock, starting up and down procedures, automatic measurements. The touch panel screens are shown in Fig. 3.20 as examples of switching on and off procedures, and control klystron HV modulator with safety interlock announcement controlled by microprocessor.

Nominal parameters of linear accelerator LAE 10/10 constructed at the INCT are as follows: electron energy – 10 MeV, beam power – 10-15 kW (Table 3.5). Advantages of the developed accelerator over the accelerator already installed at the Institute facility are related to: more stable accelerator exploitation, lower exploitation costs, higher accelerator availability obtained with moderate cost. Accelerator is equipped with standing wave accelerating section (NIIEFA, Russia), and supplied by klystron TH-2158 (Thales, France). Basic components of microwave route in addition to accelerating section and klystron are continuous wave microwave generator, microwave pulse amplifier and microwave waveguide. The range of work was performed during starting up of accelerator LAE 10/15 and testing, measurements and calibrations as the part of initiated accelerator commissioning procedure.

A

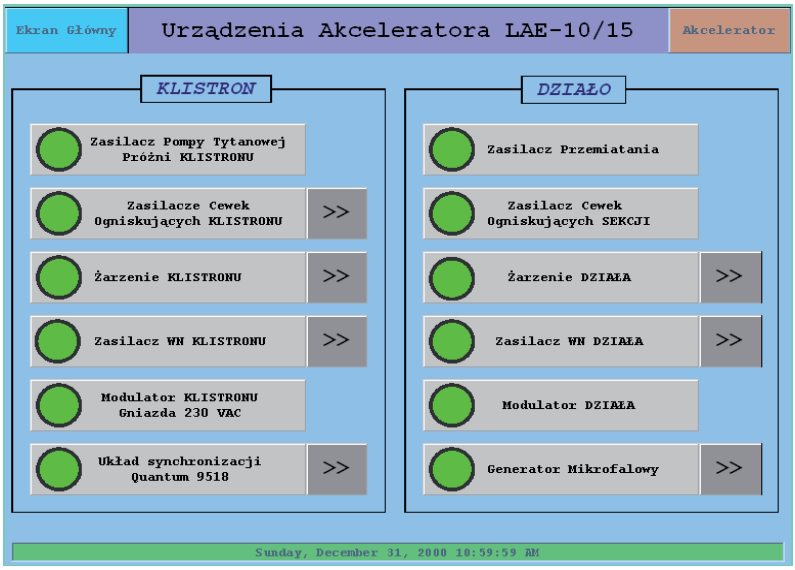


B

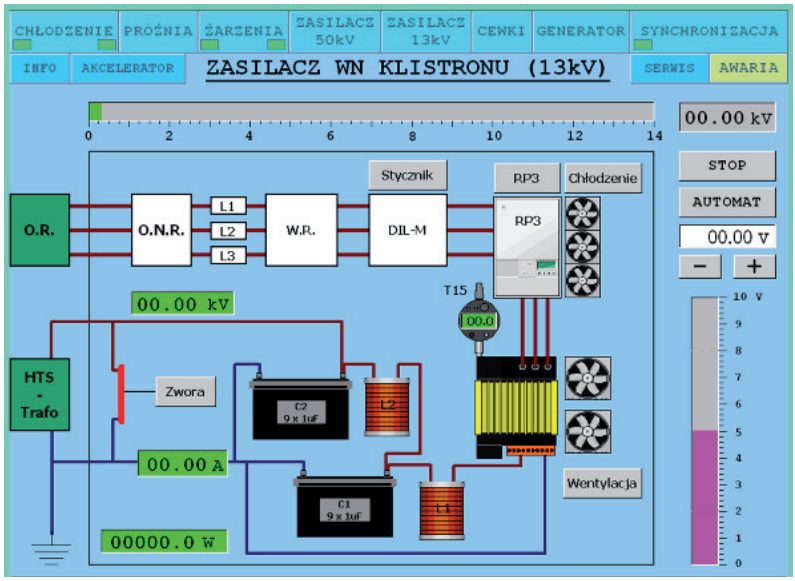


Fig. 3.20. Touch panel screens: A – switching on and off certain accelerator apparatus, B – control of safety and operation parameters of HV klystron modulator power supply

All accelerator components and installations were tested at the final stage: water cooling system, vacuum system, electron gun and gun modulator, microwave system of accelerator including pulse power supply, klystron modulator designed on the basis of high power semi-conductor HV transistor, beam scanning system and control system, and PLC control system. Electron beam alignment, beam parameters evaluation and accelerator commissioning are being performed during commissioning stage. Figure 3.21 shows pulse shape of the klystron voltage from the J2 probe and the klystron pulse current from the J1 probe (see Fig. 3.15).

Table. 3.5. Nominal parameters of linear accelerator LAE 10/10

| Nominal parameter | Value |
|---|---|
| Electron energy (nominal) | 10 MeV |
| Average beam power | 10 kW |
| Pulse beam current (nominal) | 0.3 A |
| Pulse current change | 0.2-0.5 A |
| Pulse duration (nominal) | 20 μs |
| Pulse duration change | 2-20 μs |
| Repetition frequency (max.) | 330 Hz |
| Repetition frequency change | 10-330 Hz |
| Average beam current (nominal) | 1.0-1.3 mA |
| Average beam current change | 0.05-1.3 mA |
| Scan width (nominal) | 60 cm |
| Scan frequency | 5-15 Hz |
| Scan width change | 20-60 cm |

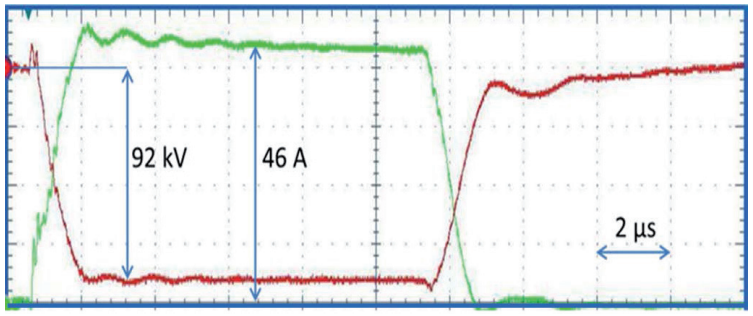


Fig. 3.21. The course of the voltage pulse on the klystron from the J2 probe and the klystron current pulse from the J1 probe (see Fig. 3.15). Time scale: 2 μs/div

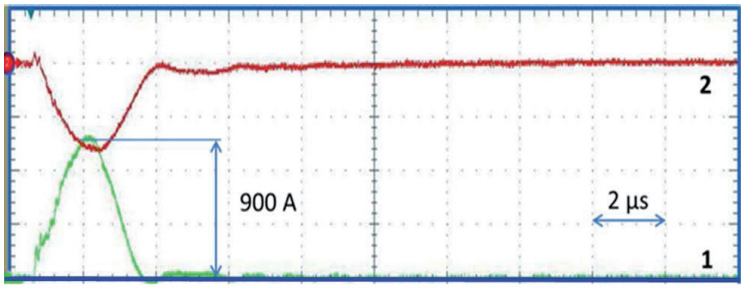


Fig. 3.22. Oscillograms of the protection test of safety shutdown over maximum load current level: 1 – HV pulse on klystron, 2 – klystron load current

The protection circuit was tested to avoid overload semiconductor switch during breakdown in klystron. The load current threshold level was established on 900 A. When load current has higher level, the semiconductor switch is turned down and voltage level goes to zero (Fig. 3.22).

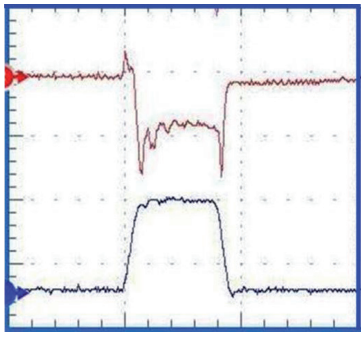

Fig. 3.23. Microwave pulse shape in the presence of beam current: envelope of the microwave pulse (upper waveform) and the shape of the klystron load current pulse (bottom waveform)

Figure 3.23 shows the registered pulse waveforms in the presence of beam current. The envelope of the microwave pulse (upper waveform) shows a characteristic shape, observed at the exit of the accelerating section indicating the absorption of microwave energy in the process of accelerating electrons. It can also be seen on Fig. 3.24. Visible at the bottom of the screen, the shape of the klystron load current pulse is regular, due to the circulator installed; the loading conditions of accelerating section are not influenced by electron beam presence.

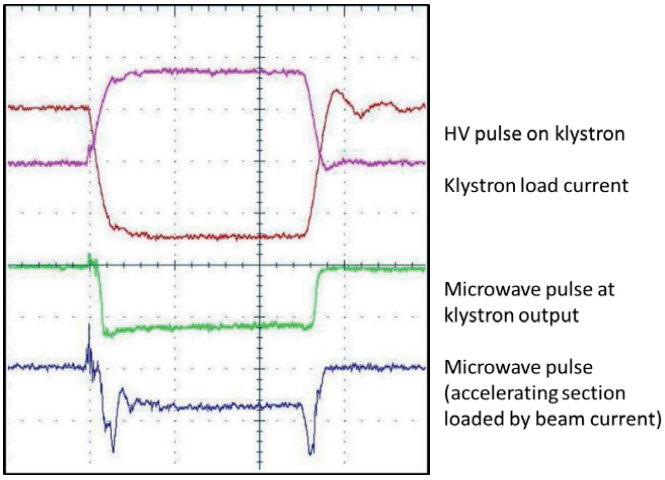


Fig. 3.24. Time relation between HV pulse on klystron, klystron load current, microwave pulse at klystron output, microwave pulse when accelerating section is loaded by beam current

Results of the preliminary beam current measurements are presented in Fig. 3.25. Electron beam alignment, beam parameters evaluation and accelerator commissioning are in the final stage of the project. The objective of the project partly supported by the IAEA was construction 10 MeV, 15 kW linear electron accelerator equipped with the microwave source based on modern klystron device operated at frequency 2856 MHz and standing wave accelerating section. The klystron modulator was designed with high power semiconductor

HV transistor as the switch. Microwave accelerators are more costly to operate due to their more complex construction and expensive spare parts such as magnetrons which are characterized by relatively short living time. The only way to lower the irradiation cost is intensive facility utilization. On the other hand, higher accelerator reliability is especially important for intense accelerator exploitation when share of maintenance and spare parts cost in exploitation cost grows significantly. Spare parts availability becomes another major problem to achieve continuous services required by facility customers.

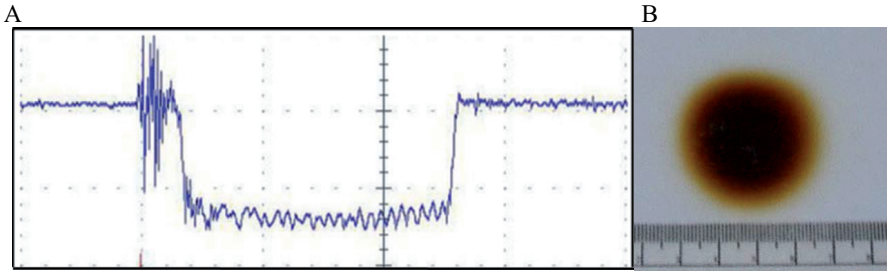


Fig. 3.25. Beam current measurements: A – shape of the pulse measured on the beam exit by Faraday cup, B – beam spot size at conveyor surface recorded by dosimetric foil

The better accelerator availability, more stable beam parameters, better spare parts availability, reduced exploitation costs and higher beam power are expected after successful project realization. Implementation of the project will provide opportunity to develop skills and knowledge of the personnel engaged. It will make also possible to transfer the results to another facilities in Poland and abroad.

## 3.2. POLYMER PROCESSING FACILITY

Accelerator ILU 6 was installed at the Department of Radiation Chemistry and Technology (currently Center for Radiation Research and Technology) of the INCT in 1988. The accelerator was purchased from the Budker Institute of Nuclear Physics, Novosibirsk, Russia, with a financial support of the IAEA under Technical Assistance Program. On the basis of the

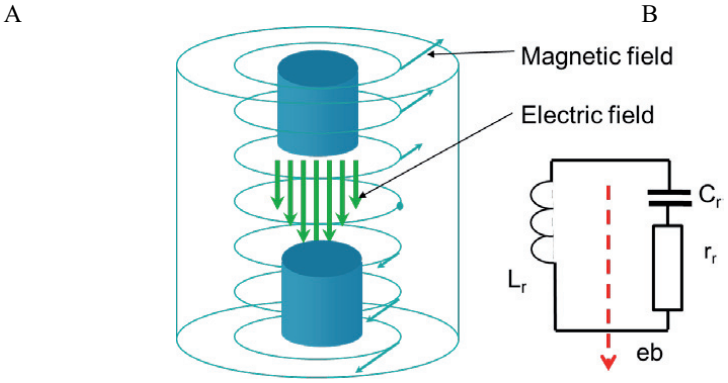


Fig. 3.26. The principle of ILU 6 accelerator operation: A – electric and magnetic distribution inside of resonator, B – equivalent resonator electric circuit ($L_r$ – resonator inductance, $C_r$ – resonator capacitance, $r_r$ – resistance (equivalent of thermal losses in resonator))

ILU 6 accelerator a pilot radiation installation was designed for the radiation processing of polymers, investigating the processes of removing impurities from the liquid and gas phase and research covering a range of other radiation technologies. ILU 6 type accelerators (nominal electron: 2 MeV, nominal beam power: 20 kW) are manufactured mainly for application in industry.

Accelerating process in ILU 6 accelerator takes place in a single concentric resonator which is operated with a standing wave mode. The principle of operation is shown in Fig. 3.26, where distribution of electromagnetic wave is presented. The electric component of electromagnetic way is used to accelerate electrons (A). Figure 3.26B shows equivalent electric circuit loaded by electron beam.

Single cavity, high frequency, pulsed accelerator was equipped with self-excited generator (working frequency: 127 MHz). Instead of expensive microwave energy sources (klystrons, magnetrons), relatively cheap generators with high power vacuum tubes are used in ILU 6 accelerator, which ensures relatively low operating costs of this device. The linear scanning (window dimension: 75 mm × 980 mm) and quasi-ring scanning (three windows 50 mm × 220 mm) can be applied to extract electron beam into open air. The electrical efficiency of the accelerator is 27%. Figure 3.27 illustrates the general idea of ILU 6 accelerator construction which is composed as the pulse linear accelerator. The basic parameters of the accelerator are shown in Table 3.6. The main accelerator parameters can be changed in a wide range.

Figure 3.28 shows cross-section of the resonator of ILU 6 accelerator. External envelope made of stainless steel forms vacuum housing (1) for resonator, the main component of accelerating system (2). The concentric cavity is made as two isolated halves, partly entering each other. The side surface of resonator forms a coaxial capacitor which shorts out the cavity RF current. The lower part of the cavity is isolated and connected by the choke (3) to DC power supply for suppressing the multipack discharge and prevent the ion leakage from the accelerating gap. Four ion vacuum pumps (4, 13) are used to keep suitable vacuum level. Electron gun (5) with cathode made of $LaB_6$ is located on the top halve of resonator where electric field is concentrated. The accelerating gap is formed by grid (electron gun)-anode (bottom part of resonator) distance which for 127 MHz and energy of accelerated electrons range 1.5-2 MeV amounts 20 cm. The electron beam is evacuated into the open air through RF generator based on GI-50A triode (8).

Electron gun cathode is located inside of upper part of resonator. The grid is mounted centrally on the top of upper half of resonator, whereas top of lower part of resonator represents the anode of the triode type gun (Fig. 3.29). The beam current can be controlled by varying the positive cathode bias (Fig 3.29B).

The RF generator exciting resonator by coupling elements (9, 10) is composed as a common grid circuit (Fig. 3.30). This circuit is characterized by simplicity and substantially decrease overall accelerator dimension. Back coupling movable plate (11) is used for RF generator tuning.

The coaxial, ceramic, industrial triode GI-50A type is the electron vacuum lamp with three electrodes (Fig. 3.31). Directly heated cathode being the source of electrons based on thermionic emission, anode polarized in relation to the cathode positively and placed among them grounded grid. The main parameters of GI-50A triode are presented in Table 3.7. The lifetime of this triode is approximately 8000 h.

The effective way to change the range of electron energy adjustment and keep nominal beam power is arrangement of the gap distance between cathode and anode. When the grid-anode distance is reduced to 15 cm the optimal energy range is 1-1.5 MeV and frequency 115 MHz, and adequately 10 cm corresponds to energy 0.5-1 MeV and frequency 105 MHz. Much simpler method of electron energy adjustment is based on RF peak power regulation. Table 3.8 shows main parameters of the acceleration process.

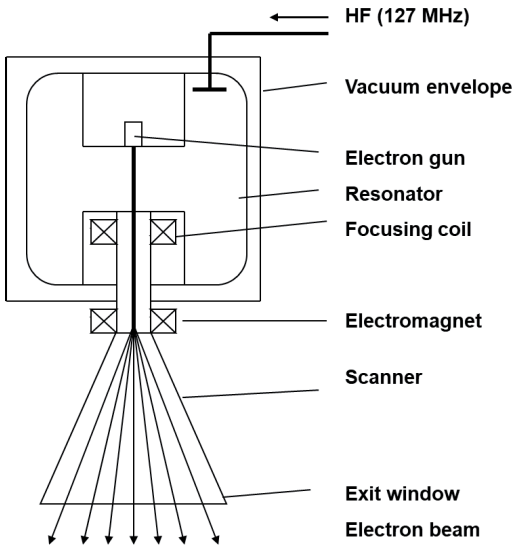


Fig. 3.27. The general idea of ILU 6 accelerator construction

Table 3.6. Technical parameters of electron accelerator ILU 6 type

| Type of parameter | Value | |
|---|---|---|
| Range of electron energy | 0.5-2 MeV | |
| Nominal energy of electrons | 1 MeV | 2 MeV |
| Nominal beam power | 20 kW | 20 W |
| Inhomogeneity of linear beam current density along scan on the distance 800 mm | < 10 | < 10% |
| Beam power delivered at distance 800 mm with inhomogeneity 10% | 85% | 85% |
| Electron energy instability | < 2% | < 2% |
| Average beam current | 20 mA | 10 mA |
| Beam current instability at nominal beam power | < 2% | < 3% |
| Pulse current (max.) | 1 A | 0.6 A |
| Pulse duration | 400 μs | 400 μs |
| Pulse repetition rate | 2-60 Hz | 2-50 Hz |
| Power line needed | < 100 kW | |
| Switching on time after automatic shoutdown | 1 min | |
| Switching on time after brake 10-60 min | 2 min | |
| Switching on time after break 2-48 h | 30 min | |
| Width of scanned beam | 30-80 cm | |
| Electron energy (maximum with reduced beam power 16 kW) | 2.4 MeV | |
| Average beam power (maximum with energy 1.7 MeV) | 24 kW | |

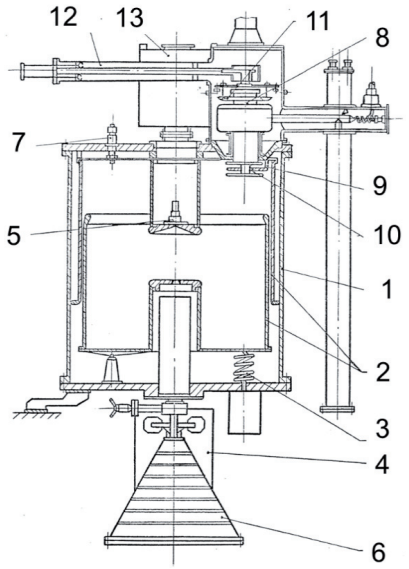


Fig. 3.28. Cross-section of the resonator of ILU 6 accelerator: 1 – vacuum housing, 2 – concentric resonator, 3 – coil, 4 – titanium vacuum pump, 5 – electron gun, 6 – beam scanning and extracting device, 7 – control loop, 8 – GI-50A triode, 9 – induction loop, 10 – coupling capacitor, 11 – movable plate of the feedback capacitor, 12 – cathode RF loop. 13 – titanium vacuum pump

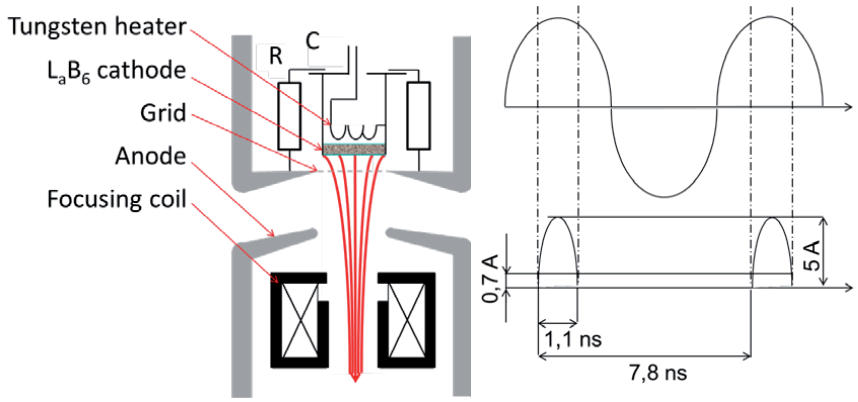


Fig. 3.29. Electron gun of ILU 6 accelerator: A – configuration of electron gun electrodes, B – sub--pulses of electrons formation (total pulse length: 400 μs, working frequency: 127 MHz)

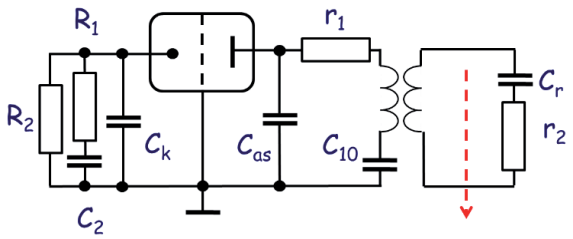


Fig. 3.30. RF self-excited generator based on GI-50A ceramic industrial triode

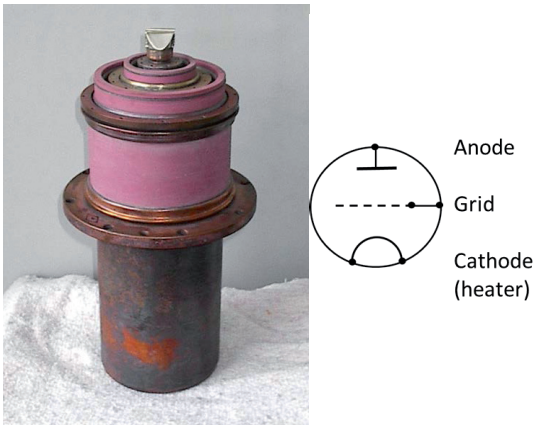


Fig. 3.31. The coaxial, ceramic, industrial triode GI-50A type

Table 3.7. The main parameters of the acceleration process

| Parameter | Value |
|---|---|
| Pulse power | 2 MW |
| Frequency | 170 MHz |
| Cathode | heated directly (carbureted paved tungsten) |
| Casing | metal-ceramic with external copper rings to provide heat removal from anode and ring type cathode and grid |
| Cooling water (anode) | 40 l/min |
| The air cooling | 200 $m^3$/h |
| Height/diameter | 420 mm/210 mm |
| Mass | 18 kg |

Table 3.8. The main parameters of the acceleration process

| Parameter | Value |
|---|---|
| The power lost in the anode lamps | 20 kW |
| Pulse voltage amplitude | up to 30 kV |
| HF pulse power | 2 MW |
| Power lost in the resonator | 0.7 MW |
| Power used in the acceleration process | 1.3 MW |
| Maximum beam average power (50 Hz) | 24 kW |
| Q factor (measured) | 20 000 |
| Thermal losses in resonator | 5.3 kW |

Figure 3.32 shows time-related characteristics of ILU 6 accelerator operated with nominal parameters.

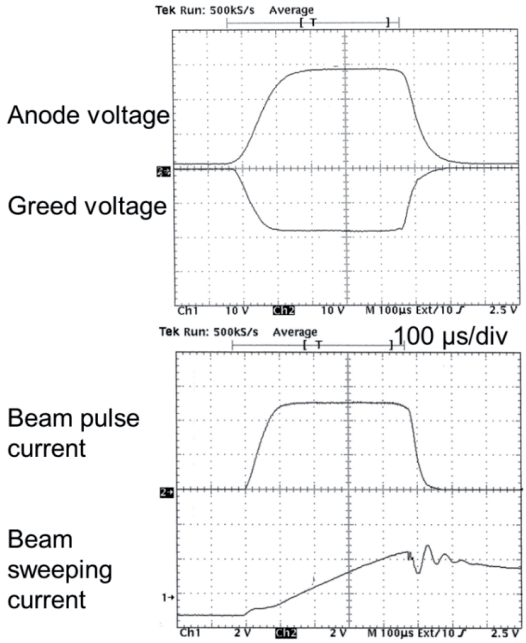


Fig. 3.32. Time-related characteristics of ILU 6 accelerator

A long term of experience in the operation ILU 6 accelerator has demonstrated significant advantages over accelerators other type, e.g. small dimensions of the unit, easy control, free of insulation gas and HV connections, simple maintenance and relatively cheap spare parts (triode GI-50A).

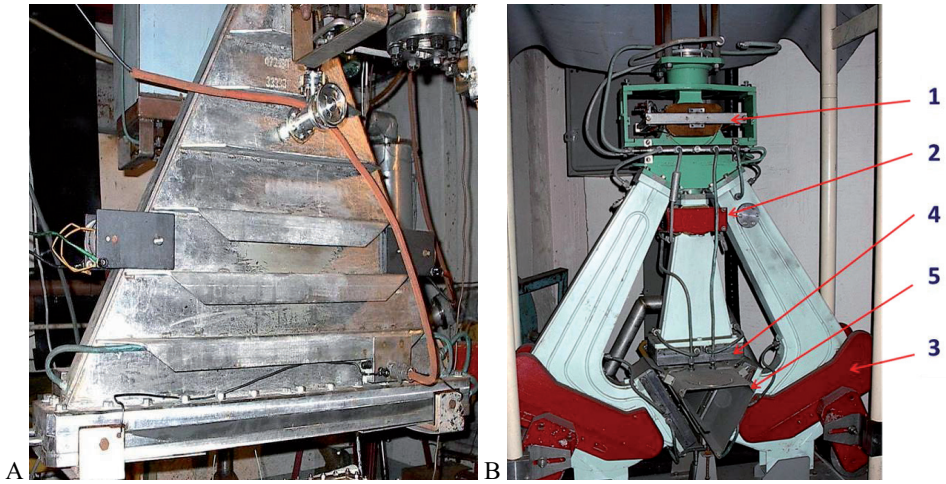


Fig. 3.33. ILU 6 accelerator beam exit devices: A – linear scaning, B – quasi-ring electron exit device (1 – switching magnet; 2, 3 – scanning magnets; 4 – exit window; 5 – irradiation zone)

The pilot plant facility was built on the basis of an industrial accelerator ILU 6 type. The facility is used as a pilot plant for radiation processing technologies as well as for applied research and as a large scale irradiator. The electron energy can be easily adjusted in a relatively large range by changing RF power level or by much more difficult way when the resonator accelerating gap length is changed. The accelerator was designed for continuous operation. Linear scanning (window dimension: 75 mm × 980 mm) and quasi-ring scanning beam exit device (three windows: 50 mm × 220 mm) can be applied to extract electron beam into the open air (Fig. 3.33).

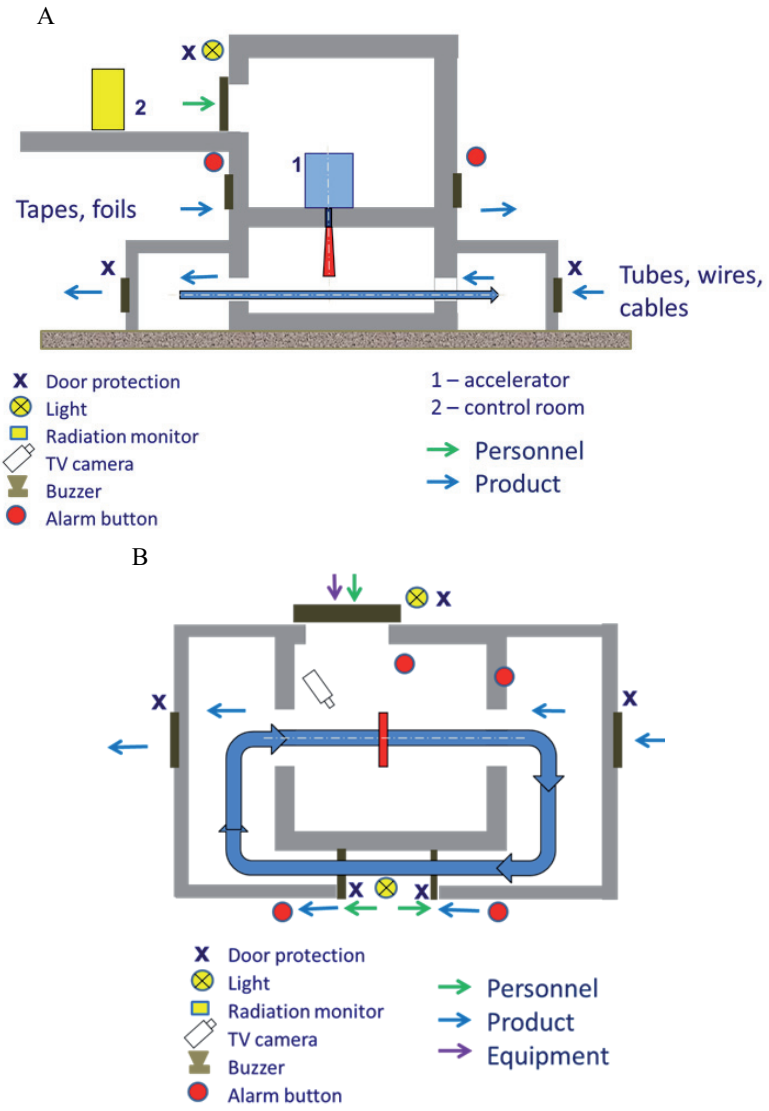


Fig. 3.34. Layout of ILU 6 pilot plant facility: A – side view, B – top view (ground level)

The use of the ILU 6 accelerator requires powering auxiliary electrical equipment necessary to run accelerator and technological lines:

- electrical equipment of a technological lines,
- accelerator water cooling systems (primary and secondary),
- supply and exhaust ventilation system.

Total electricity consumption in nominal conditions of the accelerator (beam power: 20 kW) is < 100 kW.

The accelerator and auxiliary equipment are located in three-level building with required shelter with wall made of heavy concrete to perform irradiation process (Fig. 3.34). The accelerator room with a labyrinth and the experimental hall are placed on the first level (Fig. 3.34B). The control room, technological and storage rooms are located on the second floor. The third level is used for laboratory purposes. Three independent transport systems have been foreseen for the pilot plant. A close loop conveyor system has been built and installed. It can carry samples with a maximum size of 2 m × 1 m. The speed of the conveyor can be varied continuously (0.15-15 m/min). The other technological lines with specific product transport systems allow to continuously irradiate different materials (Fig. 3.35). Separate technological lines were built to investigate pollution removal process from flue, irradiating heat-shrinkable products (tapes and tubes) and independent technological line for radiation modification of electrical wires and cables [8, 9].


Fig. 3.35. Pilot plant facility arrangement with different irradiated product transport systems: A – heat--shrinkable tapes, B – electrical wires and cables, C – gaseous pollutants removal, D – close loop conveyor

Optimization of the conditions of the radiation treatment process of polymer products assumes the analysis of specific parameters affecting the amount of absorbed dose and the uniformity of the irradiation process. It became a problem when treatment of circular objects such as wires and cables is performed. Two-sided irradiation is required to meet minimal quality standards. Four-sided irradiation system application significantly improves dose

homogeneity. The basic parameters analysis of crosslinking process of polymeric insulation towards obtaining the highest possible speed of the process with acceptable quality guarantees obtaining favorable economic indicators. It is worth noting that the average power of the accelerated electron beam affecting the process productivity. For a change, the specified insulation thickness requires the use of an electron beam with adequate energy. Process optimization should ensure maximum utilization of the electron beam while maintaining the assumed uniformity of irradiation of electric wires of a given geometry. In particular, the following parameters should be analyzed and optimized:

- average beam current in relation to the nominal electron energy value (10 mA with the energy of electrons 2 MeV, 20 mA with the energy of electrons 1 MeV) $I_{av}/I_{avn}$;
- average beam current can be changed by changing the pulse repetition frequency (F = 1-50 Hz) and the pulse current (I = 0.2-1 A); for pulse duration $\tau$ = 0.4 ms; average beam current determines the relationship $I_{av} = I \times \tau \times F$;
- use of the sweep beam range s in relation to the beam nominal sweep distance $s/s_n$;
- changing the electron energy (different average beam current for a nominal beam power level 20 kW) and the difference in electron energy utilization $E_n/E$;
- filling the irradiation area $l/l_{opt}$.

Utilization coefficient ($F_u$) can be calculated by using the following formula:

$$F_u = I_{av}/I_{avn} \times s/s_n \times E_n/E \times l/l_{opt}$$

An important parameter resulting from the above analysis determines the efficiency of the process to achieve the assumed radiation dose. The highest linear velocity of the radiation treatment process is related to the use of low energy (small insulation thickness), while the lowest speed will refer to high energy. The radiation treatment system should be designed to allow full use of the nominal beam power in the ILU 6 accelerator, i.e. 20 kW. In industrial conditions, the maximum speed should be as high as possible, even up to 1000 m/min. The selection of the energy of the accelerated electrons is directly related to the geometrical dimensions of the object and the assumed uniformity of the irradiation process. For the optimization of economic indicators, it is preferable to use the lowest possible electron energy for a wire with defined geometrical dimensions. It may be necessary to use higher energies to achieve a better uniformity of the irradiation process. In practice, materials containing, besides polyethylene, a number of components determining performance parameters as well as increasing the density of these materials, what requires an increase in the energy of electrons, are used for radiation processing.

Initial dosimetry measurements, i.e. without the use of a technological line intended for the radiation treatment of cables and electrical wires, were carried out to assess the spatial distribution of the electron beam at the output of the ILU 6 accelerator for different energies of accelerated electrons. The definition of the absorbed dose determines the amount of energy absorbed per unit of mass. The international SI unit of the absorbed dose is 1 Gy (gray), with: 1 Gy = 1 J/kg = 1 Ws/kg = $6.241 \cdot 10^{15}$ eV/g, 1 kGy = 1 kJ/kg = 1 kWs/kg = 0.239 cal/g = 1/3600 kWh/kg. The relationship between the absorbed dose and the power of the electron beam applied in radiation treatment process can be determined as:

$$D_{av} = F_u \times P \times T/M$$

where: $D_{av}$ – average dose [kGy], P – beam power [kW], T – time of radiation treatment [s], M – mass [kg], $F_u$ – the coefficient of beam power utilization.

The SI international unit defining electron energy is 1 J and the derived units are: 1 J = Ws = kg·m$^2$/s$^2$. In practice, the non-systemic unit is most often used: 1 eV = $1.602 \cdot 10^{-19}$ J. The power of the accelerated electron beam is determined by formula:

$$P = E \times I_{av}$$

where: E – energy of electrons [MeV], $I_{av}$ – average beam current [mA].

The efficiency of the radiation treatment process for a given dose determines the beam power and the efficiency of elctron beam utilization:

$$M/T = F_u \times P/D_{av}$$

In the case of radiation treatment of cables and wires, the coefficient of beam current utilization is determined by the dependence:

$$F_p = D/s$$

where: D – diameter of the channel for each wire, s – distance between the cable axes in the irradiation area.

Beam utilization coefficient depends on the relation between the energy of electrons and, more precisely, the range of the electron beam in a given material and the thickness of the layer of material subjected to radiation treatment. Table 3.9 presents the practical parameters relating to the range of electrons for polyethylene.

Table 3.9. Normalized range of electrons in polyethylene. R(opt) – optimal range where the depth dose reaches the surface dose value, R(50) – range for which the depth dose reaches 50% of the maximum dose, R(50e) – range for which the depth dose reaches 50% of the surface dose, R(p) – practical range of electrons

| Energia [MeV] | R(opt) [g/cm$^2$] | R(50) [g/cm$^2$] | R(50e) [g/cm$^2$] | R(p) [g/cm$^2$] |
|---|---|---|---|---|
| 0,4 | 0.0000 | 0.0538 | 0.0538 | 0.0828 |
| 0,6 | 0.0750 | 0.1258 | 0.1288 | 0.1688 |
| 0,8 | 0.1608 | 0.2018 | 0.2138 | 0.2618 |
| 1,0 | 0.2428 | 0.2818 | 0.3018 | 0.3578 |
| 1,5 | 0.4488 | 0.4858 | 0.5288 | 0.6096 |
| 2,0 | 0.6518 | 0.6988 | 0.7538 | 0.8608 |
| 3,0 | 1.0538 | 1.1278 | 1.2088 | 1.3730 |

The range of electrons for polyethylene can be determined for different electron energies by the following relationships:

$$R(opt) = 0.404E - 0.161$$
$$R(50) = 0.435E - 0.152$$
$$R(50e) = 0.458E - 0.152$$
$$R(p) = 0.510E - 0.145$$

Dosimetry measurements are an integral part of the radiation treatment activities. The calorimetric method commonly used in radiation sterilization has little practical significance in continuous processes, such as radiation treatment of cables and electric wires. Dosimetric measurements were made to assess the distribution of the beam in a plane perpendicular to the accelerator axis, located at a certain distance in relation to the position of the starting film. For this purpose, dosimetry PVC films were used. This allows select the optimal conditions for conducting the radiation treatment process from the viewpoint of the beam power utilization and determine the parameters of electron beam divergence, which can be useful in computer calculations of dose distribution in irradiated objects. In the ILU 6 accelerator, the beam sweep occurs each time during the pulse of the accelerated electrons (0.4 ms). The width of the sweep length is adjustable depending on the requirements in the range of 30-80 cm. The transverse dimensions of the beam in the direction perpendicular to the direction of its sweep is determined mainly by the beam scattering effect.

The phenomena affecting the transverse dimensions of the beam include the beam focusing in the accelerator's vacuum area, Coulomb forces dependent on the beam current amplitude, beam spread in the output window material and first of all the beam scattering in the air highly dependent on the electron energy. Figure 3.36 shows the curves of transverse dimensions of the electron beam in ILU 6 accelerator for the energy 1.75 MeV. Transverse beam dimenssion is of some importance for the uniformity of irradiation. The main problem of the optimization of radiation treatment process is optimization of the electron beam utilization, with maintaining the homogeneity of the irradiation process as uniform as possible. The spatial distribution of the electron beam at the output of the accelerator is determined first of

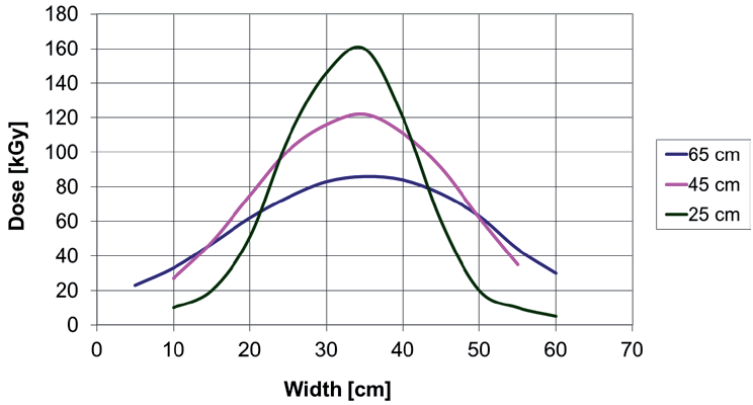


Fig. 3.36. Transverse dimensions of the electron beam for 1.75 MeV electron energy at different distances from the ILU 6 accelerator exit window

all by the parameters of the beam sweep system and the phenomenon of beam scattering in the air, significantly dependent on the energy of electrons. Figure 3.37 shows the trace of the electron beam along the sweeping direction, obtained for a PVC film placed directly at the output of the electron beam, depending on the parameters of the sweep system, i.e. current amplitude in the coil winding of the beam sweeping electromagnet.

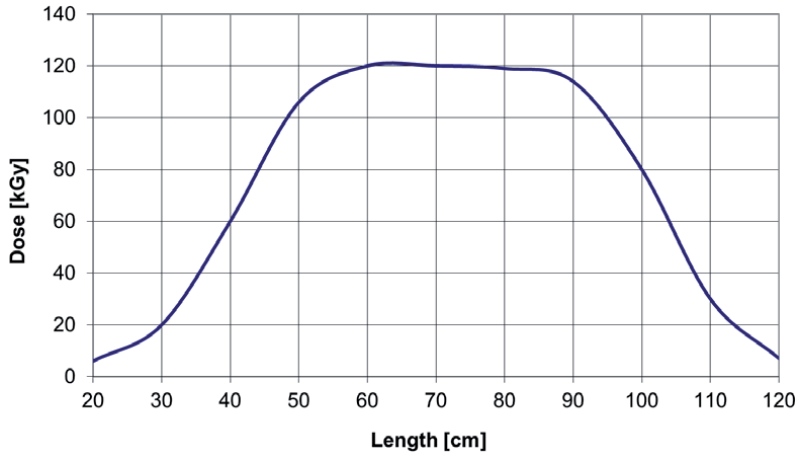


Fig. 3.37. Distribution of the intensity of the electron beam measured along the scann direction at a distance of 45 cm from the exit window (the sweep length of the beam 40 cm)

As it is easy to see in Fig. 3.38, using higher electron energies irradiation zone is more narrow. The use of the electron beam in the irradiation of wires and electric cables creates significant difficulties in obtaining an even distribution of the dose due to the shielding action of the copper wire. As shown in Fig. 3.39, “s” the longest distance covered by electron beam in polymer material with two-sided irradiation significantly exceeds “w” the thickness of the insulating layer.

As can be seen from the geometry, the distance “s” can be calculated from the following relationships:

$$s = (D^2 - d^2)^{0.5}$$
$$s = [w(D - w)]^{0.5}$$

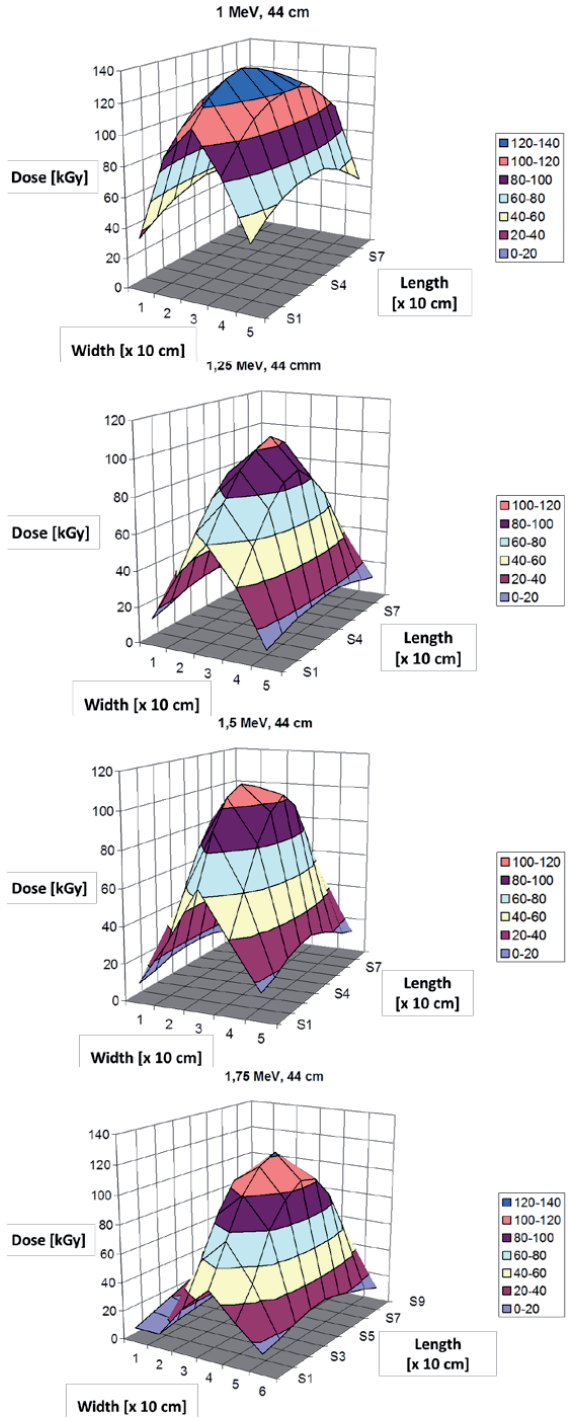


Fig. 3.38. Spatial distribution of the beam for various electron energies measured 45 cm from the exit window of the accelerator (44 cm from the floor)

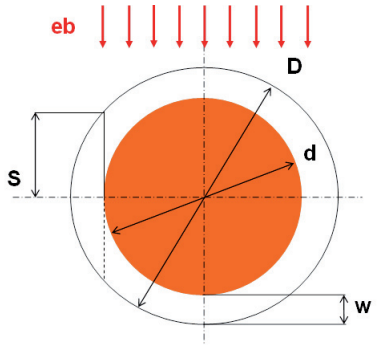


Fig. 3.39. Cross-section geometry of electric wire

where: D – diameter of the duct, d – diameter of conductive conductor, w – insulation thickness.
It is easy to notice that the thickness of the insulation, and more precisely the length of the section s, determines the minimum energy that should be used during radiation treatment. The size of the section s is influenced not only by the thickness of the insulation, but also by the geometrical dimensions of the cable. One of the ways to improve the distribution of the absorbed dose measured around the circumference is the use of two accelerators inclined at an angle of 45$^{o}$ with respect to the longitudinal axis of the conduit, placed on both sides with a beam swept along the direction of travel of the conduit. Another way is a properly constructed electron beam output system with four windows forming four independent irradiation areas. This results in the possibility of using four-sided irradiation of cables and electric wires.

The improvement of uniformity of the deep-dose distribution with two sided irradiation of electric wires can be obtained due to specific irradiation geometry of scanned electron beam. This effect is additionally aggravated by the discrepancy of the beam caused by the phenomenon of electrons scattering in the air, the characteristics of the beam focusing system, and finally the Coulomb forces that increase the divergence of the electron beam. In a similarly beneficial way, the uniformity of the dose distribution is influenced by the use of an electron beam with a significant energy distribution. Figure 3.40 schematically presents the process of irradiation of the wire with electron beam with different spatial orientation in the area of conducting the radiation treatment process.

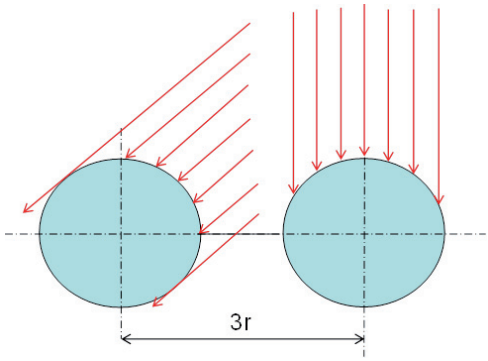


Fig. 3.40. Irradiation of the wire with electron beam of different orientation in the area of radiation treatment

A significant improvement in the homogeneity of irradiation can be achieved by using four-sided irradiation. However, that requires the use of two accelerators or a significant

construction of the accelerator output device. It is worth noting that in order to cover the full range of diameters, it is necessary to build at least two devices for rewinding cables and wires. Another important technological aspect is the production of cables with a more complex construction, e.g. containing a series of twisted pairs in one common shell. In practice a separate radiation treatment for individual wires is conducted and the process for radiation crosslinking of a common coating is repeated. The basic determinant of the radiation treatment process is the electron beam parameters determined by the accelerator operating conditions and the beam geometry.

Table. 3.10. Increase in temperature of materials with different specific heat treated with radiation

| Item | Specific heat [J/g °C] | Temperature increase [°C/kGy] |
|---|---|---|
| Water | 4.19 | 0.24 |
| Aluminum | 0.90 | 1.11 |
| Copper | 0.38 | 2.63 |
| Silver | 0,235 | 4.26 |
| Polyethylene | 2.30 | 0.43 |
| Polymethylmethacrylate | 2,09 | 0.48 |
| Polypropylene | 1.92 | 0.52 |
| Nylon | 1.67 | 0.60 |
| Polyvinyl chloride | 1.34 | 0.75 |
| Polycarbonate | 1.26-1.17 | 0.79-0.85 |
| Polytetrafluoroethylene | 1.05 | 0.95 |

One of the effects of the irradiation process is the temperature change of the material treated by radiation, directly related to the energy absorption in the form of ionizing radiation. The increase in temperature as a function of the absorbed dose is determined by the relationship:

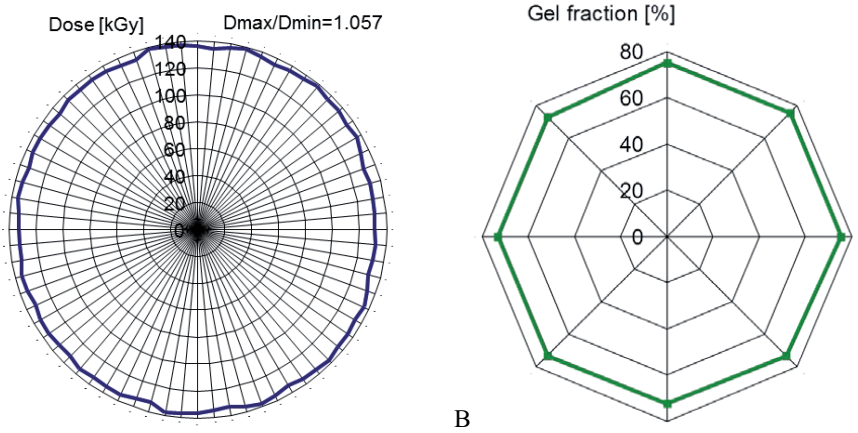


Fig. 41. A – Dose distribution around the perimeter of the polymer layer (cover + insulation) for two-sided irradiation of electric cable with aluminum wire determined by computer simulation method (electron energy: 1 MeV, energy spread: ΔE/E = 20%, beam divergence: 30°, depth between the cable axes: d = 1.5 cm), B – gel fraction distribution for above case

$$\Delta T = H/c$$
$$\Delta T = D/c$$

where: $\Delta T$ – temperature increase [$^oC$], H – heat per unit of mass [J/g], c – specific heat [J/g $^oC$], D – absorbed dose [kGy].

Table 3.10 presents the amount of specific heat and temperature increases of selected materials subjected to radiation treatment.

The size of the exposure dose determined by the process conditions has a fundamental influence on the temperature effects of the radiation treatment. A significantly higher temperature increase is recorded for a copper wire due to the low level of specific heat as compared to the polymeric materials constituting the insulating coating of the duct (Table 3.10). The geometrical dimensions of the conductor as well as the energy of the electron beam are of particular importance, especially when they exceed the level required to obtain an adequate homogeneity of the irradiation process.

Figure 3.41 shows dose and gel fraction distribution around the perimeter of the polymer layer (cover + insulation) for two-sided irradiation of electric cable with aluminum wire determined by computer simulation method gel fraction measurements method.

## 3.3. RADIATION STERILIZATION PLANT

The idea of radiation sterilization derives from the work of Maria Skłodowska-Curie published in 1929, where the mathematical analysis of the bactericidal action of gamma radiation was carried out. Currently, after many years of using the process on an industrial scale, radiation sterilization has been commonly accepted as the best method of single use medical devices sterilization. This is evidenced by the permanent increase in the global radiation installations used to conduct this process.

The effects of radiation degradation of pathogens are of statistical nature. The effectiveness of ionizing radiation depends on a number of factors, including the electronic density of the sterilized material, the dose of ionizing radiation used, as well as the water content in the sterilized material (induction of active chemical products). In addition, there are biological effects associated with the ionizing radiation (effects of DNA and key elements of bacteria damage). These phenomena are the basis of the radiation sterilization process of disposable medical devices as well as implants and transplants. An important advantage of the process is the ability to conduct sterilization in the final packaging, using the irradiation techniques provided for a given type of product. The traditional method of thermal sterilization cannot be applied to most plastics as well as transplants. The short exposure time and a small increase in temperature during the process with the use of ionizing radiation allow to sterilize the transplants in a frozen state. In contrast, the unfavorable side effects of gas sterilization with ethylene oxide cause a departure from this method in highly developed countries. Other advantages of radiation sterilization are the following:

- guaranteed degree of sterility in the entire mass of the product,
- certainty of sterility based on measuring the dose,
- sterilization in completely sealed unit and collective packaging,
- the simplicity of the procedure and the implementation of sterilization at room temperature,
- absence of impurities after the sterilization process.

The radiation sterilization process includes, in addition to a wide range of disposable medical devices, a range of products important from the point of view of medical applications, in particular: implants and transplants, cosmetics, hydrogels, packaging for medical applications and food products, pharmaceutical products.

The first electron accelerator was invented and constructed in the early 1930s. In 1956, the electrostatic electron accelerator with electron energy 2 MeV and 0.5 kW beam power was

used in the first commercial facility for radiation sterilization. Currently, two types of ionizing radiation sources are used in sterilization process: electron accelerators and radioactive isotopes. Currently, approximately 90% of industrial devices are gamma installations with a total activity of 220 MCi operating on the basis of the radioactive Co-60 isotope (most) or cesium Cs-137 (approx. 10%). It is estimated that there are approximately 200 sterilization stations around the world in 55 countries with cobalt sources, with more than half being industrial size facilities. In addition, about 60 accelerators in various countries are used to carry out radiation sterilization. Recently, a dynamic growth of applications of electron accelerators to conduct the sterilization process has been observed. This is due to intense development of accelerator technology (high power and high reliability accelerators) and the fact that the accelerators prices do not grow so fast as the prices of $^{60}$Co sources. The decisive factor may be the dissemination of the sterilization method with the use of X-ray radiation. The degree of social acceptance of nuclear devices is also very important.

The idea of the first accelerator installation for radiation chemistry and technology at the Institute of Nuclear Research (currently the Institute of Nuclear Chemistry and Technology) came after collaboration with Denmark, where such installation was finished in 1958. The Danish example of versatile accelerator facility was followed. Pulse radiolysis experimental set-up and large scale irradiation were performed in one complex. It was used as an assumptions for the construction accelerator facility in Poland. Accelerator was finally ordered and manufactured at the D.V. Efremov Institute of Electrophysical Apparatus in Saint Petersburg, Russia [10].

Practical activities in the field of chemistry and radiation technology based on the use of accelerators began in Poland when the LAE 13/9 electron accelerator was installed and put into operation at the Institute of Nuclear Research under government financial support. Nominal accelerator parameters were as follows: electron energy – 13 MeV; average beam power – 9 kW; electron pulse duration – 0.5, 2.5, 5.5 μs with corresponding repetition rate 900, 300, 150 Hz, respectively. The beam of accelerated electrons was obtained for the first time in January 1971.

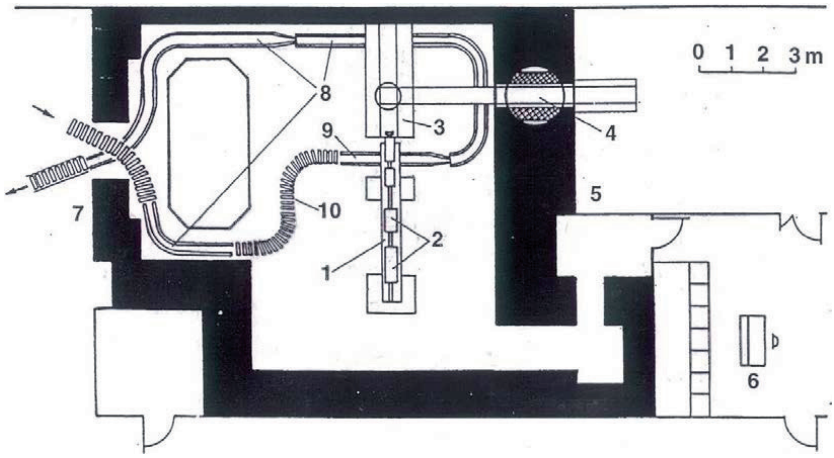


Fig. 3.42. Plan of the multipurpose LAE 13/9 electron accelerator facility: 1 – LAE 13/9 electron accelerator, 2 – accelerating sections, 3 – irradiation zone for horizontal beam, 4 – gate, 5 – measurement room, 6 – control room, 7 – technological room for radiation processing, 8 – input and output conveyors, 9 – conveyor with controlled speed, 10 – rollers

This multipurpose facility was design and build to fulfill specific requirements and provide opportunity to perform: pulse radiolysis experiments, applied study in the field of radiation chemistry and technology and large scale radiation processing activity. The layout

of the facility is shown on Fig. 3.42. As a result several radiation technologies were developed and radiation processing service has been started at the INCT on semi-industrial scale in such radiation processes as sterilization of single use medical products, biostatic grafts for transplantology and biomedical materials, crosslinking of polymers and copolymers, modification of the semiconductors and related products, food preservation. The intensive basic study investigations have been started with pulse radiolysis experimental set-up in microsecond time scale and other research programs.

The first industrial scale application of radiation technology in Poland took place in 1974, starting systematic quantitative and assortment increase, and since the mid-1975s the Institute has been involved in large scale radiation sterilization of single use medical devices including several dozen different products such as surgical clothing, catheters, bacteriological containers, eye droppers as well as biostatic grafts (bones, skin) for a tissue bank. The facility has been intensively exploited up to 4000 h per year.

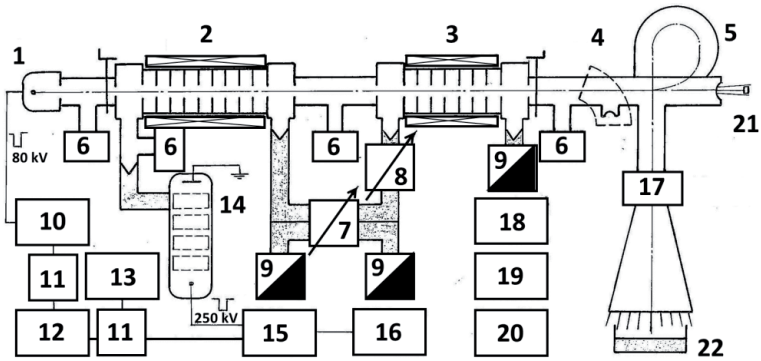


Fig. 3.43. Block diagram of LAE 13/9 electron accelerator: 1 – electron gun; 2, 3 – first accelerating section with focusing coils; 4 – electron energy analyzing magnet; 5 – bending magnet; 6 – ion vacuum pump; 7 – microwave energy divider; 8 – microwave energy phase shifter; 9 – microwave energy load; 10 – 80 kV gun pulse modulator; 11 – delay line; 12 – pulse sequence generator; 13 – driving generator; 14 – klystron KIU 15; 15 – 250 kV klystron pulse modulator; 16 – HV power supply; 17 – beam scanning coil; 18 – water cooling system;, 19 – AC power line; 20 – control circuit; 21 – process vessel; 22 – irradiated object

LAE 13/9 was constructed as a linear accelerator in which electrons are accelerated by traveling electromagnetic wave. The accelerating structure consisted of two sections powered successively by a single klystron. Accelerator was equipped with two output windows (Fig. 3.43): a horizontal beam exit used for pulse radiolysis experiments and R&D study, and a vertical scanned beam exit for radiation processing. Electron beam current density up to 80 $\mu A/cm^2$ was extracted horizontally into air through a 50-µm titanium window with air cooling system. It was also possible to use a double titanium window with water cooling system with beam current density up to 1 $mA/cm^2$. The vertical beam was formed by a $270^o$-electromagnet and a scanning device. Finally, electron beam is directed down towards a conveyor through a 50-µm titanium window 60 cm long.

The klystron KIU 15 was energized through a pulse transformer with pick voltages on secondary winding up to 250 kV. A diode electron gun with a cathode made of pressed BaNi was used. The gun was powered from a modulator operating in pulse regime at a voltage of 80 kV. A regulated power divider and regulated phase shifter are the principal components of the waveguide line between accelerating sections. Adjustment of microwave power and phase at the input of second section was making possible to vary the electron energy in a wide range including the case when the electrons are deaccelerated in second section. Practical range of electron energy adjustment was 5-13 MeV.

Fig. 3.44. Control room of LAE 13/9 electron accelerator and data collection system for radiation sterilization process

Figure 3.44 shows the control room of LAE 13/9 electron accelerator where control desk and racks with auxiliary equipment were located. In addition to accelerator equipment a computer controlled data acquisition and processing system designed by the INCT staff was installed, for control radiation sterilization process and archiving the collected data.

A 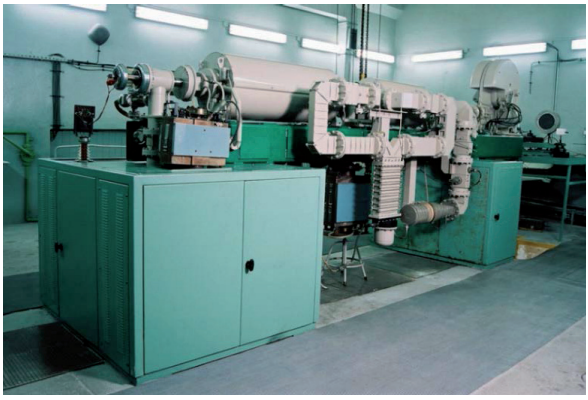 B 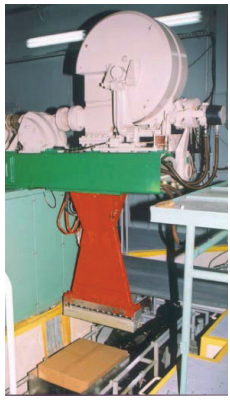

Fig. 3.45. View of accelerator facility: A – accelerator LAE 13/9 main components (electron gun, accelerating section, waveguide system and bending magnet), B – beam exits of accelerator LAE 13/9

Figure 3.45A shows electron accelerator LAE 13/9 which consisted of such components as electron gun, accelerating section, waveguide system, and bending magnets. Horizontal and vertical beam exits are displayed in Fig. 3.45B. Electron gun was the weakest part of LAE 13/9 accelerators. Figure 3.46A shows the statistic of 48 cathodes lifetime. Half of them was characterized by lifetime < 400 h. On the other hand, some of the cathodes were in service nearly 5000 h. The cathode construction was quite simple (Fig. 3.46B). the main reason of their failure was damage of insulation layer made of $Al_2O_3$. That led to shortening heater active part, decreasing heater power, reduction cathode temperature, and reduction electron emission of the cathode. Fortunately cathode price was very low and replacement was easy and quick.

Beam diagnostics devices of LAE 13/9 accelerator are presented in Fig. 3.47. Except different size of water cooled Faraday's cups which are usually applied as beam current collectors, pulse beam charge and average beam current inductive sensors were installed. Non electron beam destructive secondary electrons monitor was used for continuous registration average beam current. Thermocouple with mechanical shifting devices along exit window of

scanned beam was applied for homogeneity of electron beam intensity distribution. Separate analyzing magnet was installed to evaluate electron beam energy spectrum.

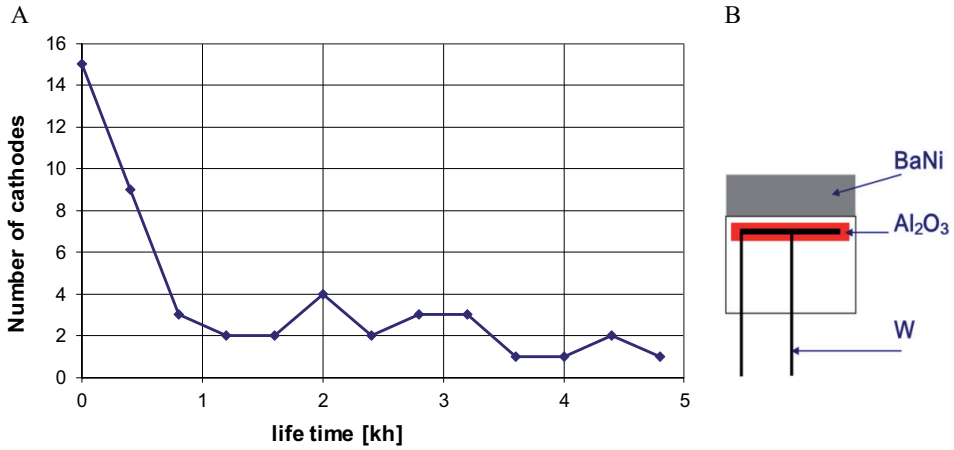


Fig. 3.46. BaNi cathode lifetime statistic (A) and a cathode construction (B)

Radiation sterilization was introduced in Poland in the early 1970s. It was preceded with research studies and testing of radiation tolerance of different plastic materials, microbiological studies on sterilization effectiveness, and elaboration of suitable dosimetry systems for routine dose and depth dose determination. The electron beam parameters affordable by LAE 13/9 (electron energy 10-13 MeV, 6 kW average beam power) were sufficient to perform regular radiation sterilization service in certain period of time. Difficulties with regular supply of spare parts, and lack of the time for scientific experimental work due to commercial load of the accelerator were the main reasons for new investments. In contrast to the LAE 13/9 accelerator, which was originally a universal accelerator, subsequent installations installed at the INCT have a specific, more specialized purpose [11].

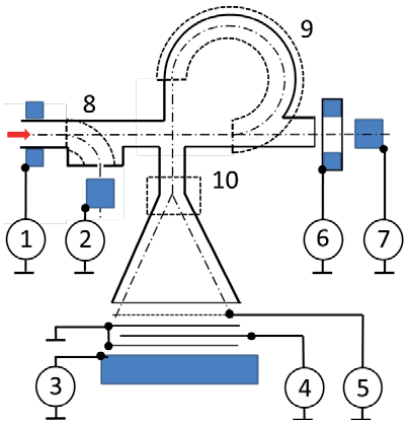


Fig. 3.47. Electron beam control devices of LAE 13/9 accelerator: 1 – inductive sensor (average beam current), 2 – Faraday cup (electron energy spectrum), 3 – Faraday cup (average beam current, shape of the pulse), 4 – secondary electrons monitor (average beam current), 5 – thermocouple (beam intensity distribution), 6 – inductive sensor (charge within the pulse), 7 – Faraday cup (shape of the pulse), 8 – analyzing magnet, 9 – bending magnet, 10 – scanning magnet


Fig. 3.48. Dedicated facility for radiation sterilization of disposable medical devices was designed and put into operation at the INCT in 1993

Dedicated facility for radiation sterilization of disposable medical devices was designed and put into operation in 1993 [12]. This industrial type facility is located in a new building at the INCT (Fig. 3.48). A microwave linear electron accelerator, with traveling wave and 10 MeV electron energy, 10-15 kW average beam power was designed and built by the NPO Toriy, Moscow, Russia. One accelerator was installed at the first stage of the investment. The accelerator was placed vertically to avoid a bending magnet and related beam power losses. The accelerator main components arrangement is shown in Fig. 3.49. The source of electrons triode type is equipped with indirect heated cathode made of porous activated tungsten. Its lifetime in regular exploitation conditions can be as high as 20 000 h. High power microwave magnetron is used as a source of microwave energy. It is transmitted to accelerator section through ceramic window. The unused microwave energy during electron accelerating process

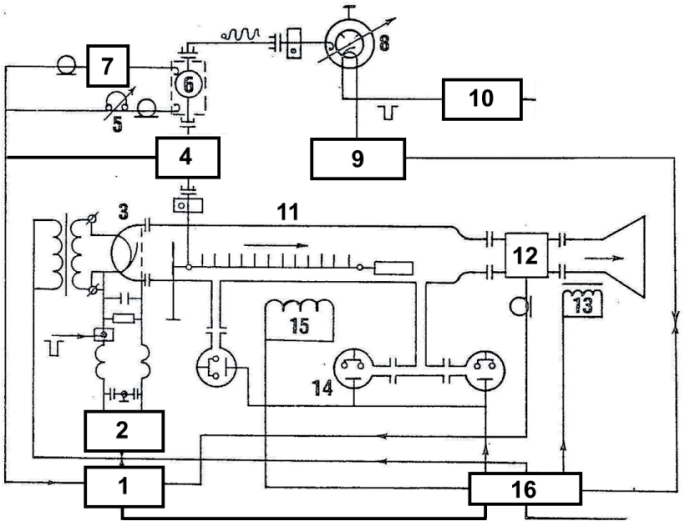


Fig. 3.49. Block diagram of electron accelerator Elektronika 10/10: 1 – control unit, 2 – power supply, 3 – electron gun, 4 – circulator, 5 – UHF sensor, 6 – coupler, 7 – UHF envelope pulse detector, 8 – magnetron, 9 – transformer, 10 – magnetron pulse modulator, 11 – accelerating section, 12 – inductance beam current sensor, 13 – scanning coils, 14 – ion vacuum pump, 15 – focusing coils, 16 – power supply units

is deposited in UHF load located in volume under vacuum. Beam exit system is equipped with scanning magnet. Figure 3.50 shows a general view of Elektronika 10/10 main components: magnetron stand, microwave circulator and accelerator section with electron gun and ion vacuum pump.

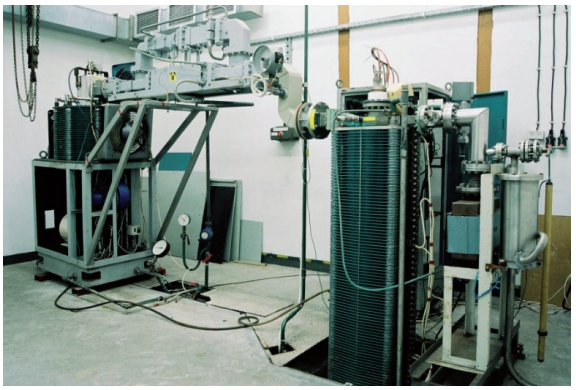

Fig. 3.50. Radiation sterilization facility equipped with UHF linac Elektronika 10/10 with electron energy 10 MeV and average beam power 10 kW

Microwave energy sources play a crucial role in linacs of this type because of their stability, price level, lifetime, and electrical efficiency. The klystrons are more stable in frequency and they frequently have lifetime 10 000 h and more, but they have an electrical efficiency of 40% in comparison with 70% efficiency of magnetrons and usually are more expensive. Magnetron – microwave self-excited oscillate device is based on the phenomenon of the resonance which transfers energy of the accelerated beam current on the energy of the electromagnetic wave at high frequency.

The shaped especially anode chamber is placed in the strong magnetic field. Electrons emitted by the cathode are directed to the polarized anode (Fig. 3.51). Electrons tracks and their speed are modified through magnetic field and the shape of the anode chamber. Magnetron generates microwave energy in the final effect.

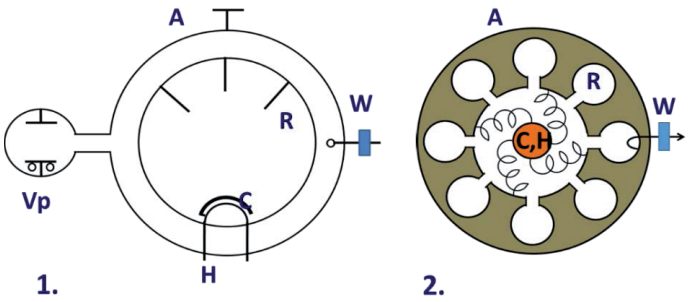


Fig. 3.51. Magnetron: 1 – graphic symbol of magnetron, 2 – magnetron cross-section with marked electrons trajectories, C – cathode, H – heater, R – resonator, W – microwave power output, Vp – vacuum ion pump

The high power pulse magnetron type MI 435 was originally applied in accelerator Elektronika 10/10. Its warranted lifetime was only 1000 h, and typical device was in service less than 2000 h. The upgrading program of high energy linear electron accelerator Elektronika 10/10 towards higher technical and economical effectiveness has been started due to limited reliability of pulsed magnetron MI 435 type and needed higher productivity and

lower unit cost of irradiation service. The accelerator upgrading program started after 10-year exploitation. The main goals of upgrading activities were as follows:

- increase in the reliability of the microwave energy source,
- increase in the beam power of accelerated electrons,
- increase in the stability of irradiation process (dose rate) by application the feedback loop between beam current and conveyor speed.

The upgrading program was divided in time to avoid long periods when accelerator is out of operation. The first step of upgrading program was application pulse magnetron MI 470 type provided by Elektronika 10/10 accelerator producer. Table 3.11 presents the main parameters of old and new magnetrons. It should be noticed that geometrical dimensions of both magnetrons are in acceptable tolerance. The main advantages of new instrument are related to twice higher warranted lifetime and more than twice higher average beam power. Practically replacement of the magnetron did not require any correction of supporting system including pulse power modulator construction.

Table 3.11. Technical specifications of high power pulse magnetrons

| Parameter | Pulse magnetron | |
|---|---|---|
| | MI 435 | MI 470 |
| Frequency [MHz] | 1883-1889 | 1883-1889 |
| Power pulse [MW] | 10 | 10 |
| Power average [kW] | 22 | 50 |
| Pulse duration [μs] | 6.0 | 10 |
| Anode voltage [kV] | 50 | 42-46 |
| Magnet system | solenoid | solenoid |
| Cooling | water | water |
| Weight [kg] | 70 | 70 |
| Warranty [h] | 1000 | 2000 |

The second step of accelerator upgrading was related to replacement of accelerating section traveling wave type. The new one was ordered from NPO Toriy. The new model of accelerating section was slightly longer with the same diameter, what required small modification of focusing coil and water cooling loop. Better electrical efficiency and suitable cooling conditions made possible significant average beam power enlargement up to 15 kW. The accelerator productivity increased by 50% due to implemented upgrading program.

The accelerator Elektronika 10/10 and the auxiliary equipment are located in a separate building consisting of three levels (Fig. 3.52): the basement with a total surface of 715 $m^2$ (irradiation chamber, auxiliary equipment rooms), the ground floor – 855 $m^2$ (accelerators rooms, storage surface 2 × 288 $m^2$) and the first floor – 244 $m^2$ (operating room, auxiliary equipment rooms). The storage area is divided into two separate parts: one for untreated and the other for irradiated and sterile products. The total storage surface can be increased by using a part of the basement surface. One more accelerator can be installed in the building to increase the total capacity of the facility. AC power consumption of the sterilization facility is 120 kVA.

A microprocessor controlled roller and belt conveyor systems are used to carry irradiated boxes of a typical size of 560 mm × 450 mm × 100-300 mm. The speed of the conveyor located in the irradiation chamber, where a stainless steel belt has been applied, can be varied continuously within the range 0.3-0.7 m/min. The irradiation process can be seen in

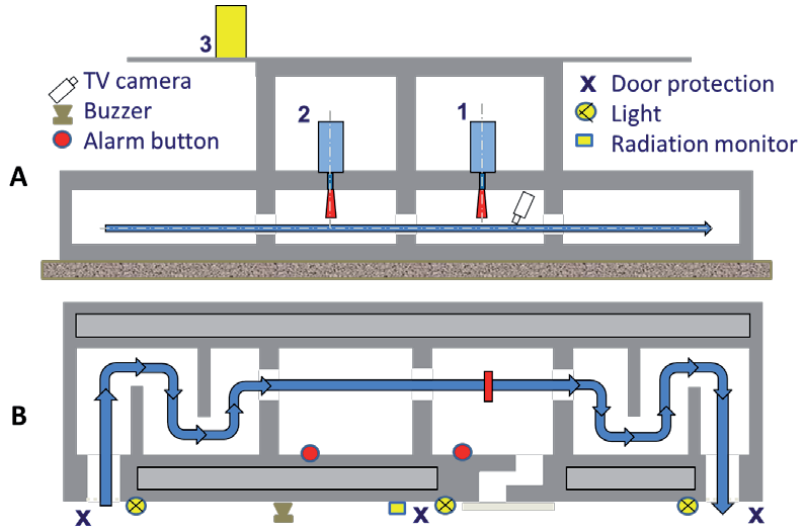


Fig. 3.52. Radiation sterilization facility arrangement: A – side view (1 – accelerator Elektronika 10/10, 2 – accelerator LAE 10/15 (under commissioning), 3 – control room), B – top view on basement level

Fig. 3.53. Additional equipment for two-sided irradiation can be used when necessary. Plastic belts are used for convening boxes between the basement and the ground level, continuous recording of the electron beam parameters and the speed of the conveyor is foreseen to meet routine monitoring requirements. Electron accelerator Elektronika 10/10 is capable to provide 24 h/day, 5 days/week service with availability better than 96%. The capacity of this facility amounts 18 000 kg kGy/h. Sterilization services should be provided without interruptions resulting from ongoing scientific research and repairs of the accelerator. The new investment has fully secured the current demand for sterilized products manufactured in the country. The validation process for the radiation sterilization of disposable medical devices, implants and transplants has been introduced, including the qualification of the installation, and process qualification.

Fig. 3.53. Radiation sterilization process

Radiation sterilization facility offers radiation process service to the medical, pharmaceutical and industrial sectors. Effective and efficient quality assurance (QA) program was established and maintained to provide service in a systematic manner with formalized procedures designed to prevent the occurrence of deficiencies in the standard work and ensure that all requirements for quality are recognized and the consistent and uniform control of these requirements is adequately maintained [13-15]. Sterilization facility provides service of irradiation of medical devices for domestic and international companies according to certificate of management system for medical devices in conformances with the standard PN-EN ISO 13485:2005. The Radiation Sterilization Plant has been certificated by the Polish Centre for Testing and Certification (Fig. 3.54A). The objective of the management of the facility is to provide service in a manner that conforms to the specified requirements of the customers, all applicable regulations, relevant safety standards and the facility quality assurance (QA) program. Radiation Sterilization Plant is certified GMP (Good Manufacture Practice) providing the highest quality products (Fig. 3.54B).

A

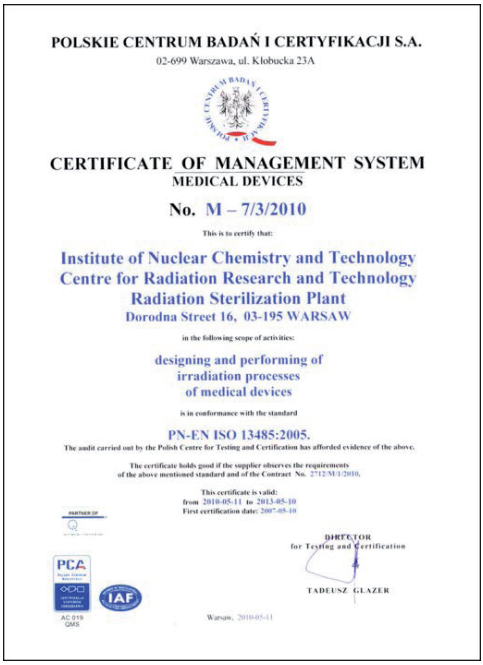

POLSKIE CENTRUM BADAŃ I CERTYFIKACJI S.A.
02-699 Warszawa, ul. Kłobucka 23A

CERTIFICATE OF MANAGEMENT SYSTEM
MEDICAL DEVICES
No. M – 7/3/2010

This is to certify that:

Institute of Nuclear Chemistry and Technology
Centre for Radiation Research and Technology
Radiation Sterilization Plant
Dorodna Street 16, 03-195 WARSAW

in the following scope of activities:

designing and performing of
irradiation processes
of medical devices

is in conformance with the standard

PN-EN ISO 13485:2005.

The audit carried out by the Polish Centre for Testing and Certification has afforded evidence of the above.

The certificate holds good if the supplier observes the requirements of the above mentioned standard and of the Contract No. 2712/M1/2010.

This certificate is valid:
from 2010-05-11 to 2013-05-10
First certification date: 2007-05-10

DIRECTOR
for Testing and Certification
TADEUSZ GLAZER

Warsaw, 2010-05-11

B

GŁÓWNY INSPEKTORAT FARMACEUTYCZNY 1/2

CERTIFICATE No. GIF-IW-N-4022/67/13

Main Pharmaceutical Inspector

CERTIFICATE OF GMP COMPLIANCE OF A MANUFACTURER

Part 1

Issued following an inspection in accordance with Art. 111(5) of Directive 2001/83/EC as amended

Main Pharmaceutical Inspector
/the Competent Authority of Poland/

confirms the following:

the manufacturer

Instytut Chemii i Techniki Jądrowej
16, Dorodna Str., 03-195 Warszawa, POLAND

site address

Instytut Chemii i Techniki Jądrowej
16, Dorodna Str., 03-195 Warszawa, POLAND

has been inspected under the national inspection programme in connection with manufacturing authorisation No. GIF-IW-N-4001/152/10 in accordance with Art. 40 of Directive 2001/83/EC transposed in pharmaceutical law of 6th of September 2001 (Dz. U. z 2008 r. Nr 45, poz. 271, z późn. zm.).

From the knowledge gained during inspection of this manufacturer, the latest of which was conducted on 26-27/02/2013, it is considered that it complies with the Good Manufacturing Practice requirements laid down in Directive 2003/94/EC.

This certificate reflects the status of the manufacturing site at the time of the inspection noted above and should not be relied upon to reflect the compliance status if more than three years have elapsed since the date of that inspection, after which time the issuing authority should be consulted.

This certificate is valid only when presented with all pages and both Parts 1 and 2.

The authenticity of this certificate may be verified with the issuing authority.

date: 2013 -05- 22

Main Pharmaceutical Inspectorate
38/40, Długa Str., 00-238 Warsaw, Poland
Tel. +48 22 630 99 01, fax. +48 22 630 99 07

Zofia Ulz
Main Pharmaceutical Inspector

Fig. 3.54. Certificate in the following scope of activities: designing and performing of irradiation processes of medical devices (A); GMP certificate on sterilization of active substances/excipients/ finished products with use of electron beam (B)

According to European standard EN 552:1994 related to electron beam irradiation process control the system should be established and documented which ensures that the operation of the irradiator and its maintenance are carried out so that the established and documented process specifications are met. Electron energy, average beam current, scan width and conveyor speed shall be monitored and recorded. Conveyor control system for delivering required dose and data acquisition in sterilization process were developed and implemented to fulfill necessary requirements (Figs. 3.55 and 3.56). Introduced irradiation control system is based on the following assumptions:

- Products and/or dosimetry devices is transported in Al-containers only.
- Product packages size match Al-containers.

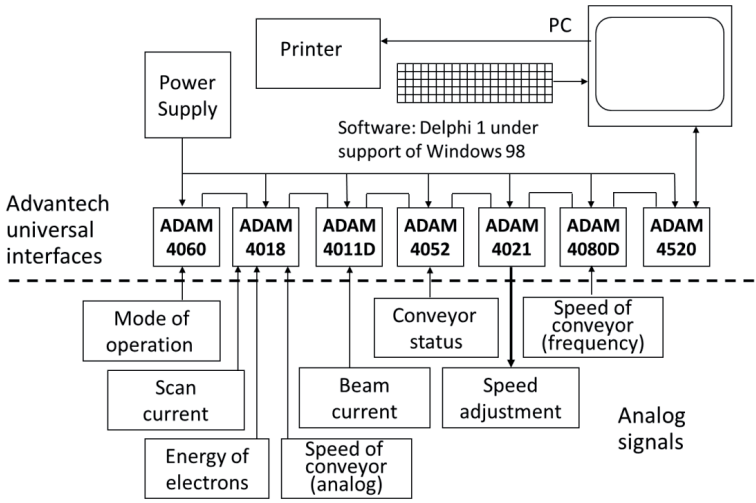


Fig. 3.55. Computer based data acquisition system and dose rate automatic control

- Each container has unique tag with barcode and number.
- Products loading into and unloading from containers is carried out according to specific procedures.
- Each product package gets unique label printed before unloaded from container.
- Product label barcode is a key to database record containing complete information regarding system status at the moment when box is irradiated. The moment when the box appears at the scanner position determines the time when it was under electron beam treatment.

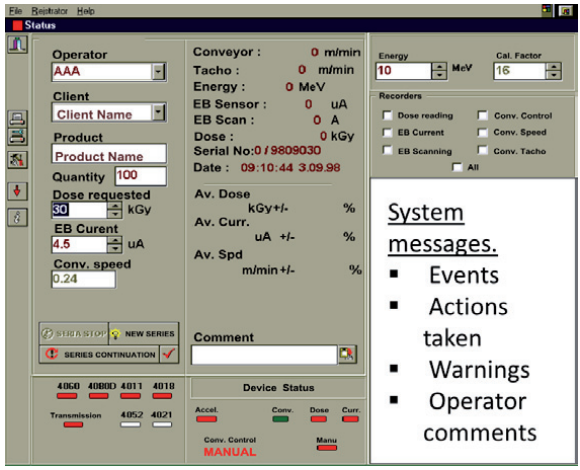


Fig. 3.56. Accelerator control system for delivering required dose and data acquisition in sterilization process

Computer based data acquisition system was designed to collect continuously information related to beam current level, conveyor speed and dose rate. Collected information is displayed and stored. The number of other information directly related to the sterilization process is included. The feedback loop were organized with help of universal interface system

ADAM type to stabilize dose rate by automatic conveyor speed correction due to actual beam current level.

It should be noticed that according to EN ISO 13485 the organization shall plan and implement the monitoring, measurement, analysis and improvement processes to: demonstrate the conformity of the product, ensure conformity of the quality management system and maintain the effectiveness of the quality management system. All the requirements for implementation of the plant's policy on radiation processing are laid down in written procedures. These documents are numbered and catalogued in the document control procedure. The issue of each procedure document is recorded. The following records are procedural documents directly involving irradiation of products: permanent records, procedural documents, and job description. Permanent records consists of:

- Customer ledger (individual consignment sheet for each customer).
- Batch book (details of the processing of product batches through the plant in consecutive order. Each page is checked and signed by the head of the plant. This is done each week).
- Dosimetry record book (record of dose measured together with the raw data showing optical density and dosimeter thickness. Each page is signed and dated by the person who read the dosimeters with the date of the reading).
- Batch control sheet (record of the irradiation process for each consignment processed. Individual responsibilities for each step during processing is accounted for. A list of initial for all relevant staff is maintained at the plant).
- Instrument calibration record (refers to the spectrophotometer, thickness gauges, timers and weighing scales).
- Certificate of irradiation (The head of the plant or other authorized person certifies treatment with reference to customer order and irradiation batch number. A list of specimen signatures for personnel authorized to sign certificates of irradiation is maintained at the plant).

Procedural documents includes:

- quality manual;
- standard operating procedure;
- step by step procedure for the receipt, processing and dispatch of products;
- document control procedure;
- maintenance schedules.

The objective of the management of the plant is to provide a service in a manner which conforms to the specified requirements of the customers, all applicable regulatory authorities, relevant safety standards and the quality assurance (QA) program. The QA program of the plant is designed to ensure that all requirements for quality are recognized and the consistent and uniform control of these requirements is adequately maintained. The QA program is designed to ensure that customer requirements are determined and are met with the aim of enhancing customer satisfaction.

Electronic system of documents circulation and archiving was implemented under upgrading program of radiation sterilization plant (Fig. 3.57). This system enables end-users to copy and move content stored in SharePoint document libraries and lists. Copy and move documents, pictures, list items and folders, export and import documents circulation and archiving are based on Microsoft SharePoint 2010 platform and MS Office program. The following content is accessible for personnel with certain capability to read and process provided information. Main library includes: archiving, QMS documents, QMS certifications, training, SMF, standards, literature, customers, low and administrative rules, technological instructions. Letter content includes: news, tasks, links, calendar, timetable of accelerator activity.

Practical sterilization of surgical transplants with the use of ionizing radiation is of great practical importance. The development of restorative and repair surgery contributes to the growing demand for tissue grafts. In addition to bones, this demand applies to cartilages, tendons, sclera, cornea, heart valves, skin and amniotic grafts. During the 40-year activity of the tissue banks, about 250 000 biostatic transplants were prepared in Poland, including

150 000 allografts sterilized by radiation (75% are bone grafts) and for the last 10 years the demand has increased over ten times. The use of biostatic grafts, especially bone grafts, eliminates or significantly limits the degree of disability of many patients and significantly shortens their treatment time.

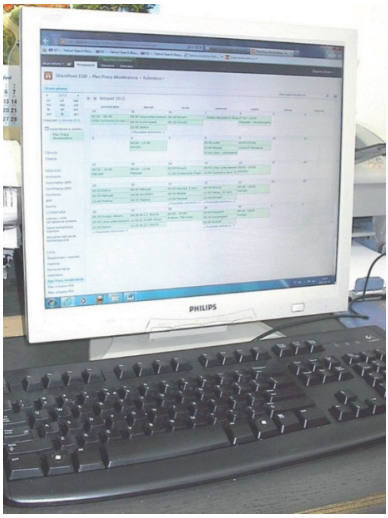


Fig. 3.57. Electronic system of documents circulation and archiving

Recently, research and radiation sterilization of packaging materials has been significantly developed. Electron beam irradiation of empty packaging (cartons, cans, boxes, bottles) is more and more often a separate treatment in the production cycle of products intended for medical applications.

## 3.4. ELECTRON BEAM PLANT FOR FOOD IRRADIATION

In the frame of the national program on the application of irradiation for food preservation and hygienization an experimental plant for electron beam processing has been established in the INCT. The pilot plant has been constructed inside an old fort what decreases significantly the cost of the investment. The pilot plant is equipped in an industrial unit Elektronika (10 MeV, 10 kW, producer: NPO Toriy, Moscow, Russia), which has been installed in the Experimental Plant for Food Irradiation (INCT) in 1990 [16]. This accelerator is a prototype unit, prior to the use for food treatment a period of optimization was involved in its experimental operation in 1993. The accelerator is capable to produce scanned beam of electrons with the energy 10 MeV and beam power of 10 kW. Radiation dose at minimal conveyor speed of 0.25 m/min reaches 50 kGy.

Accelerator Elektronika 10/10 is the linear resonance system in which electron beam is accelerated in microwave traveling – wave structure. Block diagram of the system is given in Fig. 3.58. Its technical characteristics are as follows:

- electron energy: 5-10 MeV;
- average beam current: 1 mA;
- average beam power: 6-10 kW;
- pulse duration: 2-6 μs;
- pulse repetition frequency: 50-300 Hz;

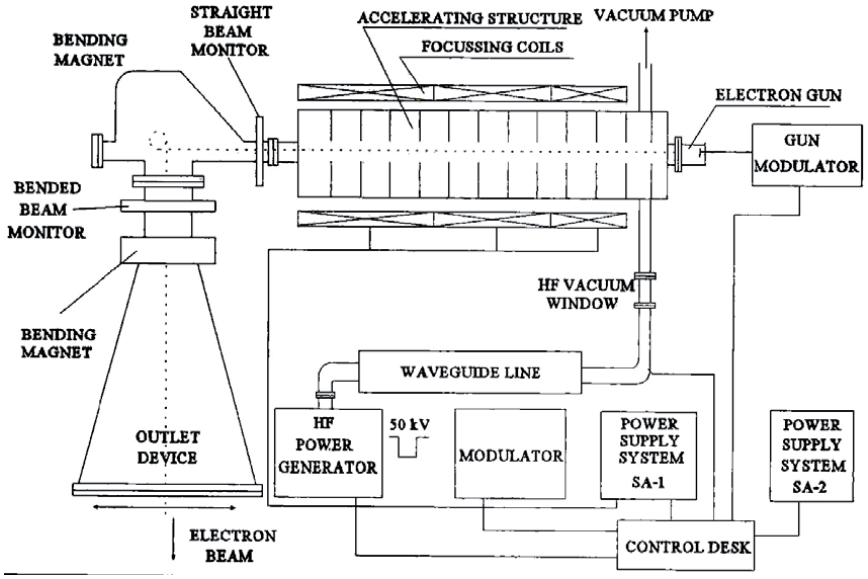


Fig. 3.58. Elektronika 10/10 accelerator's block diagram [17]

- scanning frequency: 1, 2, 5 Hz;
- scanning length: 60 cm;
- microwave generator frequency: 1886 MHz.

Fig. 3.59. Operation hall of the INCT Plant for Food Irradiation

The main parameters controlled during irradiation with electron beam are energy of electrons and the dose. In Plant for Food Irradiation has been installed a computer system which assures to obtain the desired dose of electron beam with energy 9.0-9.5 MeV by controlling accelerator parameters with the use of analog-digital steering system and collecting the data under technological conditions. Basing on the dose measurements at adjusted parameters and actual conveyor speed, the system calculates on-line the dose which is

recorded on computer hard disk. The system enables simultaneous on-line control of irradiation parameters dedicated to food products in agreement with EC directives 1999/2/EC and 1999/3/EC.

Accelerator Elektronika 10/10 is used for research and commercial scale irradiation. Operation hall of the INCT Plant for Food Irradiation is presented in Fig. 3.59. In recent years, the aim of the research study has been application of radiation methods to treatment of spices [18], medical herbs [19, 20], natural honey [21], meat lyophylized products [22], bait production to the control of crawling insects in urban areas [23] and plant growth substrates [24, 25].

During 25-year activity about 8000 tons of dry spices, mushrooms, vegetables and herbs was microbial decontaminated in the Plant. Additionally more then 10 000 000 pieces of packing materials for cosmetic and pharmaceutical industry and about 500 tons of cosmetic raw materials were irradiated.

## References


[1]. Zimek, Z., Waliś, L., & Chmielewski, A.G. (1993). EB industrial facility for radiation sterilization of medical devices. *Radiat. Phys. Chem.*, *42*, 1-3, 571-572.

[2]. Zimek, Z., Dźwigalski, Z., Warchoł, S., Roman, K., & Bułka, S. (2006). *Modernizacja Stacji Sterylizacji Radiacyjnej wyposażonej w akcelerator elektronów Elektronika 10/10. Część I*. Warszawa: Instytut Chemii i Techniki Jądrowej. Raporty IChTJ. Seria B, nr 3/2006.

[3]. Zimek, Z., Dźwigalski, Z., Warchoł, S., Bułka, S., Roman, K., & Barć, B. (2008). *Modernizacja Stacji Sterylizacji Radiacyjnej: układy i instalacje liniowego akceleratora elektronów LAE-10/15. Część II*. Warszawa: Instytut Chemii i Techniki Jądrowej. Raporty IChTJ. Seria B nr 8/2008.

[4]. Zimek, Z., Dźwigalski, Z., Warchoł, S., Roman, K., & Bułka, S. (2010). *Modernizacja Stacji Sterylizacji Radiacyjnej: montaż i uruchomienie układów i instalacji liniowego akceleratora elektronów LAE 10/15. Część III*. Warszawa: Instytut Chemii i Techniki Jądrowej. Raporty IChTJ. Seria B nr 5/2010.

[5]. Zimek, Z., Roman, K., Długoń, S., & Bułka, S. (2014). *Układ chłodzenia wodnego akceleratora elektronów LAE 10/15 stacji sterylizacji radiacyjnej*. Warszawa: Instytut Chemii i Techniki Jądrowej. Raporty IChTJ. Seria B nr 8/2014.

[6]. Zuev, Yu.V., Klinov, A.P., Krestianinov, A.S., Maslennikov, O.L., & Terentyev, V.V. Modifications of electron linear accelerators produced in NIIEFA for sterilization. In *XXV Russian Particle Accelerator Conference Proceedings, RuPAC-2016 : 21-25 November 2016, St. Petersburg, Russia* (pp. 505-507).

[7]. Zimek, Z., Roman, K., Długoń, S., & Bułka, S. (2015). *Tor mikrofalowy akceleratora elektronów LAE 10/15 stacji sterylizacji radiacyjnej*. Warszawa: Instytut Chemii i Techniki Jądrowej. Raporty IChTJ. Seria B nr 1/2015.

[8]. Zimek, Z., Przybytniak, G., & Kałuska, I. (2006). Radiation processing of polymers and semiconductors at the Institute of Nuclear Chemistry and Technology. *Nukleonika*, *51* (Suppl. 1), S129-S132.

[9]. Sun, Y., & Chmielewski, A.G. (2017). *Applications of ionizing radiation in materials processing* (Vol. 1 and 2). Warszawa: Insitute of Nuclear Chemistry and Technology. http://www.ichtj.waw.pl/ichtj/publ/monogr/m2017_1.htm.

[10]. Zimek, Z., Kołyga, S., Levin, V.M., Nikolaev, V.M., Rumyantsev, V.V., & Fomin, L.P. (1972). An Institute of Nuclear Research electron linac. *Nukleonika*, *17*, 1-2, 67-75.

[11]. Zimek, Z., Rzewuski, H., & Migdał, W. (1995). Electron accelerators installed at the Institute of Nuclear Chemistry and Technology. *Nukleonika*, *40*, 3, 93-114.

[12]. Zimek, Z., Waliś, L., & Chmielewski, A.G. (1993). EB Industrial Facility for Radiation Sterilization of Medical Devices. *Radiat. Phys. Chem.*, *42*, 1-3, 571-572.

[13]. Zimek, Z., & Kałuska, I. (2001). Sterylizacja radiacyjna sprzętu medycznego jednorazowego użytku przeszczepów. *Compedium Stomatologii*, 1, 21-23.

[14]. Zimek, Z., & Kałuska, I. (2002). Sterilization dose auditing for various types of medical products. *Radiat. Phys. Chem.*, *63*, 673-674.
[15]. Lazurik, V.T., Lazurik, V.M., Popov, G.F., Rogov, Yu.V., & Zimek, Z. (2008). Integration of computation methods into radiation sterilization process. *Journal of Kharkiv University, Physical Series: Nuclei, Particles, Fields,* 832, 77-82.
[16]. Migdal, W., Walis, L., & Chmielewski, A.G. (1993). The pilot plant for electron beam food processing. *Radiat. Phys. Chem.*, *42* (1-3), 567-570.
[17]. Migdal, W., & Maciszewski, W. (1995). Application of "Elektronika 10-10" electron linac for food irradiation. *Radiat. Phys. Chem.*, *46* (4-6), 749-752.
[18]. Chmielewski, A. G., & Migdal, W. (2005). Radiation decontamination of herbs and spices. *Nukleonika*, *50* (4), 179-184.
[19]. Owczarczyk, H.B., Migdal, W., & Kędzia, B. (2000). The pharmacological activity of medical herbs after microbiological decontamination by irradiation. *Radiat. Phys. Chem.*, *57*, 331-335.
[20]. Migdal, W., & Owczarczyk, B. (1998). The effect of ionizing radiation on microbiological decontamination of medical herbs and biologically active compounds. *Radiat. Phys. Chem.*, *52* (1-6), 91-94.
[21]. Migdal, W., Owczarczyk, H.B., Kędzia, B., Hołderna-Kędzia, E., & D. Madajczyk. (2000). Microbiological decontamination of natural honey by irradiation. *Radiat. Phys, Chem.*, *57*, 285-288.
[22]. Migdal, W., & Owczarczyk, H.B. (2000). Radiation deconatamination of meat lyophylized products. *Radiat. Phys. Chem.*, *63*, 371-373.
[23]. Migdal, W., Owczarczyk, H.B., Świętosławski, J., & Świetosławski, J. (2000). Application of irradiation in bait production to the control of crawling insects in urban areas. *Radiat. Phys. Chem.*, *57*, 551-553.
[24]. Orlikowski, L.B., Migdał, W., Ptaszek, M., & Gryczka, U. (2011). Effectiveness of electron beam irradiation in the control of some soilborne pathogens. *Nukleonika*, *56*(4), 357-362.
[25]. Migdał, W., Orlikowski, L.B., Ptaszek, M., & Gryczka, U. (2012). Influence of electron beam irradiation on growth of *Phytophthora cinnamomi* and its control in substrates. *Radiat. Phys. Chem.*, *81*, 1012-1016.

**Chapter 4**

# ACCREDITED LABORATORIES

**Marta Walo, Anna Korzeniowska-Sobczuk, Grażyna Liśkiewicz, Magdalena Miłkowska, Grzegorz Guzik**

## 4.1. INDUSTRIAL DOSIMETRY

Quantitative measurements of absorbed energy in radiation processing are based on many dosimetry systems described in the standards ISO and ASTM [1]. Combined with control systems, it is possible to precisely deliver the appropriate dose to the irradiated object. Radiation dosimeters allow to determine directly or indirectly absorbed dose, its spatial distribution and dose rate. The dosimeter and its reader are referred to as a dosimetry system [2]. The following properties of the dosimetry systems require characterization: relationship between the dosimeter response and the absorbed dose, influence of ambient conditions (temperature, humidity, exposure to light, etc.), dosimeter stability and detection threshold.

In order to conduct dosimetry correctly, several factors have to be taken into account, particularly the level of accuracy and precision in determining the dose and traceability of the results. Such activity is an integral part of quality control in radiation processing. Process control includes the correlation between parameters of irradiation facility and dose deposited in the irradiated product.

According to ISO/ASTM 52701:2013 dosimetry systems are classified as type I, when they play a role of reference or standard system, or type II applied usually in routine dosimetry. Type I dosimeters represent high metrological quality, therefore they are applied for calibration of type II dosimeters. Such systems are characterized by low uncertainty and traceability and should fulfill international standards. The primary standards used to specify a unit of quantity from its definition are verified by the primary standard dosimetry laboratories to ensure consistency of the dose determination. They are used to calibrate dosimeters for secondary standard dosimetry laboratories having appropriate accreditation. Then, based on the reference dosimeters, routine dosimeters are calibrated and then used for monitoring absorbed doses in industrial radiation processing with electron beam or gamma rays.

Dosimetry systems are essential for quality control of radiation processing because they demonstrate that the treatment is well-established technology and that has been carried out under control and according to the standards.

Requirements for radiation processing cover development, validation and routine control of the process. Installation qualification (IQ) of radiation facility is the first important stage in the implementation of technology. IQ proves that radiation source together with associated facilities and measuring instruments have been provided and installed in accordance with the specification. The procedure also includes devices applied in dosimetry systems.

The purpose of operational qualification (OQ) is to demonstrate that installed source of ionizing radiation meets the predetermined acceptance criteria and is capable of delivering the appropriate doses. The procedure allows finding relationships between parameters of the facility and determine their effect on the doses absorbed by irradiated products.

Performance qualification (PQ) program refers to the quality of the service performed for the specific objects. For each product the controlled set of parameters is determined in order to confirm that the desired absorbed dose can be achieved. The results obtained by dose mapping are needed to determine whether the absorbed energy does not exceed a specified range.

Everyday industrial practice requires proof that radiation treatment has been carried out in a controlled manner. For this purpose routine dosimetry is performed which verify whether applied process parameters are correct and in accordance with PQ.

Electron beam irradiators are described by the position and the shape of the beam spot, the electron energy, the beam current, the scan width and the scan uniformity [3]. The electron beam profile and the scan width need to be known to ensure a proper dose distribution pattern in the volume of the irradiated product. At the INCT in order to check whether the beam covers the entire width of the conveyor, it is necessary to irradiate the dosimetric film in a static manner for 30-40 s. After heating the foil, a very clear trace of the electron beam along the conveyor plane is observed (Fig. 4.1). These tests are carried out twice a year.

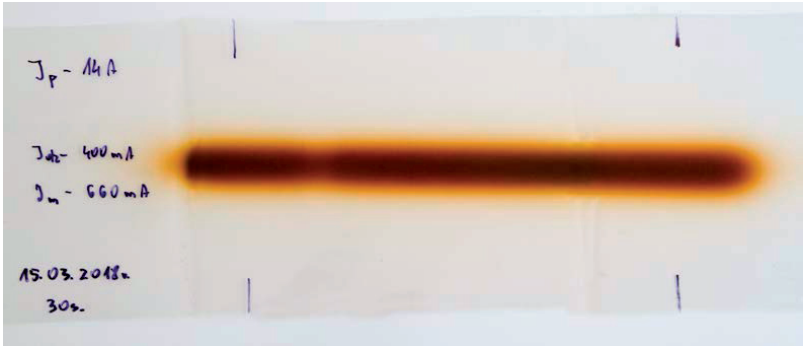


Fig. 4.1. PCV foil used for showing the electron beam width

In spite of many dosimeters available on the market, accurate and reproducible high dose dosimeters are difficult to choose due to many variables. Additionally, selection of dosimetry system usually is accompanied by an assessment of individual and combined uncertainties, the procedure critical to ensure traceability of the results.

*Alanine*

Alanine is used as a transfer standard and in routine dosimetry [4]. It shows reliable results covering a wide range of doses with one type of detector (electron paramagnetic resonance spectroscopy) and unusual stability at ambient conditions. Amplitude of the detected signal is proportional to the population of radicals generated by ionizing radiation. The commercial dosimeters are available in the form of pellets (L-α-alanine in paraffin, polystyrene or poly-ethylene) or as a coating on a polyester matrix. They were successfully applied in radiation processing in the dose range 1-100 kGy and the radiation energy for photons and electrons is between 0.1 and 30 MeV. The irradiation temperature is from -78°C to +70°C. Amplitude of the EPR signal for the selected dose increases with increasing temperature by about 0.24%/°C [5]. However, McLaughlin from NIST reported that the coefficient depends on dose and from 3 kGy to 100 kGy rises from 0.159%/deg to 0.194%/deg, respectively [6]. It was also observed that during the first 8 days after irradiation the value increases slightly around 2%. No influence of the four dose fractions on the response of alanine to electron beam irradiation was confirmed by Lundahal et al. [7].

*Thin films*

Thin film dosimeters have many advantages over liquid. They are smaller, have longer durability and are easy to use. Films provide mapping with high spatial resolution. They can be used to measure large doses in various industrial processes giving accurate data up to 1 MGy. The dosimeters can be used as undyed polymeric membranes (cellulose acetate, polyvinyl chloride, polychlorostyrene, polyethylene terephtalate, polystyrene) which after irradiation demonstrate absorption bands in the region of 290-400 nm. Plastic dye dosimeters based usually on celluloid/cellophane matrix might absorb analytical light in the whole visible range. Colors of the films sometimes bleach upon exposure to ionizing radiation [8]. There are also several

commonly used dosimeters based on methyl metacrylate – red Perspex, amber Perspex and the Gammachrome YR [9].

Some film dosimeters show instability of the dosimetry signal and tendency to saturate at high doses. Because they might reveal dose rate dependent response, careful selection of the film dosimeters is necessary. Fading of the colors of unirradiated and irradiated dyed films, particularly stored in sunlight, is another phenomenon requiring attention [10]. Usually optical absorption readout is used for film dosimetry.

Routine radiochromic dosimeters containing tetrazolium salts found application in radiation processing performed in the kGys range which could be increased by increasing concentration of the dyes. The data requires corrections with respect to thermal effects, humidity and post-irradiation stability.

B3 dosimeter has been developed at the Risø National Laboratory as a polyvinyl butyral film containing leucocyanide of pararosaniline. During irradiation up to 100 kGy, the additive gradually becomes pink. B3 dosimeter has found a widespread application in both gamma and electron beam radiation processing.

Sunna film consists of LiF dispersed in a polymeric matrix. In order to optically determine absorbed dose simulating luminescence method is applied. Response of the dosimeter to gamma radiation is higher than to electron beam irradiation at the same dose. The radiation energy for photons is 0.05-10 MeV and for electron is 0.1 MeV to 10 MeV. For Sunna film the absorbed dose range is between 50 Gy and 300 kGy. The irradiation temperature can be from -20$^{o}$C to +60$^{o}$C.

*Solutions*

Liquid dosimeters usually consist of inorganic solutes in solvents which during irradiation create oxidizing or reducing environment. Radiolytic products modify solutes which allows detection of absorbed dose via indirect effect of ionizing radiation.

Ferrous-sulfate solution (Fricke dosimeter) is the best known dosimeter for which detection of absorbed doses based on the formation of ferric ions with radiation yield of 1.65 μJ/mol.

The absorbed dose within the range between 20-400 Gy can be measured using this dosimeter. The irradiation temperature is 10-60$^{o}$C. The measurement absorbance values for Fricke dosimeter is at wavelength of 304 nm.

Potassium dichromate dosimeter is reduced to chromic ion when exposed to ionizing radiation. The reaction is followed by UV-Vis spectrophotometry or by electrochemical potentiometry. Dose measurements within the range of 2-50 kGy are based on color changes in the solution at a 440 nm due to radiolytic reduction of dichromate ions to chromic ions. The irradiation temperature is 0-80$^{o}$C.

Ceric-cerous sulfate solutions give consistent response in the dose range of 5-50 kGy or 0.5-5 kGy, depending on the initial content of ceric ions. The changes in concentration of ceric ions are assessed either by UV-Vis spectroscopy or by potentiometry method. The irradiation temperature is 0-62$^{o}$C.

Ethanol-monochlorobenzene (ECB) solution is used to follow deposited dose by oscillometric read-out or by UV-Vis spectrophotometry. The dosimeter is capable of measuring doses form 1 kGy to 300 kGy. The temperature coefficient is 0.05%/$^{o}$C. The absorbed dose range is 10 Gy-2 MGy for gamma and 10 Gy-200 kGy for electron beam. The irradiation temperature is between -40 and +80$^{o}$C.

For all dosimeters presented above, initial energy for photons is greater than 0.6 MeV, for X-radiation is equal to or greater than 2 MeV and for electron beams is greater than 8 MeV.

*Calorimeters*

Calorimetry is an absolute dosimetry method. Calorimeters consist of disks thermally insulated by polystyrene foam. Temperature increase during irradiation measured by a calibrated thermistor placed in the disk is proportional to absorbed dose [11]. The proportionality factor is specific heat of the disk, usually made of graphite (Fig. 4.2), water or polystyrene. The geometry of the disk depends on energy of the electron beam [12]. Its thickness decreases with decreasing electron energy to avoid total absorption of radiation in the dosimeter. The practice

A B

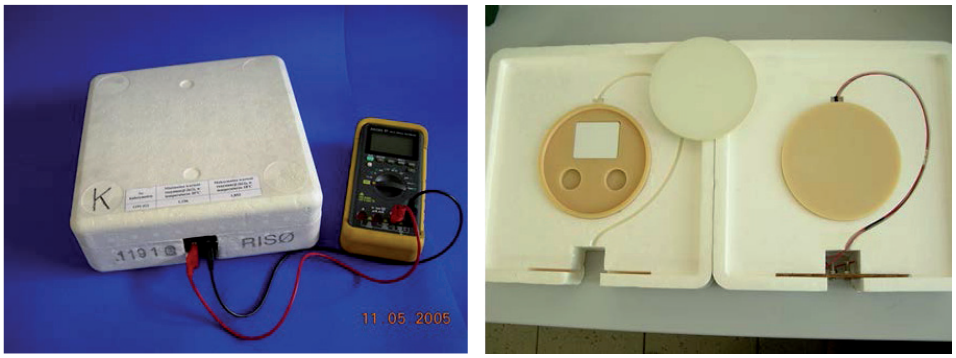


Fig. 4.2. Calorimetric dosimeters: graphite (A) and polystyrene (B) used for electron beam related measurements

POLSKIE CENTRUM AKREDYTACJI
POLISH CENTRE FOR ACCREDITATION

PCA POLSKIE CENTRUM AKREDYTACJI

Sygnatariusz EA MLA
EA MLA Signatory

CERTYFIKAT AKREDYTACJI
LABORATORIUM BADAWCZEGO
ACCREDITATION CERTIFICATE OF TESTING LABORATORY
Nr AB 461

Potwierdza się, że: / This is to confirm that:

INSTYTUT CHEMII I TECHNIKI JĄDROWEJ
LABORATORIUM POMIARÓW DAWEK TECHNOLOGICZNYCH
ul. Dorodna 16, 03-195 Warszawa

spełnia wymagania normy PN-EN ISO/IEC 17025:2005
meets requirements of the PN-EN ISO/IEC 17025:2005 standard

Akredytowana działalność jest określona w Zakresie Akredytacji Nr AB 461
Accredited activity is defined in the Scope of Accreditation No AB 461

Akredytacja pozostaje w mocy pod warunkiem przestrzegania wymagań jednostki akredytującej określonych w kontrakcie Nr AB 461
This accreditation remains in force provided the Laboratory observes the requirements of Accreditation Body defined in the Contract No AB 461

Certyfikat akredytacji ważny do dnia 26.02.2020 r.
The certificate of accreditation is valid until 26.02.2020

Akredytacji udzielono dnia 27.02.2004 r.
Accreditation was granted on 27.02.2004

POLSKIE CENTRUM AKREDYTACJI

DYREKTOR
POLSKIEGO CENTRUM AKREDYTACJI
LUCYNA OLBORSKA

Warszawa, dnia 24 lutego 2016 roku

Fig. 4.3. Accreditation certificate of the Laboratory for Measurements of Technological Doses

use of calorimeters applies to electron beam in energy range from 1.5 MeV to 12 MeV. The absorbed dose range depends on the absorbing material and the irradiation and measurement conditions. Minimum dose is approximately 100 Gy and maximum dose is approximately 50 kGy. Reproducible measurements were confirmed for a range of doses from 3 kGy to 40 kGy for a polystyrene calorimeter.

*Dosimetry at the INCT*

At the Institute of Nuclear Chemistry and Technology (INCT) measurements of doses of gamma radiation and high energy electron radiation and development on new methods of chemical dosimetry is performed by the Laboratory for Measurements of Technological Doses (LMTD).

The LMTD was established in 1998 to ensure reliable technological dose measurements and to enhance quality assurance of the INCT technological plants. The LMTD is accredited by the Polish Centre for Accreditation (PCA) as a testing laboratory according to the requirements of the PN-EN ISO/IEC 17025:2005 standard (Fig. 4.3).

The Polish Centre of Accreditation is a member of the European co-operation for Accreditation (EA), and thus all laboratories accredited by the PCA are recognized as fulfilling the EA requirements.

The scope of the LMTD accreditation includes measurements of absorbed doses of gamma radiation from 20 Gy to 80 kGy and high energy electrons from 1.5 kGy to 40 kGy. All results of the measurements are traceable to the National Physical Laboratory (NPL) primary standards and presented together with expanded uncertainty values.

The LMTD maintains the following accredited dosimetry systems:

- Fricke dosimetry system,
- CTA film dosimetry system,
- calorimetric dosimetry system.

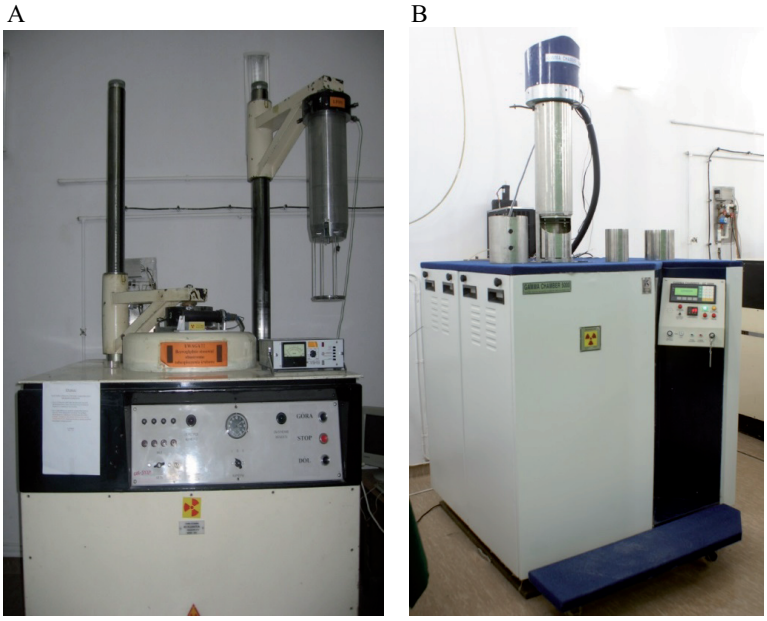


Fig. 4.4. Gamma cells: (A) Issledovatiel (dose rate: 0.25 kGy/h) and (B) GC5000 (dose rate: 2.5 kGy/h)

Other accredited LMTD activities are as follows:

- irradiation of customer's dosimeters or small samples with gamma radiation (using gamma cells with different activities: Issledovatiel (dose rate: 0.25 kGy/h; Fig. 4.4A) or GC5000

(dose rate: 2.5 kGy/h, Fig. 4.4B) to doses higher than 20 Gy or with 10 MeV electrons to the doses higher than 1.5 kGy;
- investigation of sensitivity of dosimeters for ionizing radiation.

The LMTD quality system is based on the PN-EN ISO/IEC 17025:2005 standard and the ISO/ASTM standard 51400:2003(E), what assures a proficiency of the dose measurements and high accuracy of the results.

Activities of LMTD are used in many fields such as medicine (radiation sterilization of medical devices and allografts), ecology (biological materials), plastic industry (radiation modification of polymeric materials).

Currently, the following activities are performed:
- traceability of dose measurements for routine dosimetry in radiation sterilization of medical devices using graphite and polystyrene calorimeters and the sensitivity investigation of dosimeters used for routine film dosimetry process (ISO 11137-3 standard);
- dose mapping performed during operational and performance qualification. (ISO 11137-3 standard);
- dosimetry of sealed $^{60}$Co sources (using Fricke dosimeter and CTA) for later use in: radiation modification of polymers, radiation biology and medicine;
- estimation of the dose distribution homogeneity in the products of biological importance;
- development of the dosimetric methods for controlling the sterilization of tissue allografts, carried out at a temperature of dry ice using film dosimeters B3, PVC, CTA and calorimeters in room temperature.

Customers satisfaction is a primary goal of the LMTD quality system. Thus, the LMTD cooperates with the customers in clarifying their requests and in monitoring the laboratory performance in relation to their work. The LMTD procedure of sample identification ensures confidentiality of the client data. The feedbacks from the customers are used to improve the management system, testing and calibration activities and customer service. The quality system also includes the policy and procedures for the resolution of customer complaints.

Besides providing assistance in testing and calibration of the customers' dosimetry systems, the LMTD also offers the following services and products:
- individual or group training in high dose dosimetry for gamma radiation and high energy electrons using such dosimetry systems as: Fricke, CTA films, PVC films, B3 films, graphite and polystyrene calorimeters;
- for sale: water-proof, routine alanine-polymer dosimeters alanpol® (patented) [13, 14].

Very important activities are related to the dosimetry intercomparison tests performed in the frame of IAEA Regional Project RER1019 "Enhancing standardized radiation technologies and quality control procedures for human health, safety, cleaner environment and advanced materials" active for years 2018-2019. In the frame of previous project RER 1017 "Using advanced radiation technologies for materials processing" active in the years 2016-2017 the following countries were participating in such exercise: gamma facilities – Azerbaijan, Bulgaria, Croatia, Hungary, Portugal, Romania, Serbia, Turkey; and electron beam facilities – Romania, Russia, Slovakia, Ukraine. In the present intercomparison tests 23 units are participating, among them new countries such as Belarus (electron beam + gamma), Russian Federation (electron beam) and Uzbekistan (electron beam).

## 4.2. IRRADIATED FOOD DETECTION

### 4.2.1. Introduction

In 1994, the Laboratory for Detection of Irradiated Food was created at the Institute of Nuclear Chemistry and Technology (INCT). Since then, the professional and highly experienced staff have been working to improve irradiation detection methods adapted in the

Laboratory and to make them more sensitive and reliable for an extended group of food articles [15].

The adoption of a quality assurance system resulted in the accreditation of the Laboratory in 1999 by the Polish Centre for Testing and Certification (PCBC; presently the Polish Centre for Accreditation, PCA). Since that time, the Laboratory for Detection of Irradiated Food has constantly maintained the status of an accredited R&D unit and is authorized to carry out the examination of food samples and to classify them as being either irradiated or non-irradiated. Every four years, the Laboratory accreditation certificate must be renewed after successfully passing the PCA expert audit. The current accreditation certificate, which is the 6th, was received on 24th July 2018 and is valid until 24th October 2022 (Fig. 4.5).


POLSKIE CENTRUM AKREDYTACJI
POLISH CENTRE FOR ACCREDITATION

PCA

Sygnatariusz EA MLA
EA MLA Signatory

CERTYFIKAT AKREDYTACJI
LABORATORIUM BADAWCZEGO
ACCREDITATION CERTIFICATE OF TESTING LABORATORY
Nr AB 262

Potwierdza się, że: / This is to confirm that:

Instytut Chemii i Techniki Jądrowej
Samodzielne Laboratorium
Identyfikacji Napromieniowania Żywności
ul. Dorodna 16, 03-195 Warszawa

spełnia wymagania normy PN-EN ISO/IEC 17025:2005
meets requirements of the PN-EN ISO/IEC 17025:2005 standard

Akredytowana działalność jest określona w Zakresie Akredytacji Nr AB 262
Accredited activity is defined in the Scope of Accreditation No AB 262

Akredytacja pozostaje w mocy pod warunkiem przestrzegania wymagań jednostki akredytującej określonych w kontrakcie Nr AB 262
This accreditation remains in force provided the Laboratory observes the requirements of Accreditation Body defined in the Contract No AB 262

Certyfikat akredytacji ważny do dnia 24.10.2022 r.
The certificate of accreditation is valid until 24.10.2022

Akredytacji udzielono dnia 25.10.1999 r.
Accreditation was granted on 25.10.1999

POLSKIE CENTRUM AKREDYTACJI

DYREKTOR
POLSKIEGO CENTRUM AKREDYTACJI
LUCYNA OLBORSKA

Warszawa, 24 lipca 2018 roku

Fig. 4.5. Accreditation certificate of the Laboratory for Detection of Irradiated Food

The *Scope of Accreditation*, an integral part of the accreditation certificate, offers customers five methods suitable to detect radiation treatment in almost all of food available on the open market. Nowadays, many food items such as herbal pharmaceuticals, diet supplements, and food extracts, are received by the Laboratory for examination of irradiation from our domestic and foreign customers. The application of five standardized detection methods

(Table 4.1) to specified groups of foods that were validated in the Laboratory guarantees the accurate analysis and reliable classification of food samples delivered to the Laboratory for testing.

Table 4.1. The detection methods used in the Laboratory for Detection of Irradiated Food

| Method in the Laboratory use | Method for the detection of irradiated food | Method based on an analytical procedure described by the CEN European standard |
|---|---|---|
| Electron paramagnetic spectroscopy (EPR/ESR) | containing bone | EN 1786 [16] |
| | containing cellulose | EN 1787 [17] |
| | containing crystalline sugars | EN 13708 [18] |
| Thermoluminescence (TL) | from which silicate minerals can be isolated | EN 1788 [19] |
| Photostimulated luminescence (PPSL) | containing silicate minerals | EN 13751 [20] |

Since 2017, the Laboratory has reported a large increase in the number of samples delivered by domestic customers to be analyzed. Samples were also delivered by foreign customers from Germany, Italy, Denmark, Latvia, Hungary, Spain, France, Norway, Malta, China and USA. The assortment of samples received comprised food extracts, herbal pharmaceuticals, diet supplements, spices, dried vegetables and red fermented rice.

Normative regulations of EU Parliament respected in member states and many other countries qualify vegetal extracts as food, following FAO/WHO Codex Alimentarius classification of diet supplements containing vegetal extracts, vitamins and microelements considered foodstuffs [21]. In order to assure microbial safety of vegetal extracts and diet supplements, as well as to extend their safe storage time, the articles are subjected the conservation or preservation procedure, preferentially by exposure to ionizing radiation [22, 23]. These articles therefore undergo inspection to determine whether have been irradiated or not. The most important group of foodstuffs analyzed in the Laboratory of Detection of Irradiated Food are extracts obtained from herbs by water-alcohol extraction. There are widely used in pharmaceutical industry as important components of popular diet supplements.

Among ten of CEN (European Committee for Standardization) standardized methods for the detection of irradiated food, only three are considered adaptable for the detection of radiation-treated vegetal extracts, food supplements and animal bonds or nuts shells. One is based on thermoluminescene (TL) released from silicate minerals isolated from vegetal extracts while the other one is based on the photo-stimulated luminescence (PSL) released from the product as a whole. But detection of irradiated food containing fat is investigated by gas chromatographic analysis of hydrocarbons or gas chromatographic with mass spectrometry analysis of 2-alkylocyclobutanones [24, 25]. The Laboratory offers analytical services in detection of irradiated foodstuffs to domestic and foreign customers for an extended assortment of food articles *via* the use of five appropriate and normalized analytical methods presented in Table 4.1.

### 4.2.2. Electron paramagnetic resonance method based on three European standards

The most interesting in Laboratory practice are three of electron paramagnetic resonance (EPR) methods. Unfortunately, it is possible to use them only for several kind of products, for example bones of animals, shrimps, some seasonings or herbs, fruits containing sugars and nuts. Analytical aspect of detection of their potential irradiation is in accordance with the protocol of

CEN European standard listed in Table 4.1. Depending on the species examined by the EPR method, the food components tested are bones, peels, stones, shells, skins, pulp or flesh of fruits. The samples taken for investigation were dried for 48 h at 40°C in a dryer machine under a flow of dry air. A suitable portion of each samples was placed in a signal-free glass ampoule 4 mm in diameter and subsequently measured with a Bruker EMX plus EPR spectrometer equipped with Xenon software.

The dried fruit components of diet supplements and fruit extracts are supposed to positively influence human condition and health. These components are usually dried in a traditional manner and contain many impurities and microbial contaminants, including dangerous pests. For that reason, dried fruits undergo disinfection leading to microbial decontamination. One of the most effective methods of microbial decontamination of dried and fresh fruits is irradiation [22, 23]. As recommended by a FAO/WHO expert group, the safe dose of ionizing radiation as applied to food is 0.2-10 kGy [21], while in the case of dried spices and fruits it is 5-10 kGy, depending on the content of microbial contaminants. The most popular fruits for preservation with the use of ionizing radiation are: plum, apricot, strawberry, cherry, cranberry, date, raisin, mulberry, fig, and blackcurrant. All the fruits are irradiated with doses of 0.3 kGy and 0.5 kGy, it means the lowest recommended technological doses in factory use [26, 27].

### 4.2.3. Thermoluminescence method based on EN 1788 European standard

Irradiation detection obtained by the termoluminescence method is based on the TL measurement of silicate minerals isolated from the herbs, spices and plant extracts. The TL method is found to be more sensitive than PSL method and suitable for the routine control of vegetal extracts in specialized laboratories. Silicate minerals isolated from the samples were placed in stainless steel TL measuring cups and heated overnight at 50°C. Thermoluminescence measurements were carried out with a Risø TL/OSL DA 20 reader. That instrument adjustments are presented in Table 4.2.

Table 4.2. Operational parameters of TL measurements

| Measurement parameters | |
|---|---|
| Initial temperature | 70°C |
| Final temperature | 450°C |
| Heating time | 30 s |
| Speed of the heating | 6°C/s |

Two subsequent TL measurements should be conducted with each sample: the primary measurement (glow 1) and the calibrated measurement (glow 2) which has been carried out after 1 kGy normalizing $^{60}$Co irradiation of TL measuring cups containing the isolated minerals.

### 4.2.4. Photo-stimulated luminescence method based on EN 13751 European standard

The PSL measurements were conducted with the irradiated food screening system (measuring set) by the Scottish Universities Research and Reactor Centre (SURRC) in darkness at ambient temperature with a relative humidity of 85%. The operational parameters of the measuring set were adjusted as presented in Table 4.3.

Each sample should be measured twice with the use of PPSL (pulsed PSL) method; firstly time untreated and secondly after re-irradiation with a 4 kGy dose of $^{60}$Co gamma rays. All the measurements have been carried out 48 h after radiation treatment at room temperature (it means about 20°C).

Table 4.3. Operational parameters of PPSL measurements

| Measurement parameters | |
|---|---|
| Frequency of counting | 60 cpm |
| Lower threshold value of PPSL | 700 cpm |
| Upper threshold value of PPSL | 5000 cpm |
| Approximate light count | 35 cpm |
| Approximate dark count | 20 cpm |

### 4.2.5. Final remarks

The PPSL method is less time-consuming and markedly faster than TL method. The methods is applied in the industry for the control of crude unprocessed herbs and spices typically in the form of dried leaves or roots. But the EPR method is dedicated for bones from mammals or fish, nuts shells as well.

Nowadays, thermal or high pressure treatment combined with irradiation have been applied for the decontamination of foodstuffs. In such combined disinfection processes markedly lower doses of ionizing radiation than those recommended are required. On the other hand, detection of potential irradiation is more difficult if such a low dose irradiation was applied for fresh products, especially when the products were examined after a long period of storage. In other words, the possibility of irradiation detection in food products irradiated with low doses of ionizing radiation and stored for a prolonged period is complicated. That is why the Laboratory for Detection of Irradiated Food is actively and effectively implementing improved analytical and measurement procedures that are suitable for detection of irradiation in complex food articles containing low or very low concentrations of irradiated ingredients. These are typically aromatic herbs, spices and powders of dried fruits or plant pharmaceuticals admixed to the product. It has been experimentally proven that modification of the mineral isolation procedure, the determination of isolated mineral content, and the effectiveness of mineral thermoluminescence are the important factors that influence the detection ability of the employed analytical method.

From 19th June 2012 the Laboratory for Detection of Irradiated Food has held the status of the reference laboratory (National Reference Laboratory No. 5) in the field of the detection of irradiated food in Poland under the nomination of the Ministry of Health. As such, the Laboratory is responsible for the organization of the control and monitoring of irradiated food around the country.

### References


[1]. Farrar, H. (2000). Twenty new ISO standards on dosimetry for radiation processing. *Radiat. Phys. Chem.*, *57*, 717-720.

[2]. Abaza, A.M.H. (2018). New trend in radiation dosimeters. *American Journal of Modern Physics*, *7*(1), 21-30.

[3]. IAEA. (2013). *Guidelines for the development, validation and routine control of industrial radiation processes*. Vienna: IAEA. IAEA Radiation Technology series No. 4.

[4]. OIML. (2001). *Alanine EPR dosimetry systems for ionizing radiation processing of materials and products*. International Organization of Legal Metrology. OIML R 132, edition 2001 (E).

[5]. Desrosiers, M.F., Cooper, S.L., Puhl, J.M., McBain, A.L., & Calvertet, G.W. (2004). A study of the alanine dosimeter irradiation temperature coefficient in the 77°C to 50°C range. *Radiat. Phys. Chem.*, *71* (1-2), 365-370.

[6]. McLaughlin, W.L. (2000). Reference dosimetry and calibrations with x and gamma rays and electron beams. In K. Mehta (Ed.), *Dosimetry for radiation processing* (pp. 125-129). Vienna: IAEA. IAEA-TECDOC-1156.
[7]. Lundahl, B., Logar, J., Desrosiers, M., & Puhl, J. (2014). Effects of dose fractionation on the response of alanine dosimetry. *Radiat. Phys. Chem.*, *105*, 94-97.
[8]. Kattan, M., Kassiri, H., & Daher, Y. (2011). Using polyvinyl chloride dyed with bromocresol purple in radiation dosimetry. *Appl. Radiat. Isot.*, *69*, 377-380.
[9]. McLaughlin, W.L. (2003). Radiation chemistry of anionic disazo dyes in cellophane films applications for high-dose dosimetry. *Radiat. Phys. Chem.*, *67*, 561-567.
[10]. Dolo, J.M., Feaugas, V., & Pichot, E. (2000). Modelization of the physical and chemical phenomenon of fading and control of the parameters for quality assurance of EPR/alanine measurements. In: K. Mehta (Ed.), *Dosimetry for radiation processing* (pp. 125-129). Vienna: IAEA. IAEA-TECDOC-1156.
[11]. McLaughlin, M.L., & Walker, J.C. (1995). Humphreys calorimeters for calibration of high dose dosimeters in high energy electron beams. *Radiat. Phys. Chem.*, *46*, 1235-1242.
[12]. Miller, A. (1995). Polystyrene calorimeter for electron beam dose measurements. *Radiat. Phys. Chem.*, *46*, 1240-1243.
[13]. Stuglik, Z., Bryl-Sandelewska, T., & Mirkowski, K. (2006). *Alaninowo-polimerowy dozymetr promieniowania jonizującego* (Alanine-polymer type ionising radiation disimeter). Polish Patent 194369.
[14]. Stuglik, Z. (2012). *Dozymetr alaninowo-polimerowy o podwyższonej czułości* (Alanine-polymer dosimeter). Polish Patent 212895.
[15]. Stachowicz, W., Malec-Czechowska, K., Dancewicz, A.M., Szot, Z., & Chmielewski, A.G. (2002). Accredited laboratory for detection of irradiated foods in Poland. *Radiat. Phys. Chem.*, *63*, 427-429.
[16]. European Committee for Standardization. (2000). Foodstuffs – *Detection of irradiated food containing bone – Method by ESR spectroscopy*. PN-EN 1786:2000.
[17]. European Committee for Standardization. (2001). *Foodstuffs – Detection of irradiated food containing cellulose by ESR spectroscopy.* PN-EN 1787:2001.
[18]. European Committee for Standardization. (2003). Foodstuffs – *Detection of irradiated food containing crystalline sugar by ESR spectroscopy*. PN-EN 13708:2003.
[19]. European Committee for Standardization. (2002). *Foodstuffs – Thermoluminescence detection of irradiated food from which silicate minerals can be isolated.* PN-EN 1788:2002.
[20]. European Committee for Standardization. (2009). *Artykuły żywnościowe – Wykrywanie napromieniowania żywności za pomocą fotoluminescencji*. PN-EN 13751:2009.
[21]. FAO/WHO. *General Standard for Irradiated Foods*. Codex Stan 106-1983, Rev.1-2003.
[22]. Council of the European Union, European Parliament. (1999). *Directive 1999/2/EC of the European Parliament and of the Council on the approximation of the laws of the Member States concerning foods and food ingredients treated with ionizing radiation*. Publications Office of the European Union.
[23]. Council of the European Union, European Parliament. (1999). *Directive 1999/3/EC of the European Parliament and of the Council on the establishment of a Community list of foods and food ingredients treated with ionizing radiation*. Publications Office of the European Union.
[24]. European Committee for Standardization. (2004). *Foodstuffs – Detection of irradiated food containing fat – Gas chromatographic analysis of hydrocarbons.* PN-EN 1784.
[25]. European Committee for Standardization. (2003). *Foodstuffs – Detection of irradiated food containing fat – Gas chromatographic/mass spectrometric analysis of 2-alky/cyclobutanones.* PN-EN 1785.
[26]. Raffi J., & Agnel J.-P. (1989). Electron spin resonance identification of irradiated fruits. *Radiat. Phys. Chem.*, *34*, 6, 891-894.
[27]. Raffi, J., Agnel, J.-P., Buscarlet, L.A., & Martin, C.C. (1988). Electron spin resonance identification of irradiated strawberry. *J. Chem. Soc., Faraday Trans. 1*, *84*, 3359-3362.

Chapter 5

# NEW DEVELOPMENTS BASED ON THE INCT FACILITIES

**Marta Walo, Urszula Gryczka, Dagmara Chmielewska-Śmietanko, Andrzej G. Chmielewski, Janusz Licki, Yongxia Sun, Andrzej Pawelec, Liang Zhao, Sylwester Bułka, Zbigniew Zimek, Marcin Sudlitz**

## 5.1. POLYMERS GRAFTING

Radiation-induced grafting is a useful tool for surface modification of a wide range of polymers dedicated to different applications. This method, thanks to choice of suitable monomers (methacrylamides, acrylamides, methacrylates, acrylates, acrylonitrile, styrene, vinyl acetates, vinyl chlorides, acrylic acid, N-vinylpyrrolidone, *N*-isopropylacrylamide), enables the introduction of new properties to the polymer layer such as hydrophilicity, hydrophobicity, adhesion, barrier properties, friction resistance. Radiation grafting has found application in industry and medicine [1]. Currently, intensive work has been carried out in the field of production of polymer membranes (fuel cells membrane, battery separators), production of selective adsorbents (e.g. scandium, cesium, uranium adsorbents) or to design polymers for medical and biotechnological applications (thermosensitive cell culture surfaces, antibacterial masks, intelligent packagings). Among these applications, membrane systems are one of the most effective and fast-growing technologies used for separation and purification processes [1].

The grafting process initiated by gamma or electron beam (EB) radiation allows to easy control the parameters of grafting (by the changes in the radiation exposure and reaction conditions, e.g. dose, dose rate, atmosphere, temperature), modify any type of synthetic and natural polymers in the various forms (film, fiber, membrane, fabric, powder), carry out the reaction in non-demanding conditions in a wide range of temperatures and obtain product with high degree of purity, free from initiating agent or catalyst [2].

The modification of polymer surfaces can be achieved by conventional grafting (mutual and pre-irradiation technique) or by reversible addition-fragmentation chain transfer (RAFT)-mediated grafting methods as shown in Fig. 5.1.

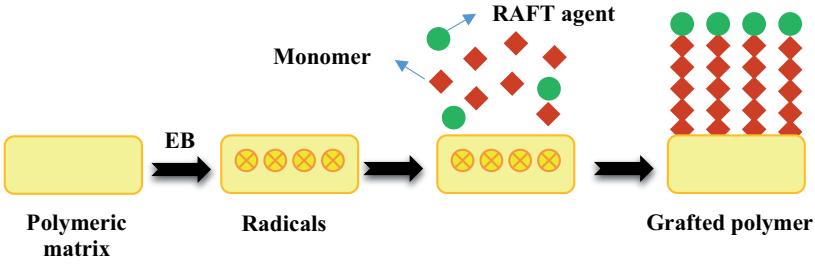


Fig. 5.1. Pre-irradiation grafting using RAFT-mediated polymerization initiated by electron beam radiation

In both cases, gamma rays or EB radiation can be used to generate active sites (free radicals) on polymeric surface which can then react with vinyl monomers to form a graft copolymer having combination of properties of these compounds. Grafting by RAFT-mediated method, in contrast to the conventional radiation grafting, enables to control length of the

grafted chains (molecular weight, polydispersity), leading to obtain new materials of different topologies and specific surface properties [3].

Research work in the field of radiation grafting at the Institute of Nuclear Chemistry and Technology (INCT) has been carried out on preparation of selective adsorbents of heavy ions [4, 5] and synthesis of polymers dedicated to medical applications for many years [6-8]. Both gamma radiation ($^{60}$Co) and electron beam radiation have been applied for these purposes. Experimental parameters (polymer nature, type and concentration of monomer, dose and dose rate, type of atmosphere, additives, etc.) affecting the grafting process were studied. Selection of irradiation facilities (gamma or electron beam irradiation) depends on the grafting system (type of polymer and reactivity of monomer) and application of modified materials. In gamma sources, the dose rate is relatively low (kGy/h), while for electron beams it is high (kGy/s), therefore the irradiation time in a gamma source is much longer (hours) than when using a high energy electron beam (minutes or seconds). The higher the dose, the greater the amount of radicals is generated in the polymeric material, which has a direct impact on the degree of grafting. The dose rate affects the lifetime and concentration of radicals and the termination process as well. In mutual grafting, for the same dose, increase in the dose rate results in lower efficiency of grafting, because the high concentration of radicals increases yield of their recombination leading to a rapid termination process and to enhanced homopolymerization [9]. In general, grafting by the mutual method is usually performed using a gamma source, as compared to the pre-irradiation technique, where the preferred radiation is an electron beam [10]. The pre-irradiation method is useful when the access to accelerator or a gamma source is limited. Then, a polymer may be pre-irradiated (in air or in vacuum) and even after a certain storage time can be used to initiate the graft polymerization.

Experiments of radiation-induced grafting by pre-irradiation methods were performed at ambient temperature with a 10 MeV electron beam generated in a linear electron accelerator Elektronika 10/10 located in the Radiation Plant for Sterilization of Medical Devices. Grafting either by conventional or by RAFT-mediated polymerization was carried out in gamma sources with different dose rates at the Centre of Radiation Research and Technology at the INCT.

## 5.2. LOW ENERGY ELECTRONS FOOD IRRADIATION

Energy of electrons is a parameter determining ability of the beam to penetrate irradiated object. Industrial electron beam accelerators can be divided into three major categories based on the energy of accelerated electrons:

- high-energy units (5.0 MeV to 10 MeV),
- mid-energy (400 keV to 5.0 MeV),
- low-energy, self-shielded units (80 keV to 300 keV) [11].

In contrary to the high energy electron beam which can penetrate centimeters of irradiated material the low energy electrons are absorbed over a few micrometers. There is a number of factors which must be considered when determining range of electrons having energy below 300 keV in irradiated product. Penetration ability of low energy electron beam depends not only on density of irradiated material but also on accelerator construction, such as thickness of the foil in accelerator window, and on irradiation conditions, because significant energy of the beam can be absorbed in air.

For any irradiation process the key parameter is absorbed dose. In the case of low energy electron beam the control of the dose is problematic due to limited penetration of the beam in compression to the thickness of most available dosimeters. For low energy electron radiation, a new dosimetry term has been introduced, namely Dμ, which is the dose in the first micrometer of an absorbing medium [12]. The other tested method for dose measurement when irradiating with low energy electron beam is application of specially constructed calorimeters [13].

The lower thickness of dosimeter, the lower gradient of the dose will be observed. One of the thinnest dosimeters available is RISO B3 dosimetric foil, which is manufactured as a highly uniform, thin film with a nominal thickness 18 μm. Using stack of B3 foil it is possible to measure range of electrons depending on energy of the beam. Examples of the beam ranges for dosimetric foil irradiated using ILU 6 accelerator are presented in Fig. 5.2. The real energy of electron beam that the material was exposed to, was lower due to absorption in 50 μm titanium foil of the accelerator extraction window, and about 10 cm air gap between the window and the irradiated samples.

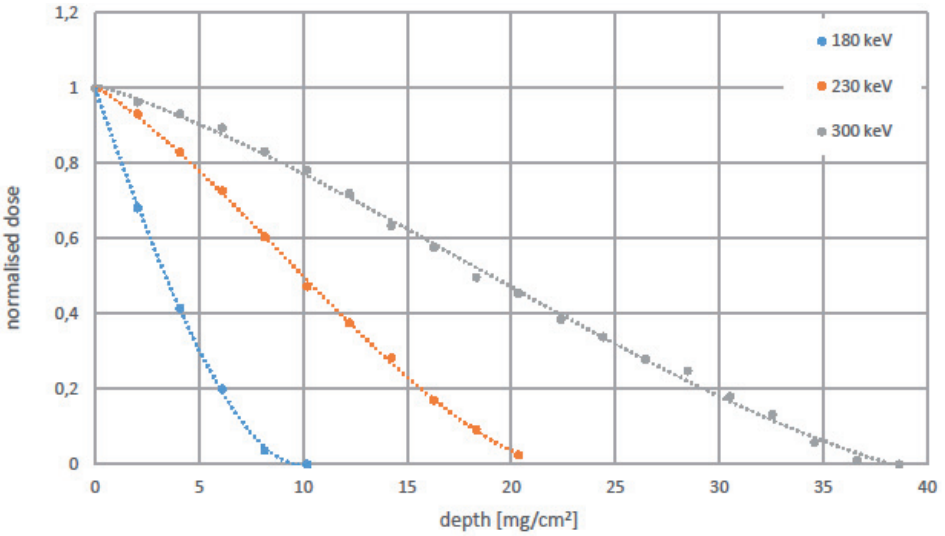


Fig. 5.2. Range of electrons having energy 180, 230 and 300 keV measured in stack of B3 dosimetric foil irradiated using ILU 6 accelerator

Food irradiation is a process of exposing food to ionizing energy in order to eliminate insects, fungi or bacteria that cause human disease or spoilage. Dried foods such as spices or nuts are often contaminated with high levels of bacteria, moulds and yeasts originated from the plant environment, namely soil, water and air. In the process where high energy electrons are used, the whole volume of food is irradiated. However, in recent years, the application of low energy electron beam has been developed as an alternative to currently used highly penetrating ionizing radiation [14]. Since microorganisms reside mostly on the surface of dry food, the irradiation of the external layer should be sufficient to eliminate food-borne microorganisms. The effectiveness of such beam in comparison with high energy electrons was proved for reduction of microbial load in dried spices [15]. Most of commonly used methods of food treatment interacts with food components causing decrease in its nutritional value. In contrary to commonly used ionizing radiation sources, low energy electrons can be used for surface treatment not affecting its internal part, thus reducing its negative impact on food quality.

There are advantages of application of low energy electron beam which make it promising technology for many applications. In addition to food processing low energy electrons can be used for surface microbial decontamination of seeds, flower bulbs or packagings. In terms of energy conversion lower energy electron accelerators are more efficient. Thus this technology is more economically profitable and friendly for the environment. Accelerators generating beam of energy below 300 keV are constructed as self-shielded units and it makes them easy to be used in-line of existing processes.

## 5.3. PAPER PRESERVATION

Paper provides the ideal nutrient base for mould fungi. Therefore, large volumes of books and archival collections are affected by bioburden because of improper storage conditions or accidents such as floods. Protection of books, archives and artifacts from destruction caused by insects and microorganisms is one of the main aims of the cultural heritage objects conservation. Moreover, the microbiological burden is harmful for the librarians' and archivists' health as well.

Decontamination of microbiologically infected paper-based objects is the area for the new application of electron beam irradiation.

Currently the most common method used for decontamination of library and archival collections is ethylene oxide treatment, which is toxic to human and natural environment. Moreover, resistance of some microorganisms (e.g. *Pyronema domesticum*) to ethylene oxide has been observed [16]. The promising alternative for this technique can be ionizing radiation. Gamma irradiation has already been applied to the treatment of large volumes of books and archives as well as wooden sculptures [17-20]. However, the most prevalent literature on applications of ionizing radiation to paper-based objects decontamination was related to treatment with gamma radiation, because of its high penetration. Nevertheless electron beam irradiation can be effectively applied for decontamination of biodeteriorated archives as well as for preventive conservation of large volumes of books in short time. Moreover, due to high dose rate of electron beam irradiation appropriate dose is delivered to the treated objects in several seconds therefore post-oxidation related effects of paper degradation are significantly limited.

The only one well-documented application of electron beam irradiation to decontamination of paper-based object on a large scale is irradiation of mail to recipients at the Congress, the White House and the federal agencies that started in October 2001 after spores of the deadly bacterium *anthrax* were found in mail sent to members of the news media and congressional leaders.

According to available data, about 1.2 million containers of D.C. federal mail were irradiated from November 2001 till April 2008 [21]. Two different facilities are used to irradiate mail. A Rhodotron continuous wave electron beam accelerator (energy: 10 MeV, power: 170 kW) located in Bridgeport, New Jersey is applied for the mail irradiation with the dose of 56 kGy [22, 23]. Absorbed dose is measured with NIST (The National Institute of Standards and Technology) alanine reference dosimeters. Roller conveyor system is used to transfer boxes with mail under electron beam. Mail must arrive packaged flat, double bagged, boxed, and sealed. Each box is irradiated twice, once per side. Sealed boxes are manually flipped over for second pass. Dosimetry is performed on trays. Throughput is 2040 kg/h.

Second facility is located in Lima, Ohio and is equipped with a single accelerator operating at energy 10 MeV and power 18 kW. Fixed-carrier conveyor system is being used to transfer boxes with mail under electron beam. Mail arrives packaged vertically in trays, double bagged, boxed, and sealed. Each box is irradiated four times (conveyor rotates boxes automatically for each pass). Dosimetry is performed on trays. Throughput is 450 kg/h [23].

In the INCT electron beam irradiation has been applied for the paper-based object sanitization for many years. Laboratory tests of different kinds of papers irradiated with a wide range of doses (0.4-25 kGy) were carried out. Changes in mechanical, thermal, physicochemical and color properties after papers irradiation were studied, together with the effectiveness of different absorbed radiation doses in *Aspergillus niger* elimination in different kinds of paper (Fig. 5.3) [24]. Electron beam irradiation of samples was carried out using 10 MeV, 10 kW linear electron accelerator Elektronika with dose rate $5 \times 10^3$ Gy/s. Delivered doses were confirmed using Gammachrome Harwell dosimeters for lower doses, and the calorimetric method involving graphite calorimeters was applied to measure absorbed radiation doses in a range from 5 kGy to 25 kGy. Optimization of irradiation procedure allowed to estimate a dose of 5 kGy as sufficient for the complete elimination of *Aspergillus niger* from all types of paper

(even if the level of the contamination was very high ~$10^4$-$10^5$ CFU/cm$^2$). Moreover, irradiation of the papers with the dose of 5 kGy did not influence the studied optical, thermal, physico-chemical and mechanical parameters of different papers.

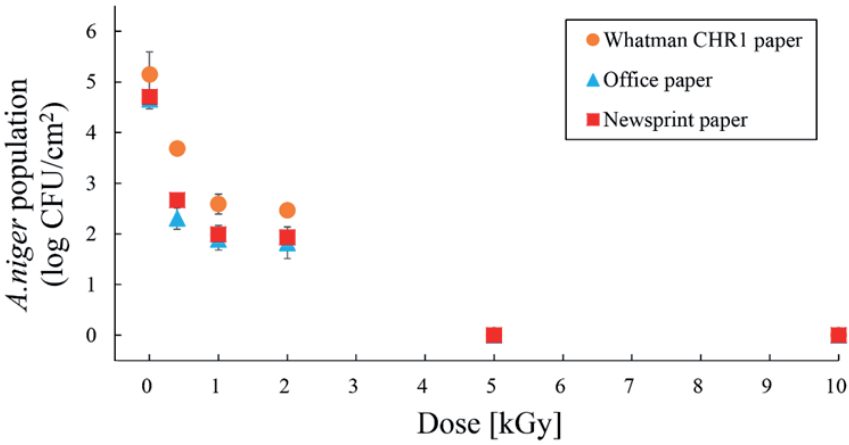


Fig. 5.3. *Aspergillus niger* population on the different kinds of paper as a function of electron beam radiation absorbed dose

Up to now ~200 m$^3$ of archives, documents and book from different libraries, museums and collections were irradiated in the INCT. Linear electron accelerator Elektronika 10-10 operating at energy 10 MeV and power 10 kW is located in the Centre for Radiation Research and Technology of the INCT. Elektronika accelerator has scanning length of 65 cm and RF 1886 MHz.

Paper-based objects must arrive packaged flat (height of the box: ~10 cm), boxed, and sealed. Roller conveyor system is used to transfer boxes with mail under electron beam. The speed of the conveyor system can be changed in order to ensure the delivery of the required dose. Each box is irradiated twice, once per side. Sealed boxes are manually flipped over for second pass. Throughput is 2 m$^3$/h. Dosimetry is performed on trays with the application of the calorimetric method involving graphite calorimeters.

The traceability of the required irradiation dose is ensured by the Laboratory for Measurements of Technological Doses (LMTD), which is a part of the INCT and is accredited by the Polish Centre for Accreditation (PCA) as a testing laboratory according to the requirements of the PN-EN ISO/IEC 17025:2005 standard.

## 5.4. DIESEL OFF-GASES TREATMENT

The laboratory unit for investigation of $SO_2$, $NO_x$ and VOC removal from flue gases has been built with ILU 6 accelerator as a source of radiation. Two heating furnaces, each of them being a water-tube boiler with 100 kW thermal power, are used as the combustion gas emitters. Proper composition of the flue gas was obtained by introducing such components as $SO_2$, NO and $NH_3$ to the gas stream. The installation consists of: an inlet system (two boilers; house heating furnace; boiler pressure regulator; $SO_2$, NO and $NH_3$ dosage system; analytical equipment); reaction vessel; and outlet system (retention chamber, filtration unit, fan, off take dust of gas, analytical equipment).

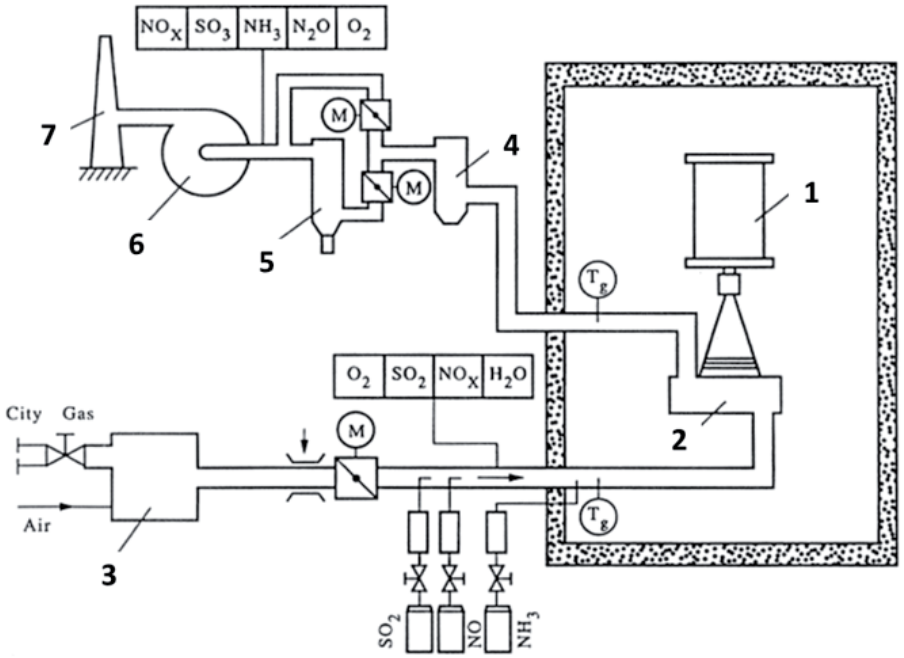


Fig. 5.4. Schematic diagram of the laboratory scale electron beam flue gas treatment installation: 1 – accelerator, 2 – reaction vessel, 3 – gas oven or oil-fired oven, 4 – retention chamber, 5 – bag filter, 6 – fan, 7 – stack

The installation shown in Fig. 5.4 was used during the tests for flue gas treatment which was basis for oil and coal fired boilers.

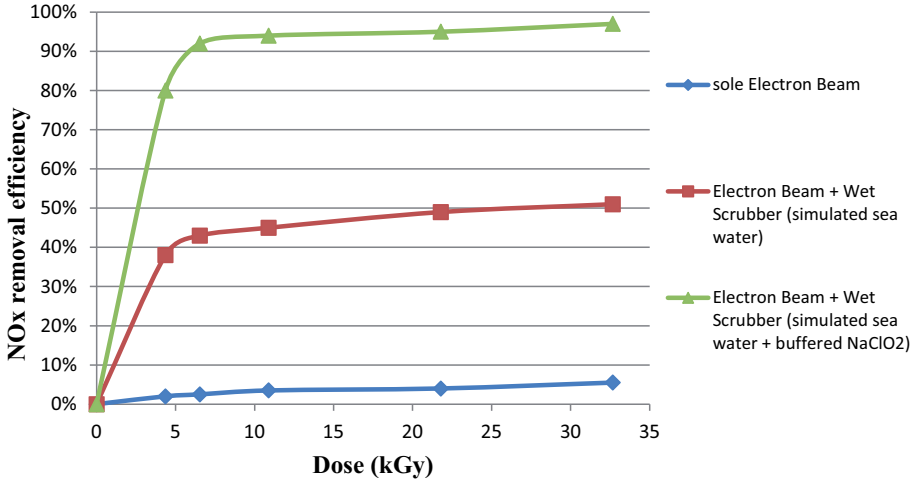


Fig. 5.5. A comparison of process efficiencies of sole electron beam method and a hybrid method, coupling electron beam with a wet scrubber in two cases: with simulated sea water and with simulated sea water and $NaClO_2$ addition with Michaelis buffer. NO initial concentration – 1500 ppm, $SO_2$ initial concentration – 700 ppm, $NaClO_2$ concentration – 25 mM, gas flow rate in the wet scrubber – 100 $dm^3/h$, time of each experiment – 15 min

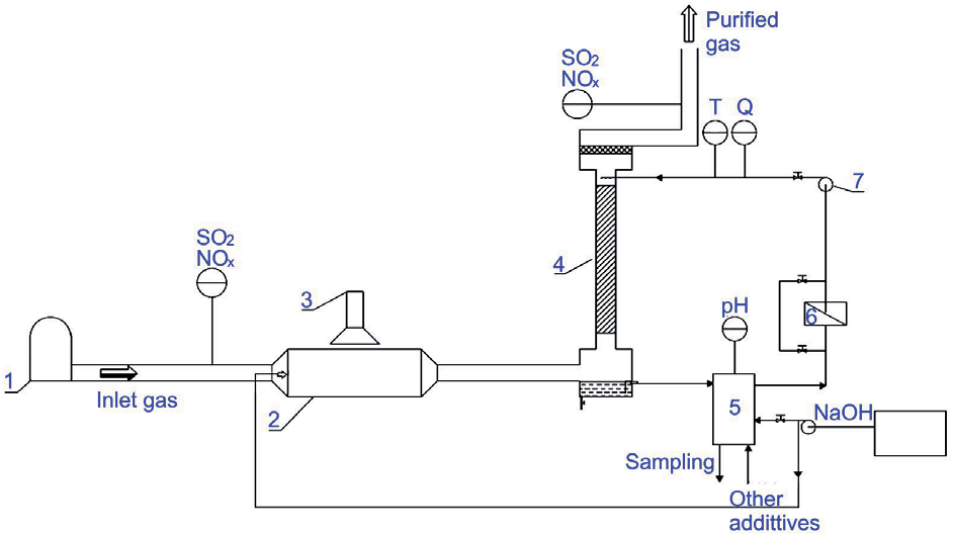


Fig. 5.6. Installation based on the laboratory scale hybrid electron beam method for flue gas treatment: 1 – burner, 2 – reactor, 3 – accelerator, 4 – scrubber (absorption column), 5 – water tank, 6 – filter, 7 – circulation pump, 8 – NaOH solution tank

The hybrid method, electron beam combined with wet scrubber, shows its advantage over electron beam in removal of $NO_x$. Figure 5.5 shows an example of electron beam combined with the wet scrubber filled with $NaClO_2$-sea water-buffer solution to remove 1500 ppm $NO_x$. $NO_x$ removal efficiency increased from 2.5% (electron beam only) to 43% (electron beam + simulated sea water as scrubber solution), till to 92.0% when oxidant $NaClO_2$ was added into scrubber solution [25] at 6.5 kGy absorbed dose.

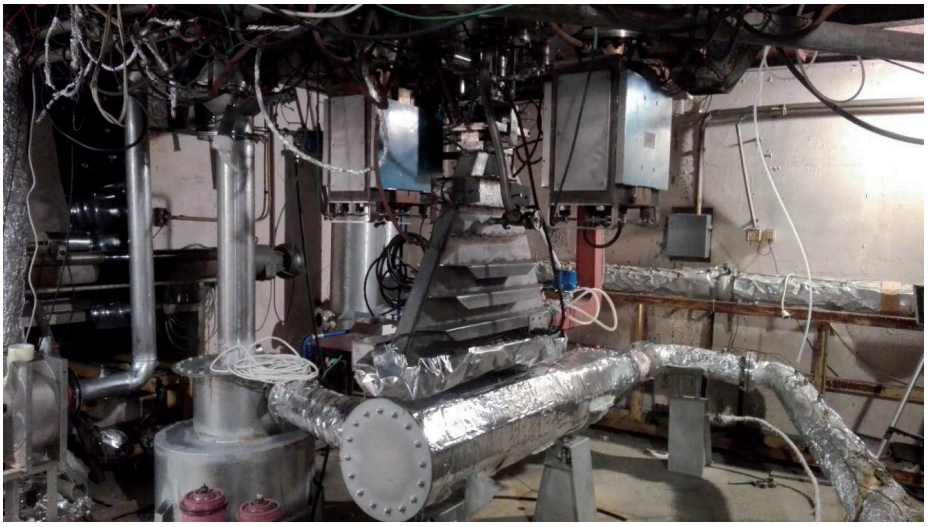

Fig. 5.7. View of the flue gas treatment installation based on the hybrid electron beam method

The results are very promising and show a big increase in the $NO_x$ removal efficiency with the use of hybrid method in comparison with the other methods. Furthermore, the influence

of the irradiation dose was minor above 10.9 kGy. Encouragingly, 90% $NO_x$ removal efficiency was achieved even when the dose was as low as 6.5 kGy or 10.9 kGy.

The new installation has been built to run the tests using hybrid method (electron beam + wet scrubber) to treat model off gases generated from diesel engine. Figure 5.6 shows the scheme of this new installation. The view of this new installation is presented in Fig. 5.7; burner and analytical equipment are not shown here.

The hybrid method enables a significant reduction in the reagent consumption. The addition of the electron beam increases the average removal of the wet scrubbing method by 10-20% depending on the dosage used. The installation will be used for the further optimization of the process.

## 5.5. WASTWATER TREATMENT

Laboratory installation was designed and constructed for radiation processing of liquids by the continuous irradiation with electron accelerator ILU 6 type [26]. The principle function of laboratory installation is radiation processing of liquid phase in continuous mode with flow rate 20-50 l and required homogeneity (the depth dose distribution). Testing the way of forming the stream of the product with suitable for the process parameters (geometrical dimensions, the speed of the flow) was conducted. The computer simulations of liquid stream irradiation were also performed in relation to suitable energy of the electron beam and depth dose distribution. The option related to the compressed air utilization for the decrease of the irradiated liquid

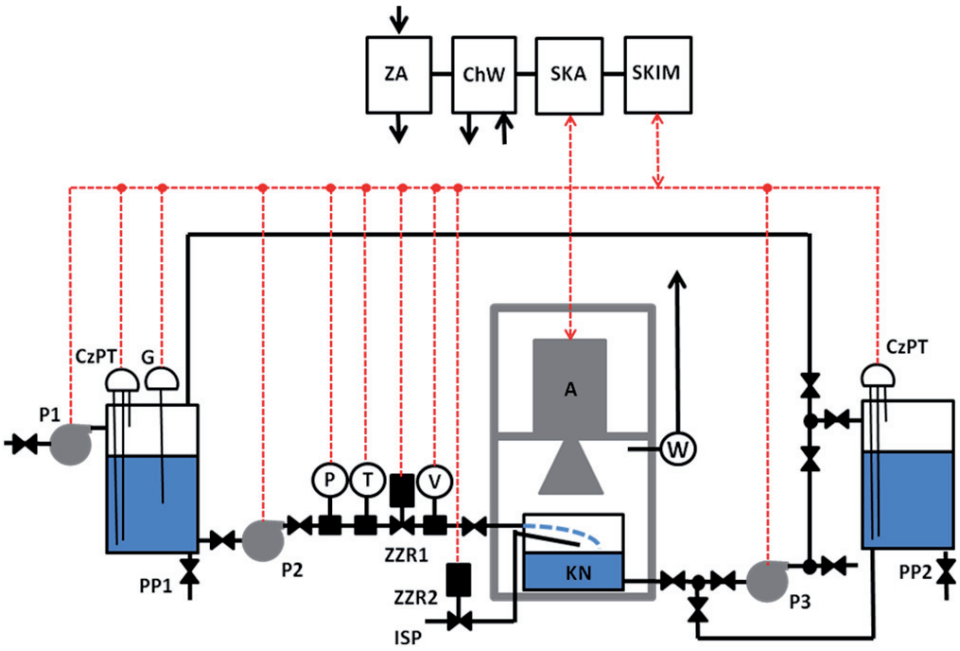


Fig. 5.8. Technological diagram of a laboratory installation: ZA – accelerator power supply, ChW – water cooling system, SKA – accelerator control system, SKIM – model installation control system, P1-P3 – liquid pumps, CzPT – level and temperature sensors, G – heater, PP1-2 – sampling, P – pressure sensor, T – temperature sensor, ZZR1-2 – valve adjusted remotely, V – flow sensor, ISP – compressed air installation, A – accelerator, KN – irradiation chamber, W – fan

density and for the improvement of the homogeneity of the irradiation process was considered. The laboratory installation was equipped in two reservoirs with the capacity 0.6 $m^3$ each. This allows performing of the irradiation process in the sufficiently long time and in the wide range of the speed of the flow. The electrical supply of the pump was associated with the micro-processor arrangement for control working conditions, what made possible regulated flow of the irradiated liquid in the proper geometry arrangement. The laboratory installation was made of materials and components (valves, pipes, pumps) resistant on corrosion induced treated liquids. The diagram of installation is presented in Fig. 5.8.

## References


[1]. Guven, O. (2016). Established and emerging applications of radiation-induced graft polymerization. In Y. Sun & A.G. Chmielewski (Eds.), *Applications of ionizing radiation in materials processing* (pp. 355-372). Warszawa: Institute of Nuclear Chemistry and Technology.

[2]. Nasef, M.M., & Guven, O. (2012). Radiation-grafted copolymers for separation and purification purposes: Status, challenges and future directions. *Prog. Polym. Sci.*, *37*(12), 1597-1656. DOI: 10.1016/j.progpolymsci.2012.07.004.

[3]. Barsbay, M., & Guven, O. (2013). RAFT mediated grafting of poly(acrylic acid) (PAA) from polyethylene/polypropylene (PE/PP) nonwoven fabric via preirradiation. *Polymer*, *54* (18), 4838-4848. DOI: 10.1016/j.polymer.2013.06.059.

[4]. Przybytniak, G., Kornacka, E. M., Mirkowski, K., Walo, M., & Zimek, Z. (2008). Functionalization of polymer surfaces by radiation-induced grafting. *Nukleonika*, *53*(3), 89-95.

[5]. Kornacka, E. M., Przybytniak, G., Fuks, L., Walo, M., & Łyczko, K. (2014). Functionalization of polymer surfaces by radiation-induced grafting for separation of heavy metal ions. *Radiat. Phys. Chem.*, *94*, 115-118. DOI: 10.1016/j.radphyschem.2013.05.047.

[6]. Walo, M., Przybytniak, G., Kavaklı, P.A., & Güven, O. (2013). Radiation-induced graft polymerization of N-vinylpyrrolidone onto segmented polyurethane based on isophorone diisocyanate. *Radiat. Phys. Chem.*, *84*, 85-90. DOI: 10.1016/j.radphyschem.2012.06.039.

[7]. Walo, M., Przybytniak, G., Męczyńska-Wielgosz, S., & Kruszewski, M. (2015). Improvement of poly(ester-urethane) surface properties by RAFT mediated grafting initiated by gamma radiation. *J. Mol. Struct.*, *68,* 398-408. DOI: 10.1016/j.eurpolymj.2015.05.019.

[8]. Walo, M., Przybytniak, G., Barsbay, M., & Güven, O. (2016). Functionalization of poly(ester--urethane) surface by radiation-induced grafting of N-isopropylacrylamide using conventional and reversible addition–fragmentation chain transfer-mediated methods. *Polym. Int.*, *65*, 192-199. DOI: 10.1002/pi.5045.

[9]. Walo, M. (2016). Radiation-induced grafting. In Y. Sun & A.G. Chmielewski (Eds.), *Applications of ionizing radiation in materials processing* (pp. 355-372). Warszawa: Institute of Nuclear Chemistry and Technology.

[10]. Nasef, M.M., & Hegazy, E.S.A. (2004). Preparation and applications of ion exchange membranes by radiation-induced graft copolymerization of polar monomers onto non-polar films. *Prog. Polym. Sci.*, *29*(6), 499-561. DOI: 10.1016/j.progpolymsci.2004.01.003.

[11]. Chmielewski, A.G., Sadat, T., & Zimek, Z. (2008). Electron accelerators for radiation sterilization. In *Trends in radiation sterilization of health care products* (pp. 27-47). Vienna: International Atomic Energy Agency.

[12]. Helt-Hansen, J., Miller, A., Sharpe, P., Laurell, B., Weiss, D., & Pageau, G. (2010). Dμ—A new concept in industrial low-energy electron dosimetry. *Radiat. Phys. Chem.*, *79*(1), 66-74.

[13]. Helt-Hansen, J., Miller, A., Duane, S., Sharpe, P., McEwen, M., & Clausen, S. (2005). Calorimetry for dose measurement at electron accelerators in the 80–120 keV energy range. *Radiat. Phys. Chem.*, *74*(5), 354-371.

[14]. Hertwig, C., Meneses, N., & Mathys, A. (2018). Cold atmospheric pressure plasma and low energy electron beam as alternative nonthermal decontamination technologies for dry food surfaces: A review. *Trends Food Sci. Technol.*, *77*, 131-142.

[15]. Gryczka, U., Migdał, W., & Bułka, S. (2018). The effectiveness of the microbiological radiation decontamination process of agricultural products with the use of low energy electron beam. *Radiat. Phys. Chem.*, *143*, 59-62.
[16]. Aoshuang, Y., Ailian, W., & Ying, Z. (2000). Study on measurement of radiation resistance of Pyronema domesticum sclerotia. *Radiat. Phys. Chem.*, *57*, 535-538. DOI: 10.1016/S0969-806X (99)00421-1.
[17]. Sinco, P. (2000, April). The use of gamma rays in book conservation. *Nuclear News*, 38.
[18]. Katusin-Razem, B., Razem, D., & Braun, M. (2009). Irradiation treatment for the protection and conservation of cultural heritage artefacts in Croatia. *Radiat. Phys. Chem.*, *78*, 729-731. DOI: 10.1016/j.radphyschem.2009.03.048.
[19]. Hanus, J. (1985, April). Gamma radiation for use in archives and libraries. *Abbey Newsletter*, 2 (9).
[20]. Moise, I.V., Virgolici, M., Negut, C.D., Manea, M., Alexandru, M., Trandafir, L., Zorila, F.L., Talasman, C.M., Manea, D., Nisipeanu, S., Haiducu, M., & Balan, Z. (2012). Establishing the irradiation dose for paper decontamination. *Radiat. Phys. Chem.*, *81* (8), 1045-1050. DOI: 10.1016/j.radphyschem.2011.11.063.
[21]. The Government Accountability Office. (2008). *Irradiation of federal mail*. Washington, DC: The Government Accountability Office. Report GAO-08-938R.
[22]. Swartz, T. (2002, April 12). Mail-related illnesses on steep decline after radiation dosage decreased. *Roll Call Daily*.
[23]. The Government Accountability Office. (2002). *Technologies for mail sanitization exist, but challenges remain*. Washington, DC: The Government Accountability Office. Report GAO-02-365.
[24]. Chmielewska-Śmietanko, D., Gryczka, U., Migdał, W., & Kopeć, K. (2018). Electron beam for preservation of biodeteriorated cultural heritage paper-based objects. *Radiat. Phys. Chem.*, *143*, 89-93. DOI: 10.1016/j.radphyschem.2017.07.008.
[25]. Chmielewski, A.G., Zwolińska, E., Licki, J., Sun, Y., Zimek Z., & Bułka S. (2018). A hybrid plasma-chemical system for high-$NO_x$ flue gas treatment. *Radiat. Phys. Chem.*, *144*, 1-7. DOI: 10.1016/j.radphyschem.2017.11.005.
[26]. Zimek, Z., Roman, K., & Długoń, S. (2016). *Laboratoryjna instalacja do ciągłej obróbki radiacyjnej ciekłych zanieczyszczeń przemysłowych*. Raporty IChTJ. Seria B nr 1/2016.

Chapter 6

# THE INCT INDUSTRIAL ELECTRON ACCELERATOR PROJECTS

**Andrzej G. Chmielewski, Zbigniew Zimek, Andrzej Pawelec**

The Institute of Nuclear Chemistry and Technology (INCT) developed and supervised construction of the plants for electron beam flue gas treatment (EBFGT) in power industry. These developments were very challenging tests for accelerators working in industrial harsh conditions. There are not too many industrial and R&D institutions that gathered such know-how all over the world related to these fields of applications [1, 2].

## 6.1. PILOT PLANT FOR EBFGT AT KAWĘCZYN POWER STATION

High emission of $SO_2$ and $NO_x$ in the process of fossil fuel combustion creates a major world environmental problem. Poland which uses for energy production mainly pit and brown coal produces these pollutants as well. Half of $SO_2$ and above 30% of $NO_x$ pollutions are contributed by heat and electricity generating boilers. Both $SO_2$ and $NO_x$ can be removed at the same time when flue gas is irradiated with an electron beam, as it was found in early experiments performed in Japan [3]. Main conclusions formulated are as follows: both gaseous pollutants can be removed in one radiation facility, irradiation process of flue gas is possible in continuous mode of operation, and the solids produced during irradiation can be collected by filtering devices such as bag filters or electrostatic precipitators. Laboratory facility for flue gas treatment with flow rate capacity 5-400 $Nm^3/h$ was organized at the Institute of Nuclear Chemistry and Technology where ILU 6 electron accelerator was applied in 1988. Electron energy range 0.5-1 MeV and beam power up to 20 kW were implemented during experimental works [4]. According to performed study OH radicals influence on initial stage of the process, temperature influences on removal pollutants efficiency, and water presence influences on $NO_x$ removal. By-product is a mixture of ammonium sulfate/nitrate salts.

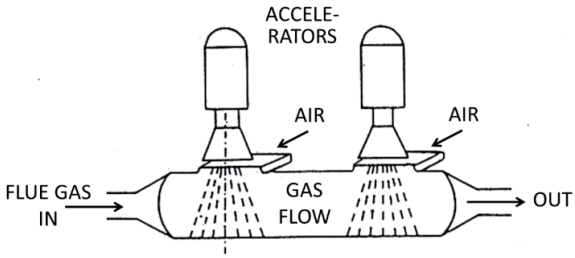


Fig. 6.1. The novelty of Polish pilot plant: cascade two-stage irradiation, longitudinal irradiation, and the air blow under the chamber window

Pilot plant for flue gas treatment has been installed at Kawęczyn Power Station at Warsaw in 1990. The flow rate was up to 20 000 $Nm^3/h$. Two electron accelerators were installed with total beam power 100 kW [5]. New elements have been introduced to the construction of the radiation chamber in Polish pilot installation (Fig. 6.1). Among them are: cascade two-stage

irradiation, longitudinal irradiation (beam scanned along the chamber axis) and the air blow under the chamber window with the purpose to create air curtain separating the window from the flue gases causing corrosion. Different system for filtration aid has been constructed and tested: bag filter, gravel bead filter and electrostatic precipitator.

Fig. 6.2. General view of Kawęczyn Power Station

The pilot plant facility was installed at Kawęczyn Power Station, heat supplier in Warsaw region (Fig. 6.2). Accelerator selection was made on the basis of available data provided by different accelerator suppliers (Table 6.1). The most important criteria were as follows: suitable range of energy and average power of the electron beam, acquaintance with the technology used by accelerator producer, positive opinion of the users and a well-developed program to increase beam power in the future. Prior to final decision the form of financial support given by the International Atomic Energy Agency (IAEA) was taken into account as well.

Table 6.1. Accelerators for flue gas treatment offered by the different manufacturers

| Type of accelerator | Producer | Energy [keV] | Current [mA] | Output window [mm] |
|---|---|---|---|---|
| 600/200/1830 Dynamitron | Radiation Dynamic, USA | 500-600 | 200 | 1830 |
| ESI 0.3/90 Electrocurtain | Energy Science Corp., USA | 300 | 300 | 1400 |
| ELV 3A Transformer | Budker Institute of Nuclear Physics, Russia | 500-700 | 100 | 1500 |
| UW-075-2-2-W Transformer | NIIEFA, Russia | 750 | 2 × 60 | 2000 |
| EPS 500 Cascade | Nissin HV, Japan | 500 | 80 | 1600 |
| ESH Transformer | Polymer Physics, Germany | 280 | 220 | 700 |

Electron accelerators of the ELV type have been applied as sources of ionizing radiation in radiation technologies such as polyethylene cables and wires insulation modification,

heat-shrinkable tubes production, grain disinfestation, artificial skin production, crosslinking silicon insulators, and flue gas treatment in electron beam process. Accelerators ELV type have been developed in the Budker Institute of Nuclear Physics, Siberian Branch of the Russian Academy of Sciences, Novosibirsk, Russia, as modular system allows constructing accelerators with electron energy 0.2-2.5 MeV and average beam power up to 400 kW [6].

Two ELV3A electron transformer accelerators were selected and installed at Kawęczyn Power Station. Accelerators were bought under POL/8/007 "Electron beam technology" project, financially supported by the IAEA technical co-operation project.

The basic construction of the ELV type accelerator is shown in Fig. 6.3. The high voltage (HV) accelerator power supply and accelerating section are placed inside pressure vessel (1) filled with insulating gas $SF_6$. One run consumption of $SF_6$ amounts 180 kg of the insulating gas in accelerator ELV 3A. Accelerator was equipped with $SF_6$ storage system. The water cooled HV transformer primary winding (2) is supplied by alternating voltage with frequency 400 Hz. Transformer is built without iron core. The source of high voltage is sectional secondary winding (5). Number of sections depends on nominal accelerator energy.

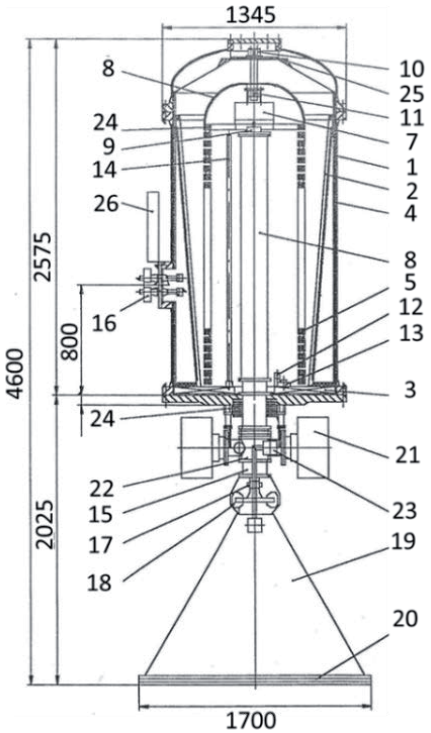


Fig. 6.3. Cross-section of ELV type electron accelerator: 1 – pressure vessel; 2 – primary winding; 3, 4 – magnetic core; 5 – HV rectifier unit; 6 – accelerating section; 7 – electron gun control unit; 8 – HV electrode; 9 – electron gun; 10, 11 – optical channels for electron gun control; 12 – divider; 13 – capacitors; 14 – HV divider; 15 – vacuum valve; 16 – electrical wires of primary winding; 17, 18 – coils of scanning; 19 – scanner; 20 – beam exit window; 21 – vacuum pump; 22 – vacuum element; 23 – vacuum valve; 24 – assembly base for HV electrode; 25 – HV screen; 26 – clamp

The amplitude of alternating voltage induced in each section is converted to doubled level of DC voltage by suitable circuit of rectifiers. All sections are connected in series according to necessary DC voltage level. Maximum DC voltage drop along the accelerating section (6) is 1 MV/m, and is independent of the accelerator energy. The accelerating section is located axially

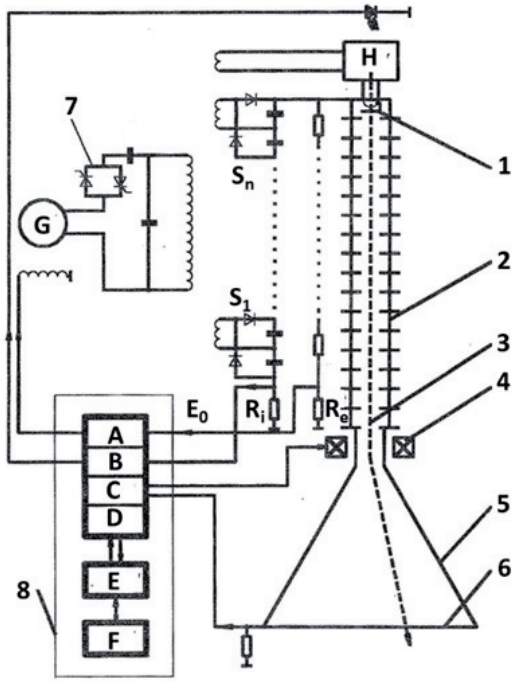


Fig. 6.4. Simplified electrical circuit of accelerator ELV type: 1 – cathode of electron gun, 2 – accelerating section, 3 – electron beam, 4 – coils responsible for X-Y beam scanning, 5 – beam scanner, 6 – titanium exit window, 7 – thyristor switch, 8 – control system, A – energy control unit, B – beam current control unit, C – X-Y scanning control unit, D – AC power line control unit, E – microprocessor control unit, F – computer, G – frequency converter, H – electron gun control unit

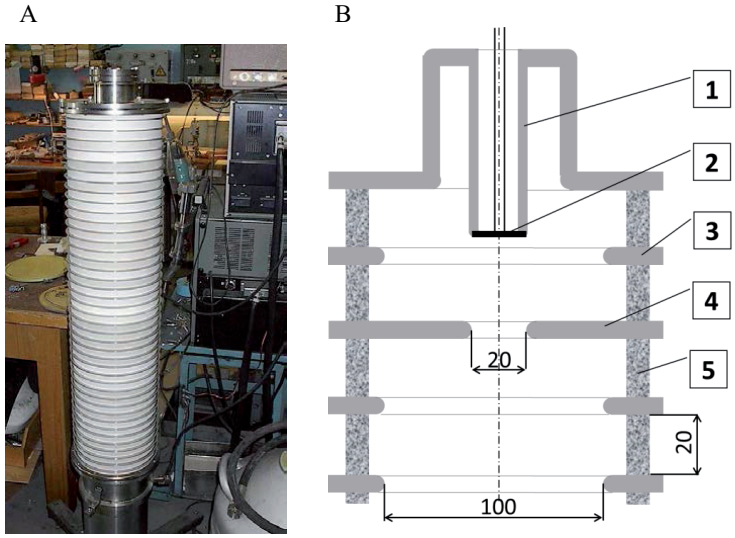


Fig. 6.5. (A) General view of accelerating tube. (B) An arrangement of the focusing electrodes at the top of accelerating section: 1 – cathode holder; 2 – $LaB_6$ cathode; 3, 4 – focusing electrodes; 5 – ceramic ring

in the column of rectifying module of the HV power supply. All these components are located in the pressure vessel filled with the insulating gas $SF_6$ under pressure up to 1.1 MPa. The basic electric diagram of the accelerator ELV type is shown in Fig. 6.4.

A hexaboride-lanthanum cathode ($LaB_6$) is a source of electrons in ELV accelerators. Cathode was externally heated tablet with diameter of 6 mm. 50 W is required for injector heating. The beam current is controlled by the cathode temperature. Electron gun is located at the top of accelerating section (Fig. 6.5). The channel aperture is 100 mm what provides good vacuum conditions in the cathode region. The outer diameter of ceramic insulator is 205 mm. 1 mm thick electrodes are connected to ceramic rings with high molecular weight PVA glue. General view of accelerating tube (A) and an arrangement of the focusing electrodes at the top of accelerating section (B) are shown on Fig. 6.5.

The electron beam is extracted through a thin titanium foil with thickness of 50 μm. The output foil is bent as a part of cylinder structure, what allows properly distribute the mechanical strength and increase the permitted temperature level. Additionally, an X-Y scanning system was applied for the homogeneous distribution of thermal load on the output window foil. The scanning signals for X and Y directions are synchronized according to the formulas:

$$f_x = f_g/n$$
$$f_y = f_g/m$$

where: $f_g$ – host generator frequency (typically $f_g$ = 900 Hz); n, m – constant dividing factors. The electron spot draws closed network in time:

$$\tau = n \times m \times f_g$$

τ is 4.2 s for n = 15 and m = 252.

In order to ensure stable operation of the output system when changing the electron energy, automatic adjustment of the beam scanning system parameters was applied. The raster size is determined by the computer according to the energy of the accelerated electrons. At the same time, the measurements of secondary electrons allow correcting the position of the beam by changing the current in the additional windings of the deflection coils. Figure 6.6 shows a block diagram of the beam scanning system. Comparison of data stored in the computer with the results of measurements ensures stable operation of the system. In the event of incompatibility, the accelerator is automatically turned off.

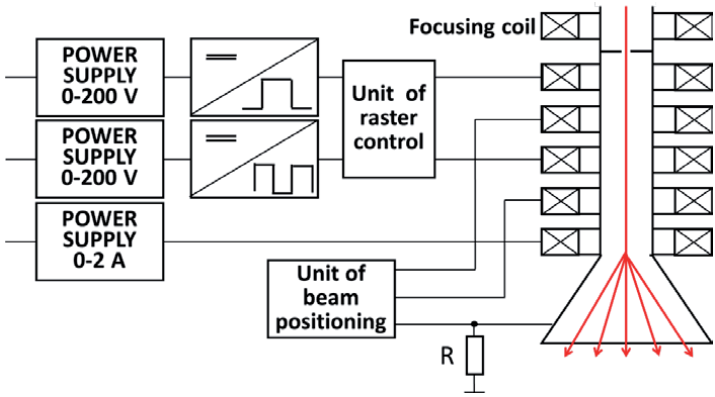


Fig. 6.6. Block diagram of electron beam scanning system

The separate blowing system for the output window is applied. The stream of air directed to the output foil has a speed of 40 m/s on the output of the nozzle. The X-Y scanning and the efficient air cooling system allow increasing the density of electron beam current up to 220 μA/cm$^2$ for the titanium window of a thickness of 50 μm. The typical current density is kept below 100 μA/cm$^2$ to increase the lifetime of the exit foil. In the case of an ELV 3A accelerator the output window has dimensions 1500 mm × 75 mm, the maximum output average

electron beam current is 100 mA. ELV type accelerators can be built as vertical or horizontal mounted devices. Round o'clock exploitation is acceptable. The starting up period after a long break (1-2 days) is usually 10 min to 30 min. Only 0.5-5 min is necessary to start the accelerator after a short break. When the vacuum is fallen down, the restore time is no longer than 4 h. The maintenance time, including the necessary service, should not exceed 10% of the total time when the accelerator works with electron beam. Because of automatic computer service neither manually adjusted parameters nor analog panel meters are used.

ELV type electron accelerators control systems are based on microcomputer program which allows:

- accelerator operation with the attachment to technological process,
- current diagnostic control of the accelerator units and systems with and without electron beam,
- diagnostic control of the separate units and systems under maintenance program,
- visual control and adjustment of the basic accelerator parameters.

The computer system was equipped with a Mera 660 microcomputer (20 MB hard disk and 360 kB floppy disk). The block diagram of the computer system is shown in Fig. 6.7. CAMAC crate equipped with proper units was used as a universal interface system between the computer and the accelerator separate units. The computer controls the accelerator interlock system. The block diagram of the accelerator interlock system and status or the separate accelerator blockades can be seen on a TV monitor screen during starting up period. The vacuum pumps discharge currents are indicated as well. The electron beam can be switch on when all the safety requirements are fulfilled and the water system, ventilation, vacuum system, power supplies are switched on.

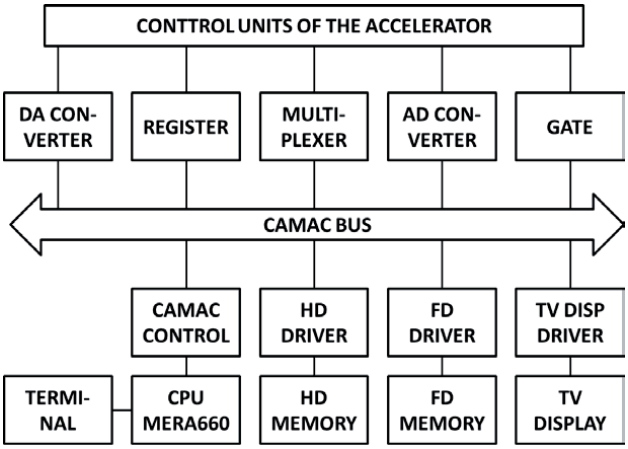


Fig. 6.7. Block diagram of the computer system applied in ELV type electron accelerators

The computer system allows maintain separate electron beam parameters (beam current, energy, spot dimensions) at the constant value. Loading current of the HV power supply is regularly compared with a given current level to control electron beam current level. The unbalanced signal is directed by a light guide to the driving circuit of the cathode heater current of the electron gun. This corrects the electron beam current by changing the temperature (emission properties) of the electron gun cathode. The circuit allows to obtain ordered value of electron beam current and to stabilize a certain value in time. The electron energy is automatically controlled as well the voltage level obtained from HV divider is compared with the level given by the computer. The unbalanced signal is directed to a high power, 50 Hz to 400 Hz, converter. It can change the output AC voltage level and the same time the accelerating voltage is changed adequately. The converter output voltage can be changed and stabilized

independently of the accelerating voltage. This feature of the system is especially important when the accelerator is tuned after installation. The electron beam parameters are chosen by the operator when he follows the instructions given by the computer. The most important accelerator parameters are the following: electron energy, beam current, secondary emission current, vacuum pump discharge current. The special command allows showing on the screen more specific information in the form of data table. The ELV 3A electron accelerator provides a continuous electron beam with the parameters given in Table 6.2.

Table 6.2. Technical characteristics of the ELV 3A electron accelerator

| Parameter | Value |
|---|---|
| Energy of electrons | 0.5-0.7 MeV |
| Instability of electron energy | ±5% |
| High voltage ripple | ±2% |
| Average electron beam power (max.) | 50 kW |
| Average electron beam current (max.) | 100 mA |
| Homogeneity of linear density of scanned beam measured at the distance 50 mm from output foil | ±10% |
| Output window dimension | 75 × 1500 mm |
| AC power line | 3 × 380 V, 50 Hz |
| AC power line conversion to frequency | 400 Hz |
| Required electrical AC power | 60 kW |
| Cooling water flow rate | 1.5 $m^3/h$ |
| Cooling air flow rate | 200 $m^3/h$ |
| $SF_6$ pressure | 1.1 MPa |
| Pressure vessel volume | 2 $m^3$ |
| Accelerator unit weight | 3700 kg |

The idea to arrange two accelerators in series is connected to well-known chemical engineering principle of the construction of cascade reactors. A sufficient decrease in the energy consumption at the same level of removal efficiency should be obtained. This idea was presented as the main objective of investigations in the IAEA Technical Assistance Program POL 8/007-1988. The existence of such phenomena in the electron beam process has been proved during the tests carried out on the pilot installations. Arrangement of the accelerators at Kawęczyn pilot plant, mounted in series, over the process vessel is shown in Figs. 6.8 and 6.9. The accelerators are located in a separate three-level building (dimensions: length – 18.2 m, width – 9.4 m, height – 7.2 m). The main equipment parameters of the accelerator building and installed auxiliary systems are given in Table 6.3.

The scanning/exit part of the accelerators is located 4 m below the ground level. The process vessel chamber was shielded by walls made of heavy hematite concrete, 70-80 cm thick (density: 3.1 g/cm). The ceiling between the underground and ground level is made of a concrete (density: 3.4 g/cm). The other inside walls are made of ordinary concrete (density: 2.3 g/cm). In the upper and bottom chambers of the accelerators shielded doors were made of a steel construction with 20 mm lead plate. Labyrinths were made of lead bricks (thickness: 100 mm).

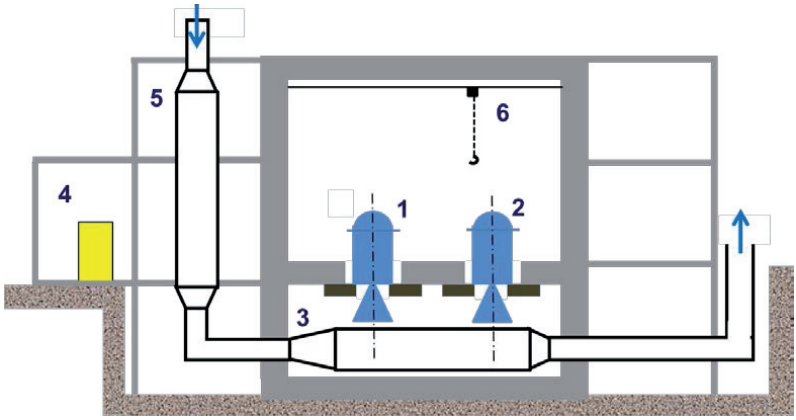


Fig. 6.8. Side view of the building with arrangement of the electron accelerators and process vessel: 1, 2 – ELV3A electron accelerators; 3 – process vessel; 4 – AC frequency converter; 5 – spray cooler; 6 – crane

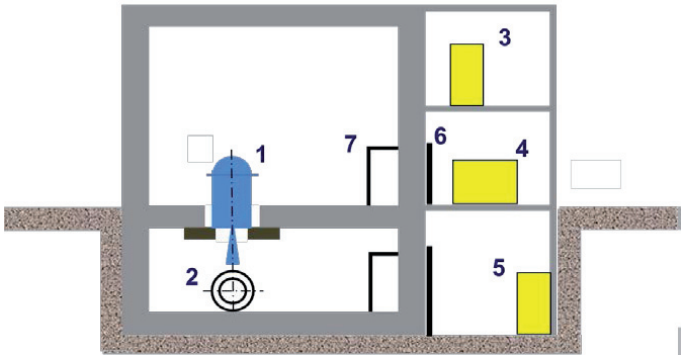


Fig. 6.9. Cross-section of the accelerator building: 1 – ELV 3A accelerator, 2 – process vessel, 3 – control rack, 4 – electrical panel, 5 – AC electrical control panel, 6 – shielded door, 7 – labyrinth shield

Table 6.3. Basic parameters of the accelerators building and installed auxiliary systems

| Parameter | Value |
|---|---|
| Covered surface | 171.1 $m^2$ |
| Useful surface | 333.1 $m^2$ |
| Cubature | 1882 $m^3$ |
| Technological water | 4.5 $m^3/h$ |
| Installed electrical power | 180 kW |
| Irradiation chamber ventilation blow | 3040 $m^3/h$ |
| Secondary windows cooling blow | 2 × 800 $m^3/h$ |
| Irradiation chamber exhaust | 3800 $m^3/h$ |

The water cooling system of the accelerators is connected with the internal water system installed at the power station. An appropriate interlock system was installed to fulfill safety and technological requirements. The process vessel was made of stainless steel 1H18N9T (equivalent to the US stainless steel no. 304). The thermal insulation was made of rock wool and covered with zinc sheets. The accelerator exit window is cooled by an air stream blown into the gap between both foils (accelerator and process vessel). The process vessel is equipped with two secondary windows made of titanium foil (thickness: 50 pm). Dimensions of the window are 1500 mm × 75 mm (active part). Stream of the air with a capacity of 800 $Nm^3/h$ is blown into the process vessel under the secondary window to make an air curtain and to prevent solid deposition. The process vessel is furnished with two screw openings for withdrawing dosimetry foil strips. Figure 6.10 shows the view of accelerator beam scanner and reaction vessel.

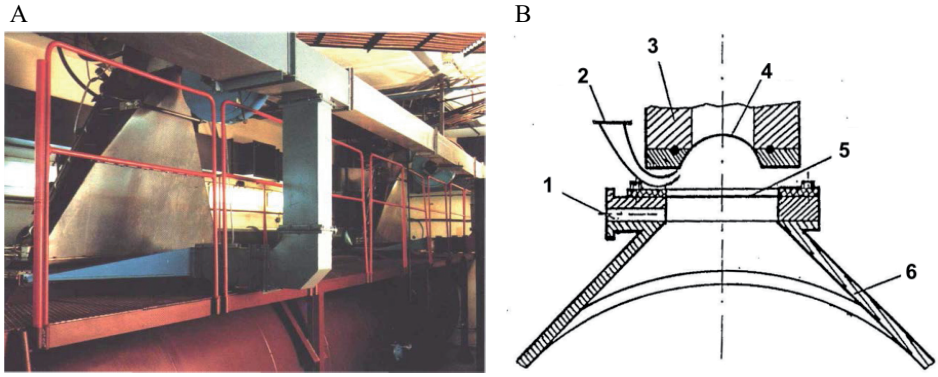


Fig. 6.10. View of (A) accelerator beam scanner and reaction vessel and (B) double window arrangement: 1, 2 – nozzle for air blowers, 3 – electron beam scanner, 4 – accelerator exit window, 5 – process vessel foil, 6 – process vessel

The nominal accelerator parameters were measured and proved after the final acceptance tests performed in the presence of manufacturer's service team. The acceptance test was based on a 72 hour non-stop operation with accelerated electrons in the energy range 0.5-0.7 MeV and a full average beam power of 50 kW for each accelerator.

The electron energy and the beam current instability were within the range ±5% during the acceptance test, in good agreement with the contract and technical parameters. After starting operation of ELV 3A accelerator measurements of spatial beam distribution inside of the process vessel were performed (Fig. 6.11). PVC foil was used as dosimeter [7]. Except electron beam dosimetry measurements of many various physicochemical effects have been tested in pilot plant facility equipped with necessary instrumentation suitable for flue gases irradiation process. Energy of electrons has to be well selected taking into account the irradiation vessel diameter and the foil thickness, what is presented in Fig. 6.12. The curves present energy losses vs. electron beam energy. The minimum losses in window and bottom wall are in the range 0.60-0.65 MeV and most of energy is deposited in flue gas [8].

Analytical system was implemented for determination gas composition at the inlet and outlet of the process vessel. Pollutants concentration was measured by two independent emission monitoring systems [9]. The general scheme of analytical system is presented in Fig. 6.13. The data were collected and stored in data acquisition computer system. Wet chemical grab samples analysis were used for control in addition to instruments for continuous emission monitoring systems.

Pilot plant for flue gas treatment continuous operation tests were performed successfully [10]. Influence of pollutants removal efficiency in two-stage irradiation were tested [11] and compared with empirical models for $NO_x$ and $SO_2$ removal in a two-stage flue gas irradiation process [12].

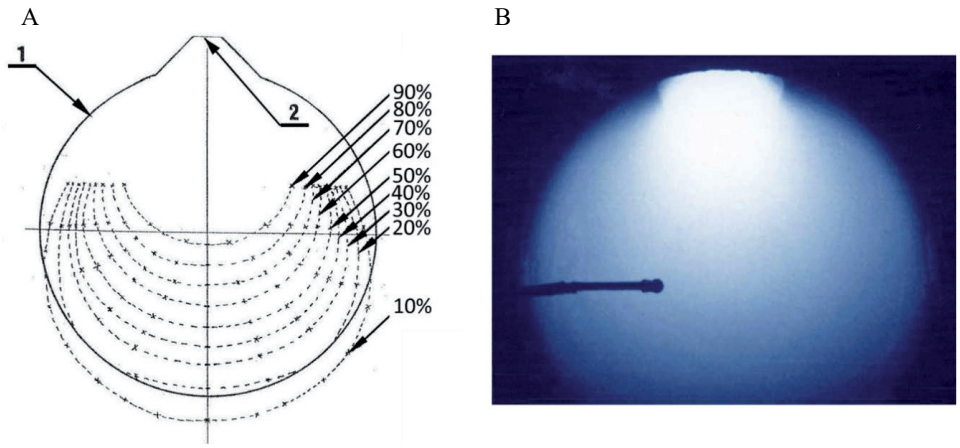


Fig. 6.11. Traversal dose distribution in air inside process vessel (A) and ionized gas photography under static conditions (B)

Final selection of by-product filtration process has been performed during the period of pilot plant for flue gas treatment operation with electron beam [13]. Scheme of pilot plant for electron beam flue gas treatment constructed at Kwęczyn Power Station is presented in Fig. 6.14 and includes three different filtration units tested: bag filter, gravel bed filter and electrostatic precipitator. Finally electrostatic precipitator (ESP) was found to be the best equipment for this particular applications.

Facility control room presented in Fig. 6.15 was equipped with two touch panels for accelerators control and monitoring and data acquisition system for measurements and data storage [14].

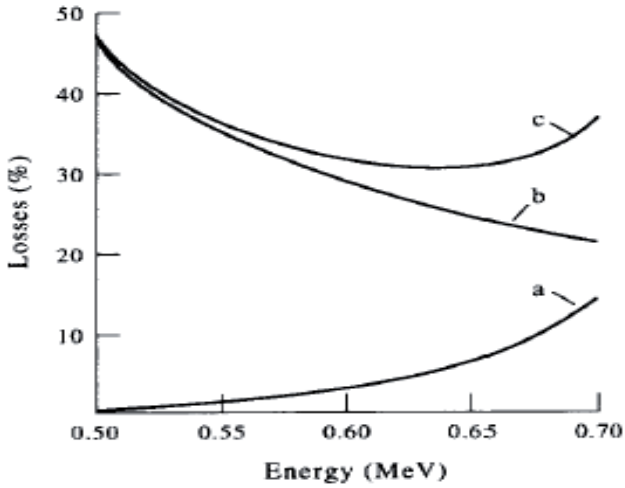


Fig. 6.12. Energy losses vs. electron beam energy (a – bottom wall, b – windows foil, c – total)

The first set of experiments was performed for low gas humidity and rather high temperatures. In the second set of experiments the gas humidification system at the Kawęczyn pilot plant has been upgraded. High enthalpy water was used, packing was introduced into the column and water recirculation was applied. The humidity of flue gases can be increased up to

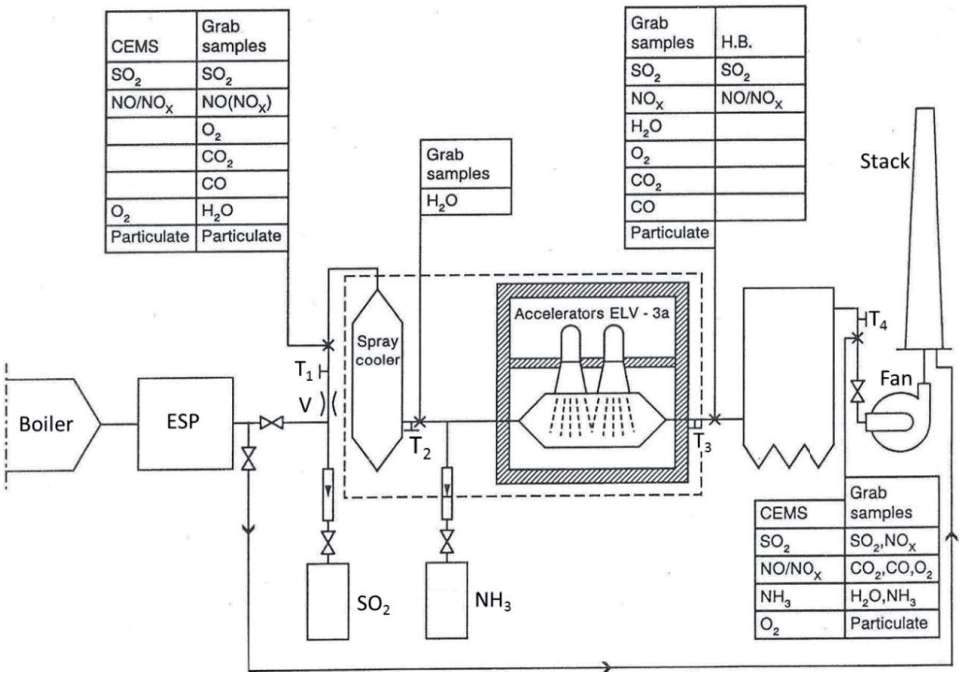


Fig. 6.13. Scheme of the pilot plant analytical system

15% per volume and the gas inlet temperature reduced to 45°C. At this condition the removal efficiency of $SO_2$ as high as 98% can be achieved. Due to thermal reaction a very low dose is required to obtain a high removal efficiency. In the case when moderate $NO_x$ removal efficiency is required the economic competitiveness of electron beam process with conventional technologies increases even further. These phenomena are well presented in Fig. 6.16.

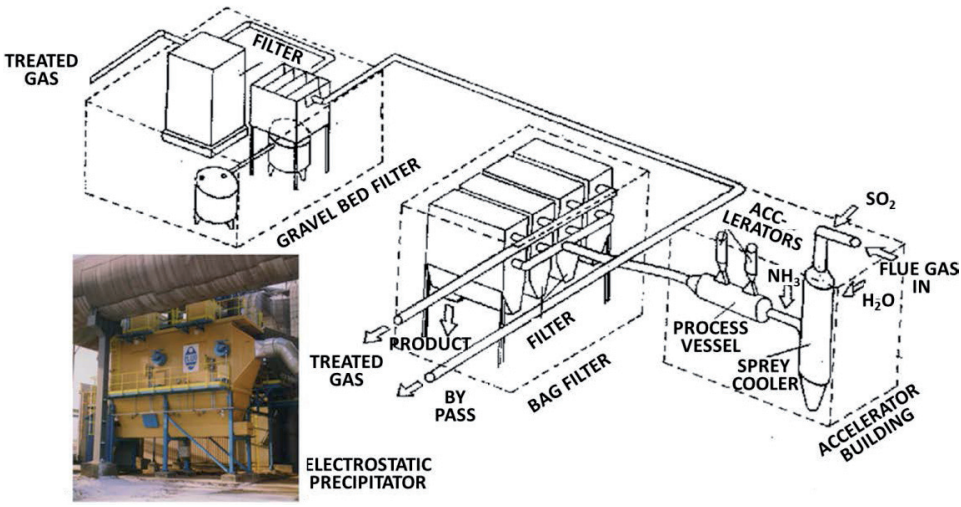


Fig. 6.14. Scheme of pilot plant for electron beam flue gas treatment constructed at Kawęczyn Power Station

Fig. 6.15. Accelerator control room and monitoring and data acquisition equipment

Average composition of by-product obtained during electron beam purification of flue gases is as follows: $(NH_4)_2SO_4$ – 95%, $NH_4NO_3$ – 5%. In principle, the by-product with small fly ash content (less than 2%) is equivalent to the c01n1nercial fertilizer – ammonium sulfate. Another possibility is to use the by-product as a component in NPK fertilizer. A test performed in Poland has proved that a blend obtained with the application of the by-product meets the standards established for this kind of fertilizers. During agricultural tests the pure by-product and a by-product with different fly ash content were used. Results were very positive. The content of heavy metals was much lower than the values allowed for commercial fertilizers.

Electron beam flue gas treatment process upscaling was implemented on the basis of experimental work results collected during pilot plant exploitation and obtained patents [15-19] related to flue gas treatment radiation process. Full scale industrial plant for $SO_2$ and $NO_x$ removal was designed and built in Pomorzany Power Station, Szczecin to treat flue gas stream 270 000 $Nm^3/h$.

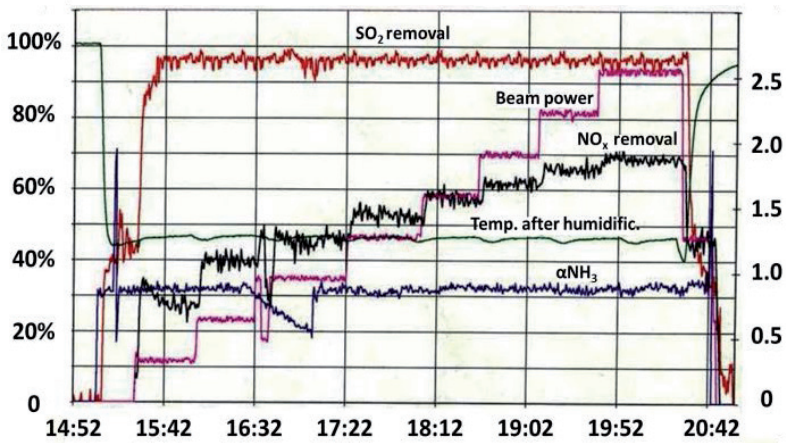


Fig. 6.16. Flow sheets from computer monitoring system of $SO_2$ (red) and $NO_x$ (black) removal efficiency as a function of time for different values of beam power (dose)

## 6.2. PILOT PLANT FOR EBFGT AT JEDDAH, SAUDI ARABIA

The pilot scale EBFGT plant was constructed in the boiler area of the Jeddah Refinery [20]. The simplified layout chart of the plant is shown in Fig. 6.17.

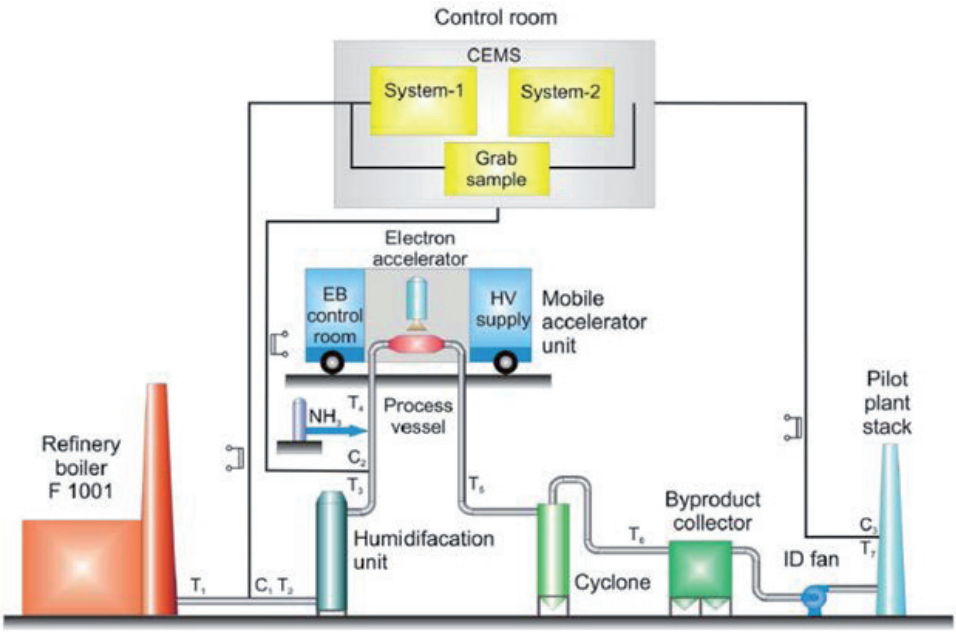


Fig. 6.17. Layout of pilot plant at the Jeddah Refinery for electron beam treatment of heavy fuel oil burned flue gas (not in scale)

The flue gas from the boiler was directed to the cooling and humidification unit and then was irradiated in the reaction chamber. A near stoichiometric amount of ammonia was added to the treated gas up-stream reaction chamber. After irradiation, the gas was directed to the by-product separation unit consisting of a cyclone and cartridge bag filter or a cyclone and electrostatic precipitator in the second part of the research. Purified flue gas was released to the atmosphere by a separate stack. The gas flow rate was controlled by an ID fan rotation speed regulation. The pilot plant was supplied by a part of exhaust gas from the boiler manufactured by Mitsubishi, Japan. The boiler may be fired by fuel heavy oil or fuel gas. During the research heavy fuel oil was combusted. The pilot plant inlet was attached to the boiler outlet upstream of the power plant stack. A flap type valve was installed at the gas inlet to the plant. Flue gas temperature at the pilot facility inlet was about 310°C, therefore, the gas conditioning unit was applied for gas cooling down. Flue gas from the installation inlet was directed to the cooling device by uninsulated steel ducts of 315 mm diameter. These ducts served as a pipe heat exchanger lowering the gas temperature before reaching the main cooling device. A counter current water spray scrubber was applied as a main cooling and humidification device. This device was also designed for dust removal as no other dust collection system was applied in the installation inlet. The water was circulating in a closed loop. Water spraying nozzles were installed under the demister located in the upper part of the column, beneath the gas outlet. Water coming out from the cooling device was filtered to prevent nozzle plugging. In order to stabilize water temperature, a water cooler in the cooling loop was applied. The ducts after the conditioning unit were thermal insulated to avoid further gas cooling and water condensation

in the ducts. Ammonia was delivered and stored in liquid form in steel cylinders and evaporated during the experiments. A battery of cylinders was used to ensure the proper amount of this reagent. Ammonia was injected into the duct via two nozzles upstream of the reaction vessel. In order to prevent particulate deposition that might lead to nozzle plugging, compressed air was used for ammonia spraying. The amount of injected ammonia was manually controlled via a rotameter with a needle valve. The accelerator ELV with radiation shielding, cooling, ventilation made by EB Tech Co., Ltd. (Fig. 6.18) was applied for flue gas irradiation [21]. The scanner window length was 640 mm. The main parameters of this accelerator are: beam energy – 400 to 700 keV, maximum beam current – 33 mA. Other auxiliary systems was assembled on a truck trailer, thereby producing a unique mobile system. The shielded irradiation room was of 1554 mm in length, 1380 mm in width and 1410 mm in height, while free space under the accelerator's scanner was of 530 mm in height. Due to space limitations, the process vessel (PV) was of 1390 mm length including inlet and outlet part of the device. The cross-section of PV had quasi hexagonal shape with a width of 434 mm and a height of 482 mm. Electrons entered PV via 640 × 70 mm window. Both the accelerator scanner and the PV windows were made of 50 μm thick titanium foil.

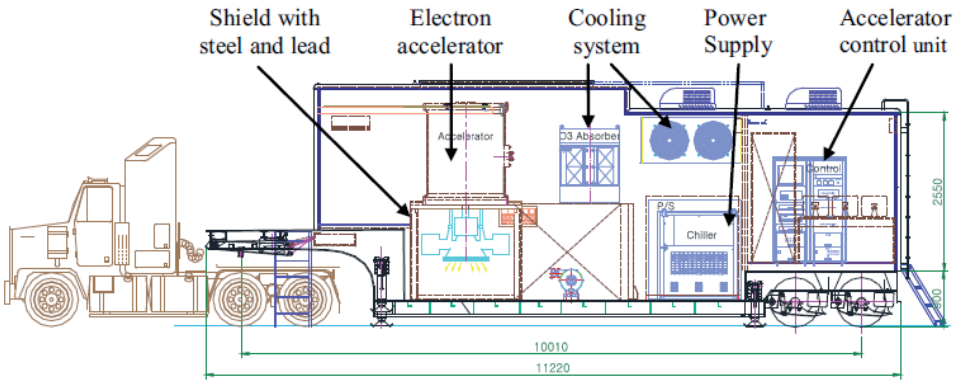


Fig. 6.18. Mobile electron beam plant (0.7 MeV, 20 kW), mounted on a trailer [21].

The by-product collection unit was composed of two elements: cyclone and bag filter. During further works the bag filter was replaced by electrostatic precipitator (ESP). The filtration equipment was supplied by EB Tech Co., Ltd.. The cyclone was installed prior to the bag filter, downstream of the reaction chamber. A typical device of nominal flow rate 60 $m^3$/min manufactured by Clean Air Tech Co., Ltd., Korea, was selected. There were two goals of cyclone application – to collect the initial by-products and to prolong the reaction time. The by-product aerosol particulates being formed as a result of EBFGT process were very fine (about 1 μm diameter) and light, therefore cyclone particulate removal efficiency was very low. On the other hand, the PV volume was very small and the residence time was also very short; therefore, the chemical reactions continued even after the gas left this device. Subsequently the cyclone acted as a retention chamber allowing the process reactions to complete. The cartridge bag filter was selected as the main by-product collecting device. A standard apparatus model CAPS-750HR of 60 $m^3$/min nominal flow rate, manufactured by Clean Air Tech Co., Ltd., Korea, was selected. The by-product from flue gas was filtered on 18 cartridges, then removed to the hopper by compressed air. Two ESPs manufactured by KC Cottrell, Korea, were applied in the second stage of research. The devices were installed parallel and the gas was directed to each of them by automatic valves. The gas exhaust unit was composed of an ID fan and a stack. The fan (MFsB-013-3-1-H3 type, Nederman, Poland) was an ID fan for the whole pilot plant system. The flow rate of treated flue gas was adjusted by fan rotation speed control. A stack of

315 mm diameter and 5 m height was constructed for gas exhaust to the atmosphere after treatment. The general view of the whole installation is presented in Fig. 6.19.


Fig. 6.19. General view of the pilot plant at the Jeddah Refinery: 1 – stack of boiler, 2 – boiler, 3 – flue gas duct, 4 – pilot plant control room, 5 – gas conditioning column, 6 – pilot plant stack, 7 – cartridge bag filter, 8 – thermal insulated duct, 9 – cyclone, 10 – ammonia dosing unit, 11 – mobile accelerator unit

Advanced analytical methods developed at the Kawęczyn pilot plant were the basis for the Pomorzany industrial plant monitoring and control systems. Similar analytical methods were applied at the Jeddah pilot plant.

Two types of monitoring systems were used for reliable and accurate flue gas composition measurements: continuous emission monitoring system (CEMS) for continuous measurements of $SO_2$ and $NO/NO_x$ concentrations by gas analyzers and grab sample system for occasional determination of various flue gas parameters (e.g. humidity). Grab samples were analyzed using manual analytical methods. Two independent extractive multi-gas monitoring systems were installed for continuous measurement of $SO_2$ and $NO_x$ concentration in the flue gas: one at the plant inlet (upstream of the humidification unit) labeled System-1 and the second at the plant outlet (downstream of the ID fan) labeled System-2. The UV pulsed fluorescent $SO_2$ analyzer, Model 40, and a chemiluminescent $NO/NO_x$ analyzer, Model 10 A/R, manufactured by Environmental Instrument Co. (EIC), USA, were applied in each system. Both systems operated by utilizing the heated sample gas dilution system Model 900 (EIC, USA) with a dilution ratio of 20:1. The flue gas leaving the by-product collector (cartridge bag filter or ESP) may contain unreacted ammonia which complicates the gas concentration measurement. The outlet gas analyzer system (System-2) was equipped with the heated ammonia scrubber, manufactured by Shimadzu Co., Japan, for selective absorption of ammonia from the extracted sample gas without changing the concentration of other components. Each gas sampling system utilized a stainless steel probe for exhaust gas extraction from duct. The probe tip was equipped with coaxial ceramic coarse and fine gas filters for particulate removal. The probe and gas filters were heated. The representative sample gas was continuously extracted from the duct using a heated sample probe, filtered at temperature above the acid dew point temperature, and transported by heating sampling line to gas analyzers system installed in the control room. Heated sampling line was kept at the same temperature as the sample probe and the gas filters. Gas sampling points were located before the humidification unit (plant inlet) and at the stack (plant outlet). An additional sampling point for flue gas humidity control (C2) was located after the humidification unit. The calibration of each continuous monitoring system was performed using standard gas mixtures. Flue gas temperature was measured at seven essential points of the Jeddah Refinery pilot plant: plant inlet, upstream and downstream of the humidification unit, upstream and downstream of PV, inlet of bag filter or ESP and plant outlet — marked Ti. K-type thermocouples were used for gas temperature measurement. The humidity of the flue gas was determined by manual analytical method based on the EPA method 4 with the use of granular silica gel filled U-tubes. The portable flue gas analyzer type Lancom Series II manufactured by

Land Combustion, UK, was applied for auxiliary measurements of CO, $CO_2$, $O_2$, $SO_2$, NO, $NO_2$, $NO_x$ and hydrocarbons (CxHy) concentrations in the flue gas as well as the gas temperature. High removal efficiencies – 85.8% for $SO_2$ and 82.8% for $NO_x$ – were obtained in this experiment (Fig. 6.20).

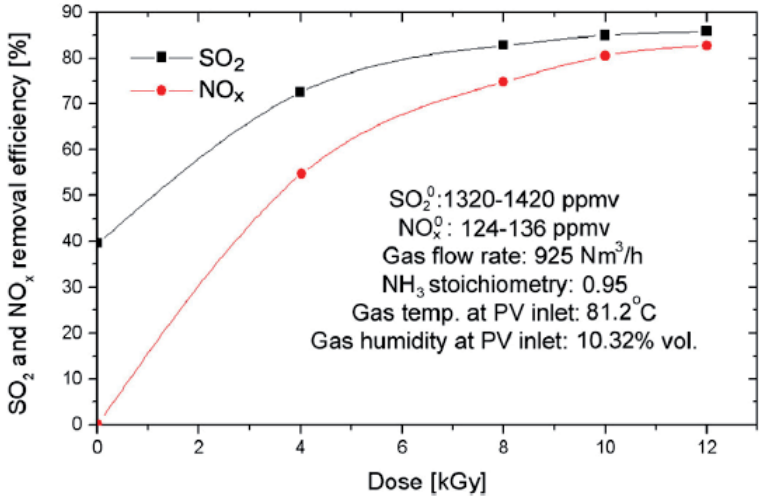


Fig. 6.20. $SO_2$ and $NO_x$ removal efficiency as a function of the irradiation dose

This dependence is typical for the EBFGT process. $NO_x$ removal is a radiation-induced process, therefore an absorbed dose (electron beam energy delivered to the gas flowing through the process vessel) is the primary factor influencing $NO_x$ removal efficiency. The process starts at zero efficiency for zero dose and indicates saturation at high doses. In the case of $SO_2$ removal, the process is based on two different pathways: thermal reaction and radiation-induced reaction. At zero dose, some $SO_2$ removal is observed due to thermal reaction of $SO_2$ and $NH_3$ in a moist environment. This reaction takes place in the gaseous phase and on the surfaces, such as those on the filter cake of the bag filter or on the plates of ESP. $SO_2$ removal increases sharply with an increase of the absorbed dose up to 8 kGy, and then the removal efficiency curve achieves saturation at high doses. The temperature of flue gas at the reactor inlet was rather high for $SO_2$ removal process, which resulted in lowering the $SO_2$ removal efficiency (only 40% $SO_2$ removal was obtained for zero dose and under 90% for 12 kGy dose). On the other hand, these conditions increased $NO_x$ removal over 80%.

The obtained by-product was a high quality fertilizer, which may be used directly or as a substrate for NPK fertilizer blends. The soluble part of by-product was almost pure ammonium sulfate (98% to 99%) with some amount of ammonium nitrate. The content of heavy metals in the by-product was very low and much lower than stated by international standards, in most cases, by two orders of magnitude.

## 6.3. INDUSTRIAL PLANT FOR EBFGT AT POMORZANY POWER STATION

The main pollutants of waste gases generated in the combustion of coal in the production of electricity and heat in power plants are: sulfur dioxide and nitrogen oxides. Aggressive effect of these pollutants adversely affects not only the devices but in the first place becomes the cause of the so-called acid rain, which is a huge threat to the natural environment. The gaseous form of these pollutants means that commonly used classical filter devices are not able to signifi-

cantly reduce the amount of them. The solution to the problem is a process initiated by a stream of electrons accelerated in an accelerator with energy enabling the ionization of gases in the entire volume of the reaction chamber. The ionized gas atoms in the presence of water vapor initiate a series of chemical reactions that form acid molecules. These molecules react with gaseous ammonia. As a result of further chemical reactions, ammonium sulfate and ammonium nitrate salts are formed as solid particles, which are easily captured by filtration devices. As a result, harmful natural gases are converted into solid products that can be applied as artificial fertilizer in agriculture. The positive results of the tests performed on laboratory and pilot installations in Poland and abroad has led to decision concerning design and construction of the industrial demonstration plant for electron beam flue gas treatment. The flue gas desulfurization system was built to remove gaseous pollutants (sulfur dioxide and nitrogen oxides) generated in the process of coal combustion in the production of electricity and heat at the Pomorzany Power Station, Szczecin. The search for effective methods led to the development of radiation technology using a stream of accelerated electrons to initiate the exhaust gas purification process [22-24].

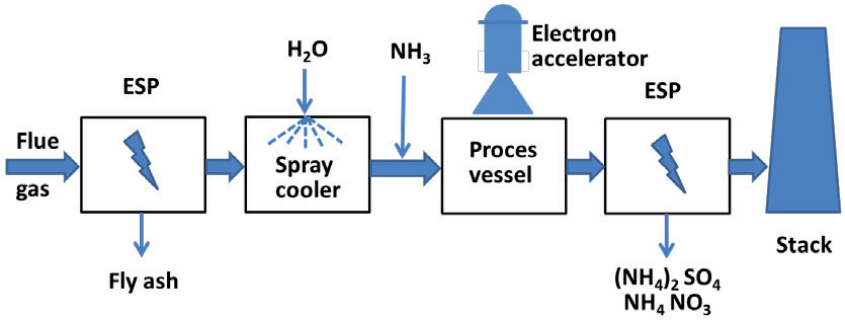


Fig. 6.21. Principal scheme of the electron beam process for flue gas treatment

Figure 6.21 shows the principal scheme of the electron beam process for flue gas treatment. Among other equipment such as electrostatic precipitators for fly ash and by-product collection, spray cooler, ammonia distribution system, accelerators play fundamentally important position as a source of accelerated electrons. Transformer electron accelerators are designed to be used as sources of ionizing radiation in various radiation treatment processes. A number of design solutions with electron energy in the range 0.7-1 MeV and power of the average beam up to 400 kW have been developed [25]. The source of accelerating voltage in these accelerators is usually a power line transformer with a sectioned secondary winding. The acceleration voltage gradient is on the order of 1 MeV/m and does not deviate from this magnitude for various accelerator design solutions, regardless of the final energy of the accelerated electrons in a given device.

The acceleration section can be placed axially in the column of the voltage generator rectifier section or installed separately from the high voltage generator. In the latter case, it is necessary to connect both elements of the accelerator with a high voltage cable. The high voltage generator is located in a housing (pressure vessel) filled with $SF_6$ gas or transformer oil. Acceleration sections installed separately are usually insulated using $SF_6$ gas. Accelerating section in transformer accelerators can be installed as horizontal or vertical devices.

Accelerators are key devices included in the installation for the removal of gaseous pollutants in the exhaust stream. They should be adapted to the requirements of the radiation method and to meet the standards and conditions for devices operating in industry, in particular in power plants. The efficiency of accelerators has a significant impact on the economic effects of radiation treatment. Changes in the construction of high power accelerators have allowed to limit energy losses by optimizing the design of these devices. It should be noted that the overall efficiency depends to the greatest extent on the principle of the type of accelerators and the

efficiency of accompanying devices. For example, transformer electron accelerators working with 50 Hz power supply, in the electron energy range 0.8-1.0 MeV reaches electrical efficiency above 80%.

Reduction of energy losses what assures increasing efficiency of accelerators depends mainly on the machine construction developed by given manufacturer. The essential role of the installation project is to properly match the accelerator output devices and the size of the reaction chamber. This allows optimizing the amount of energy transferred to the treated exhaust. The main technical requirements for the accelerator parameters to be installed in Pomorzany Power Station included: electron energy – 0.8-1 MeV, average power of the beam – max. 4 × 300 kW, efficiency – > 80%, assuming the annual use of devices in the dimension of 6500 h. The selection of the accelerator intended for radiation treatment is usually determined by the energy and medium power of the accelerated electron beam. Sometimes parameters such as: purchase cost, efficiency, reliability, presence of local shields, accelerator control method, necessary service qualifications are taken into account. Electron beam flue gas treatment process applies electron beams in the energy range of 300-1000 keV. The upper range is limited by too high electrons penetration range (above 3 m). The use of smaller diameter chambers would limit electron beam utilization coefficient and thus the efficiency of the process would be smaller. In turn, at energies of 300 keV there are significantly high losses in the output window.

An important parameter of the accelerator is the average current beam. Its size at a given electron energy determines the average power and thus this parameter determines the productivity of the installation. Due to the changes in the intensity of the radiation treatment process caused by the change of gas velocity, it is necessary to be able to automatically adjust the beam current to maintain constant irradiation conditions. Accelerators currently being built are usually equipped with a computer control system for electron beam parameters and devices included in the accelerator. This simplifies the operation of the device considerably, eliminates failures resulting from operating errors and also enables optimization of the radiation treatment process.

The selection process of suitable accelerators for installation at Pomorzany Power Station (with the participation of international experts) led to the purchase of Nissin High Voltage accelerators from Japan. These equipment was donated by the IAEA in the frame of TC project. The accelerators installed in the Flue Gas Desulphurization Installation Pomorzany consisted of two high voltage DC power supplies with nominal parameters of 800 kV, 750 mA, each of them feeding two accelerating heads with nominal parameters of the accelerated electron beam: energy of 800 keV, beam current of 375 mA. Basic parameters describing the technical capabilities of accelerators are as follows:

- acceleration voltage: 800 kV DC;,
- the maximum tested voltage: 880 keV;
- acceleration voltage stability: ±2% (max.);
- time to reach the nominal voltage: 300 s;
- beam current for one head: 375 mA (max.);
- beam current stability: ±2% (max., except for quick changes in power supply voltage);
- time to reach the nominal beam current value: 60 s;
- linear beam output: doubled 225 mm sweep length;
- frequency of sweep: 200 Hz (Y) + 60 Hz (X);
- sweep angle: 60º (max.);
- surface uniformity: ±5% (over the entire length of the sweep, measured by a CTA dosimetric foil at a distance of 100 mm from the first window);
- beam current with reduced sweep width: 1.67 mA/cm (max.).

The accelerators have been designed to maximize the efficiency of the process of converting electrical energy, supplying accelerators, to the power of the accelerated electron beam while maintaining the reliability of the devices. Each of the two high voltage DC power supplies consisted of the following components:

- A transformer reducing AC voltage from 6000 V to 1100 V, necessary to secure the appropriate voltage level at the input of the thyristor control system. The transformer has

Fig. 6.22. High voltage power supply with oil insulation

an oil insulation (750 l). Unit weight is 2800 kg, dimensions are 1.6 m × 1.5 m × 1.8 m. The transformer has additional taps on the primary winding for voltages 6.6 kV and 6.3 kV.

- The high voltage DC power supply with oil insulation in the Greinacher system is placed in a hermetically sealed housing (Fig. 6.22). In this housing, in addition to the voltage boost-

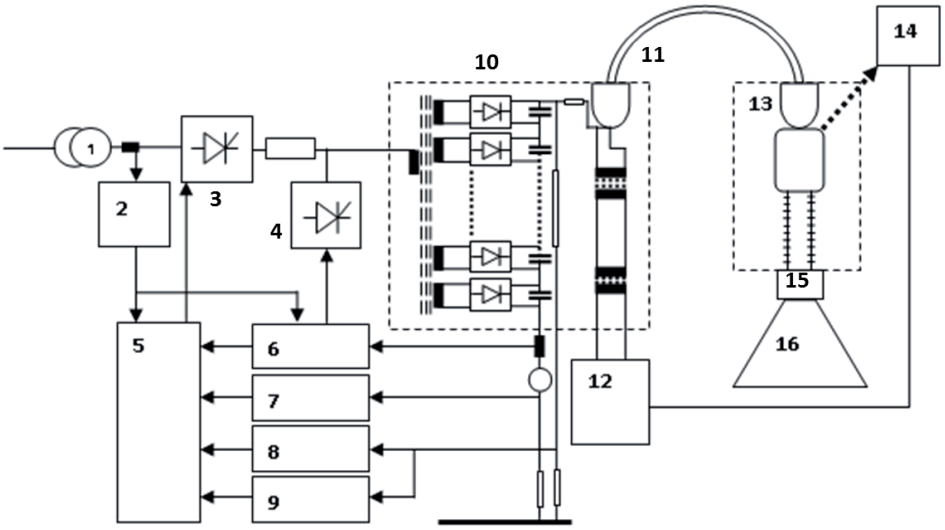


Fig. 6.23. Block diagram of the high voltage supply system of NHV accelerator with HV power supply: 1 – step-down AC power line transformer, 2 – current detector, 3 – thyristor key of the voltage regulator (serial), 4 – parallel thyristor key, 5 – serial key controller, 6 – parallel key driver, 7 – DC current detector for HV power supply, 8 – surge detector, 9 – microprocessor, 10 – HV transformer, 11 – HV cable, 12 – power supply system of the electron gun, 13 – accelerating head, 14 – signal receiver from the heater feed, 15 – beam deflection electromagnets, 16 – scanner

ing transformer, there is a system for measuring the output voltage and a power supply for the heater circuit of the electronics guns placed in the accelerating heads. There is a special diaphragm in the conservator housing that balances oil volume changes when the temperature changes. This ensures that the oil is not in contact with atmospheric air, which extends the life of the oil well. The power supply was equipped with temperature and oil pressure sensors that enable the automatic shutdown of the system in the case of violation of the work regime. The efficiency of the power supply, as a result of the applied technical solutions and power supply with 50 Hz network, is over 90%. This device is intended for installation inside the building. Unit weight is 48 t (including 27 000 l of transformer oil), dimensions are 2.8 m × 5.6 m × 4.8 m. The temperature and pressure sensors installed in the HV power supply are included in the signaling and interlocking system related to the operation of individual accelerator.

- A thyristor system designed to control the alternating input voltage for a high voltage DC power supply for controlling the DC voltage level at the HV power supply output. Control of the thyristor system is carried out from the desktop located in the control room of the accelerator. The block diagram of the high voltage supply system of NHV accelerator with HV power supply in presented in Fig. 6.23.

Each of the four accelerating heads consists of the following components: an electron gun, a vacuum accelerating column, a column of resistors, a pressure casing. The pressure housing is filled with $SF_6$ insulating gas at a pressure of 7 kg/cm$^2$. Figure 6.24 shows the general view of the accelerating head mounted on the steel plate. The gun (electron source) is connected via a high voltage connector and a limiting resistor to the DC power supply using a high voltage cable.


Fig. 6.24. General view of the accelerating head of NHV accelerator

The accelerating column is installed in the interior of the pressure enclosure, which is equipped with a lead shield, as biological cover, in the room in which the accelerating head is installed. The accelerating column consists of aluminum electrodes separated by glass isolators (Fig. 6.25). Tight metal glass connections allow to get a high vacuum inside the column. A resistor system installed on the outside with Zener diodes connected to the next electrodes ensures uniform distribution of voltage over its entire length. The accelerating column is one of the vacuum elements besides the electron gun and the electron beam scanning chamber. To

maintain appropriate conditions for accelerating and focusing the electron beam, the vacuum should be in the range of $10^{-4}$-$10^{-5}$ Pa. The electron gun is the only consuming element of the accelerator with specific technical conditions of life. Replacing the electron gun requires at least one-day accelerator stoppage. It is connected with necessity unsealing of the pressure part and the vacuum accelerator, exchange of works, obtaining adequate vacuum and pressure of the insulating gas. After obtaining a proper vacuum, it is necessary to train the accelerating section with high voltage and then the beam current to obtain the nominal accelerator parameters.

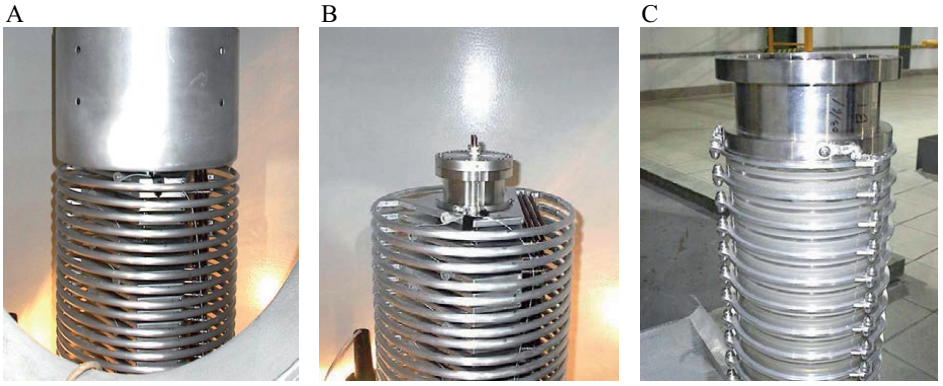


Fig. 6.25. Accelerating section arrangement: A – top of accelerating column, B – electron gun location, C – accelerating head with metal electrode and glass isolators

The electrons are emitted from the directly heated tungsten cathode of the electron gun, installed at the beginning of the accelerating column. The gun heater circuit includes a voltage reducing transformer and a heat sink for cooling. The change in the heater current changes the amount of electron emission from the cathode, which in turn allows adjust the electron beam current. The triangular shaped sweep chamber is made of stainless steel. The scanner chamber is installed at the output of each accelerating head (Fig. 6.26). The chamber is equipped with a system of sweeping coils having an adjustable mechanism allowing for precise optimization of the position of the electron beam.

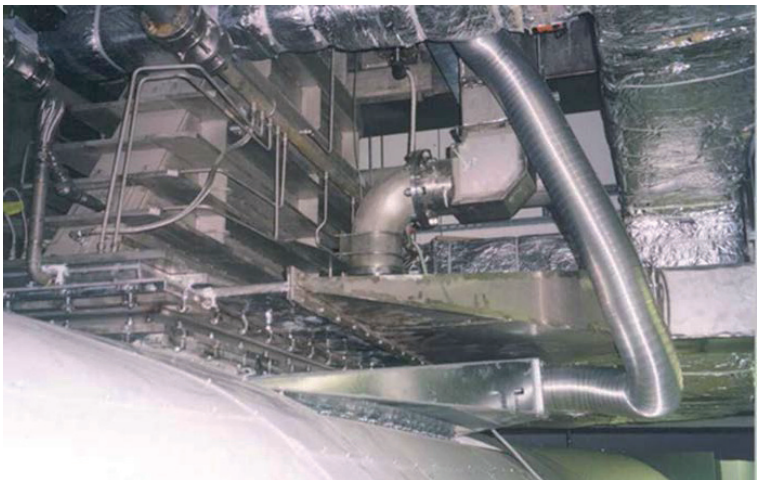

Fig. 6.26. The sweep chamber equipped with an external duct system for intensive cooling of the exit window and process vessel window

A B

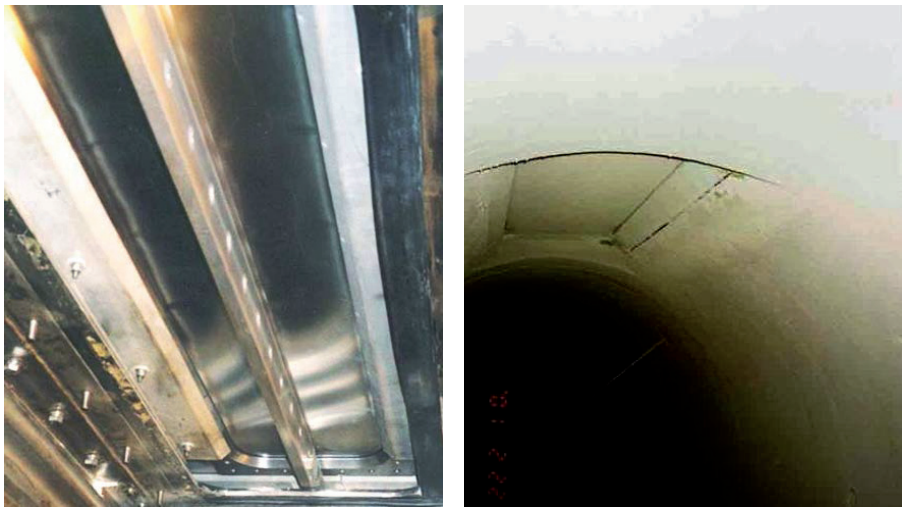

Fig. 6.27. Output system arrangement: A – two-path accelerator exit window, B – reaction chamber titanium window

The accelerator exit window is made of thin titanium foil 38 μm thick, used to deliver the electron beam outside the accelerator, and is fixed at the end of the chamber using metal gaskets that provide a proper vacuum (Fig. 6.27A). 50 μm titanium foil is used as reaction chamber inlet window (Fig. 6.27B). The mechanical properties of the foil ensure a permanent division into the vacuum part inside the chamber from the atmospheric pressure outside. At the same time, the small thickness of the foil will contribute only to a small extent to the loss of the beam's power through the stream of electrons.

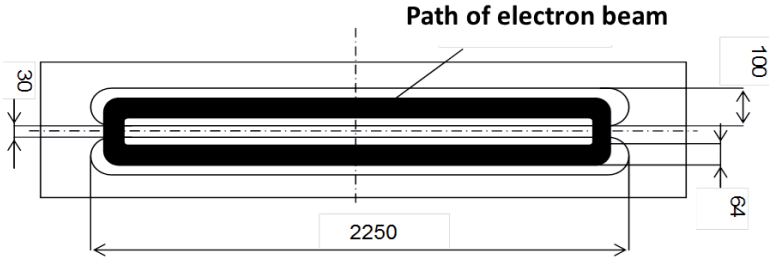


Fig. 6.28. Schematic beam sweep path on exit window in the NHV accelerator

The triangular wave current flowing through the coils marked with the Y symbol moves the electron beam along the exit window. The coils marked with X move the electron beam in the direction perpendicular to the Y axis. This deflection pattern (Fig. 6.28) provides better distribution of the thermal load caused by the absorption of a portion of the electron beam energy in the titanium exit foil. The exit foil is mounted with metal gaskets ensuring a high vacuum connections.

The high vacuum is achieved by using an ion pump and a sublimation pump assisting the vacuum system at reduced vacuum. The high vacuum is maintained in the accelerating column and in the sweep chamber by ion pumps during the routine operation of the accelerator without the need for cooling (low energy consumption). When starting up and accelerator training with the beam current and when a higher pumping speed is required, a water-cooled sublimation pump with a capacity of 2000 l/s is started. Metal seals and no oil vapors in the system (no

rotary oil pump) ensures high efficiency and durability of the vacuum system. A rotary pump equipped with a suitable valve is used after the vacuum system has been vented and is used in the initial stage of pumping.

Table 6.4. Power supply parameters

| Type of equipment | Electrical specifications | Power supply | Remarks |
|---|---|---|---|
| Accelerator | 3 × 6 000 V, 50 Hz | 950 kVA, 667 kW | one accelerator unit |
| Accelerators together | 3 × 6 000 V, 50 Hz | 1900 kVA, 1334 kW | two accelerator units |
| Control power supply | 3 × 380 V, 50 Hz | 10 kVA, 5 kW | one accelerator unit |
| Vacuum system power supply | 3 × 380 V, 50 Hz | 5 kVA, 0,4 kW | one accelerator unit |
| Exit window fan | 3 × 380 V, 50 Hz | 200 kVA, 150 kW | one accelerator unit |
| Ozone extraction fan | 3 × 380 V, 50 Hz | 15 kVA, 11 kW | one accelerator unit |
| Vacuum power supply | | 2 kVA | |
| Auxiliary equipment | 3 × 380 V, 50 Hz | 460 kVA, 332,8 kW | two accelerator units |
| Total | | 2362 kVA, 1668,4 kW | |

Requirements for powering the accelerator and electrical devices cooperating with the accelerator are presented in Table 6.4. The instability of the power supply network should be better than ±5%. Cables were provided by the Polish suppliers except four sections of the high voltage 800 kV cables to connect the high voltage DC power supply with the acceleration section, also allowing transmission of the cathode heating current. According to the recommendations of the accelerator manufacturer, a grounding installation with a resistance of less than 10 Ω was required.

The signaling, interlock and control system consists of a control panel equipped with a PLC microprocessor (A2ACPU Mitsubishi Corporation) and an operator's console. The console has the following components:

- the key – starting operation accelerator facility;
- START – after pressing the button the accelerating voltage is switched on and then the electron beam is switched on;
- BEAM STOP – after activating this button, the switching off of the electron beam is switched to zero;
- STOP – pressing the button results in first bringing the beam current to zero and then accelerating voltage;
- EMERGENCY – pressing the emergency button will immediately disable the accelerator. This button should be used only in an emergency, because it may damage some elements of the accelerator.

The operator's console provides information via the monitor screen regarding changes in the work mode and the values of individual accelerator parameters:

- current operation of accelerator or application of unintendable employment regulations;
- registration, changes and measurements of parameters;
- checking the condition of lock and security.

For direct communication with the operator, a control panel monitor screen is used, allowing the user to select the appropriate operating regime or the function performed by the measurement system.

The use of a system based on a single key is a commonly applied and recommended practice. The accelerator cannot be started if the key is not in the control console. This key

cannot be removed from the console without first switching off the accelerator. At the same time, this key allows to open the door to the room where the reaction chambers are installed. The closing of this room by the operator should be preceded by the activation of audible and visual signaling informing the persons located near this place. The button that activates the signaling is located in the room of the reaction chambers. This creates the need to inspect the room by the operator before starting the accelerator. The duration of the audible and visual signaling of a few minutes should ensure that the operator reaches the accelerator console. Extending over a specified period, the whole operation should be repeated.

The accelerator is immobilized if the room door of the reaction chambers has been opened. On the other hand, the accelerator can only be started when the door is closed. In addition, there is a blockage of the inclusion of the accelerator, manually activated by people employed in the room of reaction chambers for working time in this room. Regulation and stabilization of voltage accelerating the flow of electrons in the accelerator is based on programing the operation of the control block (PLC processor). Depending on the operator's work schedule of the accelerator through the control terminal, the following functions of the system can be distinguished: sound signaling, optical signaling, mechanical interlock systems, electrical blocking systems, authorized access to support for accelerators.

Fig. 6.29. Control room of flue gas treatment facility located at Pomorzany Power Station

Figure 6.29 shows control room arrangement of flue gas treatment facility located in Pomorzany Power Station. It can be seen three group of computer control devices to operate facility equipment: accelerator consoles, installation auxiliary equipment consoles, monitors for continuous registration process parameters.

The total beam power absorbed in the waste gases in the process of radiation removal of pollutants nominally was 1200 kW. Figure 6.30 shows view of Pomorzany Power Station. Flue gas humidifier tower of EBFGT plant can be seen on the front left side.

Beam energy was introduced into each of the two reaction chambers through each of the four beam scanners. It should be noted that one reaction chamber is equipped with two windows. Both chambers are installed in one room. The shielding walls as well as the labyrinth for pipe connections and entrance doors to the room provide the required protection against ionizing radiation. Accelerators installed in the Flue Gas Desulfurization Unit were designed for continuous operation with 800 kV accelerating voltage. Accelerating heads can work with identical or different parameters of the electron beam current. The beam current in each accelerating head can be determined by the operator or set automatically based on the current technological conditions. It was also possible to work with only one set of devices (HV power supply and two accelerating heads). Figure 6.31 shows the diagram of radiation facility for flue

Fig. 6.30. View of Pomorzany Power Station – flue gas humidifier tower of EBFGT plant

gas treatment ($SO_2$ and $NO_x$ removal) with flow rate 270 000 $Nm^3/h$ located at Pomorzany Power Station.

The flue gas was collected from two Benson boilers with an electrical capacity of 60 MWe each. The boilers were fired with coal dust and operated at variable load depending on

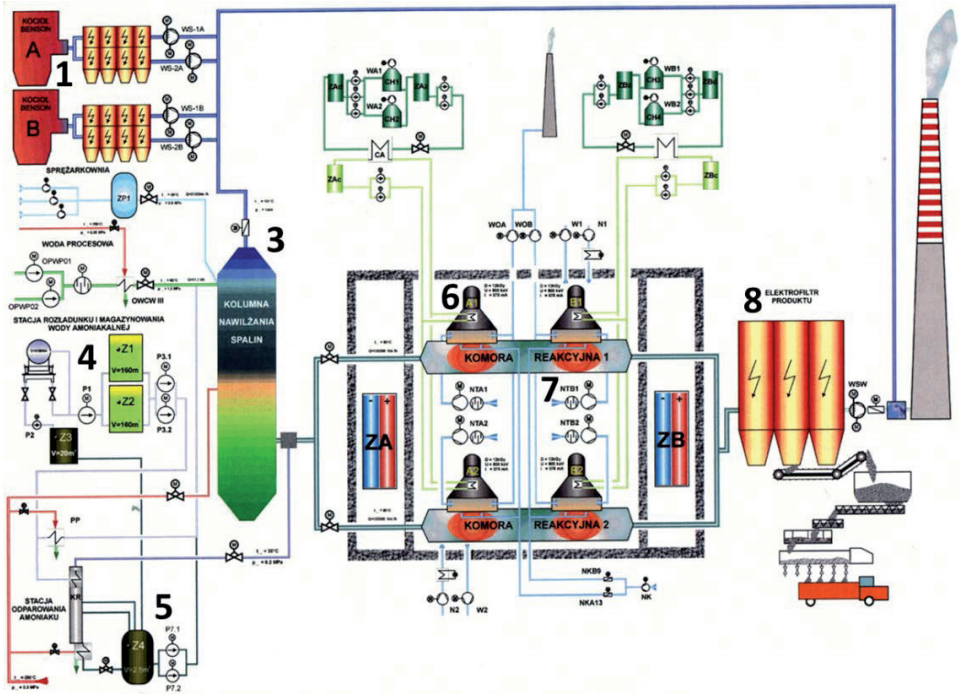


Fig. 6.31. Radiation facility for flue gas treatment ($SO_2$ and $NO_x$ removal) with flow rate 270 000 $Nm^3/h$ located at Pomorzany Power Station: 1 – boiler, 2 – electrostatic precipitator, 3 – spray cooler, 4 – ammonia tank, 5 – ammonia evaporator, 6 – accelerator, 7 – process vessel, 8 – electrostatic precipitator (by-product collection)

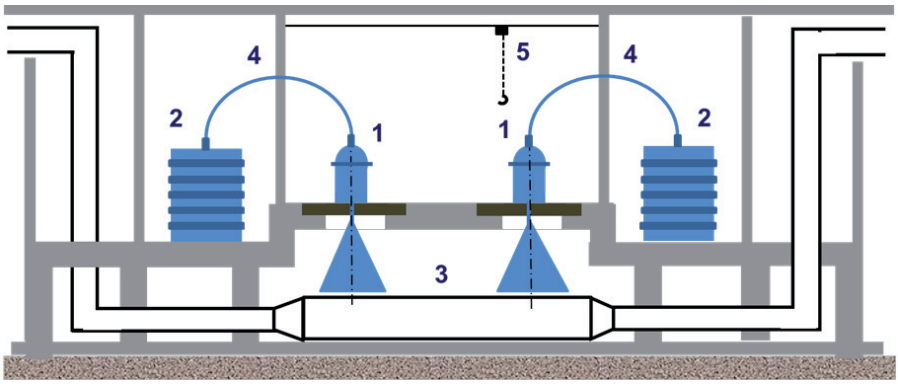


Fig. 6.32. Arrangement of flue gas irradiation process: 1 – accelerator, 2 – power supply, 3 – process vessel, 4 – HV cable, 5 – hoist

the electricity demand. The flue gas temperature ranged from 120°C to 140°C. The $NO_x$ content was 800-900 mg/Nm$^3$ and was higher than the design assumptions. Purification flue gas was taken from the collector in quantities lower by half than the total flue gas stream. Figure 6.32 shows the location of accelerators in relation to the reaction chamber (process vessel). The second analog line was arranged in parallel in the same room with shielding covers.

Industrial demonstration facility for flue gas treatment has been tested with nominal accelerator parameters. After positive results obtained during the tests performed at the beginning of facility operation, principal problem with accelerators of EBFGT facility has appeared. Isolation damage of HV transformer (800 kV) of HV power supply was stated. The main reasons of HV transformer damages were related to sparks observed in accelerating section and caused by insufficient vacuum level especially during voltage conditioning procedure. Long HV cable with relatively high dispersed capacitance response after short spark in accelerating section caused oscillations, which amplitude was 50% higher than nominal voltage level. In such conditions the existing isolation inside HV transformer was to weak. In consequence the only condition for stable accelerator operation was reduction of accelerating voltage to 700 kV. At the same time beam power from one accelerating head was reduced to 262 kW, with nominal value of average beam power. Because of electron energy reduction from 800 keV to 700 keV and beam power reduction from 300 kW to 262.5 kW, reaction vessel diameter was reduced as well and facility productivity was decreased by 12.5%. Four electron accelerators constructed by Nissin High Voltage, Kyoto, Japan were operated with electron energy 0.7 MeV and total beam 1050 kW [25]. Electron beam distribution was measured in volume of process vessel with CTA dosimetric foil application. The diagram illustrating dosimetric foil arrangement inside of process vessel under beam exit window is shown in Fig. 6.33.

As a consequence of electron energy reduction from 800 keV to 700 keV was necessary reduction of reaction vessel diameter from 2.48 m to 1.88 m. Necessary reaction chamber shape correction was done by placement inside reaction vessel profiled steel plates. Figure 6.34 shows depth dose distribution across and along reaction vessel (X – 20 cm/div; Y – 5 cm/div; isodoses every 10 kGy, max. 200 kGy) for new reaction vessel configuration.

Final tests were performed for new facility parameters. The obtained by-product composition was as follows:

- $(NH_4)_2SO_4$: 45-60%,
- $NH_4NO_3$: 22-30%,
- $NH_4Cl$: 10-20%,
- Moisture: 0.4-1%,
- water insoluble parts: 0.5-2%.

The by-product yield was up to 300 kg/h. Figure 6.35 shows part of the flue gas treatment facility used for by-product collection and transportation.

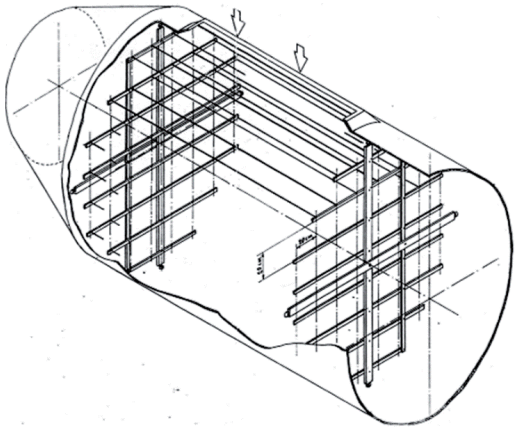

Fig. 6.33. Diagram illustrating dosimetric foil arrangement inside of process vessel under beam exit window

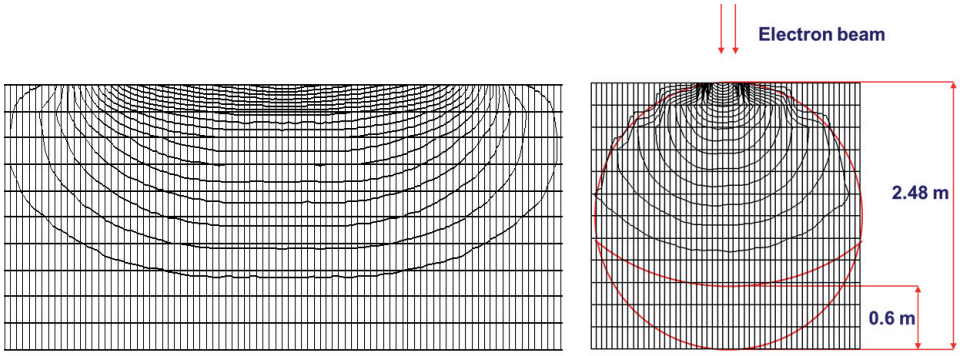


A B

Fig. 6.34. Dose distribution along (A) and across (B) reaction vessel (X – 20 cm/div; Y – 5 cm/div; isodoses every 10 kGy, max. 200 kGy; electron energy – 700 keV

Fig. 6.35. Part of the flue gas treatment facility responsible for by-product collection and transportation

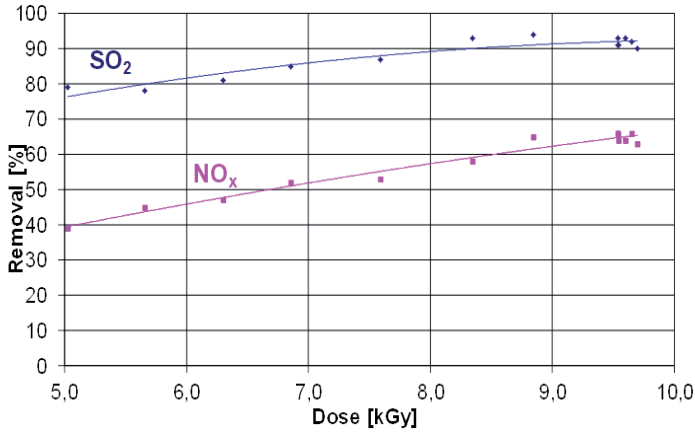


Fig. 6.36. Dependence of $SO_2$ and $NO_x$ removal efficiency on dose at Pomorzany flue gas treatment facility

The removal of $SO_2$ approaches 80-93% in the dose range up to 9.5 kGy, and that of $NO_x$ is 50-65% (Fig. 6.36). In the case of $SO_2$ removal, more parameters have impact on the removal efficiency due to process mechanism. The most important parameter is temperature of the gases at the reaction vessel inlet because of the thermal reactions pathway. $SO_2$ removal efficiency decreases rapidly with the temperature increase. Humidity is the second parameter that impact on the process efficiency; however it is hard to observe it because of the strong correlation between the humidity and the temperature of the process caused by the simultaneous cooling and humidification process in the cooling tower. Nevertheless improvement of the removal efficiency was observed when humidity increased by adding a steam into the cooling tower. Maximum $SO_2$ removal efficiency (98%) required increasing the humidity up to 14% vol. During simultaneous removal of $SO_2$ and $NO_x$, the impact of ammonia stoichiometry on $SO_2$ removal is much higher than on $NO_x$ removal. As it was previously found during laboratory and pilot plant research, the dose plays rather moderate role in $SO_2$ removal process. Low temperature, high humidity and low dose are required to obtain high $SO_2$ removal efficiency. The by-product is collected by the electrostatic precipitator and shipped to the fertilizer plant where high quality multicomponent fertilizer was manufactured (Fig. 6.37).


Fig. 6.37. NPK fertilizer manufactured on the basis of EBFGT plant by-product.

Two-stage irradiation was applied as it was tested at the pilot plant. The industrial installation located at Pomorzany Power Station consists of two independent reaction chambers,

humidification tower with water and steam supply systems, ammonia water handling system with ammonia injection, electrostatic precipitator, by-product handling system, measuring and control systems. The results of industrial facility preliminary exploitation [26, 27] indicated that $SO_2$ and $NO_x$ desired pollutants removal efficiency from the flue gas can be obtained under certain conditions such as sufficient humidity, suitable flue gas temperature, dose rate and ammonia stoichiometry. Depending on the local conditions, $SO_2$ or $NO_x$ removal can be optimized to achieve primary goals of the facility. Good reliability of the accelerators is the crucial for smooth exploitation of the facility. By-product quality may be influenced by coal and water quality used in the process.

## References


[1]. Chmielewska-Śmietanko, D. (Ed.). (2015). *The industrial and environmental applications of electron beams*. Warszawa: Institute of Nuclear Chemistry and Technology. http://www.ichtj.waw.pl/ichtj/publ/monogr/m2015_4.htm.

[2]. Zimek, Z., & Chmielewski, A.G. (1993). Present tendencies in construction of industrial electron accelerators applied in radiation processing. *Nukleonika*, *38* (2), 3-20.

[3]. Frank, N.W. (1995). Introduction and historical review of electron beam processing for environmental pollution control. *Radiat. Phys. Chem.*, *45*, 6, 989-1002.

[4]. Chmielewski, A.G., Iller, E., Zimek, Z., & Licki, J. (1992). Laboratory and industrial installation for EB flue gas treatment. In *Applications of isotopes and radiation in conservation of the environment: Proceedings of a Symposium, Karlsruhe, 9-13 March 1992* (pp. 81-92). Vienna: IAEA. IAEA Proceedings Series.

[5]. Chmielewski, A.G.. Iller, E., Zimek, Z., & Licki, J. (1992). Pilot plant for electron beam flue gas treatment. *Radiat. Phys. Chem.*, *40*, 4, 321-325.

[6]. Golubienko, Y.I., Weis, M.E., Kuksanov, N.K., Kuzniecov, S.A., Korabielnikov, B.W., Malinin, A.B., Nemytov, P.I., Prudnikov, W.W., Petpov, S.E., Salimov, R.A., Cerepkov, W.G., & Fadeev, S.N. (1997). *Electron accelerators ELV type: status, application, progress*. Budker Institute of Nuclear Physics. Russia, INP 97-7.

[7]. Chmielewski, A.G., Zimek, Z., & Panta, P. (1991). *Electron beam system and dose distribution in the process vessel in a pilot plant for flue gases treatment*. Warszawa: Institute of Nuclear Chemistry and Technology. Report INCT-2117/IChTJ.

[8]. Chmielewski, A.G., Zimek, Z., Panta, P., Drabik, W. (1995). The double window for electron beam injection into the flue gas process vessel. *Radiat. Phys. Chem., 45*, 6, 1029-1033.

[9]. Licki, J., Chmielewski, A.G., Zakrzewska-Trznadel, G., & Frank, N. (1992). Monitoring and control systems for an EB flue gas treatment pilot plant, Part I. analytical systems and methods. *Radiat. Phys. Chem.*, *40*, 4, 331-340.

[10]. Chmielewski, A.G., Tymiński, B., Licki, J., Iller, E., Zimek, Z., & Radzio, B. (1995). Pilot plant for flue gas treatment-continuous operation tests. *Radiat. Phys. Chem.*, *46*, 4-6, 1067-1070.

[11]. Chmielewski, A.G., Licki, J., Dobrowolski, A., Tymiński, B., Iller, E., & Zimek, Z. (1995). Optimization of energy consumption for $NO_x$ removal in multistage gas irradiation process. *Radiat. Phys. Chem.*, *45*, 6, 1077-1079.

[12]. Chmielewski, A.G., Tymiński, B., Dobrowolski, A., Iller, E., Zimek, Z., & Licki, J. (2000). Empirical models for $NO_x$ and $SO_2$ removal in a double stage flue gas irradiation process. *Radiat. Phys. Chem.*, *57*, 527-530.

[13]. Chmielewski, A.G., Tymiński, B., Licki, J., Iller, E., Zimek, Z., & Dobrowolski, A. (1993). Pilot plant for flue gas treatment with electron beam start up and two stage irradiation tests. *Radiat. Phys. Chem*., *42*, 4-6, 663-668.

[14]. Szlachciak, J., Kupczak, R., Obstój, I., Płomiński, M., Sowiński, M., Uzdowski, M., Chmielewski, A., & Peryt, W. (1992). Monitoring and control systems for an EB flue gas treatment pilot plant – Part II. PC based data acquisition system. *Radiat. Phys. Chem.*, *40*, 4, 341-346.

[15]. Chmielewski, A.G., & Zimek; Z. (1998). *Urządzenie wprowadzające wiązkę elektronów do komory reakcyjnej w procesie radiacyjnego usuwania $SO_2$ i $NO_x$ ze strumienia przemysłowych*

*gazów odlotowych* (Facility introducing electron beam into a reaction chamber in the process of radiation induced removal of $SO_2$ and $NO_x$ from a stream of industrial gases). Polish Patent 174442.

[16]. Zimek, Z., Jackowski, Z., & Chmielewski, A.G. (1997). *Sposób i urządzenie do usuwania niepożądanych składników z przemysłowych gazów odlotowych* (Method and an equipment for removal of undersirable components from industrial flue gases). Polish Patent 172964.

[17]. Zimek, Z., Jackowski, Z., & Chmielewski, A.G. (1997). *Sposób usuwania niepożądanych składników z gazów oraz urządzenie do usuwania niepożądanych składników z gazów* (Method and an equipment for removal of undersirable components from industrial flue gases). Polish Patent 173176.

[18]. Chmielewski, A.G., Zimek, Z., Licki, J., Tymiński, B., & Iller; E. (1997). *Sposób usuwania kwaśnych zanieczyszczeń gazowych takich jak $SO_2$ i $NO_x$ z przemysłowych gazów odlotowych* (Method for removal of acid gaseous impurities like $SO_2$ and $NO_x$ from industrial flue gases. Polish Patent 169749.

[19]. Chmielewski, A.G., Iller, E., Zimek, Z., Janowski, A., Karpiński, L., & Kurzyński, Z. (1995). *Sposób usuwania kwaśnych zanieczyszczeń gazowych zwłaszcza $SO_2$ i $NO_x$ oraz zanieczyszczeń organicznych zwłaszcza dioksyn z przemysłowych gazów spalinowych* (The method of removal of acid gas pollutants such as $SO_2$ and $NO_x$ and organic pollutants such as dioxine from industrial flue gases). Polish Patent 167481.

[20]. Pawelec A., Chmielewski A.G., Licki J., Han, B., Kim, J., Kunnummal, N., & Fageeha, O.I. (2016). Pilot plant for electron beam treatment of flue gases from heavy fuel oil fired boiler. *Fuel Process. Technol.*, *145*, 123-129.

[21]. Chmielewski A.G., & Han, B. (2016). Electron beam technology for environmental pollution control. *Top. Curr. Chem.*, (Z), *374*, 68.

[22]. Chmielewski, A.G., Iller, E., Zimek, Z., Romanowski, M., & Koperski, K. (1995). Industrial Demonstration plant for electron beam flue gas treatment. *Radiat. Phys. Chem.*, *46*, 4-6, 1063-1066.

[23]. Chmielewski, A.G., Zimek, Z., Iller, E., Tymiński, B., & Licki, J. (2000). Industrial applications of e-beam plasma to air pollution control. *Journal of Technical Physics*, *41*, 1, Special Issue, 551-572.

[24]. Chmielewski, A.G., Tymiński, B., Iller, E., Zimek, Z., Licki, J., Kostrzewski, R., Sobolewski, L., & Cybulski, J. (2002). Instalacja przemysłowa do oczyszczania gazów spalinowych za pomocą wiązki elektronów w EC POMORZANY (Industrial facility for flue gas treatment by electron beam in EPS POMORZANY). In *Technika jądrowa, w przemyśle, medycynie, rolnictwie i ochronie środowiska. T.1* (pp. 5-10). Warszawa: Instytut Chemii i Techniki Jądrowej. Raporty IChTJ. Seria A nr 1/2002.

[25]. Zimek, Z. (1995). High power electron accelerators for flue gas treatment. *Phys. Chem.*, *54*, 6, 1013-1015.

[26]. Chmielewski, A.G., Zimek, Z., Iller, E., Tymiński, B., & Licki, J. (2003). Preliminary Exploitation of Industrial Facility for Flue Gas Treatment. In *Radiation Technology in Emerging Industrial Applications. Proceedings of a symposium held in Beijing, China, 6-10 November 2000* (CD edition, pp. 1-4).

[27]. Chmielewski, A.G., Tyminski, B., Zimek, Z., Pawelec, A., & Licki, J. (2003). Industrial plant for flue gas treatment with high power electron accelerator. In J.L. Duggan, I.L. Morgan & M. Hall (Eds.), *Application accelerators in research and industry: 17th International Conference on the Application of Accelerators in Research and Industry* (pp. 873-876). Melville, New York. AIP Conference Proceedings 680.

Chapter 7

# PRE-FEASIBILITY STUDY OF SETTING UP AN ELECTRON BEAM R&D FACILITY[#]

**Zbigniew Zimek**

## 7.1. INTRODUCTION

### 7.1.1. Objectives

Electron beam (EB) accelerators technology is now commonly accepted for research study and industrial implementation. Wide field of R&D study and business opportunities exist in electron beam accelerators facilities in various fields of applications such as sterilization for medical items, crosslinking of insulation in wires and cables, modification of properties in polymers and other radiation technologies. The importance of radiation technology is related to unique properties and quality improvement of irradiated products. Initiating work for the establishment of an electron beam facility one should recognize technical and economical parameters of the process. The facility under consideration will be implemented in the field of R&D study and may offer technical capability to introduce certain radiation technology on pilot (massive) scale. The techno-economic feasibility of irradiation process will be discussed. Specifically, technical characteristics of the irradiation process in respect to product profile are recommended and type of the facility is proposed due to volume of the products to be irradiated.

The qualification of the foundations is the main object of the present study. It allows to realize feasibility study project in connection to radiation facility dedicated to research study and practical implementation.

### 7.1.2. Scope and limitations

The present study reports of the assessment carried out of technical and economical feasibility for installation the facility where electron beam technology will be implemented. This study presents comprehensive technical and financial profiles of the radiation technology. As previously stated, its principal objective is to determine whether sufficient reasons exist that will sustain the feasibility of establishing facility. Presented recommendations are limited to data gathered from official documents. Essential information for electron beam processing with the production capability for the period of one year were provided. The most important facility parameters are as follows:

- electron energy: 5-10 MeV;
- beam power: 10-50 kW;
- dose range: 1-160 kGy;
- the most probable dose rate: 25 kGy;
- standard carton dimension: 580 mm × 460 mm;
- typical efficiency of beam energy transfer: 0.3;
- the price of the electrical energy: 0.32 PLN/kWh (0.1 €/kWh);
- one shift facility operation: 8 h/5 days/week;
- average currency rate (February 2018): 1 PLN = 0.24 €, 1 USD = 0.8158 €.

## 7.2. TECHNICAL STUDY

### 7.2.1. Carton length/width

Radiation processing is usually based on moving conveyor and scanned electron beam which provides possibility to irradiate cartons containing modified (or sterilized) products. It should be noticed that usually carton length refers to the dimension parallel to the direction of the conveyor movement during irradiation process. In respect to that the carton width refers to the dimension perpendicular to the direction of movement when the box is under the beam. According to initial data the standard carton dimension is found to be 580 mm × 460 mm. The vertical dimension of the carton will depend on product density and electron energy level.

It should be noticed that two- and sometime four-sided irradiation is applied for certain product dimensions at electron energy range 10 MeV. The maximum box length is proposed to be 120 cm. The one carton weight can vary but the maximum value of surface product density for one-sided irradiation should not exceed 2.5 g/cm$^2$ for optimal dose homogeneity during radiation sterilization process.

### 7.2.2. Scan width

Width of scanned electron beam forms irradiation zone in the direction of the beam sweeping which is located perpendicularly to the product movement. Electron beam is driven by the current of the scan electromagnet according to its time characteristic. The irradiation zone dimension is directly related to electron beam scan width (SW; beam path length) in so-called linear scanning system. It depends on accelerator specification (exit window length) of certain accelerator construction. Accelerator producer usually can provide the beam scanner with required exit window length on special order.

The other option is related to additional electromagnet system which provides capability of so-called “parallel beam” after exit window. It slightly reduces electron beam losses and improves homogeneity of irradiation process.

Uniformity of the product irradiation should be evaluated according to scanning linearity (inhomogeneity of the beam current density along the window length; usually ±10%), instability of the beam current (usually ±2.5%), frequency of scanning signal and conveyor width and speed.

### 7.2.3. Irradiation layout

The typical irradiation layout in contract irradiation facilities with conveyor is presented in Fig. 7.1. The scan width is usually higher than carton box width (BW) what leads to extra electron beam losses. Typical accelerator construction usually allows to correct scan width by simple adjustment of current level in scanning electromagnet. In such case beam utilization coefficient will be improved but at the same time conveyor system should be adopted to keep the carton in center position regarding scanning device and conveyor.

In particular case (maximum cross-section: 460 mm × 400 mm) suitable distance between conveyor surface and accelerator window is required. When that distance is higher than necessary one can expect higher ozone production rate and some extra beam energy losses in air path.

One of the most important parameter is the dose homogeneity within the irradiated product. Due to product higher density two-sided irradiation is necessary. The penetration range of accelerated electrons depends mostly on electron energy level, product geometry and its density. Figures 7.2 and 7.3 show calculated depth dose distribution within irradiated box with dimension 460 mm × 400 mm, product density 0.22-0.25 g/cm$^3$, for electron energy 10 MeV and 5 MeV when one- or two-sided irradiations are applied.

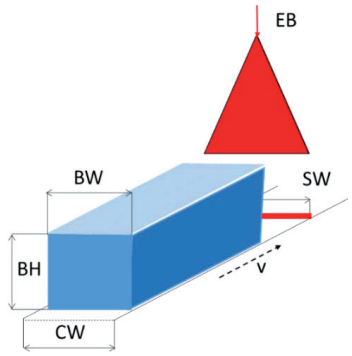


Fig. 7.1. Typical geometry of irradiation process performed in accelerator facility with conveyor as under beam equipment: EB – electron beam, CW – conveyor width, SW – scan width, BW – carton box width, BH – carton box height, v – conveyor speed. Carton box maximum cross-section (BW × BH): 480 mm × 400 mm

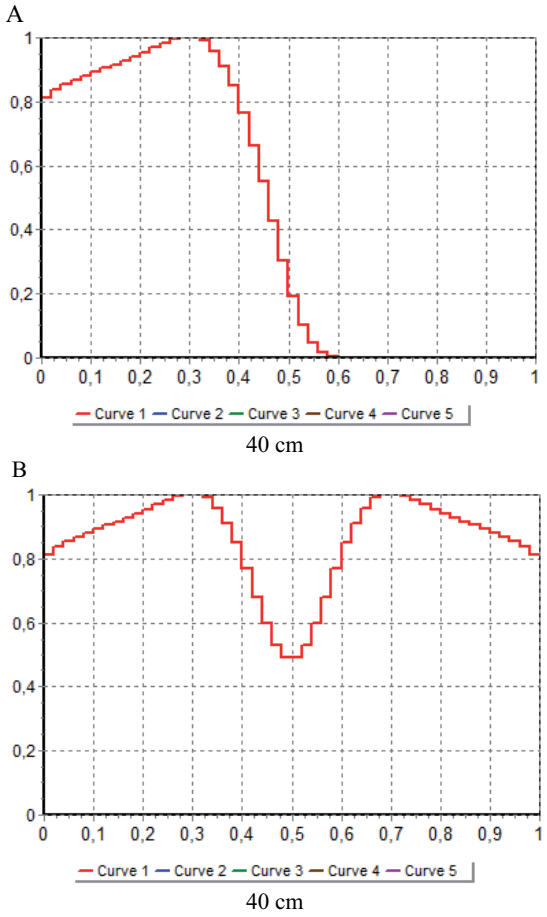


Fig. 7.2. Depth dose distribution in homogeneous object with unit density 0.25 g/cm$^3$ and thickness 40 cm irradiated by scanned electron beam with energy 10 MeV for: A – one-sided irradiation, B – two-sided irradiation

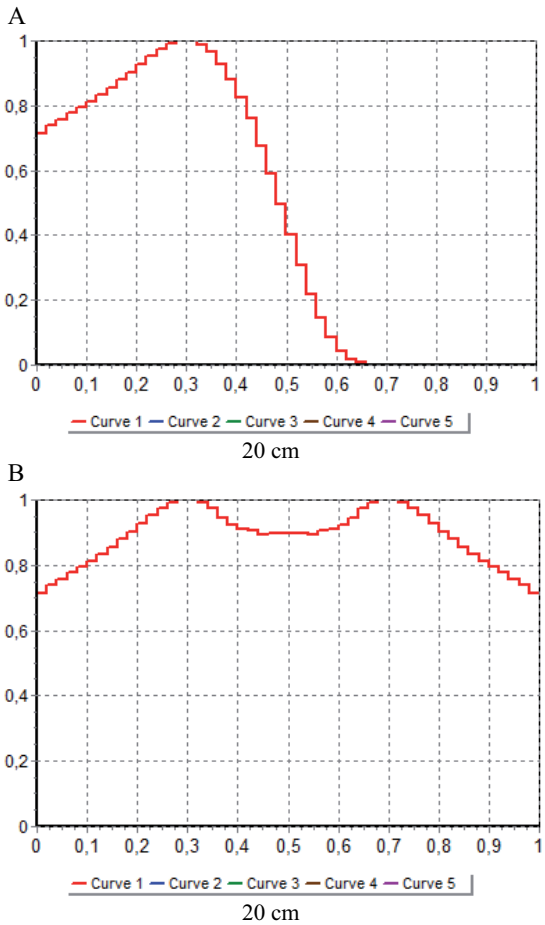


Fig. 7.3. Depth dose distribution in homogeneous object with unit density 0.22 g/cm$^3$ and thickness 20 cm irradiated by scanned electron beam with energy 5 MeV for: A – one-sided irradiation, B – two-sided irradiation

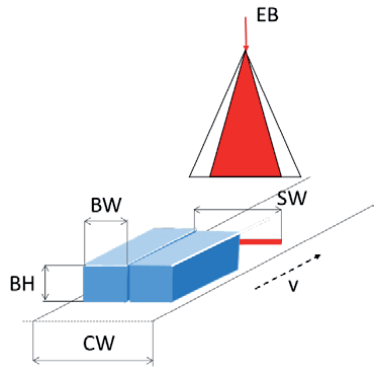


Fig. 7.4. Geometry of irradiation process performed in accelerator facility with conveyor as under beam equipment: EB – electron beam; CW – conveyor width, SW – scan width, BW – carton box width, BH – carton box height, v – conveyor speed. Carton box maximum cross-section (BW × BH): 250 mm × 250 mm

The computer simulations of circumferential dose distribution initiated by scanned electron beam in flat irradiated material were performed by Monte Carlo method with utilization of the software program ModeRTL described in the IAEA publication (Lazurik, V.T., Lazurik, V.M., Popov, G., Rogov, Yu., & Zimek, Z. (2011). *Information System and Software for Quality Control of Radiation Processing*. Warszawa). The computer program ModeRTL was designed specifically for simulation dose distribution in multilayer circular objects for the electron energy range 0.1-25 MeV. The self-consistent physical and geometrical models of the program ModeRTL include features of electron beam transport and the dose field formation in circular objects. The program ModeRTL uses as input data number of parameters related to radiation facility including electron beam spatial distribution and material properties and dimensions. The verification of simulation results was performed by dosimetry experiments.

As can be easily noticed, one- and two-sided irradiations are acceptable with defined homogeneity of depth dose distribution for exact relation between electron energy and product density and thickness.

As mentioned before, typical accelerator construction usually allows to correct scan width by simple adjustment current level in scanning electromagnet to reduce beam power losses (Fig. 7.4). In such case beam utilization coefficient will be improved but at the same time conveyor system should be adopted to keep the boxes in center position regarding scanning device.

### 7.2.4. Conveyor requirements

The conveyor shall carry cartons from the loading area to the irradiation process zone which is located inside the concrete shelter. The products should be processed at a specified speed by scanned electron beam usually coming from the top. After being irradiated, the cartons should leave the shelter.

The conveyor is divided into different subsections in order to ensure a smooth, bump free and continuous product movement under the beam. Everywhere on the conveyor, the cartons should be correctly guided avoiding any transportation disturbance such as skidding, blocking or turning head to tail. The material to be irradiated may be contained in cartons of various sizes.

The whole system should be fully controlled and driven by a PLC with its associated control features. At the vicinity of the beam, the environment will be very corrosive; stainless steel is to be used for construction of the irradiation process conveyor. Plastic parts, electronic and electric devices should not be present close to irradiation zone.

The conveyor necessary for implementation of irradiation process can be provided by accelerator manufacturer or accelerator manufacturer can recommend certain company with suitable experience in that field. It is also possible design conveyor construction based on typical components accessible on the market supported by unique mechanical equipment specifically matched to certain product and selected configuration of irradiation process.

Mechanical and electrical hazards exist during conveyor use. The supplier shall analyze the associated risks and provide appropriate guards and interlocks against such hazards. Figure 7.5 shows typical conveyor system for carton irradiation process composed of different segments.

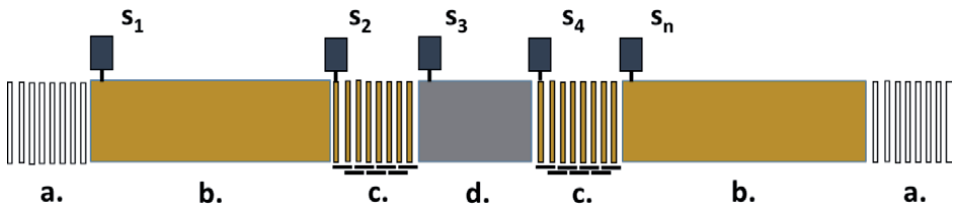


Fig. 7.5. Typical conveyor system for cartons irradiation process composed of different segments: a – rolls, b – belt conveyor, c – roll conveyor, d – conveyor with speed control located in irradiation zone, s – individual engine of the conveyor segment

Figure 7.6 shows typical conveyor bends necessary in conveyor lay out due to existence of the labyrinth through shielding walls of facility shelter. The key role of the conveyor system plays conveyor segment with speed control located in irradiation zone. Its speed should be precisely adjusted according to beam current and required dose level. Stable conveyor movement assures stable dose level. The feedback loop to beam current sensor allows to automatically compensate beam instability by conveyor speed variation to keep dose rate constant. All conveyor components located inside irradiation chamber should be protected against radiation to avoid corrosion caused by ozone presence. The belt made of stainless steel wires or rollers type conveyor are frequently used to transport irradiated product under exit window.

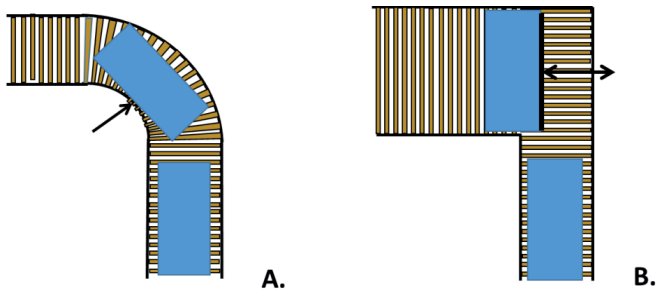


Fig. 7.6. Typical conveyor bends necessary in conveyor lay out due to existence of the labyrinth through shielding walls of facility shelter

Manual loading and unloading rolling lines with accumulation buffer action should be located at the beginning and at the end of conveyor. The number of other specific segments could be recognized depending on the conveyor configuration and complexity. These include:

- entrance conveyor with elevator section to a superior level / lowering conveyor to ground level;
- accumulation area before irradiation section to eliminate gaps between cartons;
- option to 180º flipping over section second irradiation loop (flipping over station receives the cartons which have already been irradiated once);
- special guiding for the twin cartons. This system is used to inject the cartons at the entrance of the irradiation loop. To ensure a final throughput within the specification, the cartons should be grouped. So the cartons can be driven two by two (or one by one).

During irradiation tubes or pips several product turns can be finalized to obtain necessary dose homogeneity. It is possible in advance preparation the trolley with certain tubes dimensions. The special mechanism providing necessary tube rotation should be applied for different tubes dimensions and thickness.

### 7.2.5. Process control system

The whole process should be controlled both by process control system (PCS) which will confirm that the irradiation takes place with the good parameters and a real time. The PCS should continuously measure the key parameters of the beam and conveyor (beam intensity, scan length and conveyor speed). At the end of the batch process it should be possible to issue an irradiation certificate.

*Conveyor control system*

The conveyor should carry through the irradiation process the products packaged in cartons that need to be modified by electron beam. Each carton should be irradiated from one or two sides with 180º flip over movement according to specification. The whole system should be usually designed to work 24 h a day and 5 days a week. The cartons are loaded on the conveyor at a manual loading station. The main different sections of the conveyor are as follows:

- manual loading / unloading lines with accumulation buffer action,
- entrance conveyor with elevator / lowering sections to a superior level / ground level,
- accumulation area before irradiation section,
- irradiation stainless steel conveyor able to drive each box within specification under the beam,
- 180º flipping over section second irradiation loop,
- special guiding for the twin cartons.

So-called under beam conveyor is directly under the beam. The speed should be fully controlled by a supplementary device. The tolerance should be around ±1%. The structure of this conveyor is in stainless steel and the absence of other elements is of course applicable to the whole area. The cartons should be introduced on the irradiation conveyor close to one another without bumping. Conveyor control system (CCS) including program and control features should be provided by the conveyor supplier. It should be coordinated with PCS responsible for accelerator operation. Automatic stop of the conveyor should take place when electron beam disappear suddenly due to technical reasons. Automatic electron beam stop should take place when conveyor is suddenly stopped due to technical reasons.

*Monitoring control system*

Monitoring control system can be provided by accelerator manufacturer for independent supervision of the irradiation parameters.

*Dosimetry system*

The dosimetry system should be selected and purchased to read certain film dosimeter (B3, Gex, FW, CTA) with adequate devices integrated with the UV-Vis spectrophotometer. The following items are also recommended: aluminum wedge, calibration filters thickness gauge, reference thickness blocks, PC with dosimetric program, printer.

## 7.3. ACCELERATOR SUPPLY

### 7.3.1. Accelerator specification

Accelerator is the key device of any electron beam radiation facility. It is responsible for productivity of the process and economical effects of the applied radiation technology. The energy of accelerated electrons determines their penetration into the irradiated material, what determines the geometry of the irradiation process. Sufficient average power of the beam of electrons ensures achievement of the required capacity of the process, costs minimization, and should be accessible for continuously operating installation. Differences between various types of accelerators mainly come down to the difference in the generation of electric field which is used to accelerate the electrons. Two basic ways of generating accelerating voltage are used in accelerators applied for radiation processing:

- high voltage power supplies (transformer accelerators, low energy level),
- radio- and microwave frequency generators for accelerators where the electric component of electromagnetic wave is used in the process of electrons accelerating (resonance accelerators with single accelerating gap and multi-cavity high frequency linacs, high energy level).

The process of accelerating electrons takes place in the vacuum inside of accelerating section where cathode emitting electrons is installed in one side, while the system for transporting and conveying of the beam through output foil (scanner) is installed in other side.

Industrial irradiation processes using high power electron accelerators are attractive because the throughput rates are very high and the treatment costs per unit of product are often competitive with more conventional chemical processes. The utilization of energy in electron beam processing is more efficient than typical thermal processing.

The principle of certain accelerator operation is based on difference in electric field generation, related to this accelerating section construction and the accelerated particles trajectory shape. Four accelerator constructions are described as an interesting technical solution: two

microwave resonance accelerators in which the electric component of electromagnetic wave accelerates electrons in number small resonance cavities and two RF accelerators with single cavity resonator each.

High energy scanned beam systems driven by RF sources are capable of providing from 5 to 700 kW average beam power at electron energy range 5-10 MeV. They are used for medical product sterilization and crosslinking and polymerization of even thicker materials. Microwave linacs provide electron beams with energy 10 MeV and beam power up to 100 kW.

Fundamental accelerator parameters: electron energy and average beam power define technological abilities and facility productivity. Although there are many different types of accelerators offering a wide range of performances ratings, only a few would be suitable for particular application.

*Microwave electron accelerator UELR 10-15S type*

The main feature of linear microwave accelerator is the microwave energy source use in electron accelerating process. Power supplies consist of microwave generators mainly in S-band frequencies (3 GHz). A large number of small resonant cavities are used. Microwave source parameters (price, life time) play a crucial role in implementation of linacs of this type.

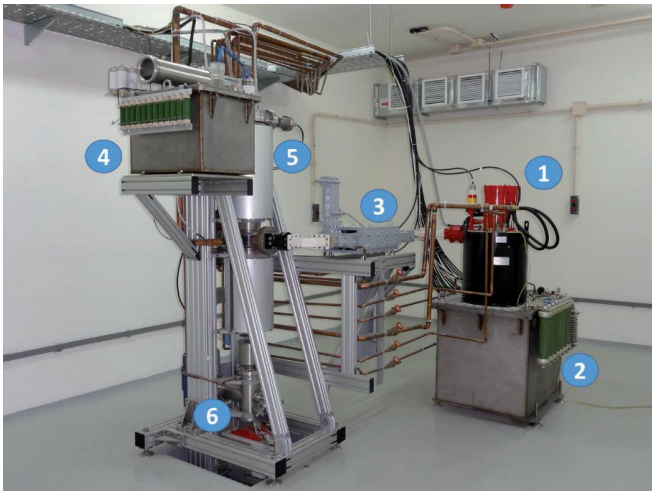


Fig. 7.7. Microwave linear electron accelerator UELR 10-15 type: 1 – klystron, 2 – pulse modulator, 3 – microwave circulator, 4 – gun modulator, 5 – accelerating section, 6 – scanner

The klystrons are more stable in frequency and power but they have efficiency of 40-50% in comparison with 70% efficiency of magnetrons which lifetime is significantly lower. Microwave linacs can be built with traveling or standing wave configuration. Radiation facility with linac (Fig. 7.7) offered by CORAD Company (Saint Petersburg, Russia) is designed for installation inside of industrial buildings or warehouses. Accelerator UELR 10-15S has following basic technical characteristics:

- electron energy: 10 MeV;
- maximum beam power: 15 kW;
- maximum pulse amplitude of the electron beam current: 0.25 A;
- pulse repetition rate: 1, 3.06, 6.125, 12.5, 25, 50, 100, 200, 400 Hz;
- electron beam pulse duration: 0.015 ms;
- maximum scan length: 700 mm;
- maximum power consumption: 110 kW;
- homogeneity of dose along the scan length on both sides of irradiated boxes: ±5%;
- beam power stability: ±2.5%;
- electron energy stability: ±2.5%;

- the accelerator supplied from three-phase networks 380/220 V, 50 Hz, with the insulated neutral wire, stability: ±5%.

The external water circuit of cooling (not included in the delivery kit) should dissipate power of 90 kW and provide following condition in the output: water temperature of cooling no more than 25ºC, water flow for 25ºC – 120 l/min. The basic features of accelerator are the following:

- high efficiency solid-state modulators for klystron and electron gun with DC voltage less 800 V on the basis of thyristors;
- continuous control of electron energy, scan length and beam current during electron beam processing.

During an operation of the accelerator periodic replacement of the klystron and the cathode of the electron gun is required.

*Resonance RF accelerator ILU 10 type*

Resonant HF accelerators are based on the large resonant cavities working at the frequency varying from one to several hundred MHz. Those cheap and reliable components require relatively simply and compact DC or pulse modulators to generate HF oscillations. Medium and high electron energy level with appropriate beam power can be obtained.

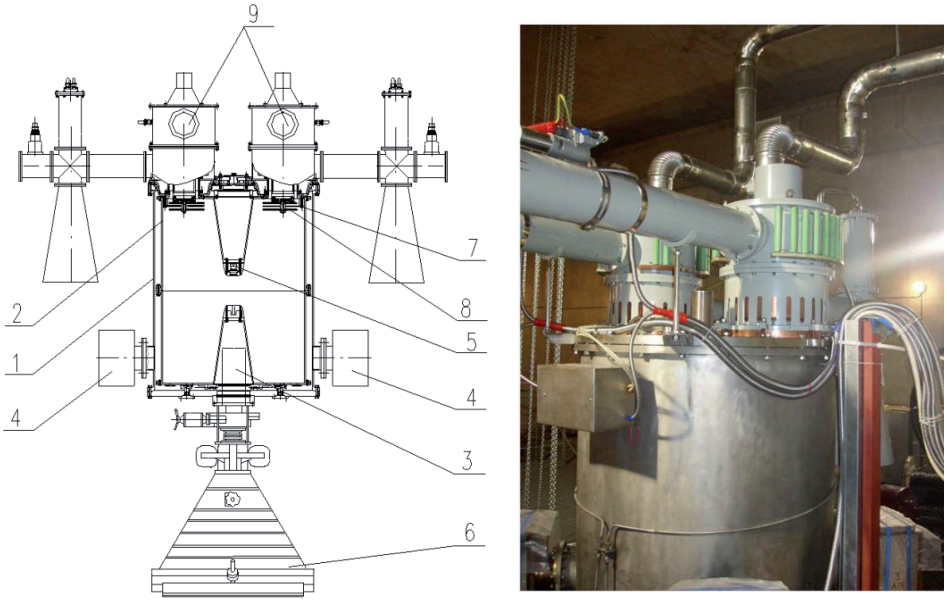


Fig. 7.8. RF electron accelerator type ILU 10: 1 – vacuum envelope, 2 – resonator, 3 – focusing coil, 4 – ion pump, 5 – electron gun, 6 – scanner, 7 – coupling loop support, 8 – vacuum capacitor, 9 – RF generators

The first industrial accelerators of this type were developed at the Institute of Nuclear Physics (INF, Novosibirsk, Russia). ILU type electron accelerators are based on one coaxial resonator operating in pulse regime (Fig. 7.8). Industrial model of HF resonant accelerator was developed to cover energy range from 0.5 MeV up to 5 MeV with average beam power up to 50 kW. Above 50 accelerators ILU type were constructed and installed in Russia and several other countries for different field of R&D and industrial applications. Main parameters of operation regime ILU 10 accelerator are as follows:

- energy: 4-5 MeV,
- average current: 0-10 mA,

- average beam power: up to 50 kW,
- pulse current: 0-400 mA,
- pulse duration: 0.5 ms,
- pulse repetition: 1-50 Hz,
- RF frequency: 115 MHz,
- dimensions: Ø1280 mm × 1480 mm.

ILU type electron accelerator family is represented by several constructions with different electron beam parameter. The units suitable for this application are listed in Table 7.1.

Table 7.1. ILU type accelerator family

| Parameter | Accelerator type | |
|---|---|---|
| | ILU 10 | ILU 10M |
| Electron energy | 4-5 MeV | 4.5 MeV |
| Beam power | up to 50 kW | 10 kW* |

* The accelerator ILU 10M can be upgraded to ILU 10 configuration

*Accelerator Rhodotron TT100 type*

Rhodotron type electron accelerators presented in Fig. 7.9 are based on relatively new conception of electron accelerator arrangement. Family of Rhodotron accelerators were developed by IBA Company (Belgium). Using multipass system across resonant cavity 5-10 MeV electron energy and up to 700 kW beam power can be obtained.

Rhodotron HF electron accelerator arrangement was invented in France. The coaxial line short-circuited on both ends was proposed to accelerate electrons in standing wave conditions. The electric field is radial with maximum at the median plane whereas the magnetic field is azimuthal and is equal to zero at the median position. That creates opportunity to accelerate electron beam crossing diametrically the cavity without distortion coming from magnetic field presence. Bending devices located outside of cavity are used to successive beam acceleration in the same electric field. There is continuous beam operation with RF modulation of the electron intensity. Accelerator is characterized as continuous beam operation device but with RF modulation of the electron intensity. The compact construction, relatively high (up to 50% of electrical efficiency) high energy and high beam power make this accelerator suitable for industrial application. Accelerators of this type can be easily upgraded by installing additional modules to increase average beam power. Rhodotron accelerator family includes several models: TT100 (10 MeV, 40 kW), TT200 (10 MeV, 100 kW), TT300 (10 MeV, 245 kW), TT1000 (7 MeV, 560 kW). Second generations of Rhodotron type accelerators is offered since 2018. Rhodotron TT100 model is recognized as compact accelerator with the following parameters:

- electron energy: 3-10 MeV,
- electron energy spread: less than 0.3 MeV,
- maximum beam power: 40 kW,
- beam current stability: better than 0.5%,
- full diameter: 1.6 m,
- full height: 1.75 m,
- weight: 2.5 t,
- number of passes: 12,
- energy gain per pass: 0.833 MeV,
- electrical efficiency: 20%,
- maximum line power: 210 kW.

As an option, Rhodotron can be supplied with a two-stage scan horn system that delivers a scanned but not-diverging (parallel) beam. Beam scan length can be varied from 30% to 100%. Electron bean can be scanned with frequency 100 Hz (optionally 200 Hz).

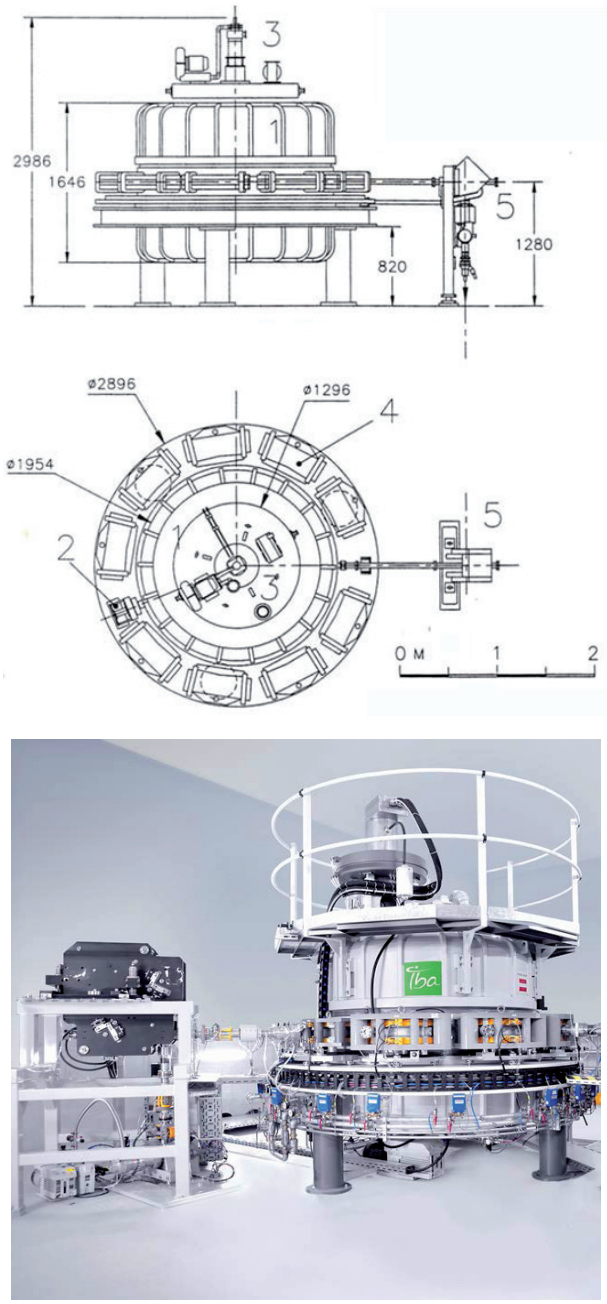


Fig. 7.9. RF electron accelerator Rhodotron TT200 type: 1 – vacuum envelope, 2 – electron gun, 3 – RF tetrode amplifier, 4 – deflecting electromagnet, 5 – bending electromagnet

*Summary of accelerator specification*

Table 7.2 shows the basic physical parameters related electron accelerators capable to be established in facility for radiation processing. The presented units with certain physical charac-

Table 7.2. Electron accelerators for facility used for radiation processing

| Energy | High energy | High energy | Medium energy | High energy |
|---|---|---|---|---|
| Accelerator type | LAE 10/10 | UELR 10-15S | ILU 10 | TT100 |
| Producer | INCT | CORAD, Russia | INP, Russia | IBA, Belgium |
| Energy | 10 MeV | 10 MeV | 5 MeV | 10 MeV |
| Power source | klystron | klystron | pulse triode | tetrode |
| Beam current | 0.1-1 mA | 1.5 mA | 10 mA | 4 mA |
| Beam power | 10 kW | 15 kW | 50 kW | 40 kW |
| Power consumption | 125 kW | 150 kW | 200 kW | 210 kW |
| | 150 kW (overall) | 175 kW | 225 kW | 235 kW |
| Energy efficiency | 10% | 10% | 25% | 20% |
| Window size | 600 mm | 600 mm | 800 mm | 800 mm |
| Shield thickness | 3 m | 2.5 m | 2.5 m | 3 m |

teristics referring to electron energy and beam power as well as economical data (Table 7.3) can be compared to optimize investment process.

Table 7.3. Delivery conditions

| Energy | High energy | High energy | Medium energy | High energy |
|---|---|---|---|---|
| Accelerator type | LAE 10/10 | UELR 10-15S | ILU 10 | TT100 |
| Delivery time | - | 12 months | 12 months | - |
| Transport | - | 1 month | 2 months | - |
| Installation | - | 4 months | 4 months | - |
| Maintenance | difficult | difficult | moderate | difficult |
| Main spare part | klystron | klystron | triode | tetrode |
| Main advantages | high energy | high energy | compact construction | high energy |
| Main disadvantages | low EB power, low electrical efficiency, high operation cost | low EB power, low electrical efficiency high operation cost | - | high operation cost |
| Conveyor (as option) | - | yes | - | yes |

### 7.3.2. General requirements

General requirements are related to accelerator rooms, accelerator equipment location, accelerator electric and water power supply, rooms ventilation, elevating mechanism.

*Power line*

Power line voltage with three phases 380/220 V ±10% and frequency 50 Hz is required.

*Note*. In some cases it is recommended to use a separate transformer with nominal parameters. Consumed power by accelerator unit is up to 210 kW (depends on accelerator type).

In some cases it is recommended to connect the accelerator to the power line through a device providing a visible disconnection in the power supply circuit when the voltage is switched off. The accelerator equipment must have a separate grounding. Power and control--measuring cables should be put into a separate cable trench or separate routs.

*Environment*

Typically the temperature in the range +10÷+35ºC and humidity no more than 90% at a temperature +25ºC are required in respect to accelerator equipment.

*Ventilation*

General ventilation with a suitable capacity should be installed. It is recommended (to reduce ozone propagation) to confine the beam damping zone by an aluminum or stainless steel screen 4-5 mm thick. The air should be exhausted from zone where electron beam is deposited into irradiated material.

*Note*. The air line of the ventilation system must be made of aluminum or stainless steel.

Accelerator chamber (irradiation room) should be equipped with the inflow-exhaustive or only exhaustive ventilation systems for air radiolysis products (ozone and nitrogen oxides) removing. Ventilation system productivity should provide the air exchange multiplicity in accordance with local sanitary rules.

An important feature of supply ventilation is a certain balance of air in the room containing accelerator scanner and irradiation zone. Air should be supplied at such a rate, as to ensure that the pressure in this room is lower than those prevailing in the neighboring rooms. This will prevent the ozone from getting out of the accelerator building.

The exhaust and supply ventilation system in other rooms, where accelerator devices are operating, should be designed in such way as to make proper provisions for the balance of power lost in those devices.

*Hoist crane*

The hoist crane should be installed in the irradiation hall with the slow rise of the hook (hand drive is possible), which allows one to serve a strip on each side from the axis lying above the center of the accelerator. The strip length should usually be no less than 4 m. Weight-carrying capacity depends on accelerator type.

*Instruction regarding anticorrosion protection*

Selection of materials used in the construction installed in the accelerator chamber should be effected in such manner as to make proper provisions for the extremely high corrosive properties of the atmosphere in this room. This is caused by factors resulting from radiation with the beam of electrons, e.g. the presence of ozone and nitrogen oxides. It is recommended to use a paint resistant to peroxide acid.

Water cooling installations in the area of reaction chambers should be made from stainless steel. As far as the air supply and exhaust ventilation systems are concerned, it is recommended to make them from stainless steel, non-corrosive aluminium or alternatively regular steel covered with anticorrosive epoxy paint.

Cables, rubber hoses, parts made of rubber and teflon as well as units, instruments, plugs, panels located in irradiation zone and non-protected against the scattered electrons and active gases should be protected by shields of 1 mm thick made of lead or 2 mm thick made of steel.

Measures should be taken to avoid dust generation in the accelerator chamber. The walls, floor and ceiling must be covered by radiation proof materials.

### 7.3.3. Requirements for radiation protection

Electron accelerators are high risk devices. Assembly and operation of such accelerators should take place in accordance with general operation, technical maintenance and safety principles applicable to electric devices operating at industrial plants, as well as in accordance with principles for operating with ionizing radiation sources.

Scale of hazards is wide and complex. The safety system is an integral part of radiation facilities operation. Hazards evolve with facility age and mission. Regulatory environment of safety system includes:

- industrial safety (handling of potentially hazardous customer products; it can be referred to safety of machinery);
- radiation safety (integrate radiation requirements into industrial safety framework; it can be referred to radiation safety of electron irradiation facilities).

Safety control systems (SCS) should include:

- personnel safety systems:
  - access controls,
  - critical devices,
  - equipment interlocks,
  - audio and visual warnings;
- machine protection systems:
  - beam loss monitoring,
  - fast shutdown;
- safety envelope monitoring (access controls and interlocks);
- radiation monitoring.

The main objectives for radiation safety system are:

- keep people out of dangerous areas;
- warn people of hazards;
- define procedures, for example:
  - to secure radiation rooms,
  - to unsecure radiation rooms and allow access after a delay for ozone removal,
  - for emergency stop and access violations;
- provide safety even when a single fault is undetected.

Modern control systems are usually based on computer technology what directly leads to significant benefits related to irradiators operation in terms of process control and cost savings. However in that case the most important issue becomes safety system and its reliability and degree of safety. It is important for both new and upgraded irradiators. Presently offered control systems cover the entire irradiation process from loading of products to the final post-irradiation report. The facility monitoring system includes video surveillance as well as data transmission through internet and GSM network. Design features are the following:

- Diversity: Each safety interlock must function independently of any other safety interlocks. It is generally accepted that when using two identical devices in a redundant configuration the probability of both failing (to “danger”) is less than that of a single device.
- Reliability: It should provide the required protection, subject to all foreseeable aging and environmental conditions at the accelerator facility. These conditions may include weather extremes, high electromagnetic fields, high radiation fields, earthquakes, and the cumulative effects of aging on components, such as corrosion, dirt, and normal wear.
- Redundancy: The SCS is duplicated throughout (input devices, wiring, logic function, outputs), and is periodically tested to ensure that both “guard-lines” are operating correctly.
- Testable: Before commissioning, the system or subsystem shall be checked to meet the requirements. Pre-test and on-line tests are necessary.
- Fail safe: In case of failure, the SCS shall maintain a safe condition.

High power electron accelerator should be recognized as a powerful source of ionizing radiation causing hazard radiation effects when an accelerated electron beam is extracted into air. The radiation protection design should be done in accordance with the radiation safety rules accepted in certain country. During radiation protection calculation it is necessary to take into account the following radiation dangerous factors, which taking place during accelerator operating: electrons scattered by irradiated subjects in various directions, bremsstrahlung occurring both while the beam deceleration in the irradiated subjects and due to its partial loss along the accelerating track and on the extraction device units.

Maximum bremsstrahlung energy for electron beam energy up to 5 MeV is lower than the threshold of photo-nuclear reactions for all elements except beryllium. Since there is no parts made of beryllium in typical accelerator facility, therefore it is radiation safe when electron beam is being switched off (with the absence of voltage on the resonator gap, or DC voltage in transformer accelerators).

With the beam absence but with high voltage presence at accelerating tube (in accelerating tube training mode, for example) it is possible the electrons auto-emission (so-called dark current) from accelerating tube upper electrodes and its electrons accelerating up to whole energy. In this case maximum air extracted electron beam can be 20-50 μA range what creates real danger for personnel. When dark current is present the entry to accelerator chamber is strictly prohibited.

Safety control system should provide a personnel access system that will prevent unauthorized access to the treatment room. A mechanical and data interface should be defined to allow elements of the safety system to be installed at the entry to the treatment vault. It means that control system must recognize the cartons on conveyor and preventing any human intrusions.

Accelerator chamber (radiation-dangerous) should be equipped with protecting door (or labyrinths) for personnel passage and for accelerator devices transporting during accelerator assembling. Before the accelerator installation safety interlocks should be installed inside and at the entry to accelerator chamber:

- radiation dangerous illuminated indicator boards. These lamps are automatically switched on by accelerator control system during all time accelerator operation in radiation dangerous mode;
- sound signal system (high sound electric bell). These bells are automatically switched on by accelerator control cabinet during one minute every time before accelerator operation in radiation dangerous mode;
- hermetic buttons (toggle switchers) for fast accelerator break down in case of emergency;
- radiation protection door interlock.

During the operation of accelerators with accelerated beam of electrons, emergency situations (caused by radiation or fire) can take place in the following circumstances:

- damage of the door blockade at the radiation room,
- breakage of the biological shield,
- fire of switched on electrical devices.

In case of any emergency situation, all equipment should be switched off, work with accelerators stopped, while all people should be prevented from accessing the danger zone, local fire department, exposure measuring authorities and the company's administrative authorities should be notified. Accelerators can be switched on once reasons for the emergency are found, all damages are fixed and consent of the fire department and exposure measuring authorities are given.

### 7.3.4. Security system

Overall security (physical security protection of radiation systems from outsiders) should be implemented. Certified redundant safety system using security elements should be designed to provide the full system to secure both the accelerator vault and the irradiation maze.

Security locks are to be engaged at different places. It shows the survey has been done inside the shielded cells and it gives the certainty there is nobody left inside the secured places. Beacons and flashing signals are associated to clearly show the status of the security system. The secured places are shown on a supervision screen and the secured status is one element of the "beam allowed general" signal.

### 7.3.5. Radiation monitoring

Installation of meter with measurement range 0.01-1000 μSv/h connected with the adequate microprocessor, display and control unit is recommended. The probe should be set on the wall, inside the irradiation maze, at the vicinity of the exit. It will give an actual value close to the background very near the exit, any improbable significant variation will be an alarm. Sometime the second meter should be set in the accelerator vault as an unhooked with a cable long enough to reach selected components during the accelerator fine tuning. Portable measuring instrument is recommended as well.

### 7.3.6. Video control

The high ionizing radiation background is present in the accelerator chamber. Installation video control system is mandatory. During the operation of the accelerator, the room will be inaccessible for maintenance services, but should be ensured by appropriately designed system of control and signalization. TV cameras installed in this room should be equipped with radiation protection shields, with the frontal parts of the cameras equipped with lead glass.

### 7.3.7. Ozone extraction

An important problem of radiation installations is the level of ozone generated during the operation of the accelerator with the beam of electrons. Harmful effects of ozone are revealed at concentration above 1 ppm. It should also be mentioned that ozone can be felt at concentration as low as 0.01 ppm. For instance the American standard limits of daily exposure to ozone during an 8 h workday is set to 0.1 ppm. In some other countries this level is 0.06 ppm or even less.

The amount of ozone generated depends on the energy of electrons, electron beam current and the length of its travel through the air. The level of ozone generation is 0.11 kg/kWh where power corresponds to the electron beam energy losses per unit of time of travel through the air.

The value of calculated ozone concentration unambiguously determines the efficiency of the exhaust ventilation system. Neutralization of ozone is an additional problem. Ozone can be neutralized in the following ways:

- burning (thermal decomposition at temperature of 450ºC),
- activated coal as a filter in the shape of granules with appropriate additives,
- application of magnesium dioxide filtration aid,
- dissipation through chimney.

The volume of air to be extracted is calculated in function of the maximum quantity of ozone which could be produced by the accelerator at full power. One can consider the maximum interaction between electrons and air (no obstacle). The height of the dissipation chimney can be calculated with the use of the formula with seated mandatory limit.

### 7.3.8. Water cooling system

Several specific cooling water parameters may be taken into account: acidity value, carbonate hardness, specific resistance, input and output pressure, input water temperature. It depends on recommendation of accelerator manufacturer.

*Note*. Inlet water temperature should be not less than accelerator equipment dew-point.

Water consumption by the accelerator is specific for certain accelerator construction and it can vary between 50-200 l/min. Two close loops of water cooling system are applied the most frequently. First loop is connected to all accelerator components and heat exchanger. High quality or even distillated water is use in this particular loop. The other one usually contains ordinary

water. It is connected to cooling tower and heat exchanger. All components of the second loop are provided by investor. The water losses (consumption) in such system are very limited. The cooling system can be integrated in the whole building HVAC system.

## 7.4. FACILITY DESIGN ASSUMPTIONS

### 7.4.1. Plant production capacity

Calculation of mass productivity of radiation process is based on formula:

$$M = P \times F/D$$

where: M – mass productivity [kg/s], F – efficiency of beam energy transfer (0.2-0.7), D – absorbed dose [kGy], P – beam power [kW].

Coefficient of electron beam utilization depends on beam losses in exit window, losses in air, losses due to certain density distribution of irradiated material, losses due to geometry of scanned beam, losses due to packs density on conveyor and may be different for each type of product. The minimal F coefficient value was selected for productivity calculation and is equal to 0.3.

When four-sided irradiation is used the electron energy of accelerator can be selected within the range 2.5-10 MeV. The productivity according to the above formula for 1 kW beam power and 25 kGy dose rate can be:

$$M = 1 \text{ kW} \times 0.3/25 \text{ kGy} = 0.012 \text{ kg/s} = 43.2 \text{ kg/h}$$

Facility assumed to be operated 52 weeks/year. The national holidays can reduce this period to 50 weeks/year. It is recommended to perform general maintenance service during 5 working days after 6 months of facility operation. It reduces facility operating period to 48 weeks/year. Due to typical accelerator availability level 96%, facility operation period corresponds to 46 weeks/year, which means 1840 h/year (8 h for 5 days/week).

Table 7.4. Radiation facility productivity for different accelerators (average dose 25 kGy)

| Accelerator type | Linac | Linac | Resonance | Resonance |
|---|---|---|---|---|
| Energy | 10 MeV | 10 MeV | 5 MeV | 10 MeV |
| Beam power | 10 kW | 15 kW | 20 kW | 40 kW |
| Productivity for one shift (1552 h) | 670 t | 1006 t | 1341 t | 2682 t |
| Productivity for two shifts (3392 h) | 1465 t | 2198 t | 2931 t | 5861 t |

When one shift facility operation will be implemented the total operation time with electron beam will be limited to 1552 h/year for one shift because of 1 h/week should be devoted to current maintenance and 1 h/day (5 h/week) will be devoted to accelerator switching on and switching off procedures. Radiation facility productivity for different accelerators (average dose 25 kGy, beam utilization 0.3) is displayed in Table 7.4.

### 7.4.2. Manpower and skills requirement

One shift operation requires two accelerator operators (technicians) and two workers for loading and unloading of the conveyor. There should be a facility manager who should be responsible for the overall operation of the facility as well as coordination other works related to outside service. It is recommended to engage one engineer responsible for maintenance and service work, who could replace operator due to vacation or other type of absence. One shift personnel should count six persons.

Additionally the facility should have a radiation safety officer and person responsible for technology dosimetry which should be performed in stated periods.

### 7.4.3. Location of the irradiation facility

Usually all the accelerator equipment is recommended to be located in three rooms. The other rooms (or storage surfaces) are related to radiation facility operation:

- control room (control console),
- power supply room (cabinets, high-vacuum pump power supply units),
- irradiation chamber (accelerator itself and auxiliary systems),
- storage before treatment (loading zone),
- storage after treatment (unloading zone),
- dosimetric laboratory (optionally).

The rooms before accelerator installation should meet requirements of vacuum hygiene. Before accelerator equipment installation all the sanitary-technical and decoration works should be completed, all the constructions and pipes should be cleaned and painted, the internal electrical power and grounding circuits and the light should correspond to the design.

The valves and pressure meters should be installed on the pressure and drain ends of water pipelines in the accelerator and power supply rooms. The pipelines should be tested. Operating consumption of cooling water should be provided.

The forced and exhaust ventilation should ensure the design proportion of the air exchange in the rooms according to the sanitary requirements for building design approved in Poland, it should be tested and accepted for operation.

The internal grounding circuits for the equipment frames should correspond to the design in all rooms.

The rooms and the doors as well as the roads should enable one to transport all the accelerator units with overall dimensions given in its documentation.

The control room should be protected against noise caused by the power supply system and the accelerated beam.

Measures should be taken within accelerator chamber (irradiation room) to avoid dust generation. The walls, floor and ceiling must be covered by radiation proof materials. Transportation of the accelerator parts into accelerator chamber thorough the shielding door (or labyrinths) should be foreseen in respect to certain accelerator part dimensions. If it is not possible it is recommended to make a hole at radiation protection walls with necessary dimensions. After the accelerator equipment installation that hole should be closed. The cable channels should be provided for accelerator equipment control and power supply. These holes location and dimensions as well as cable and water channels should be agreed upon the accelerator provider specialists before accelerator equipment installation.

Table 7.5. The approximate volume of shielding walls for different accelerators

| Type of accelerator | Resonance | Linac | Resonance |
|---|---|---|---|
| Electron energy and beam power | 5 MeV<br>20 kW | 10 MeV<br>10-15 kW | 10 MeV<br>40 kW |
| Approximate shielding wall volume<br>(without floor layer on the ground level) | 625 $m^3$ | 900 $m^3$ | 1500 $m^3$ |
| Approximate cost<br>(approximate concreate price (with transport) ~100 €/$m^3$) | 0.3 M€ | 0.4 M€ | 0.6 M€ |
| Surface needed for shield installation | 90 $m^2$ | 228 $m^2$ | 372 $m^2$ |

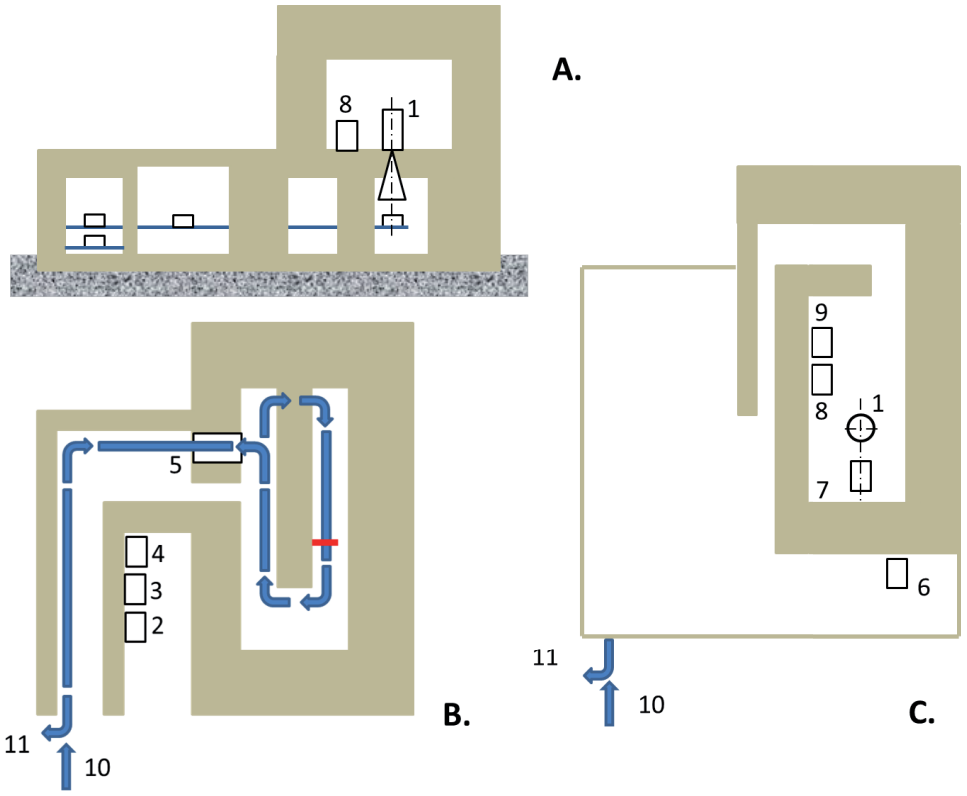


Fig. 7.10. Example of conveyor system lay out and shielding wall configuration in facility equipped with linear microwave accelerator: 1 – irradiator; 2 – control system of the conveyor; 3 – power supply rack; 4 – control system rack; 5 – overturn system; 6 – pulse modulator of the klystron; 7 – klystron; 8, 9 – two cooling system; 10 – loading zone; 11 – unloading in a zone. A – side view, B – ground floor top view, C – first floor top view

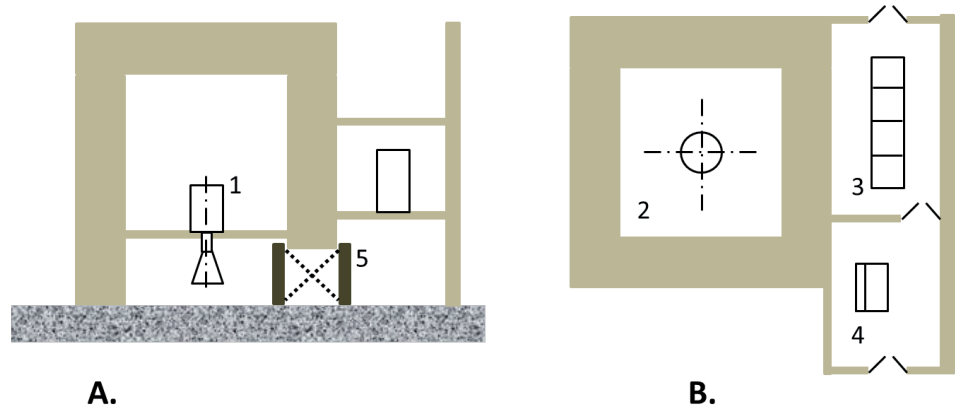


Fig. 7.11. Possible shielding wall configuration in facility equipped with RF single pass resonance accelerator: 1 – accelerator, accelerator chamber; 3 – modulator; 4 – control room; 5 – shielded door. A – side view, B – first floor top view

Arrangement of accelerator chamber depends on type of accelerator, its dimensions, conveyor system configuration and its shape of labyrinths through shielding walls. The shielding wall thickness depends mainly on electron energy, type of target material and shielding material density. The beam power level also has some influence on necessary wall thickness. The raw estimation of shielding walls shows that their thickness can vary from 2.5 m for electron energy 5 MeV to 3 m for electron energy 10 MeV. The precise calculations should be performed to evaluate exact shielding walls dimensions due to national regulation as well as due to shielding material density and shielding walls configuration including the presence of labyrinths for personnel and product entrance and channels for water pipes and electrical cables. Table 7.5 shows the approximate volume of shielding walls for accelerator chambers configuration presented in Figs. 7.10-7.12.

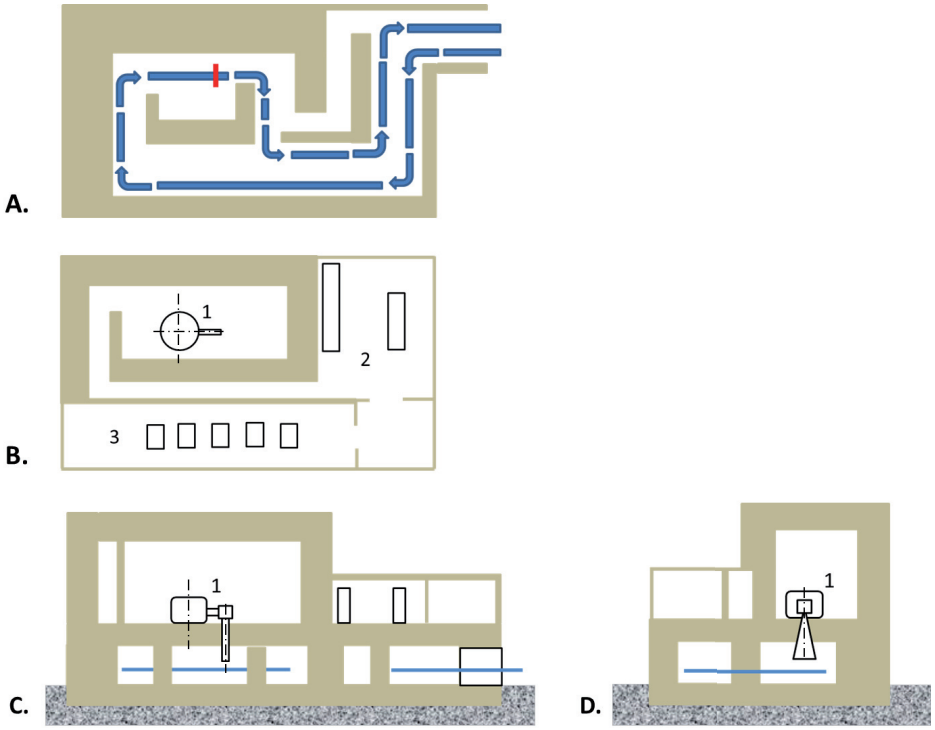


Fig. 7.12. Possible lay out of conveyor system and shielding wall configuration in facility equipped with RF multipass resonance accelerator: 1 – accelerator, 2 – control room, 3 – auxiliary equipment room. A – ground floor lay out; B – first floor lay out; C, D – side view

### 7.4.4. Cost assessment

The investment and operating costs for electron beam accelerators vary widely because of different accelerator specification, type of accelerator and accelerator producers. High facility throughput which is directly related to the beam current level may significantly reduce total unit cost of the process. The accelerators with higher energy of electrons cost more than low energy devices with the same beam power level. Therefore, the lowest energy rating with suitable dose distribution in irradiated object will give better economical parameters of the radiation process. A reduction of the operating time would increase the unit cost significantly because fixed annual cost of investment will be allocated to fewer hours of accelerator exploitation. On

the other hand the lower dose will increase the process throughput and reduce the unit costs. Investment in general includes cost of accelerator and necessary building with shielding walls, safety interlock system, conveyor and auxiliary equipment, land, documentation and installation. Investment cost is frequently connected to the bank credit and became important part of operation costs which are also related to labor and administration spending, electrical energy consumption and spare parts.

Economical and financial evaluation should be performed to obtain information about commercial economical profitability of the project before its final approval and implementation. Economical evaluation should include structure of investment and operating cost of radiation facility. The economical effects of radiation installation may be influenced by many factors. The most important are the following:

- investment cost (direct and indirect costs);
- operating cost (variable and fixed costs);
- required dose level,
- utilization of electron beam and required dose homogeneity.

Cost reduction is one of the key factors of radiation technology successful implementation. Annual cash flow projections are common techniques used for analyses of economical options.

Economic analysis based on annual fixed and variable costs evaluation is very useful to prognosis and recognition of accelerator facility economical condition. Accelerator selection criteria are as follows:

- average beam power (productivity),
- electron energy (penetration),
- price (investment cost),
- electrical efficiency (cost of accelerator exploitation),
- size (building geometry and size),
- reliability (availability > 95%).

Estimated capital costs can be referred to electron accelerator price. One should take into account the expenses related to:

- shielding walls,
- ventilation,
- building with armature,
- technological equipment,
- process control system,
- design and permission,
- installation and validation.

Capital costs (investment), $K_k$, in relation to accelerator price, $K_a$, can vary in most cases according to simple formula given bellow:

$$K_k \sim 2.2\ K_a$$

Capital costs (investment) includes direct and indirect cost components:

- direct costs:
  - the preparation of the stand,
  - construction of the building,
  - technological equipment;
- indirect costs:
  - project management,
  - facility design,
  - installation,
  - commissioning,
  - reserve.

Service (exploitation) cost can be divided on fixed and variable. Investment cost may have primary influence on fixed service cost, due to assumption related to amortization rate (5-10 years).

Exploitation fixed costs are as follows:

- administrative costs with overheads;
- security, amortization, credit;
- required license costs;
- service (planned);
- taxes, including land tax;
- insurance;
- annual regulatory permit fees;
- periodic verification or emission tests.

Exploitation cost includes variable cost components:

- labor (exploitation, supervision);
- electricity, water, pressured air, others;
- materials;
- spare parts.

In general, electron beam technology seems to have the low operating cost despite its moderate to high capital costs. The high capital cost of technology may be compensated by its relatively low annual operating costs. Full set of technical information should be collected to describe accelerator quality and evaluate the risk connected with certain accelerator design.

Table 7.6. Accelerator facility cost assessment

| Accelerator type | | Linac | Linac | Resonance | Resonance |
|---|---|---|---|---|---|
| Electron energy | | 10 MeV | 10 MeV | 5 MeV | 10 MeV |
| Maximum electron beam power | | 10 kW | 15 kW | 20 kW | 40 kW |
| Capital cost | accelerator | 0.44 M€* | 1.5 M€ | 1.0 M€ | 2.4 M€ |
| | shielding | - | 0.4 M€ | 0.3 M€ | 0.6 M€ |
| | conveyor | - | 0.25 M€ | 0.25 M€ | 0.6 M€ |
| | others** | - | 0.3 M€ | 0.3 M€ | 0.3 M€ |
| | total | 0.44 M€ | ~2.45 M€ | ~1.85 M€ | ~3.9 M€ |
| Maintenance cost | E-gun | 2.0 k€/y | 2.0 k€/y | 2.0 k€/y | 3.0 k€/y |
| | ion pumps | 2.5 k€/y | 2.5 k€/y | 2.5 k€/y | 2.5 k€/y |
| | RF source | 38.5 k€/y | 38.5 k€/y | 3.5 k€/y | 7.5 k€/y |
| | others | 2.0 k€/y | 2.0 k€/y | 2.0 k€/y | 2.0 k€/y |
| | annually | ~45 k€ | ~45 k€ | ~10 k€ | ~15 k€ |

* Labor cost is not included.

** Accelerator packaging and shipping, facility design and documentation, licensing, instrumentation, wiring and piping, security system, and ventilation.

The price of the accelerators and auxiliary equipment were evaluated on the literature data base in relation to electron energy and beam power level as well as differences in construction of particular devices. Such assumptions are necessary to calculate unit cost of operation.

Disadvantages and advantages should be discussed in details to optimize a final decision regarding accelerator selection. Table 7.6 presents the cost assessment of the radiation facility with medium or high energy high power electron accelerator. The capital cost which included the accelerator, shield vault, handling system totally amounts of 1.85 M€ to 3.9 M€. Annually, the maintenance cost depends on accelerator type and vary from 10 k€ to 45 k€ (1% to 5% of accelerator cost).

Table 7.7. Accelerator facility operating cost assessment

| Accelerator type | | Linac | Linac | Resonance | Resonance |
|---|---|---|---|---|---|
| Energy activity | | 10 MeV | 10 MeV | 5 MeV | 10 MeV |
| Initial investment | | 0.44 M€ | 2.45 M€ | 1.85 M€ | 3.9 M€ |
| Power consumption | | 150 kW | 225 kW | 155 kW | 235 kW |
| Fixed cost | administration and others* | 43.2 k€ | 43.2 k€ | 43.2 k€ | 43.2 k€ |
| | depreciation** | 88 k€ | 490 k€ | 370 k€ | 780 k€ |
| | subtotal | 131.2 k€ | 533.2 k€ | 413.2 k€ | 823.2 k€ |
| Variable cost for one shift | labor | 86.4 k€ | 86.4 k€ | 86.4 k€ | 86.4 k€ |
| | electricity | 27.6 k€ | 41.4 k€ | 28.5 k€ | 43.2 k€ |
| | spare parts | 45 k€ | 45 k€ | 10 k€ | 15 k€ |
| | service | 30 k€ | 30 k€ | 15 k€ | 30 k€ |
| | subtotal | 189 k€ | 285.1 k€ | 128.9 k€ | 154.7 k€ |
| Total annual cost | | 320.2 k€ | 818.3 k€ | 542.1 k€ | 977.9 k€ |
| Maximum one-hour productivity*** | | 432 kg | 648 kg | 864 kg | 1728 kg |
| Cost of 1 h electron beam operation | | 206 €/h | 444 €/h | 295 €/h | 630 €/h |
| Unit cost | | 0.48 €/kg | 1.26 €/kg | 0.63 €/kg | 0.36 €/kg |

* Administration, outside service for planned maintenance, dosimetry service, radiation safety oficer.
** 5-year period.
*** Dose rate 25 kGy, electron beam utilization coefficient 0.3.

The data related to accelerator facility operating cost assessment are presented in Table 7.7. In conclusion, one can find the unit cost of product irradiated by different accelerators in relation to 1 kg of the product and the one-hour productivity. The calculations were performed for one shift operation.

### 7.4.5. Permissions

The procedure of the realization of the investment should include certain steps:

- pre-feasibility study (multivariants conception),
- the choice of the variant,
- the study of feasibility – the chosen variant.
- project related to the conditions of the building and land development,
- obtainment of the conditions of the buildings and land development,
- technical project of the building and project of permission on the building,
- obtainment of permission on the building,
- the realization.

Initiation of investment process requires standard procedures related to acceptance (permission) of local authorities supported by report related to potential influence on environment.

The specific procedures are related to separate permissions which allow to initiate construction, starting up and exploitation facilities equipped with sources of ionizing radiation. Such permission is provided by the Nuclear Safety Department of the National Atomic Energy Agency, Poland (PAA).

Accelerator operators should obtain official license to operate accelerator facility. Formal proposal (document available on web page of the PAA) should be supply to the Nuclear Safety Department of the PAA. After positive results of national exam the license will be provided. The training course on radiation safety matters for accelerator operators is strongly recommended in advance to national exam. The list of organization providing necessary training courses is available on web page of the PAA.

### 7.4.6. Cooperation

The Centre of Radiation Research and Technology of the Institute of Nuclear Chemistry and Technology activities include basic research, development and applications, various services related to the profile of its activities. The Centre is the best developed in Poland in the fields of implementation of electron beam technology and radiation chemistry. The results of works have been implemented in various branches of national economy, particularly in industry, medicine, environmental protection and agriculture. Nowadays with its six electron accelerators and three laboratory gamma sources in operation and with the staff experienced in the field of electron beam application, is one of the most advanced centers of science and technology in this domain. The Centre has four pilot plants: for radiation sterilization of medical devices and transplantation grafts, for radiation modification of polymers, for removal of $SO_2$ and $NO_x$ from flue gases, for food hygienization and has long time experience in practical implementation radiation processing technologies including number technologies related to polymer modifications (thermo-shrinkable tubes and tapes, wires and cables, foams).

Gained experience would be the excellent base for future cooperation in number fields of activities:

- participation in preparation of proposals to support implementation of new energy efficient technology from national sources,
- polymer material characterization towards certain properties development,
- optimization of the irradiation process of products of different geometry and composition based on experimental and computational methods,
- training capability in operation and exploitation accelerator facility,
- participation in supervision of electron accelerator installation,
- participation in facility commission procedures,
- routine technological dosimetry with certified method,
- radiation safety and personal dosimetry.

## 7.5. CONCLUSIONS AND RECOMMENDATIONS

The data presented in Tables 7.6 and 7.7 show that electron beam facility equipped with presented accelerators are capable to irradiate required amount of required product. The electron energy levels 5 MeV and 10 MeV were considered. A more detail technical analysis should be performed to recognize optimal conditions of irradiation process. Final result depends on geometry irradiated product, nominal energy of the accelerator and configuration of irradiation process. Due to specific product dimension two-sided irradiation could be solution to improve the process efficiency, and irradiation homogeneity. Such process can be performed by electron beam with energy 5 MeV or 10 MeV.

A more detailed financial analysis on the profitability of the process should be undertaken after selection certain accelerator to implement radiation processing. Table 7.7 shows main advantages and disadvantages of certain accelerator constructions. The possible reason of difference would be the specific beam utilization coefficient or significantly lower beam power provided by the facility. Other limit can be present due to ability to perform the irradiation process fast enough (conveyor speed) to use the full beam power.

Table 7.8. The main advantages and disadvantages of certain accelerator construction

| Accelerator type | | Linac | Linac | Resonance | Resonance |
|---|---|---|---|---|---|
| Energy activity | | 10 MeV | 10 MeV | 5 MeV | 10 MeV |
| Initial investment | | 0.44 M€ | 2.45 M€ | 1.85 M€ | 3.9 M€ |
| Beam power | | 10 kW | 15 kW | 20 kW | 40 kW |
| Advantage | high beam power | | | | X |
| | compact size | X | X | X | |
| | low investment cost | X | X | X | |
| | lowest spare parts cost | | | X | |
| | lowest unit cost | | | | X |
| Disadvantages | low beam power | X | X | | |
| | high investment cost | | | | X |
| | highest unit cost | | X | | |
| | highest spare parts cost | X | X | | |
| | low energy level | | | X | |

Table 7.8 shows main advantages and disadvantages of facilities based on different accelerators. Facility based on resonance multipass accelerator is fully acceptable from technical point of view, but it is characterized by relatively high investment cost. Microwave linacs are characterized by relatively low beam power, as well as relatively high spare parts cost. More universal production profile would be obtained with resonance single pass accelerator due to high enough electron energy level (up to 5 MeV) and moderate beam power.

The detailed analysis should be performed regarding product profile and selection of irradiation configuration and conveyor technical capabilities and properties. Traditional conveyor system seems to be more universal for different types of irradiated product.

[#] This chapter was published as the INCT report – *Raporty IChTJ. Seria B nr 1/2018* and is available on the INCT website: http://www.ichtj.waw.pl/ichtj/publ/b_report/b2018_01.htm.

Chapter 8

# NEW INCT INDUSTRIAL PROJECTS UNDER PLANNING AND DEVELOPMENT

**Andrzej G. Chmielewski, Zbigniew Zimek, Małgorzata Siwek, Urszula Gryczka, Agnieszka Miśkiewicz, Dagmara Chmielewska-Śmietanko**

## 8.1. PROCESS ENGINEERING ASPECTS OF DIESEL ENGINE OFF GASES TREATMENT[#]

### 8.1.1. Introduction

The major cargo transportation mode is maritime transport, which is also responsible for approximately 90% of world trade by volume. Furthermore, travelling by sea has increased considerably in recent years – from 2003 to 2016 this touristic sector has expanded from 12.0 to 22.0 million travellers [1]. Shipping is also the most cost-effective and efficient method of international transportation for most goods. It provides a reliable means of transporting goods globally, facilitating commerce and helping to create prosperity among nations and peoples. Accordingly, worldwide emission from shipping has grown significantly, which contributes directly to the global anthropogenic emissions and it poses a serious threat to the ecosystem and public health [2].

Exhausts from marine engines may contain nitrogen, oxygen, carbon dioxide ($CO_2$) and water vapour as well as nitrogen oxides ($NO_x$), sulphur oxides ($SO_x$), carbon monoxide (CO), various hydrocarbons (HC) and complex particulate matter (PM). The maritime transport usually uses heavy fuel oil (HFO) with a high content of sulphur, which naturally leads to the three main pollutants derived from shipping: nitrogen oxides, sulphur oxides and particulate matters [3]. Around 15% of global $NO_x$ and 5-8% of $SO_x$ emissions are attributable to ocean-going ships [4].

Presence of sulphur oxides in exhausts is a direct result of the fuels' composition, which was applied. During the combustion, the sulphur is oxidized, generating sulphur dioxide ($SO_2$) with a minor proportion of sulphur trioxide ($SO_3$). $SO_2$ emission as a smog component is a precursor to acid rains and it can have a negative influence on plant life as well as on wider ecosystems. It is also possible to observe damaging of minerals used in the construction of buildings and other architecture. In the absence of wetness (rain, snow) these gases may contain particulate matter, causing harm to human health and the environment (for instance respiratory problem, damaging vegetation) [3]. The two primary nitrogen oxides present in pollution streams are nitric oxide (NO) and nitrogen dioxide ($NO_2$). The molecular nitrogen in the combustion air or in the fuel is oxidized, forming $NO_x$. Nitrogen dioxide is a brown gas with a ripe smell whereas NO is colourless and essentially odourless. Both of them can be contributors to acid rain or precursors to the formation of ground-level ozone (smog component), which causes respiratory problems and damage to vegetation [3-5].

The three modes of operation can be distinguished during the ship journey: at berth, manoeuvring and at sea. The emissions from manoeuvring comprise the lowest amount of pollutants whereas the majority of hazardous gases are emitted while the ship is at sea [6]. Emissions are also specific to a ship, as individual ships have varying machinery and equipment. For meeting specific requirements related to different areas (open sea, on/offshore, inland water) as well as to ships' parameters, in 1948, the International Maritime Organization (IMO) was established at the conference in Geneva. Nowadays, IMO is the global standard-setting authority for the safety of international shipping with a universally implemented and universally

adopted regulatory framework for the shipping industry (including manning, construction, ship design, equipment, operation and disposal, etc.) [7].

On 2 November 1973, IMO adopted the International Convention for the Prevention of Pollution from Ships (MARPOL), which is the main international convention covering prevention of pollution of the marine environment by ships from operational or accidental causes [7]. MARPOL is divided into annexes in relation to different categories of pollutants, each of which deals with the regulation of a particular group of ship emissions [8] (Table 8.1).

MARPOL Annex VI entered into force on 19 May 2005. It includes limits for the main air pollutants contained in ships exhaust gas and it prohibits the deliberate emissions of ozone-depleting substances. MARPOL Annex VI also regulates the emissions of volatile organic compounds (VOC) from tankers and shipboard combustion. Two sets of emission and fuel quality requirements are defined by Annex VI [9]:

- global requirements – a progressive reduction in global emissions of $SO_x$, $NO_x$ and particulate matter,
- more restrictive requirements dedicated to ships in deliberately established zones – emission control areas (ECA).

Table 8.1. List of the MARPOL 73/78 Annexes [8]

| Annex | Title | Entry into force |
|---|---|---|
| Annex I | Prevention of pollution by oil & oily water | 2 October 1983 |
| Annex II | Control of pollution by noxious liquid substances in bulk | 2 October 1983 |
| Annex III | Prevention of pollution by harmful substances carried by sea in packaged form | 1 July 1992 |
| Annex IV | Pollution by sewage from ships | 27 September 2003 |
| Annex V | Pollution by garbage from ships | 31 December 1988 |
| Annex VI | Prevention of air pollution from ships | 19 May 2005 |

Existing ECA can be designated for $SO_x$ and PM, or $NO_x$, as well as all three types of emissions from ships and it consists of [9]:

- Baltic Sea ($SO_x$: adopted 1997/entered into force 2005; $NO_x$: 2016/2021);
- North Sea ($SO_x$: 2005/2006; $NO_x$: 2016/2021);
- North American ECA, including most of US and Canadian coast ($NO_x$ and $SO_x$: 2010/2012);
- US Caribbean ECA, including Puerto Rico and the US Virgin Islands ($NO_x$ and $SO_x$: 2011/2014).

Due to current and upcoming regulations to address the adverse impacts of sulphur and nitrogen oxides from shipping emission, the maritime sector is required to find highly efficient and low-cost methods of gaseous pollutants removal. Outgoing methods are applied to remove $NO_x$ or $SO_2$ separately. These technologies are divided into $NO_x$-reducing devices and $SO_x$ scrubbers. There are only several studies concentrating on the simultaneous removal of $NO_x$ and $SO_2$ in one process (using electrolysis or electromagnetic techniques) [3, 10]. To accomplished major reductions in $SO_x$ and $NO_x$ emissions, the new onboard installations of exhaust emission control are required and one of them may be an electron beam flue gas treatment (EBFGT) process, which is one of the most effective methods of removing $SO_2$ and $NO_x$ from industrial flue gases.

### 8.1.2. Emission limits for marine vessels

**$SO_x$ emission limits**

$SO_x$ limits are designated under Regulation 4 and 14 of MARPOL Annex VI ($SO_x$ and particulate matter emission control). Limitations of sulphur oxide's concentration in exhausts from maritime vessels are currently met in two different ways [3]:

Table 8.2. MARPOL Annex VI fuel sulphur limits inside/outside the ECA [9]

| Outside the ECA established to limit $SO_x$ and PM emissions | Inside the ECA established to limit $SO_x$ and PM emissions |
|---|---|
| 4.50% m/m prior to 1 January 2012 | 1.50% m/m prior to 1 July 2010 |
| 3.50% m/m on and after 1 January 2012 | 1.00% m/m on and after 1 July 2010 |
| 0.50% m/m on and after 1 January 2020 | 0.10% m/m on and after 1 January 2015 |

- primary – using fuel oil with a low sulphur content (avoiding of pollutants forming),
- secondary – using $SO_x$ scrubber system (exhaust gas treatment system).

Limits of sulphur content are strictly related to areas on which ship moves. The sulphur limits and implementation dates are listed in Table 8.2 and illustrated in Fig. 8.1.

Most vessels which operate both outside and inside the ECA will, therefore, operate on different fuel oils. It is expected to have fully changed over to using the ECA compliant fuel oil before entering into the ECA. Likewise, a change from the ECA compliant fuel oil to the oil used outside cannot be started before leaving the ECA. The first crucial issue while meeting these limits is to have a knowledge about the actual sulphur content in the bunkered fuel oils. This value is to be stated in the special documents (bunker delivery note) by the fuel oil supplier. Subsequently, it is a crew's responsibility to possess the suitable fuel, service tanks as well as to avoid loading into differently part filled storage. Accordingly, accidental mixing of one fuel with other, higher sulphur content oil is unacceptable.

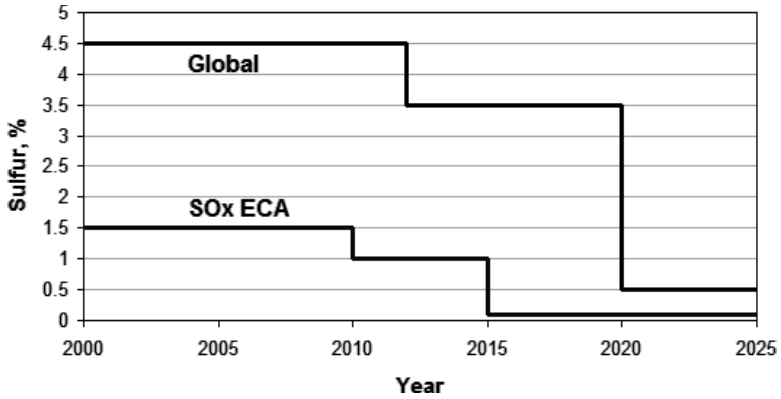


Fig. 8.1. Illustration of progressive decrease of sulphur content in fuel under MARPOL Annex VI, Regulation 14

MARPOL Annex VI determines the sulphur content in the fuel being combusted. As an equivalent for using controlled fuels, the $SO_x$ scrubbers were applied (MARPOL Annex VI, Regulation 4). In 2009, a Guidelines for Exhaust Gas Cleaning System MEPC 184 (59), which specify the regulations for the certification, test and in-service verification of $SO_x$ scrubbing systems were created. To meet restrict regulations, each scrubber should necessarily be approved by the ship's flag administration or by a classification society acting as a recognized organization on the flag administration's behalf. According to the Guidelines, there are two schemes, acceptable as the alternative methods of compliance with MARPOL Annex VI, Regulation 14 [3]:

- Scheme A – there is a need for initial certification of $SO_x$ reduction ability, followed by continuous monitoring of operating parameters and a daily spot check of emissions performance.
- Scheme B – initial certification is not required, the continuous emission monitoring using an approved system and a daily spot check of operating parameters are being used.

Using a scrubbing system always requires a $SO_x$ Emissions Compliance Plan (SECP), which introduces how the vessel will comply with MARPOL Annex VI, Regulation 14. SECP

Table 8.3. Scrubber document requirements [3]

| Document | Scheme A | Scheme B |
|---|---|---|
| $SO_x$ Emissions Compliance Plan (SECP) | X | X |
| $SO_x$ Emissions Compliance Certificate (SECC) | X | |
| EGC system – Technical Manual for Scheme A (ETM-A) | X | |
| EGC system – Technical Manual for Scheme B (ETM-B) | | X |
| Onboard Monitoring Manual (OMM) | X | X |
| EGC Record Book or Electronic Logging System | X | X |

must be prepared by ship operator and it also has to be approved by the administration. Table 8.3 shows the documents, which should be provided by the equipment manufacturer [3].

The majority of $SO_2$ in an exhaust system, as well as $CO_2$, is attributable to the fuel, combustion and operation conditions and engine design. For this reason, the ratio of $SO_2/CO_2$ is using to measure of $SO_2$ emission in proportion to the sulphur content of the fuel consumed. Therefore, in reference to scrubber system, it is possible to meet the limits included in Regulation 14 of MARPOL Annex VI on the basis of the $SO_2/CO_2$ ratio values listed in Table 8.4 (only applicable to the combustion of residual fuel oils and the petroleum-based distillate) [3].

Table 8.4. The fuel oil sulphur limits recorded in MARPOL Annex VI, Regulations 14 and corresponding emissions values [3]

| Fuel oil sulphur content [% m/m]) | Ratio emission $SO_2$ [ppm]/$CO_2$ [% v/v] |
|---|---|
| 4.50 | 195.0 |
| 3.50 | 151.7 |
| 1.50 | 65.0 |
| 1.00 | 43.3 |
| 0.50 | 21.7 |
| 0.10 | 4.3 |

Under each scheme, it is required to show that the $SO_2/CO_2$ ratio of the scrubbed exhaust is less than or equal to the required. In relation to Scheme A the value of gas flow rate and the $SO_2/CO_2$ ratio are specified by the manufacturer and they must comply with ship's operating pattern and with the $SO_2/CO_2$ emissions being at least the equivalent of the applicable fuel sulphur limit under Regulation 14. (Generally the certified value for most scrubbers is expected to be the equivalent of using 0.10% sulphur fuel.)

Under Scheme B, a continuous emissions monitoring, showing that the $SO_2/CO_2$ ratio of the scrubbed exhaust is less than or equal to the recommended at any load point (including during transient operation), is compulsory.

**$NO_x$ emission limits**

$NO_x$ limits are designated under Regulation 13 of MARPOL Annex VI ($NO_x$ emission control). Regulations are divided into three parts and they directly depend upon the date of ships construction and engine's rated speed (n). The first and the second parts of requirements are related to engines installed on ships constructed on or after 1 January 2000 (Tier I) and 1 January 2011 (Tier II). Tier III limits are in force only in $NO_x$ emission control areas, while the Tier I and Tier II standards are global. In accordance with Regulation 13, it will not be allowed for certain small ships to install Tier III engines. The nitrogen oxides emission regulation, which is posted in MARPOL Annex VI, allows installing the marine diesel engine of over 130 kW output power, other than those used solely for emergency purposes irrespective of the

Table 8.5. MARPOL Annex VI $NO_x$ emission limits, determined from the engine's rated speed [9]

| Tier | Ship construction date on or after | Total weighted cycle emission limit [g/kWh] n = engine's rated speed [rpm] | | |
|---|---|---|---|---|
| | | n < 130 | n = 130-1999 | n ≥ 2000 |
| I | 1 January 2000 | 17.0 | $45 \cdot n^{(-0.2)}$, e.g. 720 rpm – 12.1 | 9.8 |
| II | 1 January 2011 | 14.4 | $44 \cdot n^{(-0.23)}$, e.g. 720 rpm – 9.7 | 7.7 |
| III | 1 January 2016 | 3.4 | $9 \cdot n^{(-0.2)}$, e.g. 720 rpm – 2.4 | 2.0 |

tonnage of the ship onto which such engines are installed [3]. Permissible $NO_x$ emission limit for vessels, specified by the International Maritime Organization in the MARPOL Convention as Tier III standard, initially assumed its validity from 1 January 2016. However, the introduction of these requirements from 1 January 2016 has become dependent on the availability of technology applying to reduce $NO_x$ emissions to such a low level. IMO analyses have shown that the introduction of such stringent standards in the assumed period is impossible and the date of entry of the Tier III standard has been shifted, probably on 1 January 2021. Until then, $NO_x$ emission reductions should be in accordance with Tier II [11].
The $NO_x$ limits and implementation dates are listed in Table 8.5 and illustrated in Fig. 8.2.

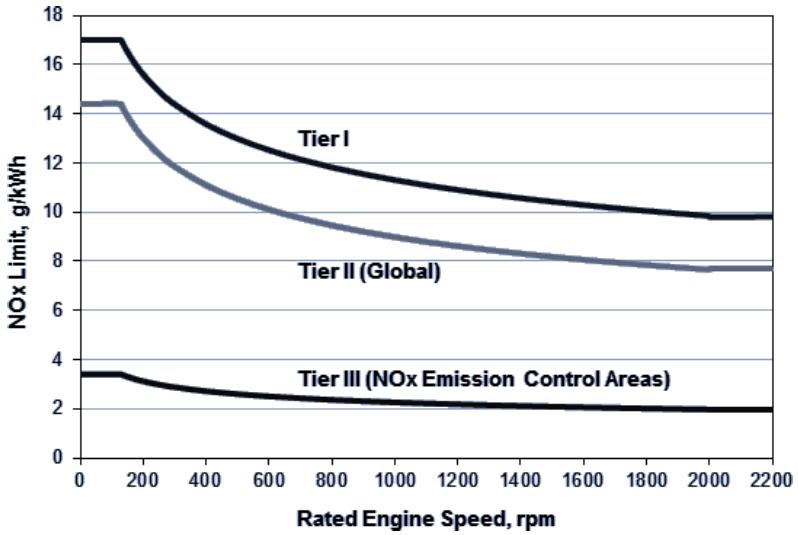


Fig. 8.2. Illustration of progressive decrease of $NO_x$ emission limits under MARPOL Annex VI, Regulation 13

Tier II regulations are expected to apply a combustion process optimization by the detailed examination of fuel injection timing, pressure, and rate (rate shaping), fuel nozzle flow area, exhaust valve timing, and cylinder compression volume. Tier III limits are expected to be met by dedicated $NO_x$ emission control technologies, such as exhaust gas recirculation (EGR) or selective catalytic reduction (SCR).

They are three methods used to confirm that the level of nitrogen oxides emission remains within the applicable limits [3]:

- Parameter check method – checking compliance of all operational parameters. Keeping the limits specified in the engine's technical file guarantees that the appropriate $NO_x$ level is maintained.

- Direct measurement and monitoring method while the engine is in service (engine + SCR together), referred to as Scheme A – completing data, using an approved emission monitoring system and determining specific g/kWh $NO_x$ emission and exhaust flow rate. To be considered as current, data have to comply within 30 days of the survey.
- Separate tests of engine and SCR referred to as Scheme B – testing of $NO_x$ emission from the engine in accordance with the appropriate test cycle and predefining of $NO_x$ reduction performance of the SCR by modelling tools using data from either a full size or scaled down version. The g/kWh $NO_x$ emission value is calculated in relation to these two dimensions and thereafter it is implemented into engine's technical file. Finally, the result of the simulation is confirming on board.

### 8.1.3. Marine diesel engines

Diesel engines, rather than gasoline engines, are distinguished by lower operating cost, longer durability, higher thermal energy as well as lower hydrocarbon and carbon monoxide emissions. Thus, there has been a continuous increase in the number of diesel engines operating in both stationary and mobile applications. Notwithstanding, this type of energy source emits the higher amount of PM and $NO_x$ than gasoline engines.

Due to lack of homogeneity in the fuel and rapid variations in the temperature inside the diesel engine, it is not possible to reach the ideal state of thermodynamic equilibrium [12]. Hence, the incomplete combustion of HC results in the formations of various types of organic and inorganic compounds, distributed among the gaseous, semi-volatile and particulate phases [13]. Products of this phenomenon are presented in Table 8.6 [14].

Table 8.6. Typical diesel exhaust composition [14]

| | Component | Concentration |
|---|---|---|
| Components naturally occurring in air | $N_2$ | 70-75 vol% |
| | $O_2$ | 5-15 vol% |
| | $CO_2$ | 2-12 vol% |
| | $H_2O$ | 2-10 vol% |
| Regulated harmful components | CO | 100-1000 ppm |
| | HC | 50-500 ppm |
| | $NO_x$ | 30-600 ppm |
| | $SO_x$ | proportional to fuel S content |
| | PM | 20-200 mg/m$^3$ |
| Unregulated harmful components | ammonia | 2.0 mg/mile |
| | cyanides | 1.0 mg/mile |
| | benzene | 6.0 mg/mile |
| | toluene | 2.0 mg/mile |
| | polycyclic aromatic hydrocarbons (PAH) | 0.2 mg/mile |
| | aldehydes | 0.0 mg/mile |

The world's leading designer and manufacturer of low and medium speed engines, using as a marine vessels' propulsion are MAN Diesel & Turbo Group and its licensees. They develop

two-stroke and four-stroke engines, auxiliary engines, turbochargers and propulsion packages, which cover approximately 50% of the power needed for all world trade.

**Four-stroke marine diesel engines**

In the maritime environment, four-stroke engine is commonly used in on-road and marine transportation and it requires four strokes of the piston to complete a power cycle during two crankshaft revolution [15]. A stroke refers to the full travel of the piston along the cylinder, in either direction (Fig. 8.3).

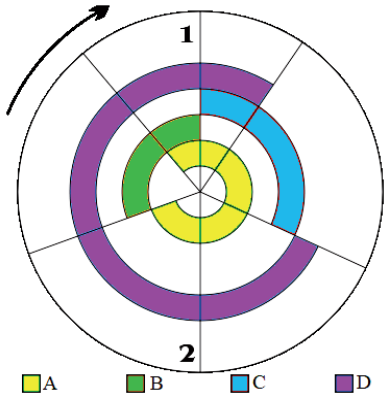


Fig. 8.3. The four-stroke cycle: A – intake, B – compression, C – power, D – exhaust; 1, 2 – crankshaft revolutions

The maximum amount of power generated by an engine is determined by the maximum amount of air ingested. The amount of power generated by a piston engine is related to its size (cylinder volume), whether it is a two-stroke engine or four-stroke design, volumetric efficiency, losses, air-to-fuel ratio, the calorific value of the fuel, the oxygen content of the air and speed (rpm). The speed is ultimately limited by material strength and lubrication. Valves, pistons and connecting rods suffer severe acceleration forces. At high engine speed, physical breakage and piston ring flutter can occur, resulting in power loss or even engine destruction. Piston ring flutter occurs when the rings oscillate vertically within the piston grooves in which they are located. Ring flutter compromises the seal between the ring and the cylinder wall, which causes a loss of cylinder pressure and power. If an engine spins too quickly, valve springs cannot act quickly enough to close the valves [15]. This is commonly referred to as 'valve float', and it can result in the piston to valve contact, severely damaging the engine. At high speeds, the lubrication of piston cylinder wall interface tends to break down. This limits the piston speed for industrial engines to about 10 m/s. The output power of an engine is dependent on the ability of intake (air-fuel mixture) and exhaust matter to move quickly through valve ports, typically located in the cylinder head. An internal combustion engine on an average is capable of converting just 30-40% of the supplied energy into mechanical work. A large part of the waste energy is in the form of heat that is released to the environment through coolant, fins, etc. It has been found that even if 6% of the entirely wasted heat is recovered it can increase the engine efficiency greatly [16]. Many methods have been devised in order to extract waste heat out of an engine exhaust and use it further to extract some useful work, decreasing the exhaust pollutants at the same time. Use of Rankine cycle, turbocharging and thermo-electric generation has been found very useful as a waste heat recovery system.

Depending on the operational location and type of the ship, different four-stroke engines with desired parameters are used. Main applications of four-stroke diesel engines are presented below.

*Offshore*: Offshore vessels require highly reliable and efficient propulsion systems that adapt easily to low-load operation. Station keeping, also known as dynamic positioning, is another

key factor when operating in heavy seas around oil platforms and installations. Offshore vessels typically operate in environmentally sensitive areas (ECA), therefore emission requirements, such as $NO_x$ and particulate matter, are of the utmost importance. Emission limits can be met with the range of dual fuel engines or by installing one of the post-treatment systems such as selective catalytic reduction to minimize $NO_x$ and scrubbers to reduce $SO_x$. While operating offshore, the highly efficient and reliable four-stroke engines are required (to power the broad variety of offshore vessels, anchor handlers, platform supply vessels, construction vessels, drill ships, etc.).

*Dredger*: In relation to the growth in the global sea transport and the size of marine vessels, greater demands have been placed on harbours and commercial waterways around the world. Part of the solution lies in excavating channel beds and modern dredgers are capable of excavating gigantic volumes of sediment daily. Modern dredgers require highly reliable, efficient, proven, medium-speed, four-stroke engines that comply with all modern emission regulations when sailing in environmentally sensitive areas (ECA). It is expected to be met by reduced rpm experienced during dredger pump operation. For engines running on heavy fuel oils, it is required to install the exhaust gas cleaning systems such as SCR to minimize $NO_x$ and to meet IMO Tier III regulations. Modern auxiliary engines usually run on the same high-viscosity fuel grades as the main engines to maximize economy.

*Fishing*: As with so many other marine segments, population growth is one of the primary market drivers in the fishing industry, in this case revolving around the need for ever-more food resources. Fishing restrictions are another key influence as regulation forces on the construction of modern, cost-optimized vessels that can operate profitably. Modern fishing vessels require cost-efficient propulsion systems (with low first-costs) as well as tough and robust technical solutions for operation in what are some of the harshest and most demanding conditions on the planet. Fishing vessels typically operate in environmentally sensitive areas, therefore emission requirements, such as $NO_x$, $SO_x$ and particulate matter, are important. It is expected to use the proven, efficient medium-speed engines that are eminently suitable for the fishing segment as well as to have the exhaust gas cleaning systems such as SCR for IMO Tier III-compliance ($NO_x$) and scrubbers for $SO_x$ reduction to comply with IMO Tier III emission regulations and their sulphur limits. Modern auxiliary engines run on the same high-viscosity fuel grades as main engines to maximize economy.

*Navy and government*: The navy and coast guard segment has grown in recent years in the face of national security concerns where nations are anxious to protect their maritime boundaries. At the same time, the growth of asymmetric threats, such as piracy, has increased the desire to provide security for world seaborne trade. Requirements within this segment include highly reliable, efficient and proven propulsion systems with excellent load acceptance. While not a strict requirement, there is still a demand for limiting emissions as much as possible. Navies often make special demands on their propulsion systems, compared to civilian vessels, such as shock-proofing, noise cancellation and antimagnetic propulsion systems. Modern auxiliary engines run on the same high-viscosity fuel grades as the main engines to maximize economy.

*Ferry*: Driven by the global growth in population and an increase in regional trade, the mobility of people – both domestically and internationally – has increased rapidly in recent decades. Modern ferries place high demands for reliability and comfort on their main engines, while silent power generation onboard is also a crucial consideration when thinking gen-sets. As this vessel type frequently sails in coastal waters, environmental sensitivity is a key issue and minimizing $NO_x$, $SO_x$ and particulate matter levels to meet stringent emission limits is a key requirement. At the same time, ferry operators seek to keep operating costs on a low level to ensure their ability to compete, also against other means of transportation. Ferry's four-stroke engines are also available as dual-fuel engines capable of running on gas, as well as on fuel oils, to ensure compliance with existing and upcoming regulations on permissible $NO_x$ and sulphur emissions. For engines running on HFO, it is required to install the exhaust gas cleaning systems such as SCR to minimize $NO_x$ and scrubbers to reduce $SO_x$. Modern auxiliary engines run on the same high-viscosity fuel grades as the main engines to maximize economy.

*LNG*: Global energy demands continue to rise year after year as existing oil reservoirs become depleted and the search for replacements spreads to deeper parts of the ocean, requiring massive investment costs. A general change in energy politics has nuclear and coal power losing popularity while gas from the USA and the Middle East is emerging as a viable alternative. Political instability has also encouraged countries to develop an energy policy that makes them more independent from pipeline supplies. In this scenario, the shipping of natural gas by LNG carrier is an obvious solution. Modern LNG tankers require highly reliable propulsion systems with excellent service support as engine availability is critical. Sailing globally through environmentally sensitive waters demands low engine emissions while the operational safety of the propulsion system is paramount. Offered propulsion systems should, therefore, be efficient and proven and they also should be able to comply with all modern emission legislation when sailing in environmentally sensitive areas and which meet the strict safety requirements that LNG carriers operate under. Some of MAN's Diesel & Turbo engines are dual-fuel and they can both operate on boil-off gas derived from a carrier's LNG payload and diesel-electric engine solutions. Modern auxiliary engines run on the same high-viscosity fuel grades as the main engines to maximize economy.
*Cruise*: As global wealth has grown in recent decades and the conception of enjoying a foreign holiday has become standard for many people, so accordingly the cruise trade has grown. Once the preserve of the very rich, cruises are now affordable to many and this segment has experienced significant growth. Today's cruise ships must accommodate high demands for reliable, comfortable and silent power generation onboard. As cruise vessels typically sail in environmentally sensitive areas, the engines employed in this segment must meet stringent emission regulations in terms of $NO_x$, $SO_x$ and particulate matter. While ensuring minimal impact on the environment operators also seek to keep operating costs at economic levels in order to offer affordable holiday experiences to their customers. Four-stroke engines, using while cruise, are available as dual-fuel engines capable of running on gas, as well as on fuel oils, to ensure compliance with existing and upcoming regulations on permissible $NO_x$ and sulphur emissions. For engines running on fuel oils, it is expected to use the exhaust gas cleaning systems such as SCR to minimize $NO_x$ and scrubbers to reduce $SO_x$. Modern auxiliary engines run on the same high-viscosity fuel grades as the main engines to maximize economy.
*Tug*: The global growth in marine transport and the accompanying increase in the volume and complexity of harbour operations have expanded the tug sector in recent years. Simultaneously, the general increase in vessel size, such as that experienced within the container and tanker sectors, has prompted the development of larger, more powerful tugs. Modern tugs require cost-efficient propulsion systems (with low first-costs), while the nature of harbour operations demands that engines possess great adaptability to low-load operation. Harbours are also environmentally sensitive areas and, accordingly, emission requirements are strict in terms of $NO_x$ and particulate matter. In this case, it is required to use medium-speed engines that are eminently suitable for the tug segment. The operation profile of a tug is pretty much as a 'sleeping bear' – many hours of standby just waiting and then full power on all engines. It requires a lot of the engine to be able to handle those load challenges a tug is requiring. All tugs' engines are therefore equipped with jet-assist which boosts the turbocharger speed if sudden load peaks occur resulting in rapid and smoke-free load increase.

**Two-stroke marine diesel engines**

In a two-stroke engine, the end of the combustion stroke and the beginning of the compression stroke happen simultaneously, with the intake and exhaust (or scavenging) functions occurring at the same time. In contrast to a four-stroke engine, it completes a power cycle with two strokes (up and down movements) of the piston during only one crankshaft revolution. Two-stroke engines have also a greatly reduced number of moving parts, and so can be more compact and significantly lighter, they are also more powerful. Due to this fact, two-stroke engines are used as a source of energy of the biggest vessels such tankers and containers. On the other hand, they create more noise as well as more pollutions (Fig. 8.4). The comparison between the four-stroke and two-stroke diesel engine is presented in Table 8.7. Depending on

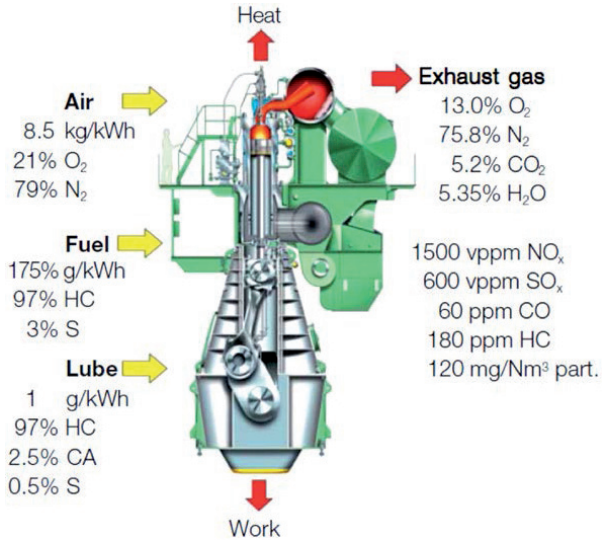


Fig. 8.4. Flow process and typical exhaust gas composition for two-stroke diesel engine [17]

the operational location and type of the ship, different four-stroke engines with desired parameters are used. Main applications of two-stroke diesel engines are presented below [18].

*Tanker*: Such ships are currently used to transport a vast variety of products such as chemicals, fresh water, wine and molasses. Modern tankers vary in size from smaller, local, coastal tankers to ULCCs (very large crude carriers), some of the largest vessels found sailing the oceans. Many modern tankers are designed for a specific cargo and a specific route with draft typically limited by harbour depth and/or the depth of straits along the preferred shipping route. Gen-sets can play a vital role as cargoes with the high vapour pressure at ambient temperatures may require pressurized tanks or vapour-recovery systems, while heaters may be required to maintain heavy crude oil, residual fuel, asphalt, wax, or molasses in a fluid state for offloading. Tankers frequently sail in environmentally sensitive areas, hence emission requirements ($NO_x$, $SO_x$, particulate matter) are important factors when choosing the main driver.

MAN Diesel & Turbo offers two-stroke engines for all tanker sizes that meet strict safety requirements. It is required to have exhaust gas cleaning systems such as SCR for IMO Tier III-compliance ($NO_x$) and scrubbers for $SO_x$ reduction. Modern auxiliary engines run on the same high-viscosity fuel grades as the main engines to maximize economy.

*Bulker*: Modern bulk carriers prioritize capacity, safety, efficiency and durability and they often demand cost-efficient propulsion systems with low first-costs. Bulkers frequently sail in environmentally sensitive areas (ECA), thus emission requirements ($NO_x$, $SO_x$, particulate matter) are important factors while choosing the main driver. Bulkers require various types of propulsion systems in accordance with all the bulk carrier sizes – from single-hole mini-bulkers to mammoth ore ships. Modern auxiliary engines run on the same high-viscosity fuel grades as the main engines to maximize economy. It is expected to have the exhaust gas cleaning systems such as SCR for IMO Tier III-compliance ($NO_x$) and scrubbers for $SO_x$ reduction to comply with IMO Tier III emission regulations and their sulphur limits.

*Container*: Containerization has greatly reduced the expense of international trade and increased its throughput, especially in relation to consumer goods and commodities. As of today, some 90% of non-bulk cargo worldwide is moved by containers stacked aboard container vessels. Container operators generally demand cost-efficient propulsion systems with low first-costs while significant auxiliary power to operate reefer containers is another key criterion. Container ships frequently sail in environmentally sensitive areas, hence emission requirements ($NO_x$, $SO_x$, particulate matter) are important factors when choosing the main driver. It is expected to

Table 8.7. The comparison between the four-stroke and two-stroke diesel engines [18]

| | Four-stroke engine | Two-stroke engine |
|---|---|---|
| Advantages | ✓ More torque – In general, four-stroke engines always make extra torque than two-stroke engines at low rpm. Although the two-stroke ones give higher torque at higher rpm but it has a lot to do with fuel efficiency.<br>✓ More fuel efficiency – four-stroke engines have greater fuel efficiency than two-stroke ones because fuel is consumed once every four strokes.<br>✓ Less pollution – As power is generated once every four strokes and also as no oil or lubricant is added to the fuel, the four-stroke engine produces less pollution.<br>✓ More durability – We all know that more the engine runs, quicker it wears out. Two-stroke engines are designed for high rpm. If an engine can go for 10,000 rpm before it wears out; the four-stroke engine with 100 rpm will run for 100 min while two-stroke engine which has a higher rpm of 500 and will run for only 20 min.<br>✓ No extra addition of oil – Only the moving parts need lubrication intermediately. No extra oil or lubricant is added to fuel. | ✓ Simple design and construction – It does not have valves. It simply has inlet and outlet ports which makes it simpler.<br>✓ More powerful – In the two-stroke engine, every alternate stroke is power stroke unlike four-stroke one in which power is delivered once every four strokes. This gives a significant power boost. Also, the acceleration will be higher and power delivery will be uniform due to the same reason.<br>✓ The position doesn't matter – two-stroke engine can work in any position as lubrication is done through the means of fuel (as the fuel passes through the whole cylinder and crankcase). |
| Disadvantages | ✓ Complicated design – four-stroke engine has complex valve mechanisms operated and controlled by gears and chain. Also, there are many parts to worry about which makes it harder to troubleshoot.<br>✓ Less powerful – As power is delivered once every two rotations of the crankshaft (four strokes), hence four stroke is less powerful.<br>✓ Expensive – A four-stroke engine has much more parts than the two-stroke engine. So it often requires repairs which leads to greater expense. | ✓ Less fuel efficiency – For every alternate power stroke, fuel is consumed every alternate stroke. This makes the engine less fuel efficient although it results in uniform power delivery.<br>✓ Oil addition could be expensive – Two-stroke engines require a mix of oil in with the air-fuel mixture to lubricate the crankshaft, connecting rod and cylinder walls. These oils may empty your pockets.<br>✓ More pollution – two-stroke engine produces a lot of pollution. The combustion of oil added to the mixture creates a lot of smoke which leads to air pollution.<br>✓ Wastage of fuel – Sometimes the fresh charge which is going to undergo combustion gets out along with the exhaust gases. This leads to wastage of fuel and also power delivery of the engine is effected.<br>✓ Improper combustion – The exhaust gases often get trapped inside the combustion chamber. This makes the fresh charge impure. Therefore maximum power does not get delivered because of improper incomplete combustion. |

have the exhaust gas cleaning systems such as SCR for IMO Tier III-compliance ($NO_x$) and scrubbers for $SO_x$ reduction to comply with IMO Tier III emission regulations and their sulphur limits. Modern auxiliary engines run on the same high-viscosity fuel grades as the main engines to maximize economy.

*LNG*: According to section titled 'Four-stroke marine diesel engines'.

*Future application*: According to MAN Diesel & Turbo Marine Engine IMO Tier II and Tier III Programme 2nd edition 2017, the two-stroke engines are shortly expected to meet the newest strict emission regulations. According to this programme, the two-stroke engines are either [19]:

- Tier II engines complying with IMO Tier II,

- Tier III engines complying with Tier II when operated in Tier II mode and with Tier III when operated in Tier III mode.

There are different parameters defined in MAN Diesel & Turbo Marine Engine IMO Tier II and Tier III Programme 2nd edition 2017 for new two-stroke engines:

- Engine power: The engine brake power is stated in kW, and the power values stated are available up to tropical conditions at sea level, i.e. [19]:

- turbocharger inlet air temperature: 45°C,
- turbocharger inlet air pressure: 1000 mbar,
- cooling water (sea/fresh) temperature: 32/36°C.

- Specific fuel oil consumption (SFOC): The SFOC is usually represented by the figures of SFOC in relation to the percentage of power which shows the values obtained when the engine and turbocharger are matched to the lowest possible SFOC values while fulfilling the IMO $NO_x$ Tier II or Tier III emission limits. The SFOC is given in g/kWh and it is based on the use of a fuel oil with a lower calorific value (LCV) equal to 42.700 kJ/kg at ISO conditions [19]:

- turbocharger inlet air temperature: 25°C,
- turbocharger inlet air pressure: 1000 mbar,
- cooling water temperature: 25°C.

Most commercially available HFOs with a viscosity below 700 cSt (7 $cm^2/s$) at 50°C can be used.

- Tolerances: The energy efficiency design index (EEDI) has increased focus on part-load SFOC. Therefore, it is possible to selects the SFOC guarantee at a load point in the range from 50% to 100%. It is recommended that the SFOC guarantee point should be limited to the range 50% to 85% for part-load or low-load tuning methods.

All engine design criteria, for example, heat load, bearing load and mechanical stress on the construction, are defined at 100% load, independently of the selected guarantee point. This means that turbocharger matching, engine adjustment and engine load calibration must also be performed at 100% load, independently of the guaranteed point. When choosing an SFOC guarantee at or below 100%, the tolerances, adjustment and calibration at 100% will affect engine running at the lower SFOC guarantee load point. This includes tolerances on measurement equipment, engine process control and turbocharger performance. Consequently, SFOC guarantee tolerances are as follows:

- 5% tolerance for 100-85% engine load,
- 6% tolerance for < 85-65% engine load,
- 7% tolerance for < 65-50% engine load.

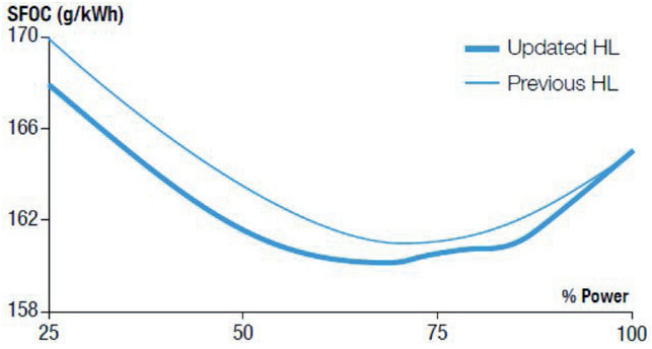


Fig. 8.5. Improvement of the G90ME-C10.5 engine [19]

- Updated fuel consumption on selected engines: As a result of tests, the fuel consumptions of G95ME-C9.5, G90ME-C10.5, G80ME-C9.5 and S90ME-C10.5 engines have been updated. Figure 8.5 shows an example of the improvement for a Tier II, L1 rated G90ME-C10.5 engine in high-load (HL) optimization:

The fuel consumption for Tier III options and dual fuel engines has also been updated. Similar improvements can be realized with part-load and low-load tuning.
- Turbocharging system: Two-stroke engines can be delivered with MAN, ABB or MHI turbochargers as standard. The SFOC figures given in the two-stroke chapter are based on turbocharging with the best possible turbocharging efficiency generally available, which means 67% for all engines with the 45-cm bore and larger, and 64% for engine bores smaller than 45 cm. Both efficiency figures refer to 100% SMCR (specified maximum continuous rating). Recently we have added exceptions to this rule. Today, the G40ME-C9.5 is available as a high-efficiency application offering all Tier II standard tunings and all Tier III options requiring a high-efficiency turbocharger. The S40ME-B9 and S35ME-B9 type engines are also available as high-efficiency applications offered with high-load tuning and Tier III options with conventional-efficiency turbocharging. Only engine specifications for which an applicable high-efficiency turbocharger is available are subject to the firm order. All Tier II engines with high-efficiency (67%) turbochargers can be ordered with lower (conventional) turbocharging efficiency. Utilizing this possibility will result in higher exhaust gas temperatures, lower exhaust gas amounts, and a slight change in SFOC. It is not possible to apply tuning methods (part- or low-load) when making such a conversion.
- Fuel consumption and optimization: Possibilities for Tier II engines various optimization are available for the MAN B&W type engines. High-load optimization is for the best possible SFOC at 100% engine load. Optimization of SFOC in the part-load range (50-85%) or low-load range (25-70%) requires selection of the exhaust gas bypass (EGB) tuning method. Also, high-pressure tuning (HPT) is available on request for engines. The above tuning methods are available for all SMCR points, but cannot be combined. The SFOC reduction potential of each tuning method at L1 rating can be seen on each individual engine page. In cases where part-load or low-load EGB tuning is applied, and a higher exhaust gas temperature is needed, a solution exists for additional automatic control of the EGB, the so-called economizer energy control (EEC). Forcing an open EGB at loads where the EGB is normally closed results in a higher exhaust gas temperature, but with an SFOC penalty.

Table 8.8. EGR-matching conceptions

| EGR conception | Description |
|---|---|
| EGRTC | T/C cut-out matching for engines with bores ≥ 80 cm and more than one turbocharger applied |
| EGRBP | Bypass matching for engines with bores ≤ 70 cm and one high-efficiency turbocharger and for engines with bores ≤ 40 cm and one conventional efficiency turbocharger |

- Tier III technologies: To ensure compliance with IMO Tier III regulations, one of the two major $NO_x$ reduction technologies must be selected – EGR or SCR (details about this installation in section 8.1.4). Which technology is preferred depends on market demands, engine size, other requirements and operational pattern.

Table 8.9. SCR-matching conceptions [19]

| SGR conception | Description |
|---|---|
| MAN SCR-HP | High-pressure SCR with a static mixer and SCR reactor installed upstream the turbocharger(s) |
| MAN SCR-LP | Low-pressure SCR with a static mixer and SCR reactor installed downstream the turbocharger(s) |

All Tier III engines have two operating modes:
- Tier III mode fulfilling the IMO Tier III regulations
- Tier II mode fulfilling the IMO Tier II regulations.

## MAN B&W S70ME-C8.5

Tier III

| Cyl. | $L_1$ kW |
|---|---|
| 5 | 16,350 |
| 6 | 19,620 |
| 7 | 22,890 |
| 8 | 26,160 |

Stroke: 2,800 mm

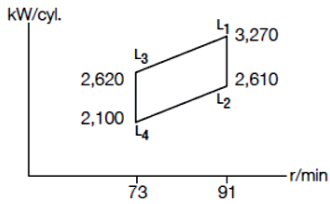


### Dual Fuel Mode for GI (Methane)

$L_1$ MEP: 20.0 bar

**MAN B&W S70ME-C8.5-GI-EGRTC**

**$L_1$ SFOC equivalent gas + pilot fuel (42,700 kJ/kg) [g/kWh]***

| | 50% | 75% | 100% |
|---|---|---|---|
| Tier II mode | 162.5 | 164.5 | 171.0 |
| Tier III mode | 170.5 | 169.0 | 174.0 |

**$L_1$ SGC 50,000 kJ/kg (SPOC pilot fuel 42,700 kJ/kg) [g/kWh]**

| | | | |
|---|---|---|---|
| Tier II mode | 131.7 (8.3) | 135.2 (6.3) | 141.6 (5.2) |
| Tier III mode | 138.5 (8.3) | 139.0 (6.3) | 144.1 (5.2) |

**MAN B&W S70ME-C8.5-GI-HPSCR**

**$L_1$ SFOC equivalent gas + pilot fuel (42,700 kJ/kg) [g/kWh]***

| | 50% | 75% | 100% |
|---|---|---|---|
| Tier II mode | 162.5 | 164.5 | 170.5 |
| Tier III mode | 164.0 | 165.5 | 171.0 |

**$L_1$ SGC 50,000 kJ/kg (SPOC pilot fuel 42,700 kJ/kg) [g/kWh]**

| | | | |
|---|---|---|---|
| Tier II mode | 131.8 (8.2) | 135.3 (6.2) | 141.2 (5.1) |
| Tier III mode | 133.1 (8.2) | 136.1 (6.2) | 141.7 (5.1) |

**MAN B&W S70ME-C8.5-GI-LPSCR**

**$L_1$ SFOC equivalent gas + pilot fuel (42,700 kJ/kg) [g/kWh]***

| | 50% | 75% | 100% |
|---|---|---|---|
| Tier II mode | 162.5 | 164.5 | 170.5 |
| Tier III mode | 163.5 | 165.5 | 171.5 |

**$L_1$ SGC 50,000 kJ/kg (SPOC pilot fuel 42,700 kJ/kg) [g/kWh]**

| | | | |
|---|---|---|---|
| Tier II mode | 131.8 (8.2) | 135.3 (6.2) | 141.2 (5.1) |
| Tier III mode | 132.7 (8.2) | 136.1 (6.2) | 142.1 (5.1) |

* *Gas fuel LCV (50,000 kJ/kg) is converted to fuel oil LCV (42,700 kJ/kg) for comparison with a fuel oil operated engine.*

Fig. 8.6. Sample specification of the new two-stroke engine S70ME-C8.5 [19]

## Engine Dimensions

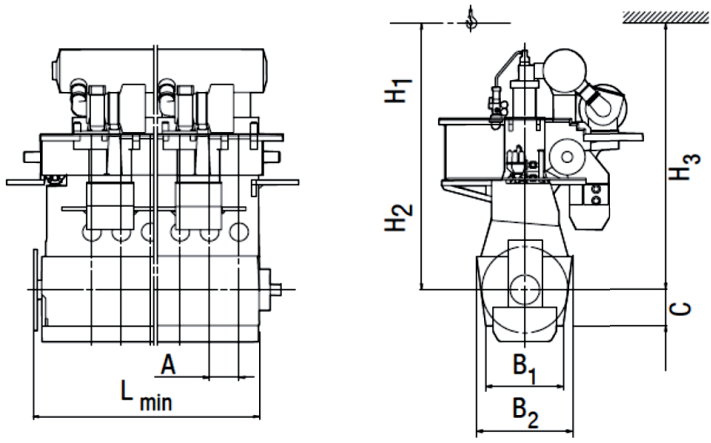


**Specifications**

| Dimensions: | | A | $B_1$ | $B_2$ | C | $H_1$ | $H_2$ | $H_3$ |
|---|---|---|---|---|---|---|---|---|
| | mm | 1,190 | 4,390 | 4,454 | 1,521 | 12,550 | 11,725 | 11,500 |

| Cylinders: | | 5 | 6 | 7 | 8 |
|---|---|---|---|---|---|
| $L_{min}$ | mm | 7,781 | 8,971 | 10,161 | 11,351 |

**Tier II**

| Dry mass: | t | 451 | 534 | 605 | 681 |
|---|---|---|---|---|---|

**Tier III**

| Dry mass (added): | | | | | |
|---|---|---|---|---|---|
| EGR | t | 15 | 16 | 17 | 18 |
| HP SCR | t | 4 | 5 | 6 | 6 |
| LP SCR | t | - | - | - | - |

Fig. 8.7. S70ME-C8.5 engine dimensions [19]

The Tier III technologies are designed for the use of low-sulphur fuels (0-0.1% sulphur) in Tier III mode. This limitation for sulphur content applies to Tier III operation only. In Tier II operation, the engine is in all cases capable of using fuels with a high sulphur content. Tier III designs for use of high-sulphur fuels in Tier III mode are available on request. Fuel consumption guarantees can be given for engines for both Tier II and Tier III mode.

- EGR: Two EGR-matching conceptions are available depending on engine type [19]. They are presented in Table 8.8.

For the smallest bore engines, especially with five and six cylinders, the availability of applicable turbochargers makes it difficult to apply EGR. Therefore, SCR is recommended for these engines. SCR-matching conceptions are presented in Table 8.9.

The SCR system must be supplied by an approved supplier. For some large-bore engines (bores ≥ 90 cm) with a high cylinder number, SCR-HP is also available.
- Application of high-sulphur fuels and $SO_x$ scrubbers: All two-stroke engines in the MAN Diesel & Turbo marine engine programme are compatible with $SO_x$ scrubbers. A $SO_x$ scrubber installation will increase the back pressure, thereby affecting engine performance. Accordingly, we require that a $SO_x$ scrubber installation does not increase the back pressure by more than 30 mbar at SMCR.
- Waste heat recovery systems: On engines with high-efficiency turbochargers, waste heat can be economically recovered by installing equipment for waste heat recovery (WHR) and matching the engine for WHR. WHR systems are available for both Tier II and Tier III engines. The following types of WHR systems have been approved for application:

- power turbines with a power output equal to 3-5% of the engine shaft power at SMCR;
- power turbines and steam turbines with a power output corresponding to 8-10% of the engine shaft power at SMCR;

Table 8.10. Properties of marine diesel fuels in accordance with ISO-8217 standard

| Limit | Parameter | DMX | DMA | DFA | DMZ | DFZ | DMB | DFB |
|---|---|---|---|---|---|---|---|---|
| Max. | Viscosity at 40ºC [$mm^2/s$] | 5.500 | 6.000 | | 6.000 | | 11.00 | |
| Min. | Viscosity at 40ºC [$mm^2/s$[ | 1.400 | 2.000 | | 3.000 | | 2.000 | |
| Max. | Micro carbon residue at 10% residue [% m/m] | 0.30 | 0.30 | | 0.30 | | - | |
| Max. | Density at 15ºC [$kg/m^3$] | - | 890.0 | | 890.0 | | 900 | |
| Max. | Micro carbon residue [% m/m] | - | - | | - | | 0.30 | |
| Max. | Sulphur [% m/m] | 1.00 | 1.00 | | 1.00 | | 1.50 | |
| Max. | Water [% V/V] | - | - | | - | | 0.30 | |
| Max. | Total sediment by hot filtration [% m/m] | - | - | | - | | 0.10 | |
| Max. | Ash [% m/m] | 0.010 | 0.010 | | 0.010 | | 0.010 | |
| Min. | Flash point [ºC] | 43.0 | 60.0 | | 60.0 | | 60.0 | |
| Max. | Pour point in winter [ºC] | - | -6 | | -6 | | 0 | |
| Max. | Pour point in summer [ºC] | - | 0 | | 0 | | 6 | |
| Max. | Cloud point in winter [ºC] | -16 | report | | report | | - | |
| Max. | Cloud point in summer [ºC] | -16 | - | | - | | - | |
| Max. | Cold filter plugging point in winter [ºC] | - | report | | report | | - | |
| Max. | Cold filter plugging point in summer [ºC] | - | - | | - | | - | |
| Min. | Calculated cetane index | 45 | 40 | | 40 | | 35 | |
| Max. | Acid number [mg KOH/g] | 0.5 | 0.5 | | 0.5 | | 0.5 | |
| Max. | Oxidation stability [$g/m^3$] | 25 | 25 | | 25 | | 25 | |
| Max. | Fatty acid methyl ester (FAME) | - | - | 7.0 | - | 7.0 | - | 7.0 |
| Max. | Lubricity, corrected wear scar diameter (wsd 1.4 at 60ºC) [µm] | 520 | 520 | | 520 | | 520 | |
| Max. | Hydrogen sulphide [mg/kg] | 2.00 | 2.00 | | 2.00 | | 2.00 | |
| Max. | Appearance | Clear and bright | | | | | - | |

- steam turbine system – with a power output corresponding to 4-6% of the engine shaft power at SMCR;
- turbochargers with a motor/generator attached to the turbocharger shaft, and with a power output equal to 3-5% of the engine shaft power at SMCR.

- Lubricating oil consumption: The system oil consumption varies according to engine sizes and, operational and maintenance patterns.
- Specific cylinder oil consumption: Alpha ACC (adaptive cylinder-oil control) is the lubrication mode for MAN B&W two-stroke engines that involves lube oil dosing proportional to the engine load and to the sulphur content in the fuel oil being burned. The specific minimum dosage for low-sulphur fuels is set to 0.6 g/kWh. The typical ACC dosage for a BN 100 cylinder oil is 0.3 g/kWh × S%.

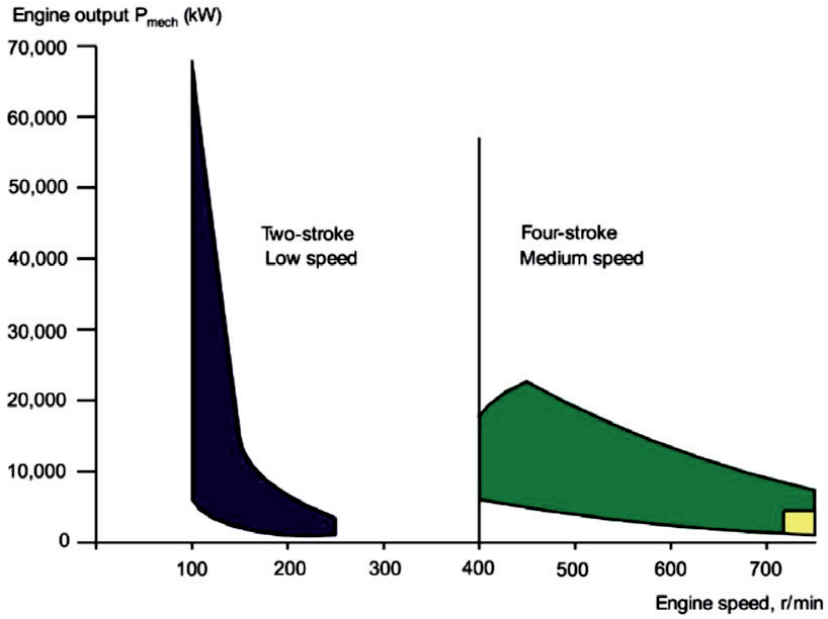


Fig. 8.8. The application of piston engines as a marine propulsion

Sample specification of the new two-stroke engine (S70ME-C8.5) is presented in Figs. 8.6, 8.7 and properties of marine diesel fuels in accordance with ISO-8217 standard are presented in Table 8.10 [19]. The application of piston engines as a marine propulsion is presented in Fig. 8.8.

### 8.1.4. Currently available $SO_X$/$NO_X$ emission control systems

**$SO_x$ pollution control**

Emission of $SO_2$ is directly proportional to the sulphur content of the fuel. The simplest and the least labour-intensive way to reduce it is to go over to using fuel oil in a low sulphur content. Another possibility, as mentioned before, is to use the $SO_x$ scrubber. There are two different types of such devices [3]:

- wet scrubbers – using a water (fresh/seawater) as the scrubbing medium,
- dry scrubbers – using a dry adsorbent as the scrubbing medium.

Wet scrubbers can also be divided into open loop, closed loop and hybrid systems, which is illustrated in Fig. 8.9.

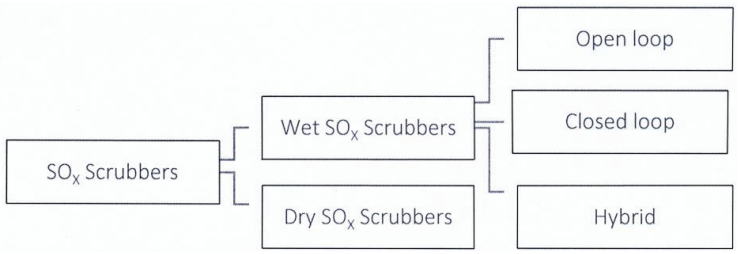


Fig. 8.9. Division of currently available wet $SO_x$ scrubbing systems [3]

In general, each wet scrubbing system consists of the same basic elements: a scrubber unit (directly contact of water and exhaust gas from one or more combustion unit, typically mounted high up in the ship in or around the funnel), a treatment plant (conditioning of wash-water before discharge overboard), residue handling facility (managing with sludge separated from the washwater), pipes, tanks, monitoring and control systems, various pumps and coolers concerning the scrubbing system configuration. It may be also necessary to include a reheater (lowing the exhaust gas temperature) or demister. Due to highly corrosive washwater, the wet $SO_x$ scrubber system should be constructed of suitable corrosion-resistance materials. The main dimensions of typical scrubber unit, which can be used in maritime industry are presented in Table 8.11 and Fig. 8.10.

Table 8.11. Main dimensions of typical scrubber unit applied in maritime engines exhaust gas treatment system

| Dimension | Description | Scrubber unit | | | | | | |
|---|---|---|---|---|---|---|---|---|
| | | 1 MW | 2 MW | 4 MW | 6 MW | 8 MW | 11 MW | 15 MW |
| | Exhaust gas mass flow [kg/s] | 2.15 | 4.30 | 8.60 | 12.90 | 17.20 | 23.65 | 32.25 |
| A | Vessel diameter [mm] | 850 | 1 350 | 1 750 | 2 000 | 2 500 | 2 900 | 3 500 |
| B | Overall length [mm] | 1 730 | 2 240 | 3 295 | 3 850 | 4 660 | 5 360 | 6 250 |
| B1 | Overall width [mm] | 1 250 | 1 580 | 1 980 | 2 240 | 2 740 | 3140 | 3 660 |
| C | Outlet height [mm] | 4 020 | 4 460 | 4 835 | 5 810 | 6 150 | 6935 | 8 205 |
| D | Inlet height [mm] | 4 670 | 5 200 | 7 015 | 8 495 | 9 635 | 10 665 | 12 130 |
| E | Drain below base [mm] | 40 | 120 | 150 | 190 | 250 | 315 | 595 |
| F | Scrubber inlet height [mm] | 1 480 | 1 660 | 2 050 | 2 435 | 2 985 | 3 330 | 3 680 |
| X | Difference between bottom part and inlet [mm] | 0 | 0 | 200 | 200 | 250 | 150 | 300 |
| S | Distance between support [mm] | 690 | 745 | 745 | 790 | 1 015 | 1 160 | 1 260 |
| N1 | Inlet nominal bore [mm] | 400 | 600 | 900 | 1 100 | 1 300 | 1 500 | 1 700 |
| N2 | Outlet nominal bore [mm] | 400 | 600 | 850 | 1 000 | 1 100 | 1 300 | 1 600 |
| N3 | Drain nominal bore [mm] | 150 | 200 | 273 | 400 | 400 | 450 | 500 |
| | Dry weight [tones] | 1.2 | 2.0 | 2.8 | 4.1 | 5.9 | 7.4 | 10.4 |
| | Wet weight [tones] | 1.5 | 2.7 | 3.7 | 5.4 | 8.6 | 11.5 | 16.9 |
| Hw | Water level [mm] | 600 | 500 | 435 | 420 | 550 | 580 | 610 |
| | Water weight [tones] | 0.30 | 0.7 | 1.0 | 1.3 | 2.8 | 4.1 | 6.5 |

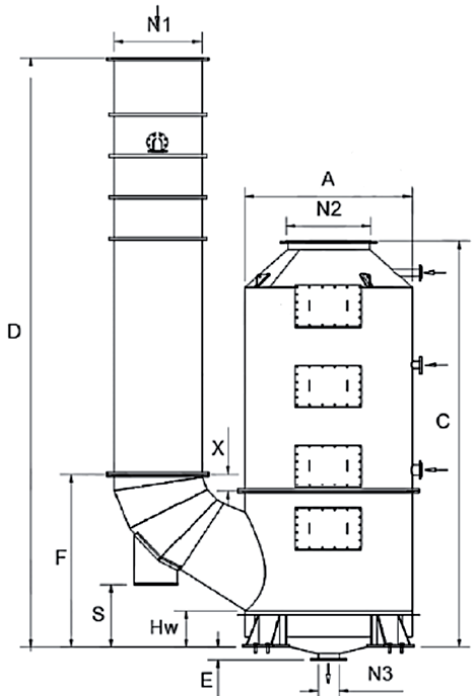


Fig. 8.10. Main dimensions of typical scrubber unit applied in maritime engines exhaust gas treatment systems

*Wet $SO_x$ scrubber – open loop*: This system is accomplished by extraction of water directly from the sea. Thereafter water is contacted with the exhaust gas and discharged back to the sea. There is no recirculation of washwater in this system. The washwater rate in open loop is approximately 45 $m^3$/MWh and removal rate is close to 98% (with full alkalinity water). An open loop wet $SO_x$ scrubbing system is presented in Fig. 8.11. The chemical reactions are the following [20]:

- for $SO_2$:

$SO_2 + H_2O \rightarrow H_2SO_3$ (sulphurous acid) $\rightarrow H^+ + HSO_3^-$ (bisulphite) (8.1)

$HSO_3$ (bisulphite) $\rightarrow H^+ + SO_3^{2-}$ (sulphite) (8.2)

$SO_3^{2-}$ (sulphite) $+ 1/2O_2 \rightarrow SO_4^{2-}$ (sulphate) (8.3)

- for $SO_3$:

$SO_3 + H_2O \rightarrow H_2SO_4$ (sulphuric acid) (8.4)

$H_2SO_4 + H_2O \rightarrow HSO_4^-$ (hydrogen sulphate) $+ H_3O^+$ (8.5)

$HSO_4^-$ (hydrogen sulphate) $+ H_2O \rightarrow SO_4^2$ (sulphate) $+ H_3O^+$ (8.6)

Conclusion: The high efficiency of $SO_2$ removal renders that it is possible to use a 3.50% sulphur fuel, which after scrubbing will be an equivalent of 0.10% sulphur fuel [20]. On the other hand, there are several parameters, which should be considered before the decision of using the wet scrubber in the open loop system. First of all, marine's scrubbing and denitration systems are expected to be compatible. $NO_x$ reducing systems usually require a high temperature of activation, close to 300°C. Simultaneously, $SO_2$ solubility reduces at higher seawater temperatures. For this reason, equipment manufacturers are expected to provide guidance on the maximum sulphur content of fuel that can be consumed by an engine or boiler with a scrubbed exhaust, so that emissions remain within applicable limits, together with any seawater temperature limitations that may apply and, if applicable, the engine's $NO_x$ certification limits. As always, it is also necessary to mix the washwater with the exhaust without making a back-

pressure that exceeds the regulations and to reduce the space required for installation, which will decline manufacturing costs.

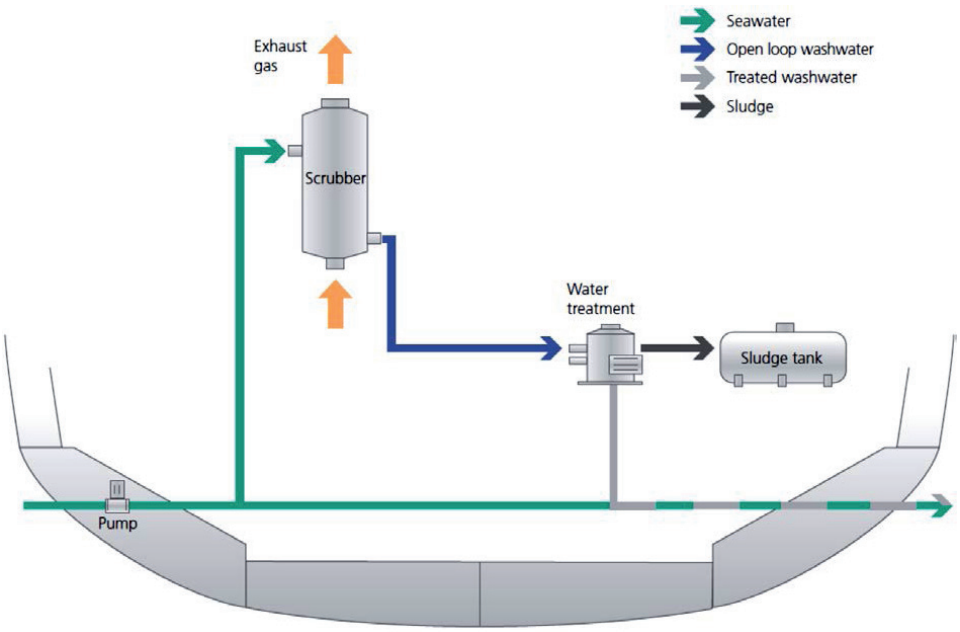


Fig. 8.11. An open loop wet $SO_x$ scrubbing system [3]

*Wet $SO_x$ scrubber – closed loop*: This system uses fresh water treated with sodium hydroxide (NaOH) as the scrubbing media. Rather than open loop scrubbing system, the washwater from closed loop after the cleaning is recirculated. The composition of wastewater from scrubber operating in closed loop mode is presented in Table 8.12. The washwater rate in the closed loop is approximately 20 $m^3$/MWh and the washwater discharge is around 0.1 $m^3$/MWh. The concentration of typically used NaOH solution is 50% (with 1530 kg/$m^3$ density at 15°C) which directly appeals to the dosage rate around 15 L/MWh. The chemical reactions are the following [20]:

Table 8.12. The composition of wastewater from scrubber operating in closed loop mode

| Wastewater component | Content [% mas.] |
|---|---|
| Water | > 75 |
| Sulphates | < 25 |
| Sulphite | < 1 |
| Nitrite | < 0.2 |
| Nitrates | < 0.2 |
| Metals as sum | < 0.006 |
| Hydrocarbons as sum C10-C40 | < 0.0001 |

- for $SO_2$:

$Na^+ + OH^- + SO_2 \rightarrow NaHSO_3$ (aqueous sodium bisulphite) (8.7)

$2Na^+ + 2\ OH^- + SO_2 \rightarrow Na_2SO_3$ (aqueous sodium sulphite) + $H_2O$ (8.8)

$2Na^+ + 2\ OH^- + SO_2 + 1/2O_2 \rightarrow Na_2SO_4$ (aqueous sodium sulphate) + $H_2O$ (8.9)

- for $SO_3$:

$SO_3 + H_2O \rightarrow H_2SO_4$ (sulphuric acid) (8.10)

$2NaOH + H_2SO_4 \rightarrow Na_2SO_4$ (aqueous sodium sulphate) $+ 2H_2O$ (8.11)

Conclusion: The efficiency of $SO_2$ removal renders that it is possible to use a 2.70% sulphur fuel, which after scrubbing will be an equivalent of 0.10% sulphur fuel [20]. A huge advantage of closed loop system is the possibility of its operation when the ship is in enclosed waters where the alkalinity would be too low for open loop. Moreover, power consumption while the marine vessel sailing in the closed loop can be up to two times lower. Additionally, closed loom system can operate in zero discharge mode for a period of time, which depends on the size of holding the tank and which may be helpful while operating in areas such as ports and estuaries.

There are also plenty of disadvantages related to closed loop wet $SO_x$ scrubbing system. Firstly, the result of the $SO_x$ removal from the exhaust gas stream is sodium sulphate, which requires a recirculation of small quantities of treated washwater to reduce the concentration. If uncontrolled, the sodium sulphate crystals will degrade the washwater system in a short time. The rate of water replenishment to the system also depends on the losses to the exhaust through evaporation (influenced by exhaust and scrubbing water temperature) and via the washwater treatment plant.

Sodium hydroxide is corrosive to glass, aluminium, tin, bronze, brass, zinc and mild steel at over 50°C, thus it is usually transported in temperature of around 40°C. The required temperature while pumping is 20°C, as the viscosity rapidly rises below this temperature. It is therefore advisable to store NaOH onboard at the temperature between 20°C and 50°C. Sodium hydroxide, having the pH of 14, is hazardous and it may cause eye injury, respiratory damage as well as severe skin burns. The restrict regulations about the usage of NaOH are expected to be met by appropriate personal protective equipment (PPE) in accordance with material safety data sheets (MSDS).

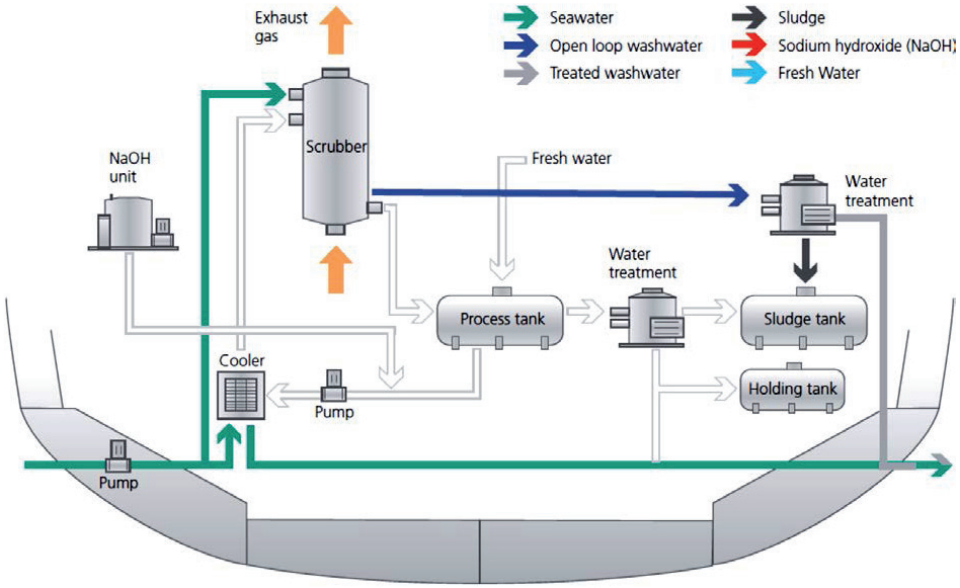


Fig. 8.12. A hybrid $SO_x$ scrubbing system, operating in open loop mode [3]

*Wet $SO_x$ scrubber – hybrid*: This system is a combination of open and closed loop and it can operate in both modes. This flexibility allows working in zero discharge mode as well as full washwater discharge mode without consuming sodium hydroxide. It is required to only use the NaOH when necessary, reducing handling and storage; fresh water consumption is also reduced.

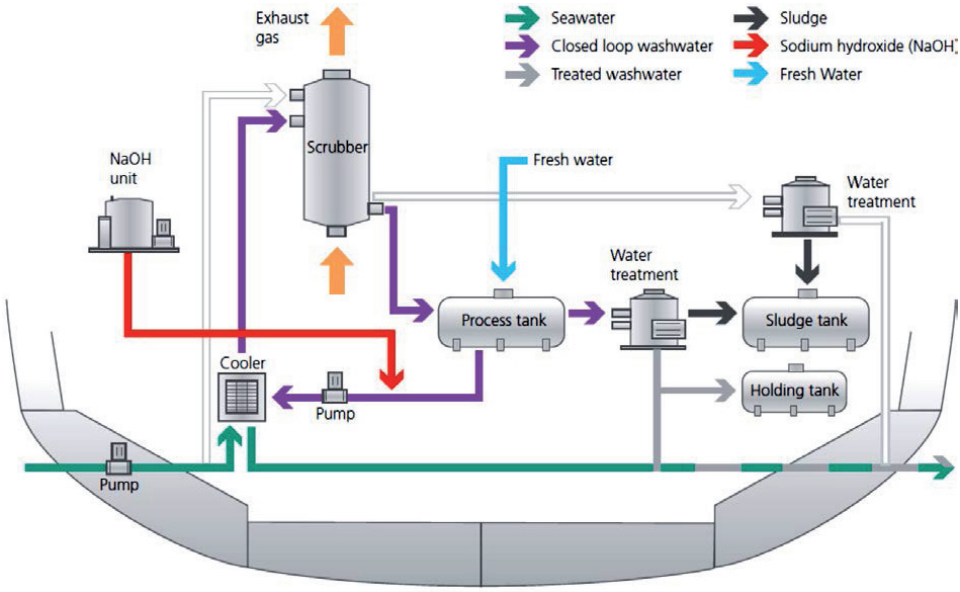


Fig. 8.13. A hybrid $SO_x$ scrubbing system, operating in closed loop mode [3]

The hybrid scrubber is more complicated than the open loop or closed loop devices. A hybrid wet $SO_x$ scrubbing system is presented in Figs. 8.12. and 8.13.

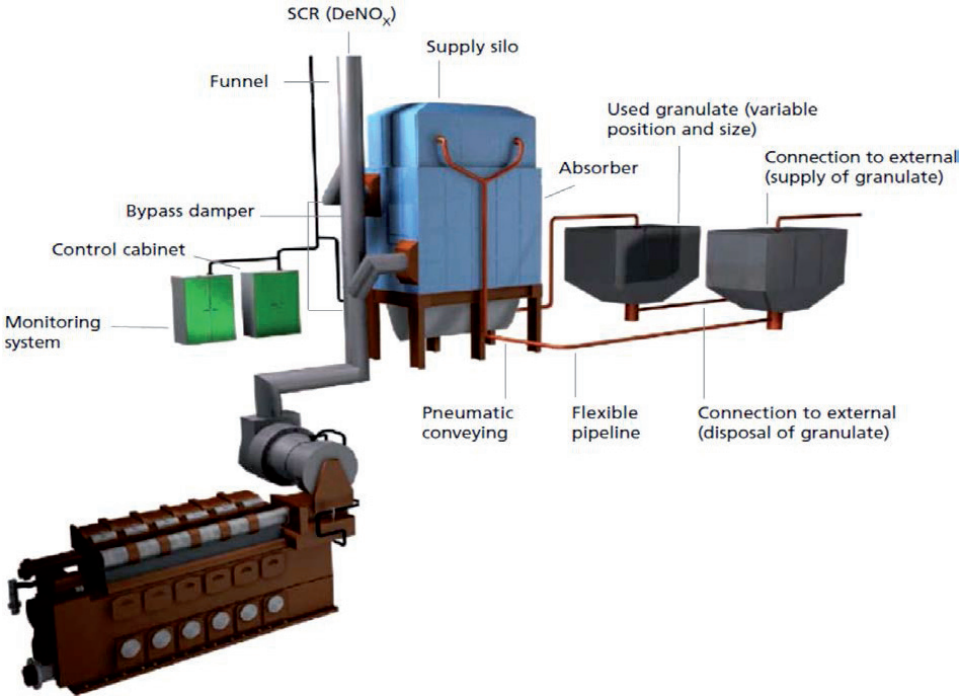


Fig. 8.14. A dry $SO_x$ scrubber system [3]

Table 8.13. Comparison of different $SO_x$ scrubbing technologies [3, 20, 21]

| | Wet (open loop) | Wet (closed loop) | Wet (hybrid) | Dry | Comment |
|---|---|---|---|---|---|
| Main components | Scrubber, washwater pumps, washwater piping, washwater treatment equipment, sludge handling equipment | Scrubber, washwater pumps, washwater piping, washwater processing tank, washwater holding tank, sodium hydroxide storage tank, washwater treatment equipment, sludge handling equipment | Scrubber, washwater pumps, washwater piping, washwater processing tank, washwater holding tank, sodium hydroxide storage tank, washwater treatment equipment, sludge handling equipment | Adsorber, fresh granulate hopper, used the granulate hopper, granulate transport system, additional granulate storage (new/used granules) | More complicated systems naturally require more auxiliary devices. While using wet $SO_x$ scrubber systems it is necessary to handle with washwater tanks and accessories as well as with sludges. The hybrid system is more flexible but requires more complex scrubber unit than other installations. Dry systems are less complicated in terms of quantity of necessary apparatus, but they require the granulate transport system and storage. |
| Weight | 30-55 tons (excluding washwater system and treatment equipment) | 30-55 tons (excluding washwater system, treatment equipment, washwater processing tank and washwater holding tank) | 30-55 tons (excluding washwater system, treatment equipment, washwater processing tank and washwater holding tank) | ~200 tons (excluding additional granulate system) | The filled dry scrubber unit for a 20 MW engine is usually heavier than comparable exhaust capacity wet scrubbers. Nonetheless, in reality, the overall weight of both systems may be similar once the washwater systems, such as the processing tank, holding the tank and chemical storage, are taken into account. |
| Power consumption [% of max. scrubbed engine power] | 1-2% | 0.5-1% | 0.5-2% (depending on whether it is operating in open or closed loop mode) | 0.15-0.20% | The washwater flow rate in a closed loop $SO_x$ scrubber is lower (≈ 20 $m^3$/MWh) than in open loop $SO_x$ scrubber (≈ 45 $m^3$/MWh) because the buffering capacity of seawater is less than the buffering capacity of fresh water dosed with sodium hydroxide. Consequently, open loop $SO_x$ scrubbers require larger pumps and have higher power requirements. The power requirement of dry $SO_x$ scrubber systems is mainly related to a screw conveyor hence it is considerably less than for wet $SO_x$ scrubbers. |
| Operation in fresh water | No | Yes | Yes | Yes | Alkalinity or the buffering capacity of seawater is a key parameter for the effective operation of wet open loop $SO_x$ scrubbers (including hybrid $SO_x$ scrubbers when operating in open loop mode). When exhaust gas is mixed with seawater inside the scrubber, sulphur oxides are dissolved, increasing the acidity and lowering the pH of the washwater. Alkalinity is a measure of the ability to resist changes in pH; in seawater, alkalinity is naturally provided by bicarbonates, carbonates, borates and anions of other 'salts' in more minor quantities. Areas within the Baltic Sea do not have sufficient alkalinity to support the operation of wet open loop $SO_x$ scrubbers. Closed loop wet $SO_x$ scrubbers (including hybrid $SO_x$ scrubbers operating in closed loop mode) and dry $SO_x$ scrubbers do not use seawater as their scrubbing medium; therefore they are unaffected by the properties of the water the ship is operating in. The energy consumption will affect any operational energy efficiency key performance indicators that include actual energy consumption of auxiliary systems |

Table 8.13. Contd.

| | Wet (open loop) | Wet (closed loop) | Wet (hybrid) | Dry | Comment |
|---|---|---|---|---|---|
| Operation without discharge to sea | No | For a limited time depending on the size of the washwater holding tank | For a limited time depending on the size of washwater holding tank | Yes | The high washwater discharge rate (≈ 45 $m^3$/MWh) of open loop systems (and hybrid systems in open loop mode) means that when operating they have to discharge washwater into the sea continuously. The much lower discharge rate (0.1 $m^3$/MWh) of closed loop systems (and hybrid systems operating in closed loop mode) means that it is possible to retain washwater to be discharged on board for a limited period of time. Dry $SO_x$ scrubbers have no discharges to sea. Being able to operate in zero discharge mode is ideal for areas where there is sensitivity to washwater discharges, such as ports and estuaries. |
| Scrubbing chemical consumable | No consumable | Sodium hydroxide solution | Sodium hydroxide solution (while operating in closed loop mode) | Calcium hydroxide granules | Due to highly corrosive washwater, the wet $SO_x$ scrubber system should be constructed of suitable corrosion-resistance materials, which can generate additional costs. Sodium hydroxide is corrosive to glass, aluminium, tin, bronze, brass, zinc and mild steel at over 50°C. The restrict regulations about the usage of NaOH are expected to be met by appropriate personal protective equipment in accordance with material safety data sheets. Calcium hydroxide is strong alkali and it is classed as harmful to eye and skin. The regulations about the usage of $Ca(OH)_2$ are expected to be met in accordance with material safety data sheets, but calcium hydroxide is significantly less hazardous than 50% aqueous NaOH solution used in wet systems. |
| Compatibility with the waste heat recovery system | Yes, provided the scrubber is installed after the waste heat recovery system | Yes, provided the scrubber is installed after the waste heat recovery system | Yes, provided the scrubber is installed after the waste heat recovery system | Yes. Can be placed before or after the waste heat recovery system | All wet $SO_x$ scrubbers significantly cool the exhaust gas and are therefore not suitable for installation before a waste heat recovery unit. For the same reason, it would not be possible to install a wet $SO_x$ scrubber before an SCR system unless a reheater was fitted after the wet scrubber to raise the exhaust gas temperature back up to around 300°C – the temperature required for SCR systems to work effectively. Dry $SO_x$ scrubbers do not cool the exhaust gas so they are suitable for installation before both waste heat recovery units and SCR systems. |
| Compatibility with SCR system | No, unless a reheater is fitted after the wet scrubber to raise the exhaust gas temperature | No, unless a reheater is fitted after the wet scrubber to raise the exhaust gas temperature | No, unless a reheater is fitted after the wet scrubber to raise the exhaust gas temperature | Yes | |
| Compatibility with EGR system | Yes | Yes | Yes | Yes | - |
| Particulate matter removal | Yes | Yes | Yes | Yes | $SO_x$ scrubbers can be an effective means of reducing PM both indirectly by removal of $SO_x$ and by direct mechanical cleaning when particles come into direct contact with either washwater or chemical granules. $SO_x$ scrubber manufacturers typically claim between 70% and 90% removal rates. The sulphates, which make a significant contribution to PM, are formed post-combustion in the exhaust plume. Oxidation of $SO_2$, followed by further oxidation and condensation processes, contributes to the growth of complex particles after the cylinder and the majority of sulphates form in reactions after release from the stack. |

*Dry $SO_x$ scrubber*: This system consists of a scrubber unit (adsorber, which contacts exhaust gas from one or more combustion unit with calcium hydroxide granules), a granule supply silo and screw conveyor (for discharge, positioned at the top and bottom of the absorber, respectively) and a scrubber control and emission monitoring system. This kind of scrubber typically works at exhaust temperatures between 240°C and 450°C. Calcium hydroxide granules are between 2 mm and 8 mm in diameter with a very high surface area to maximize the masses exchange. The rate of calcium hydroxide granules is approximately 40 kg/MWh and, based on a density of 800 kg/m$^3$, the volume of granulate would be 0.05 m$^3$/MWh. A dry $SO_x$ scrubbing system is presented in Fig. 8.14. The chemical reactions are the following [20]:

- for $SO_2$:

$$SO_2 + Ca(OH)_2 \rightarrow CaSO_2 \text{ (calcium sulphite)} + H_2O \quad (8.12)$$

The sulphite is then oxidized and hydrated in the exhaust stream to form calcium sulphate dihydrate or gypsum:

$$2CaSO_3 + O_2 \rightarrow 2CaSO_4 \text{ (calcium sulphate)} \quad (8.13)$$

$$CaSO_4 + 2H_2O \rightarrow CaSO_4 \cdot 2H_2O \text{ (calcium sulphate dihydrate – gypsum)} \quad (8.14)$$

- for $SO_3$:

$$SO_3 + Ca(OH)_2 + H_2O \rightarrow CaSO_4 \cdot 2H_2O \text{ (calcium sulphate dihydrate – gypsum)} \quad (8.15)$$

Conclusion: The efficiency of $SO_2$ removal renders that it is possible to use a 2.70% sulphur fuel, which after scrubbing will be an equivalent of 0.10% sulphur fuel [20]. Electrical power consumption is lower than for wet systems at approximately 0.15-0.20% of the power of the engine being scrubbed. During the dry scrubbing, it is no necessity to have the washwater treatment system and its associated tankage, instrumentation, pipework and controls. However, there is a requirement for used granules storage before disposal ashore.

Calcium hydroxide is strong alkali and it is classed as harmful to eye and skin. The regulations about the usage of $Ca(OH)_2$ are expected to be met in accordance with material safety data sheets, but calcium hydroxide is significantly less hazardous than 50% aqueous NaOH solution used in wet systems. The main problem is to keep granules dry and away from contact with acids.

Table 8.14. Major types of wet scrubbers [22-25]

| General category of scrubbers | Particle capture mechanism | Liquid collection mechanism | Specific types of scrubbers |
|---|---|---|---|
| Performed-spray | impaction | droplets | spray towers, cyclonic spray towers, vane-type cyclonic towers, multiple-tube cyclones |
| Packed-bed scrubbers | impaction | sheets, droplets (moving-bed scrubbers) | standard packed-bed scrubbers, fibre-bed scrubbers, moving-bed scrubbers, cross-flow scrubbers, grid packed scrubbers |
| Tray-type scrubbers | impaction, Brownian diffusion | droplets, jets and sheets | perforated-plate, impingement--plate scrubbers, horizontal impingement-plate (baffle) scrubbers |
| Mechanically aided scrubbers | impaction | droplets and sheets | wet fans |
| Venturi and orifice scrubbers (gas atomized scrubbers) | inertial impaction, Brownian diffusion | droplets | standard venturi scrubbers; variable-throat venturi scrubbers: flooded disc, plump bob, movable blade, radial flow; variable rod orifice scrubbers |

The dry scrubbing is ideally suited for use in conjunction with SCR $NO_x$ reducing system, which, as mentioned, requires hot exhaust gas to gain an operating temperature of above 300°C. Comparison of different $SO_x$ scrubbing technologies is presented in Table 8.13.

*Scrubbing equipment and key operating parameters – wet scrubbing*: There are many different types of wet scrubber vessels. The type of scrubber selected is based on factors such as the gas temperature, pollutants to be removed, space available and desired efficiency. Some types of scrubbers are mainly designed to remove particulate pollutants (e.g. venture scrubbers) and others are designed to mostly remove gaseous pollutants or soluble particulates (e.g. packed towers and tray towers). Spray chambers are often added ahead of the scrubbers to condition the gas by saturating the gas stream, by cooling the gas stream via evaporative cooling or by removing larger particulates. Examples of various categories of wet scrubbers and related types of scrubbers are presented in Table 8.14.

Wet scrubbing is a two-step process, the first step being the capture of the gas stream contaminants in the liquid and the second step being the separation of the scrubbing liquid droplets from the gas stream after leaving the scrubber. This step is important in the ultimate collection of pollutants because poor liquid separation will cause reentrainment of the droplets containing pollutant. There are four basic types of liquid entrainment separators (demisters): mesh-pad, chevron, centrifugal and cyclonic. The mesh-pad and chevron types utilize inertial impaction of the liquid droplets to cause their agglomeration and removal. The centrifugal and cyclonic types utilize centrifugal inertia to collect the liquid droplets. Different types of demisters are presented in Fig. 8.15.

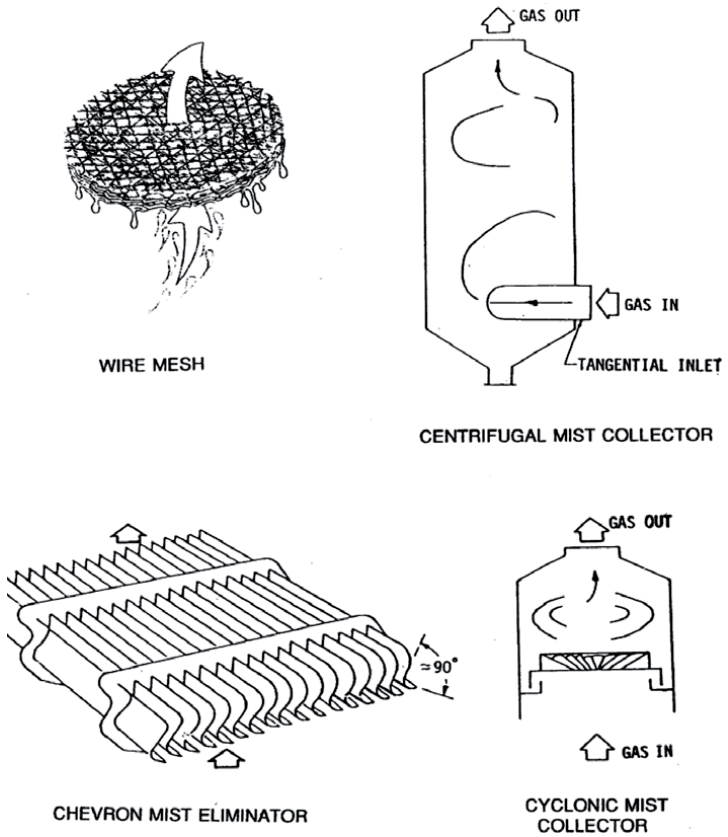


Fig. 8.15. Liquid entrainment separators [23]

A wet scrubbing system could contain more than one different type of scrubber. A typical air pollution control system for a hazardous waste incinerator, for example, might contain a spray chamber or quench chamber to cool and saturate the exhaust gases as they leave the incinerator.

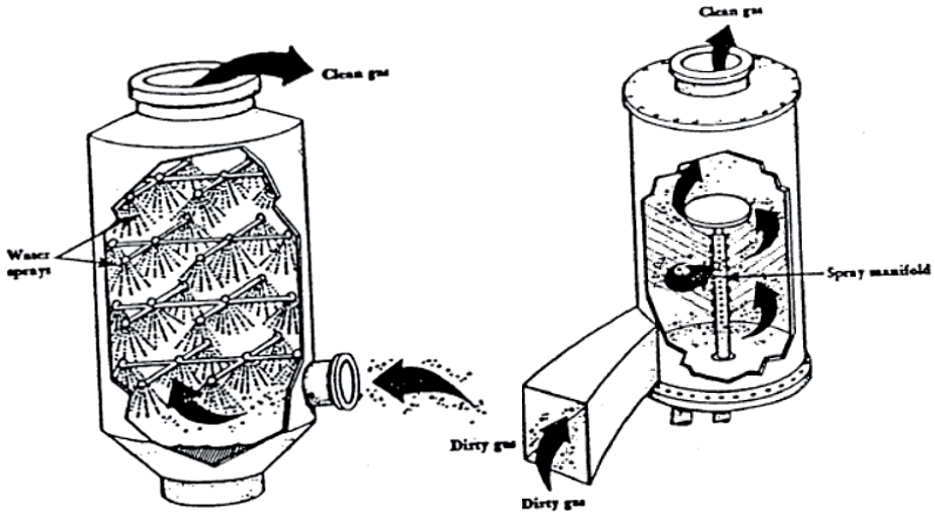


Fig. 8.16. Simple spray tower (left) and cyclonic spray tower (right) [23]

A venturi scrubber would follow the spray chamber to remove most of the particulates before the gas stream enters a packed column for gaseous contaminant removal. Liquid entrainment separators would follow both venturi scrubber and packed column to remove the water droplets and their contained pollutants before going to the next air pollution control stage. In most of these systems, an included draft fan follows the air pollution controls to pull the gases through the control system and force the cleaned exhaust gases through the stack. Different types of scrubbers are presented in Figs. 8.16-8.18.

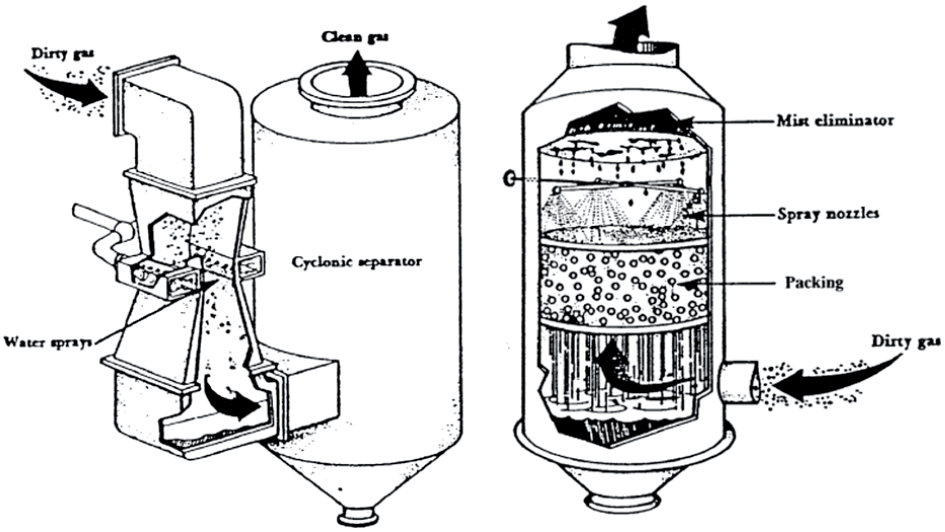


Fig. 8.17. Fixed throat venturi scrubber (left) and packed-bed scrubber (right) [23]

Gas and vapour collection in wet scrubber air pollution control devices is achieved by adsorption. The process of absorption refers to the contacting of the mixture of gases with a liquid so that part of one or more of the constituents of the gas will dissolve in the liquid. The necessary condition for absorption is the solubility of pollutants in the absorbing liquid. The rate of mass transfer of the soluble constituents from the gas to the liquid phase is determined by diffusional processes occurring on each side of the gas-liquid interface. Equilibrium is another important factor to be considered in controlling the operation of absorption systems. The rate at which pollutant will diffuse into an absorbent liquid will depend upon the departure from equilibrium that is maintained. The rate at which the pollutant mass is transferred from one phase to another depends on a so-called mass transfer or rate coefficient, which equates the quantity of mass being transferred with the driving force. As can be expected, this transfer process ceases upon the attainment of equilibrium.

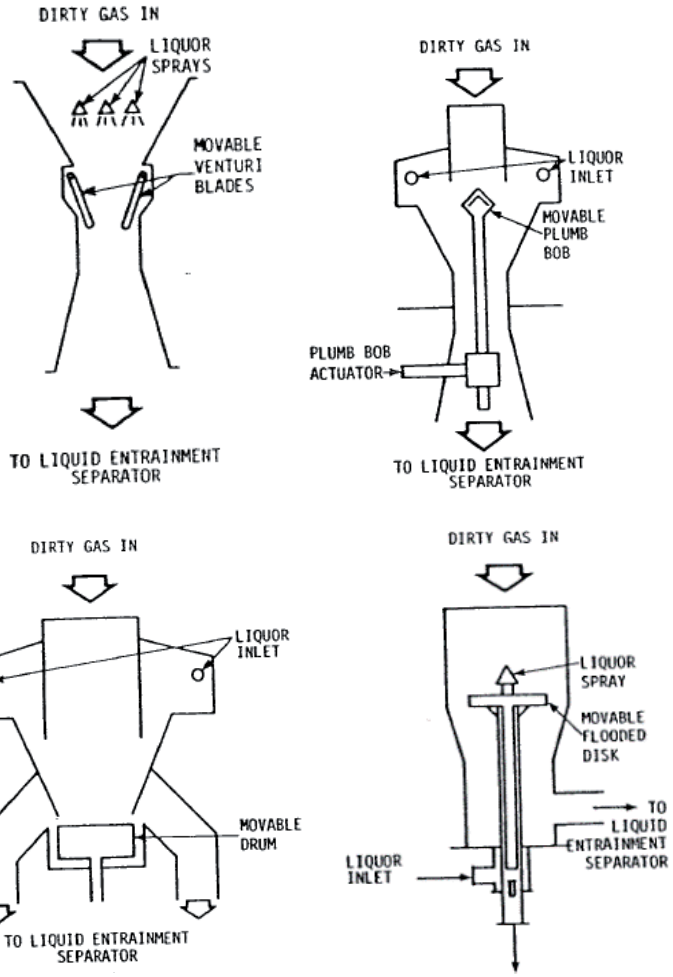


Fig. 8.18. Movable blade venturi (upper left), plump bob venturi (upper right), radial flaw venturi (bottom left), flooded disc venturi (bottom right) [25]

The scrubbing system is composed of exhaust hoods and ducts handling airborne contaminants. Gas pre-treatment equipment may be required for coarse particulate removal and for

cooling before the contaminants enter the scrubber vessel. The contaminant-laden droplets are removed by the entrainment separators. The clean gas is then passed through an induced-draft fan and up the stack. Forced-draft fans upstream of the scrubber are also used.

The key operating parameters affecting the pollution collection are the following [22-25]:

- liquid-to-gas ratio,
- pressure drop,
- velocity/gas flow rate,
- temperature,
- particle size distribution (particulate).

The liquid-to-gas flow rate (L/G) is a calculated value, reflecting the liquid recycling rate for every volume of gas cleaned. High L/G ratios are used for high-temperature gas streams and high-grain loadings. If the L/G ratio falls below the design value, collection efficiency will diminish. Typical liquid-to-gas ratios are presented in Table 8.15.

Table 8.15. Typical L/G ratios for wet scrubbers [25]

| Scrubber type | L/G ratio [gal/1000 $ft^3$] |
|---|---|
| Venturi | 5-8 |
| Cyclonic spray tower | 5-10 |
| Spray tower | 10-20 |
| Impingement-plate | 3-5 |
| Packed-bed | 1-4 |

High L/G ratios are required for high-temperature gas streams to prevent pollutant re-entrainment. When the L/G ratio is not sufficient to saturate the gas stream, pollutant-laden droplets reentering the scrubber from recycled liquors will evaporate (evaporative cooling) and leave the previously captured particulate re-entrained in the gas stream. Should this occur, pre-treatment with clean liquor (for quenching) may be required. The quenching stage saturates the gas stream to minimize evaporation in the scrubbing stage.

The pressure drop across the scrubber includes the energy loss across the liquid-gas contacting section and entrainment separator, with the former accounting for most of the pressure loss. A low-pressure drop scrubber ranges from 2 in $H_2O$ to 10 in $H_2O$, medium from 10 in $H_2O$ to 30 in $H_2O$ and high, 30 in $H_2O$ and above. The higher the pressure drop, the greater the particulate collection efficiency for both particle size and concentration. Typical pressure drops for various types of wet scrubbers are presented in Table 8.16.

Table 8.16. Typical scrubber pressure drops [25]

| Scrubber type | Pressure drop [inches water] |
|---|---|
| Venturi | 10-70 |
| Centrifugal (cyclonic) spray | 1-3 |
| Spray tower | 1-2 |
| Impingement-plate | 1-10 |
| Packed-bed | 1-10 |
| Wet fan | 4-10 |
| Self-induced spray (orifice) | 2-20 |
| Irrigated filter (filter bed scrubber) | 0.2-3 |

The collection of most scrubbers depends upon the velocity of the gas stream through the liquid-contacting section of the scrubber vessel. For particulates, the relative velocity between washing liquids (droplets) and particulates is critical to contaminant collection. In the case of high-energy venturi scrubbers, a velocity of 40 000 ft/min can be delivered. Fine droplet size and high density lead to increased removal efficiency.

When a high-temperature gas stream exhaust enters the scrubber, the volumetric flow rate diminishes accordingly (based on the temperature of the scrubber liquid) because the gas is being cooled by the scrubber liquors. When the system flow rate decreases, the resulting relative velocity may not be sufficient to collect the desired amount of particulate and emissions will increase. For a packed tower or tray tower, low or no gas flow might indicate plugged packing in the absorber, fan problems, duct leaks or an increase in liquid flow to the tower. The increased gas flow might indicate a low liquid flow rate, packing failure or a sudden opening of a system damper.

Wet scrubber inlet and outlet temperatures are also key parameters that should be monitored when controlling gas streams with elevated temperatures. An increase in temperature could indicate a failure of the cooling equipment, which would result in decreased pollutant collection efficiency and perhaps damage to the scrubber.

Performance of a scrubber controlling particulate emissions depends on the gas stream particulate size distribution. Efficient collection of submicron contaminants challenges the application of any type of control system. High-energy venturi scrubbers are designed for submicron contaminant collection. Changes in process equipment or operation can change the particle size distribution and, in turn, impact collection efficiency

$SO_2$ absorption at an industrial scale in maritime sector is most commonly practised in packed or spray towers, which are often combined with venturi nozzle. In the spray tower, the liquid is sprayed into a gas stream by means of a nozzle which disperses the liquid into a fine spray drops. The flow may be countercurrent, as in vertical towers with the liquid sprayed downward, or parallel, as in horizontal spray chambers. These devices have the advantage of low-pressure drop for the gas but also have a number of disadvantages. There is a relatively high pumping cost for the liquid, owing to the pressure drop through the spray nozzle. The tendency for entrainment of liquid by the gas leaving is considerable, and mist eliminators will almost always be necessary.

Unless the diameter/length ratio is very small, the gas will be fairly thoroughly mixed by the spray and full advantage of countercurrent flow cannot be taken. Ordinarily, however, the diameter/length ratio cannot be made very small since then the spray would quickly reach the walls of the tower and become ineffective as a spray.

A packed tower is essentially a piece of pipe set on its end and filled with inert material or ‘tower packing’. Liquid poured into the top of the tower trickles down through the packing, gas pumped into the bottom of the tower flows countercurrently upward. The intimate contact between gas and liquid achieved in this way effects the gas abortion. Analysing the packed tower involves both mass transfer and fluid mechanics. The mass transfer, detailed in the following section, determines the height of the packed tower. This mass transfer is described as molar flows, partly because of the chemical reactions that often occur. The fluid mechanics determines the cross-sectional area of the packed tower. The fluid mechanics is described as mass flows, a consequence of the physics that control the process.

The fluid mechanics in the packed tower is dominated by the inert material in the packed tower. This material can be small pieces dumped randomly or larger structures carefully stacked inside the tower. Random packing is cheaper and more common whereas structured packing is more expensive but more efficient. Different types of packings are presented in Figs. 8.19 and 8.20.

Generally, random packings offer larger specific surface area (and larger gas pressure drop) in the smaller sizes, but they cost less per unit volume in the larger sizes. As a rough guide, packing sizes of 25 mm or larger are ordinarily used for gas rates of 500 $ft^3$/min (0.25 $m^3$/s), 50 mm or larger for gas rates of 2000 $ft^3$/min (1 $m^3$/s). During installation, the packings are poured into the tower to fall random and in order to prevent breakage of ceramic or carbon

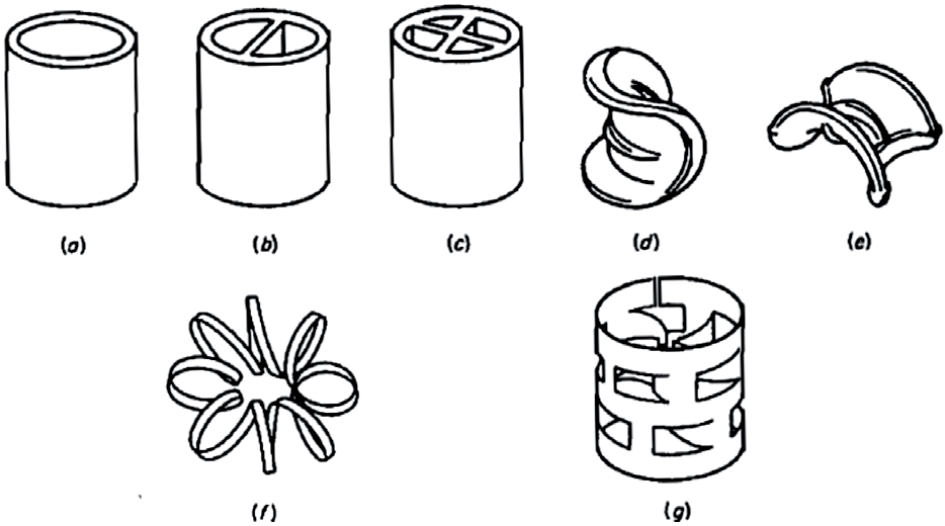


Fig. 8.19. Some random tower packings: (a) Raschig rings, (b) Lessing rings, (c) partition ring, (d) Berl saddle, (e) Intalox saddle, (f) Tellerette, (g) pall ring [23]

packings, the tower may first be filled with water to reduce the velocity of fall. The schematic diagram of a packed gas absorption tower is presented in Fig. 8.21.

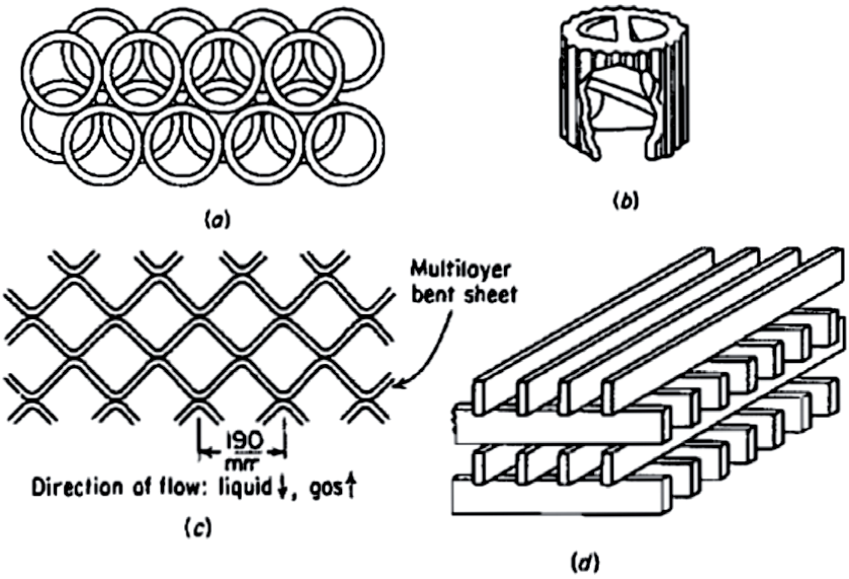


Fig. 8.20. Regular or stacked packings: (a) Raschig rings, stacked staggered; (b) double spiral ring; (c) section through expanded-metal-lath packing; (d) wood grids [23]

The regular packings offer the advantages of low-pressure drop for the gas and greater possible fluid flow rates, usually at the expense of more costly installation than random packing.

While using packed gas absorption tower another crucial issue is an adequate initial distribution of the liquid at the top of the packing. This phenomenon is presented in Fig. 8.22.

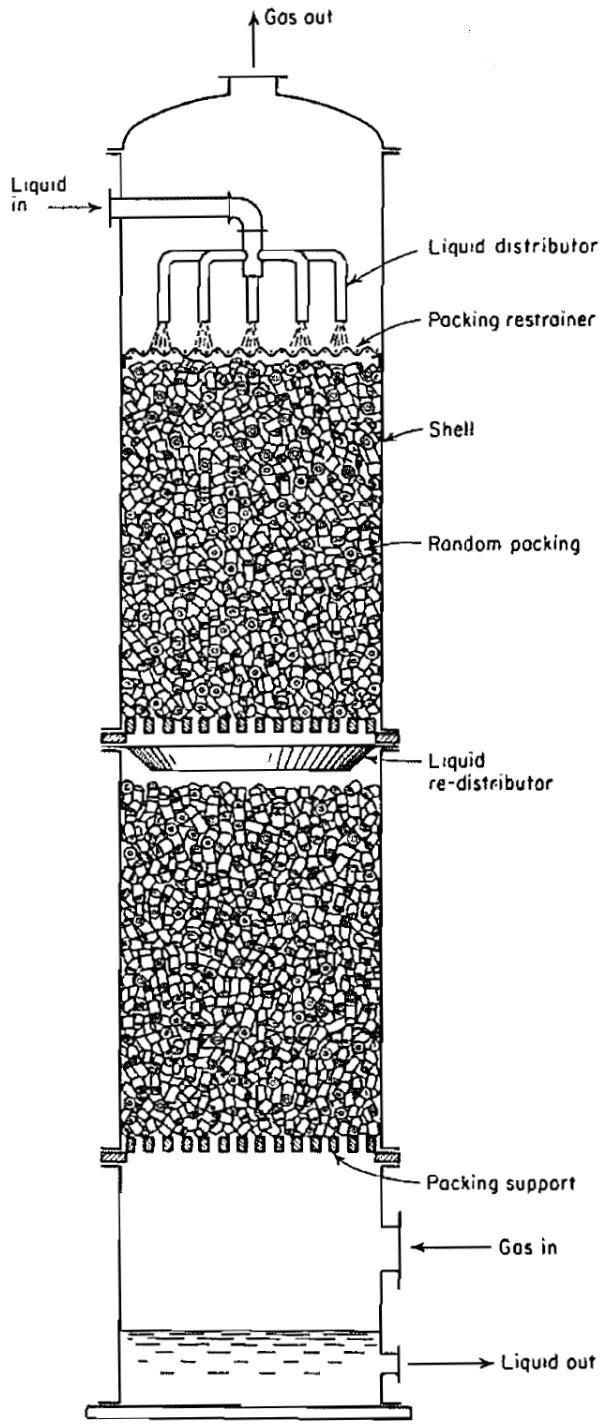


Fig. 8.21. The schematic diagram of a packed gas absorption tower [23]

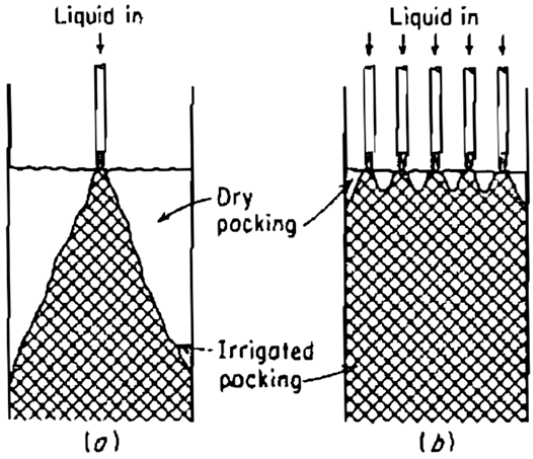


Fig. 8.22. Liquid distribution and packing irrigation: (a) inadequate, (b) adequate [23]

As dry packing is completely ineffective for mass transfer, various devices are used for liquid distribution. Spray nozzles generally result in too much entrainment of liquid in the gas to be useful. In the small tower, it is possible to use a ring of perforated pipe. For larger diameters of distributor, many other arrangements are available. It is generally considered necessary to provide at least five points of introduction of liquid for every 1 $ft^2$ (0.1 $m^2$) of tower cross-section for the large tower ($d \geq 4$ ft (1.2 m)) and a greater number for smaller diameters. In the case of random packings, the packing density, i.e. the number of packing pieces per unit volume, is ordinarily less in the immediate vicinity of the tower walls and this leads to a tendency of the liquid to segregate toward the walls and the gas to flow in the centre of the tower (channelling). This tendency is much less pronounced when the diameter of the individual packing pieces is smaller than at least one-eighth of the tower diameter, but it is recommended that, if possible, the ratio 1:15. Even so, it is customary to provide for redistribution of the liquid at intervals varying from 3 times to 10 times the tower diameter, but at least every 6 m or 7 m. Knitted mesh packings placed under a packing support make good redistributors.

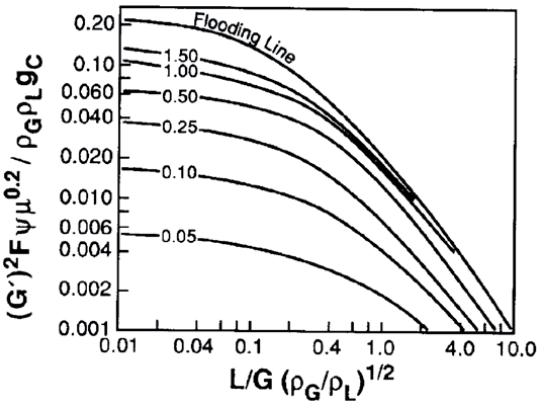


Fig. 8.23. Correlation for estimating tower cross-sectional area: gas flux G' (given in $lb/ft^3/s$), the densities $q_G$ and $q_L$ (given in $lb/ft^3$), the velocity $\mu$ is that of the liquid (expressed in cP), $\Psi$ is the ratio of the density of water to the density of the liquid, the gravitational constant $g_C$ is 32.2 and the packing factor F is roughly inversely proportional to the packing's size. Values for F for common packings can be found in the literature [23]

Another important parameter to go over is to use liquid flows that are high enough to avoid channelling and achieve loading. It is also expected to use gas flows that are low enough to avoid flooding. Such calculation can be determined using proper correlations for estimating tower cross-sectional area. The example is presented in Fig. 8.23.

*Scrubbing equipment and key operating parameters – dry scrubbing*: This process involves the separation of a substance from one phase, accomplished by the accumulation of that substance at the surface of another phase. Two types of adsorption are possible. The first, physisorption, is a physical process that occurs below 200ºC. The material is adsorbed due to molecular interactions between the adsorbent and the adsorbate. The typical heat of physisorption is 5-10 kcal/mol. The second type of adsorption, chemisorption, is a chemical process where the adsorbent adheres to the adsorbate through a chemical bond and that is the phenomenon typically used during the onboard dry scrubbing. Adsorption occurs due to the formation of chemical compounds. Chemisorption bonds can be weak, ranging from 15-40 kcal/mol, or strong, which can be greater than 50 kcal/mol. The dry scrubbing process is accomplished in column contact adsorbers, which can operate as a fixed bed, or as a moving or pulsed bed. Fixed bed operation is the oldest form of column contact adsorption. A bed of adsorbent is held in place inside the column, and the gas to be treated flows over, through and around it. The bed must be taken offline to replace or regenerate the used granules. In a moving or pulsed bed adsorber, untreated gas enters the adsorber from the bottom and flows up the column. At the same time, fresh adsorbent enters the adsorber from the top of the column and exits out the bottom. The exhausted adsorbent is continually removed, while fresh adsorbent is continually added, allowing for more efficient operation. Under fixed bed operation, adsorption columns may be arranged in series or parallel and may be run in either up flow or down flow modes. Pulsed bed operations are restricted to the up flow mode of operation. Additional equipment is required to recycle the adsorbent, which allows for a more efficient operation. In general, smaller adsorbents have a larger surface area and allow for more contact between the packing and absorbate than larger adsorbents. Therefore, small adsorbents are desirable and enhance the adsorption rate. However, if adsorbent particles are too small they may restrict the proper flow of fluid through the column. Various kind of contact columns are presented in Figs. 8.24 and 8.25.

While considering the adsorption, there are many key parameters, which can have a significant influence on the process efficiency. Certain general properties of adsorbents are involved in all adsorber design calculations. The necessary properties are as follows [22, 23, 26, 27]:

- isotherms (or other equilibrium data),
- densities and void fractions,
- kinetics,
- fluid-to-particle mass transfer coefficient,
- pressure drop,
- temperature,
- nature of adsorbent.

Isotherms: Adsorption equilibrium data are commonly gathered at a fixed temperature and plotted or tabulated as capacity or loading versus the fluid-phase concentration (or partial pressure for gases and vapours). In that format, the data comprise an isotherm. As mentioned earlier, adsorption capacity governs the capital cost because it dictates the amount of adsorbent required, which also fixes the volume of the adsorber vessels. Figure 8.26 shows classifications suggested by Brunauer, Deming and Teller (1940).

Types I, II, and IV represent ‘favourable’ equilibrium (concave downwards), while types III and V represent ‘unfavourable’ equilibrium (concave upwards). Type VI has two regions that are favourable and two that are unfavourable. Furthermore, types IV and V exhibit hysteresis, which occurs when desorption occurs along a different path than adsorption, e.g. as a result of liquid-filled pores, and implies that uptake and release may be slow. For all that, only type I of adsorbents, over the range of relevant conditions, are generally suited to cyclic applications.

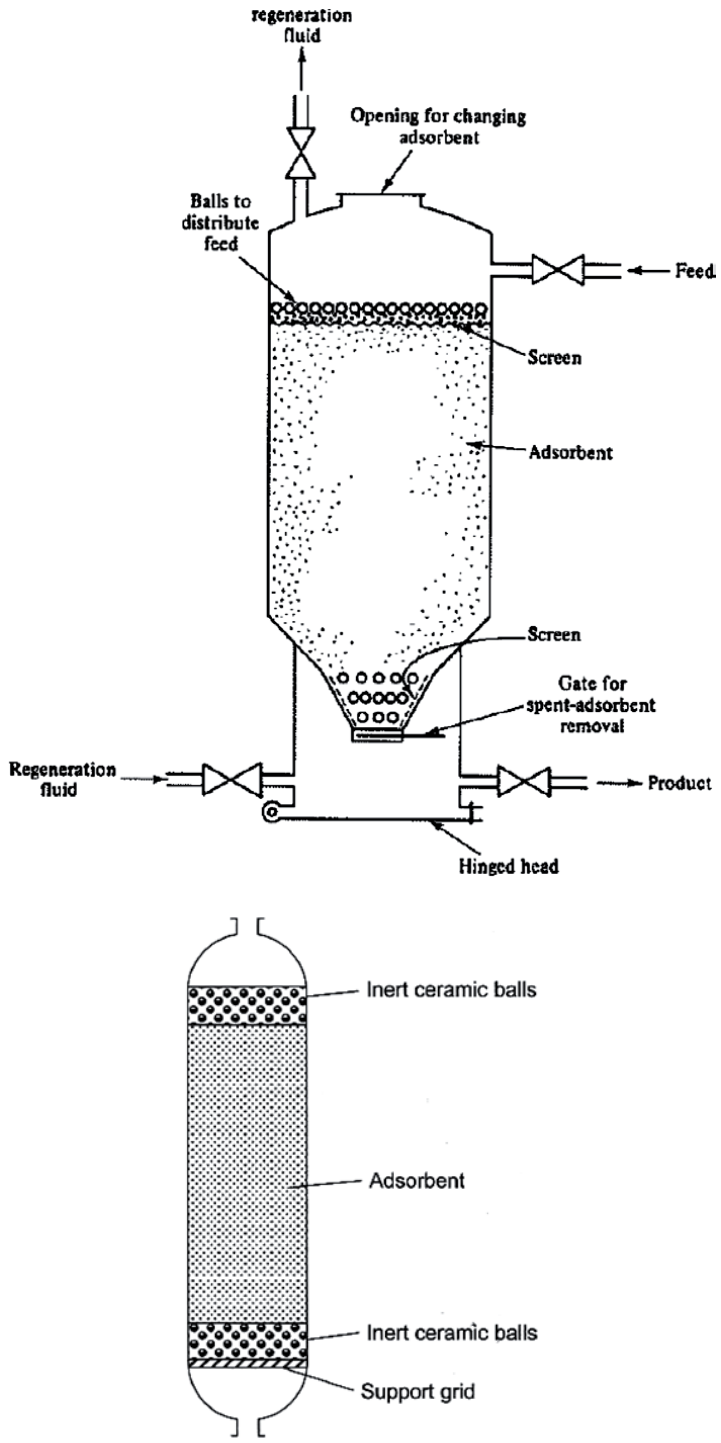


Fig. 8.24. Fixed bed adsorbers

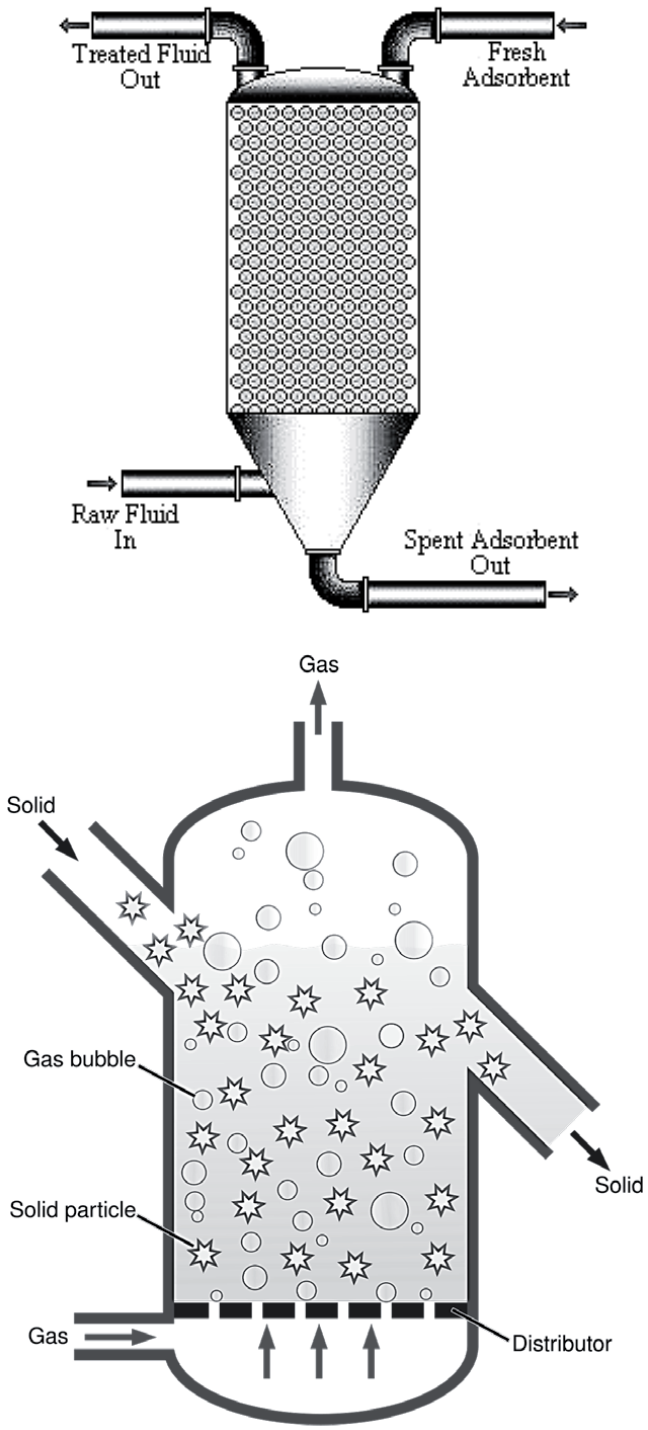


Fig. 8.25. Pulsed bed (upper) and moving (fluidized) bed (bottom) adsorbers [23]

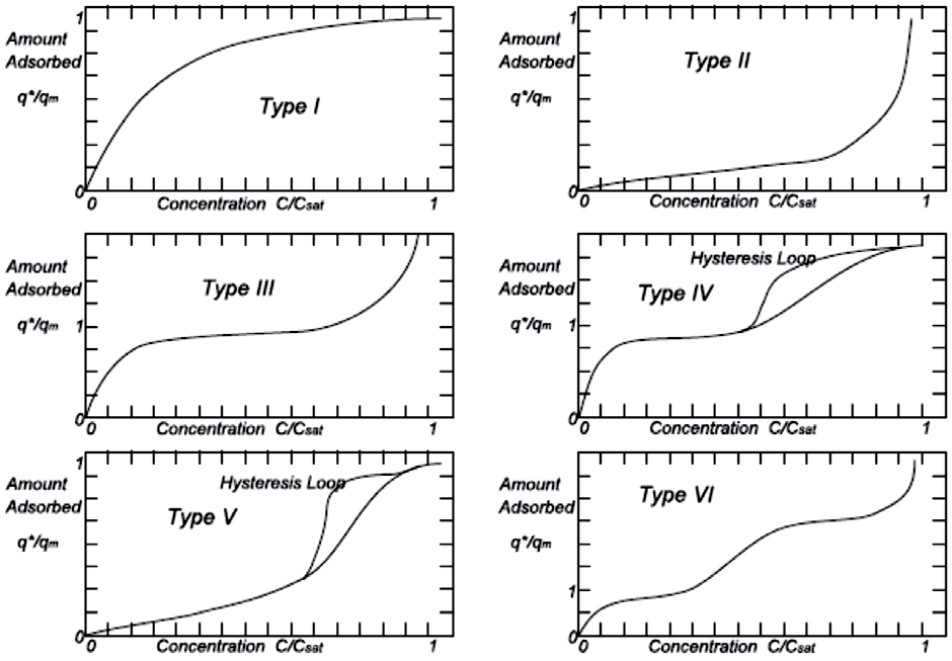


Fig. 8.26. Isotherm classifications (1940) [23]

Linear forms of the isotherm models are widely adopted to determine the isotherm parameters or the most fitted model for the adsorption system due to the mathematical simplicity. The linear forms of the Langmuir, Freundlich and Dubinin-Radushkevich isotherm models are given in Table 8.17.

Table 8.17. Linear forms of the isotherm models [28]

| Isotherm models | Linear form |
|---|---|
| Langmuir | (I) $\frac{C_e}{q_e} = \frac{1}{q_m \cdot K_L} + \frac{C_e}{q_m}$<br>(II) $\frac{1}{q_e} = \left[\frac{1}{q_m \cdot K_L}\right] \cdot \frac{1}{C_e} + \frac{1}{q_m}$<br>(III) $q_e = q_m - \left[\frac{1}{K_L}\right] \cdot \frac{q_e}{C_e}$<br>(IV) $\frac{q_e}{C_e} = K_L \cdot q_m - K_L \cdot q_e$ |
| Freundlich | $\ln q_e = \ln KF + \frac{1}{n} \cdot \ln C_e$ |
| Dubinin-Radushkevich | $\ln q_e = \ln q_s - K_D \cdot \varepsilon^2$ |

Densities and void fractions: Three densities are relevant: bulk, particle, and solid, represented by $q_B$, $q_P$, and $q_S$, respectively. Likewise, there are four pertinent void fractions, $\varepsilon_B$, $\varepsilon_P$, $\varepsilon_S$, and

ε. The first three have the same associations as the densities having the same subscripts. The last one, ε, is the overall void fraction in the bed of adsorbent. They are related as [27]:

$$q_B = (1 - \varepsilon_B)\, q_P = (1 - \varepsilon_B)(1 - \varepsilon_P)\, q_S = (1 - \varepsilon)\, q_S$$

The bed or bulk density is the mass of adsorbent in a specific volume. This can be measured simply using a graduated cylinder. Particle density is the mass of adsorbent per volume occupied by the particle. This is accurately and easily measured for true cylindrical pellets and beads, but is more difficult for distorted shapes and granular materials, though proprietary methods exist for obtaining accurate values even for those. Solid density is the mass of the adsorbent per volume occupied by the particle, but with the pores deducted. It is measured by immersing a known amount of adsorbent in a liquid of known density and known total volume, then measuring the total mass. In this case, the characteristics of the liquid may dramatically affect the resulting value, because the liquid molecules may or may not be able to penetrate certain pores in a reasonable time due to steric reasons or surface tension. The greater the fraction of pores penetrated, the greater the apparent solid density. Densities and void fractions are important because the most isotherm data are published as loading per unit mass, which is fine for determining the total adsorbent cost since prices are quoted per unit mass. Conversely, to determine the vessel dimensions from the necessary amount of adsorbent, or vice versa, $q_B$ is required. For pressure drop calculations, the relevant void fraction is $\varepsilon_B$ since the fluid in the pores of the adsorbent is usually considered to be immobile. In contrast, for material balance equations, the fluid in the pores of the adsorbent cannot be ignored, so the relevant void fraction is ε.

Fluid-to-particle mass transfer coefficient: The fluid-to-particle mass transfer coefficient (k) is mostly governed by the fluid properties (density, q, viscosity, μ, and diffusivity, $D_{AB}$) and superficial velocity ($v_s = Q/A_{cs}$, where Q is the volumetric flow rate and $A_{cs}$ is the cross-sectional area of the empty bed). Generally, a large value of k is good, but not at the expense of high velocity $v_s$, not because of pumping or compression costs, but because the time of exposure is inversely proportional to velocity. Thus, the faster the fluid is flowing, the less time the adsorbent has to respond.

Pressure drop: Most adsorbers are designed to operate with the relatively low-pressure drop, because large particles are used whenever possible, and because the velocity is typically low to allow equilibration of the fluid with the adsorbent. In addition, a small $L/d_{bed}$ (length/diameter) leads to the low-pressure drop. Conversely, achieving good flow distribution and low dead volume implies a large $L/d_{bed}$. Generally, pipes, valves, and fittings pose as much of a flow restriction as the pressure drop in the bed of adsorbent.

Kinetics: Mass transfer kinetics is a catch-all term related to intraparticle mass transfer resistance. It is important because it controls the cycle time of a fixed bed adsorption process. Fast kinetics implies a sharp breakthrough curve, while slow kinetics leads to a distended breakthrough curve. The effect of a distended breakthrough curve can be overcome by adding adsorbent at the product end, or by increasing the cycle time (which reduces the throughput per unit of adsorbent). Both of these options increase the amount of adsorbent required. To compensate for slow diffusion, it is also possible to use small particles, but there is a corresponding sacrifice due to increased pressure drop.

Temperature: Since adsorption is an exothermic process, the concentration of adsorbed gas decreases with increasing temperature.

Nature of adsorbents: Both the chemical and physical properties of the adsorbent must be considered. Chemical properties that influence on adsorbent design include the degree of ionization of the surface, functional groups present on the surface, and the degree to which these chemical properties vary with process parameters and by contact with the gas. Adsorbent solids are usually used in granular form, varying in size from roughly 12 mm in diameter to as small as 50 μm. The solids must possess certain engineering properties depending upon the application to which they are put. If they are used in a fixed bed through which a liquid or gas is to flow, for example, they must not offer too great pressure drop for flow nor must they easily be carried away by the flowing stream. They must have adequate strength and hardness so as not to be reduced in size during handling or crushed in supporting their own weight in beds of the

required thickness. If they are to be transported frequently in and out of bins, they should be free-flowing. Large surface per unit weight seems essential to all useful adsorbents (100 $m^2/g$ to over 2000 $m^2/g$). Particularly, in the case of gas adsorption, the significantly surface is not the gross surface of the granular particles which are ordinarily used but the very much larger surface of the internal pores of particles. The pores are usually very small, sometimes of the order of a few molecular diameters in width, but their large number provides an enormous surface for adsorption.
The general adsorber design considerations are presented in Table 8.18.

Table 8.18. General adsorber design considerations [27]

| Basic adsorbent properties | Application considerations | Equipment/flowsheet |
|---|---|---|
| A. Isotherm data | A. Operating conditions | A. Contactor type |
| 1. uptake/release measurements | 1. flow rate | 1. fixed: axial/radial flow |
| 2. hysteresis observed | 2. feed and product concentrations | 2. pulsed/fluidized bed |
| 3. pre-treatment conditions | 3. pressure/temperature | |
| 4. ageing upon multiple cycles | 4. desired recovery | B. Geometry |
| 5. multicomponent effects | 5. cycle time | 1. number of beds |
| | 6. contaminants | 2. bed dimensions |
| B. Mass transfer behaviour | | 3. flow distribution |
| 1. interface character | B. Regeneration technique | 4. dead volumes |
| 2. intraparticle diffusion | 1. thermal: steam/hot fluid/kiln | |
| 3. film diffusion | 2. chemical: acid/base/solvent | C. Column internals |
| 4. dispersion | 3. pressure shift | 1. bed support/ballast |
| | 4. regenerant/adsorbate recovery or disposal | 2. flow distribution |
| C. Particle characteristics | | 3. insulation |
| 1. porosity | | |
| 2. pore size distribution | C. Energy requirements | D. Miscellaneous |
| 3. specific surface area | | 1. instrumentation |
| 4. density | D. Adsorbent life | 2. materials of construction |
| 5. particle size distribution | 1. attrition/swelling | 3. safety/maintenance |
| 6. particle shape | 2. ageing/fouling | 4. operation, start-up, shut-down |
| 7. abrasion resistance | | |
| 8. crush strength | | |
| 9. composition/stability | | |
| 10. hydrophobicity | | |

**$NO_x$ pollution control**

There are different types of nitrogen oxides, existing in the environment: $N_2O$, NO, $NO_2$, $N_2O_3$, $N_2O_4$, $NO_3$, and $N_2O_5$, but the abbreviation $NO_x$ usually regards nitrogen monoxide (NO) and nitrogen dioxide ($NO_2$), which are considered toxic. Approximately 95% of $NO_x$ emitted from incineration process is insoluble and non-reactive NO and 5% – $NO_2$. NO is less toxic, notwithstanding it is also unstable but it reacts readily with oxygen through photochemical oxidation to form $NO_2$. These oxides are formed in the cylinder during combustion in two different ways:

- Thermal $NO_x$ – the main mechanism by which $NO_x$ is produced. Nitrogen oxides are formed in high-temperature reactions between $N_2$ and $O_2$ in the charge air (this process depends on temperature, available oxygen and exposure time of the combustion gases to high temperature).

- Fuel $NO_x$ – nitrogen oxides are formed through the oxidation of the nitrogen compounds predominantly contained in residual fuel oils and biofuels (this process depends on the available oxygen, the quantity of fuel-bound nitrogen and, to less extent, combustion temperature and the nature of the nitrogen compounds).

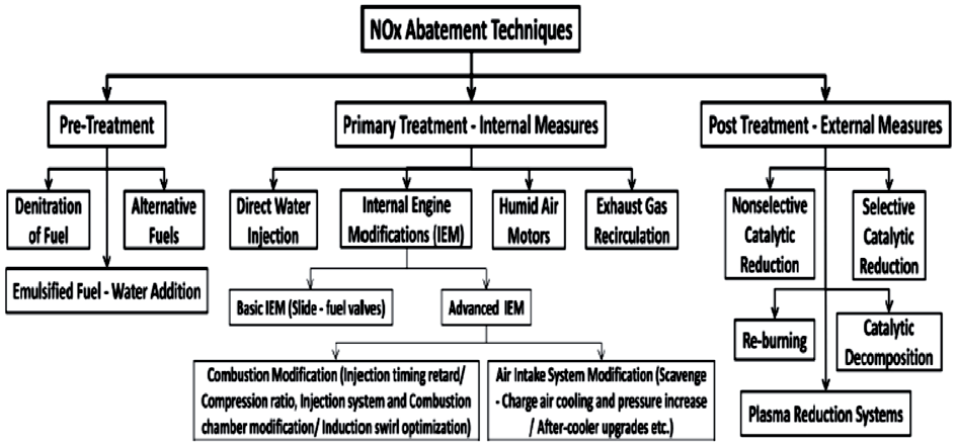


Fig. 8.27. $NO_x$ abatement techniques [29, 30]

Dealing with the emission of nitrogen oxides involves different ways of their reduction. There are various methods for reducing $NO_x$ emissions (Fig. 8.27), depending on cost and effectiveness (Table 8.19). It is possible to distinguish [3, 31]:

- Primary $NO_x$ control – aims to reduce the formation of nitric oxide at the source. It may be achieved through engine design and operational adjustments of parameters and components such as fuel injection (pressure, timing, rate, nozzle configuration), valve timing, charge air (temperature, pressure) and compression ratio. Other at-engine measures can reduce local temperatures and oxygen content in the combustion zone through various wet technologies:

Table 8.19. The $NO_x$ reduction potential of different methods [29]

| $NO_x$ abatement techniques | $NO_x$ reduction |
|---|---|
| Alternative fuels | 50-60% |
| Emulsified fuel – water addition | 50-60% |
| Basic IEM – slide fuel valves | 20% |
| Injection timing retardation | 30% |
| Compression ratio modification | 10-30% |
| Injection system modification | 30% |
| Scavenge/charge air cooling | 14% |
| Scavenge/charge air pressure increase | 10-40% |
| Direct water injection | 40-60% |
| Humid air motor | 70-80% |
| Exhaust gas recirculation | 80-98% |
| Selective catalytic reduction | 80-99% |

water-in-fuel (WIF), fuel water emulsion (FWE), direct water injection to the combustion space (DWI), water sprays into the charge air (humid air motor – HAM) or scavenging air moistening (SAM). They can be only used to meet Tier II limits. The nature of such processes can also leads to the large power losses.

- Post-combustion abatement – exhaust gas is treated to remove $NO_x$. The most commonly used method is the selective catalytic reduction (SCR). Other ways such as selective non-catalytic reduction (SNCR), exhaust gas recirculation (EGR), non-thermal plasma (NTP) and lean $NO_x$ traps (LNTs) have been also investigated by scientists.

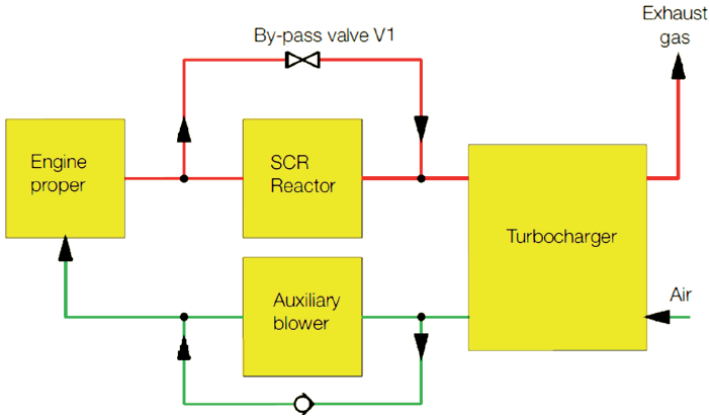


Fig. 8.28. SCR flowchart [21]

*Selective catalytic reduction*: $NO_x$ is converted into nitrogen and water by spraying urea or ammonia into the gases before they pass through a catalytic converter. This installation is able to reduce $NO_x$ emissions by 80-90% to below 2 g/kWh. Reduction costs are generally below 600 EUR/ton of $NO_x$ reduced, lower if the equipment can be installed while the ship is being built [31]. When retrofitted, SCR system replaces the exhaust silencers. SCR systems are commonly fitted to four-stroke medium-speed engines. To date, a very small number of two-stroke engines have been equipped with SCR systems, but it is planned to be done en masse for MAN Diesel & Turbo marine engines [3, 21]. The SCR $NO_x$ reducing system is presented in Figs. 8.28 and 8.29. The chemical reactions are as follows:

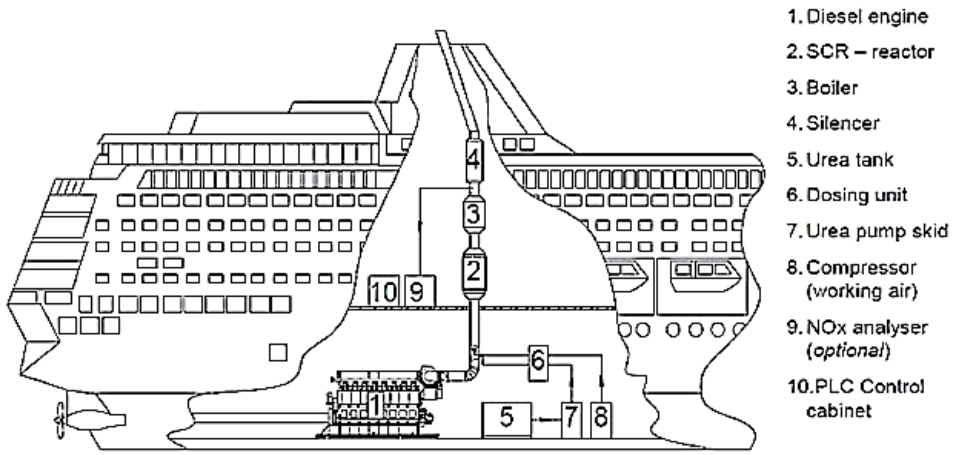


Fig. 8.29. SCR $NO_x$ reducing system – Yara Marine Technologies [32]

- Urea decomposition before the catalyst:

$(NH_2)_2CO$ (urea) → $NH_3$ (ammonia) + HNCO (isocyanic acid) (8.16)

$HNCO + H_2O \rightarrow NH_3 + CO_2$ (8.17)

- $NO_x$ reduction at the catalyst:

$4NO + 4NH_3 + O_2 \rightarrow 4N_2 + 6H_2O$ (8.18)

$2NO + 2NO_2 + 4NH_3 \rightarrow 4N_2 + 6H_2O$ (8.19)

$6NO_2 + 8NH_3 \rightarrow 7N_2 + 12H_2O$ (8.20)

Reaction (8.18) shows the main SCR reaction as nitric oxide dominates in the exhaust. The reaction (8.19) occurs at the fastest rate up to the $NO_2$: NO ratio of 1:1. Nevertheless, at higher ratios, the excess $NO_2$ reacts slowly – reaction (8.20).

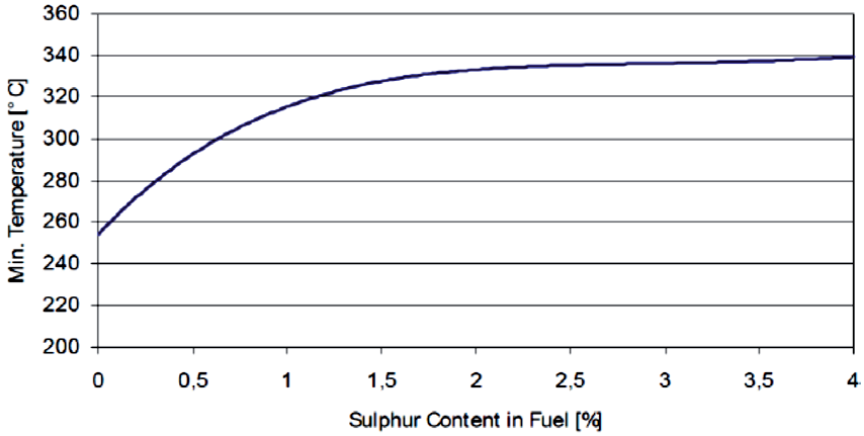


Fig. 8.30. Dependence between the minimum temperature required for the catalyst and the sulphur content in fuel

SCR $NO_x$ reduction system usually consists of a pumping unit (for transfer of urea solution from storage), a reactor housing containing replaceable catalyst blocks, a urea dosing unit, a mixing duct with urea injection point, a soot/ash cleaning and control systems. If there is a necessity to fit the SCR system to two-stroke low-speed engines it is also required to bypass the reactor during various engine operating modes. The position of the reactor containing the catalyst is related to the exhaust temperature. That is the reason for installing marine SCR systems on four-stroke engines, as there is a sufficiently high exhaust temperature. The recommended temperature is over 300°C, but below 500°C to prevent thermal damage to the catalyst. Dependence between the minimum temperature required for the catalyst and the sulphur content in fuel is shown in Fig. 8.30.

It is possible to run at lower temperatures, but only after the reducing of the sulphur content in the fuel. Another crucial issue is to completely mix urea with the exhaust gas before entering SCR reactor. A typically used urea's concentration is a 40% solution, which is injected as a fine spray into the mixing duct before the catalyst by means of compressed air. The amount of $NH_3$ injected into the exhaust gas is controlled by a process computer dosing the $NH_3$ in proportion to the $NO_x$ produced by the engine as a function of the engine load. The relationship between the $NO_x$ produced and the engine load is measured during test runs on the engine testbed. The relationship obtained is programmed in the process computer and used for the feed-forward control of the $NH_3$ dosage. The ammonia dosage is subsequently adjusted for bias by a feedback system on the basis of the measured $NO_x$ outlet signal [31].

As the effective dispersion of the urea in the exhaust stream is pivotal to efficient SCR performance, suitable injection nozzles, atomizing air, high-pressure injection (typically 25 bar), duct design, or a combination of all four are required. The main reason for using urea instead of ammonia is that urea is classed as non-hazardous and can be stored in existing tanks

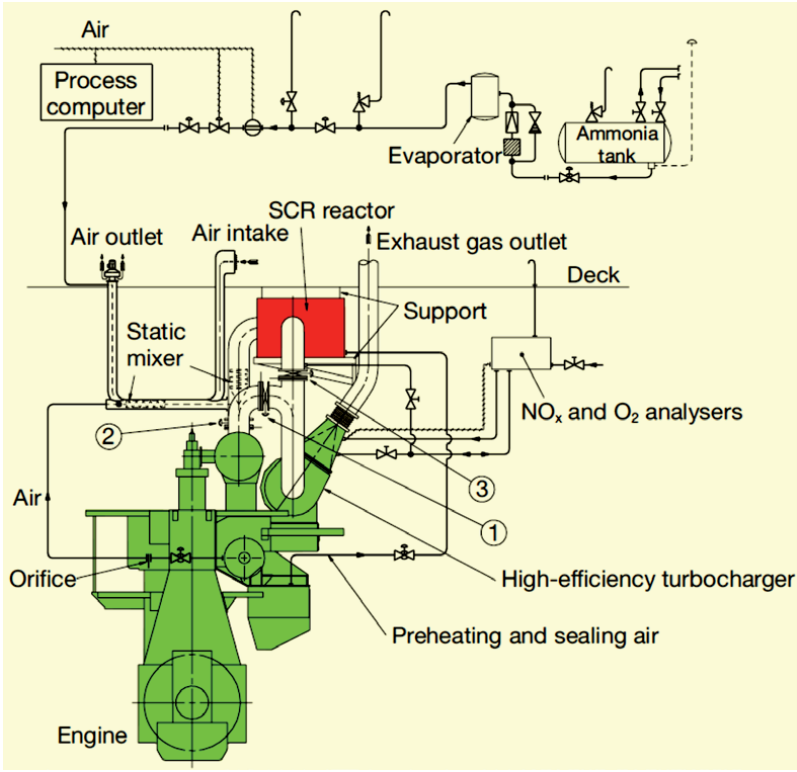


Fig. 8.31. SCR system layout [21]

if epoxy-coated whereas ammonia is both toxic and corrosive. The catalysts used in typical marine SCR system are made up of porous titanium dioxide ($TiO_2$), vanadium pentoxide ($V_2O_5$) or tungsten trioxide ($WO_3$) [3, 31]. Figure 8.31 shows the actual system layout of the 6S50MC engine [21] and Table 8.20 presents the SCR current reference list for MC type engines [17].

Table 8.20. SCR reference list for MC type engines [17]

| No | Engine | Application | Function | Efficiency |
|---|---|---|---|---|
| 1 | 6S50MC | ship | $NO_x$ reduction | 93-95% |
| 2 | 6S50MC | ship | $NO_x$ reduction | 93-95% |
| 3 | 6S50MC | ship | $NO_x$ reduction | 93-95% |
| 4 | 6S50MC | ship | $NO_x$ reduction | 93-95% |
| 5 | 9K80MC-GI-S | power plant | $NO_x$ reduction | up to 98% |
| 6 | 4L35MC-S | power plant | $NO_x$ reduction | > 93% |
| 7 | 2 × 7K60MC-S | power plant | $NO_x$ reduction | > 93% |
| 8 | 6S35MC | ship | $NO_x$ reduction | > 93% |

High-efficiency turbochargers have to be used. The measured exhaust gas temperature is slightly higher than for engines without SCR system because of the ammonia/urea heat release

in the SCR process. The SCR reactor is designed as a semi-rectangular pressure vessel for horizontal or vertical installation and flow. As an example, the main dimensions (excluding support structure and insulation) for a 11K90MC engine are presented in Table 8.21.

Table 8.21. Main dimensions of 11K90MC engine [21]

| Dimension | Value |
|---|---|
| Diameter [m] | 2.4 |
| Height [m] | 4.5 |
| Length [m] | 15 |
| Weight, including catalyst [tons] | 42 |

The design and dimensions of an SCR reactor are influenced by the exhaust gas flow, the exhaust gas temperature window, and the $NO_x$ reduction rate. The optimum and most common solution, therefore, is that the SCR reactor is tailor-made for a specific installation and it is, of course, more convenient to build-in the SCR during the construction of the ship. Retrofit is also possible. The space requirement for an SCR unit in the engine room is considerable, on top of which the piping and the mixer between the engine and the SCR catalyst also require a lot of space, so the designer's task is to make the SCR system as compact as possible while, at the same time, ensuring easy access for maintenance and operation. As can be seen in Fig. 8.32 there are a number of alternative designs of SCR reactors. Location of the SCR module in the four-stroke engine and two-stroke engine is presented in Fig. 8.33.

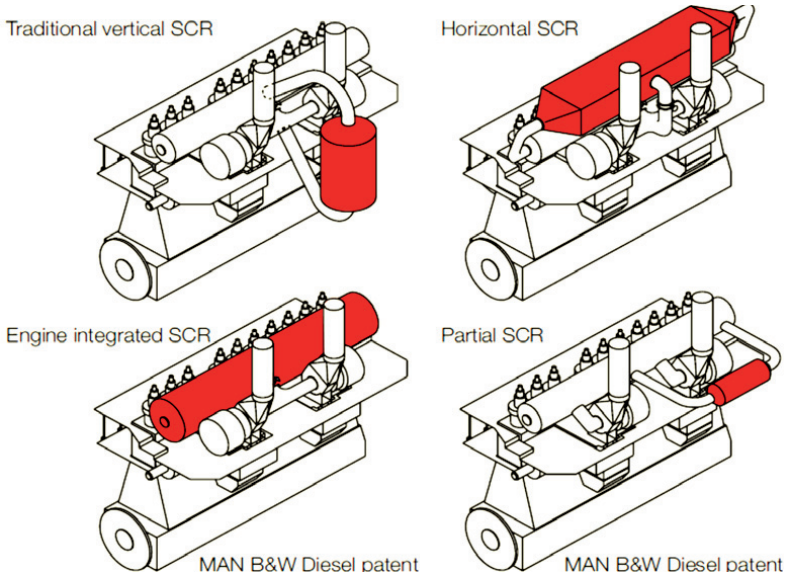


Fig. 8.32. SCR configurations [17]

If ammonia is used as the medium for denitrification, the tank should be located on deck. In the case of urea, we recommend that a tank in the hull structure be used, to lower the cost. Having such a tank in the hull will also minimize the space requirements, compared with the installation of a tank on deck. If it is not possible to find an appropriate tank on board, the tank could be built into containers.

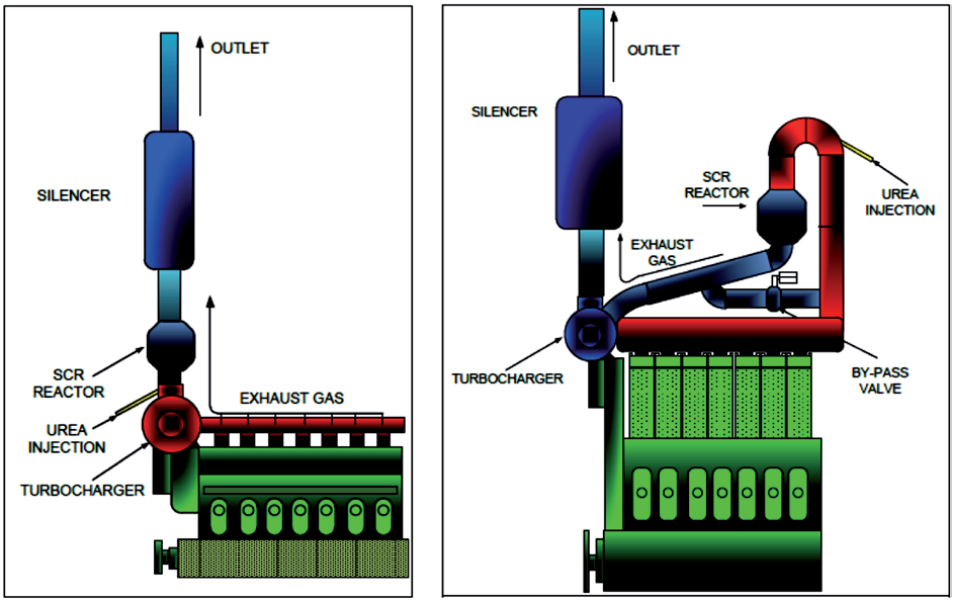


Fig. 8.33. Location of the SCR module in the four-stroke engine (left) and two-stroke engine (right)

As mentioned before, retrofit is also possible and after the test trial, the vessel can operate with reduced $NO_x$ emission. For example, the reduction of $NO_x$ emission for an exemplary 6S35MC engine can be obtained between 40-100% engine load, when running on HFO with a sulphur content of up to 2.4%. Below 40% engine load, the injection of urea is stopped due to low exhaust gas temperatures. The risk of creation of ammonia sulphate is thereby avoided. Performance data are shown in Table 8.22, and the actual system layout is shown in Fig. 8.34.

Table 8.22. Engine performance data [17]

| Parameter | Prior to installation of SCR | DeNO$_x$ mode with injection of urea |
|---|---|---|
| Engine load | 75.8% | 77% |
| Turbochanger | 15 600 rpm | 15 700 rpm |
| T/C inlet temperature | 440°C | 440°C |
| Scavange air pressure | 2.02 barg | 2.10 barg |
| $NO_x$ emission | 1 100 ppm | 132 ppm (< 2 g/kWh) |
| Urea consumption | - | 62 L/h |

For the two-stroke engines, too low exhaust gas temperature after the turbine has called for a solution where the SCR may be placed on the high-pressure side of the turbine. The efficiency of $NO_x$ removal in relation to the flue gas temperature is presented in Fig. 8.35.

Depending on the engine load, this makes it possible to obtain exhaust gas temperatures that are between approximately 50°C and 175°C, higher than after the turbine. The comparison is presented in Table 8.23.

This means that the SCR system works according to the following: When $NO_x$ reduction is needed (inside ECA), the exhaust gas is guided to the SCR according to the flow direction.

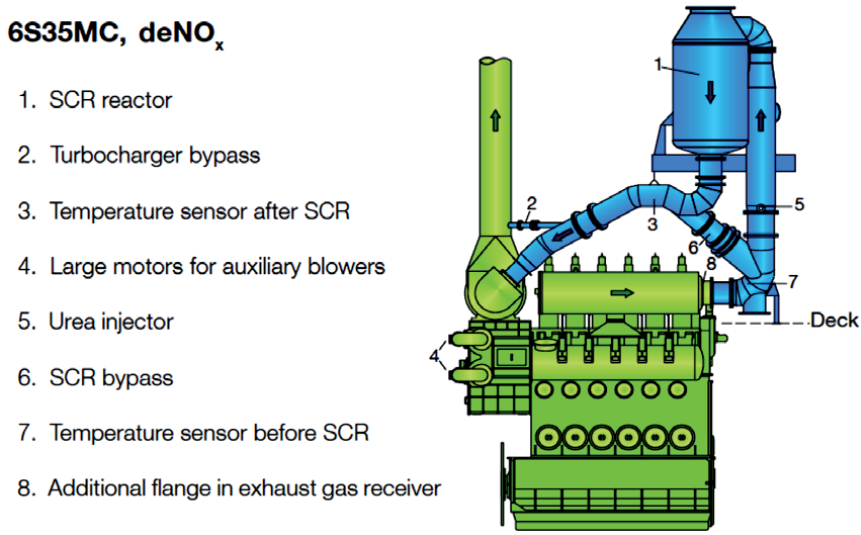


Fig. 8.34. 6S35MC engine with SCR catalytic reactor installed [17]

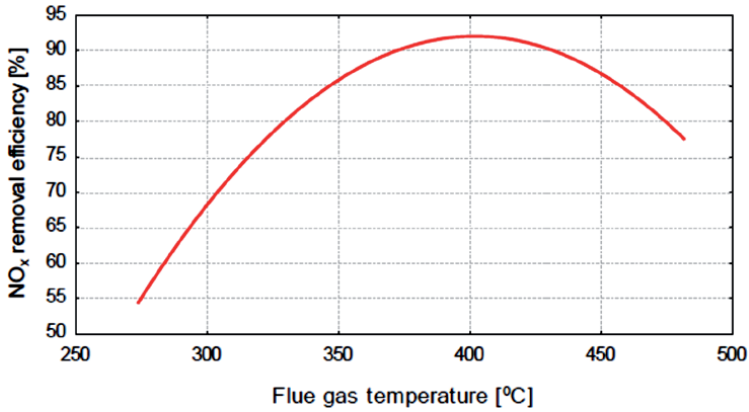


Fig. 8.35. $NO_x$ removal efficiency in relation to the flue gas temperature

Table 8.23. Temperature before and after the turbine (turb.), based on a 6S50ME-C two-stroke diesel engine [19]

| Temperature | Use of engine | | | |
|---|---|---|---|---|
| $T_{amb}$ = 10ºC | 25% load | 50% load | 75% load | 100% load |
| $T_{in}$ turb. [ºC] | 299 | 308 | 337 | 395 |
| $T_{out}$ turb. [ºC] | 245 | 217 | 207 | 221 |
| $T_{gain}$ [ºC] | 54 | 92 | 130 | 174 |

When no SCR operation is needed (outside ECA), the exhaust gas is passed directly to the turbine in the turbocharger (T/C) and the SCR is sealed by two valves. Table 8.23 reveals that even though the reactor is placed before the turbine, the exhaust gas temperature is still too low at loads below approximately 50%. Therefore, it has been necessary to develop a 'low load method', which can be used to increase the exhaust gas temperatures. The cylinder and SCR bypass are shown in Fig. 8.36.

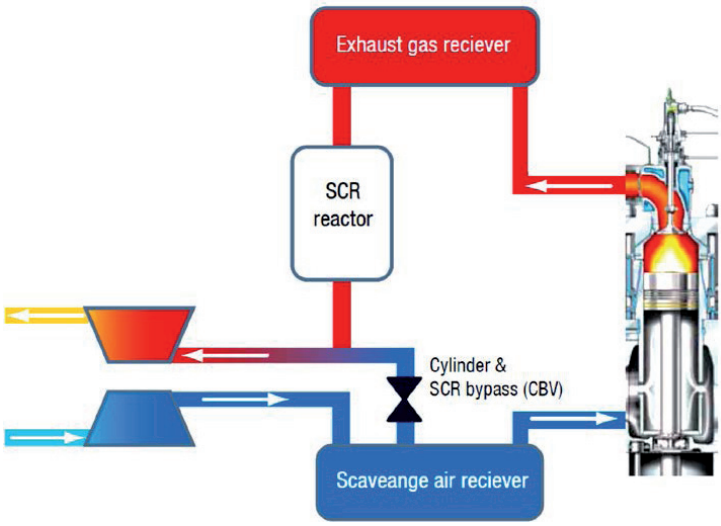


Fig. 8.36. Low-load method to increase exhaust gas temperatures [3]

The cylinder bypass valve (CBV) increases the exhaust gas temperature by reducing the mass of air through the cylinders at a fixed amount of fuel combustion. This means that higher exhaust gas temperatures for the SCR are obtained. Calculations have shown that this method is suitable because the mass flow through the T/C remains almost unchanged. This means that the scavenge air pressure is maintained and thus that the combustion is nearly unaffected. It was also verified that the engine and SCR system was able to meet the IMO Tier III $NO_x$ limits, and the results are presented in Table 8.24.

Table 8.24. $NO_x$ emissions at the four IMO engine load points [21]

| | 25% | 50% | 75% | 100% | Cycle |
|---|---|---|---|---|---|
| Tier III [g/kWh] | 2.9 | 3.1 | 2.9 | 2.5 | 2.8 |

The table reveals that the SCR system ensures a $NO_x$ cycle value of 2.8 g/kWh, which is well below the IMO Tier III limit of 3.4 g/kWh (reduction of 80%).
Conclusion: This system may reduce the emissions of $NO_x$ by more than 90%, (obligatorily requires comparatively low-sulphur fuel), with the cost-effectiveness of 873.5 $/ton and $SO_x$ emissions by 98% with 3115 $/ton in case of using seawater scrubbing. Researchers have indicated that the urea consumption of SCR system is 8.5% of the consumption of diesel oil, which will surely have a significant influence on the size and weight of installation.
The main challenges for marine SCR applications are sulphur resistance and low-temperature activation. Currently, SCR catalyst mainly relies on $V_2O_5$–$WO_3$–$TiO_2$, but $V_2O_5$ is a kind of highly poisonous material and the active temperature is above 300°C. The mechanism for deposit formation involves an undesirable parallel reaction (to the $NO_x$ conversion) at the catalyst whereby sulphur dioxide in the exhaust is oxidized to sulphur trioxide ($SO_3$), which

can then react with ammonia to form ammonium sulphate and bisulphate. Such a process reduce the effective area and shorten the lifespan of the catalyst, with fuel-related hydrocarbon and particulate matter adding to the fouling. As conditions deteriorate, $NO_x$ reduction is impaired and more unreacted ammonia will slip past the catalyst. Manufacturers recommend minimizing the oxidation of sulphur dioxide with their reduction catalyst materials and by specifying that only fuels with a sulphur content of less than 1.00% should be used. This treatment prevents the formation of ammonium sulphates as well as sulphuric acid. Systems capable of operating with higher sulphur content are possible, but in this case, the higher exhaust temperatures are required. As an alternative to low-sulphur fuel, a $SO_x$ scrubber fitted before the reactor is possible to use. When installed after a wet $SO_x$ scrubber the exhaust gas would require reheating from around 50ºC to at least 300ºC. No reheat would be required for a dry scrubber. An additional undesirable parallel reaction will take place if calcium is present, resulting in calcium sulphate deposits. SCR catalyst material is extremely sensitive to the presence of sulphur in the fuel and it is also subject to poisoning (chemical attack of the active element of the catalyst), fouling (deposition of material which masks the catalyst, preventing contact between the catalyst surface and the reactants, possible to be seen during a visual inspection) and plugging (which refers to the plugging of the catalyst pores, may not be seen during the visual inspection). Additionally, as pressure drop is a function of the bed length and the catalyst configuration, depositing of fly ash or other solid particles on the catalyst can have a profound effect on the engine performance and the back pressure growth may be observed. In order to minimize the pressure losses, the diameter of SCR reactor can be increased, which is most likely impractical onboard.

SCR system has been used for many years for inland installations, which are characterized by long periods of operation under the constant load. The different nature of marine engines' service has become a challenge for producers of SCR technology.

Onboard, there are two types of engines:

- auxiliary engines (aggregates),
- main engines (vessel's propulsion).

As the aggregate, four-stroke self-ignition engines are usually used. In this case, using of SCR technology is definitely a simpler solution, but it is necessary to take into account the presence of the installation at the ship construction stage. Another solution is to try to place it in the existing ship's engine room. While considering main engines, the installation of SCR system is much more problematic. Propulsion engine operates under variable load conditions, especially while working inside the ECA, where sailing at reduced speed is required and thereby the exhaust gas temperature is too low for the catalysis. It may be also a crucial issue for ammonia or urea dosing systems. SCR technology involves a periodic check of the catalyst efficiency and thereafter there may be a necessity to replace it.

*Exhaust gas recirculation*: In this technology a proportion of the exhaust from before the turbocharger is recirculated to the cylinders with the charge air, which allows lowering the oxygen content of the mixture as well as increases its heat capacity. It brings about reduction of peak combustion temperatures and suppresses the formation of thermal $NO_x$. EGR installation consists of: high-pressure exhaust gas scrubber fitted before the engine turbocharger (used to remove sulphur oxides and particulate matter from the recirculated exhaust and to prevent corrosion and reduce fouling of the EGR system and engine components, typically working in the closed loop mode), a water mist catcher (WMC) to remove entrained water droplets, a cooler to further reduce the temperature of the recirculated gas, a high-pressure blower to increase recirculated gas pressure before reintroduction to the engine scavenge air and automated valves for isolation of the system [3, 33]. The EGR installation and its parameters are presented in Figs. 8.37-8.39. The natural result of using EGR is the negative effect on the engine efficiency, which decreases with the increasing EGR ratio almost linearly, as shown in Fig. 8.40.

The investigation on the two-stroke marine diesel engine (4T50ME-X) has shown that IMO Tier III $NO_x$ compliance is achievable by the use of high-pressure EGR solely. A cycle value below 3.4 g/kWh of $NO_x$ was obtained, and also the not-to-exceed (NTE) level of 5.1 g/kWh

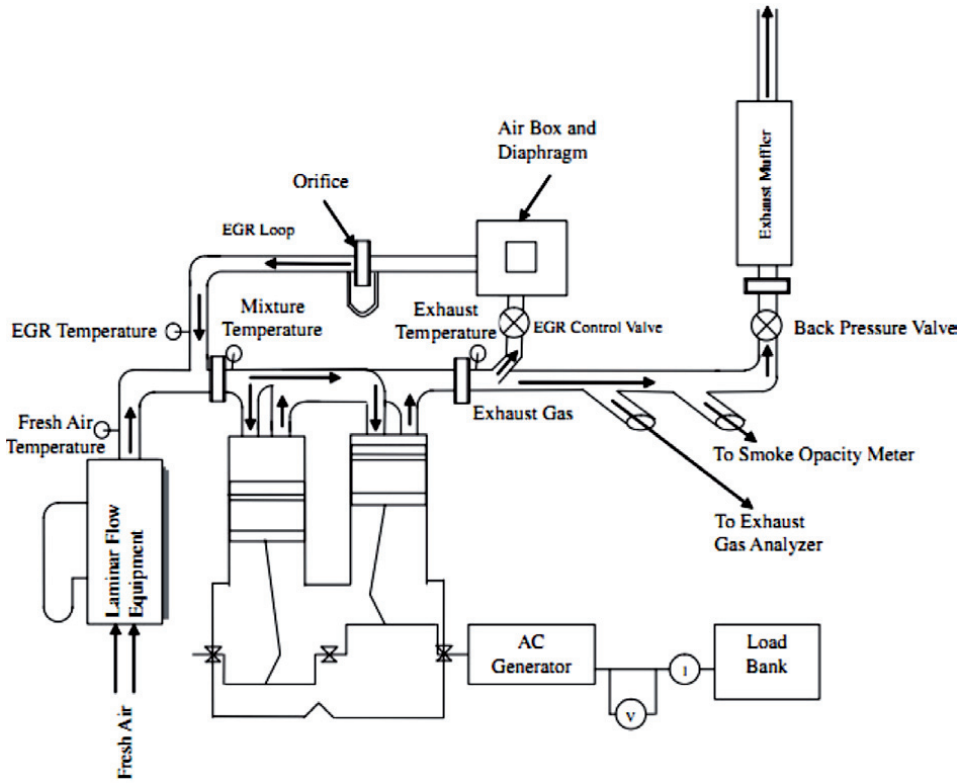


Fig. 8.37. An EGR system arrangement [31]

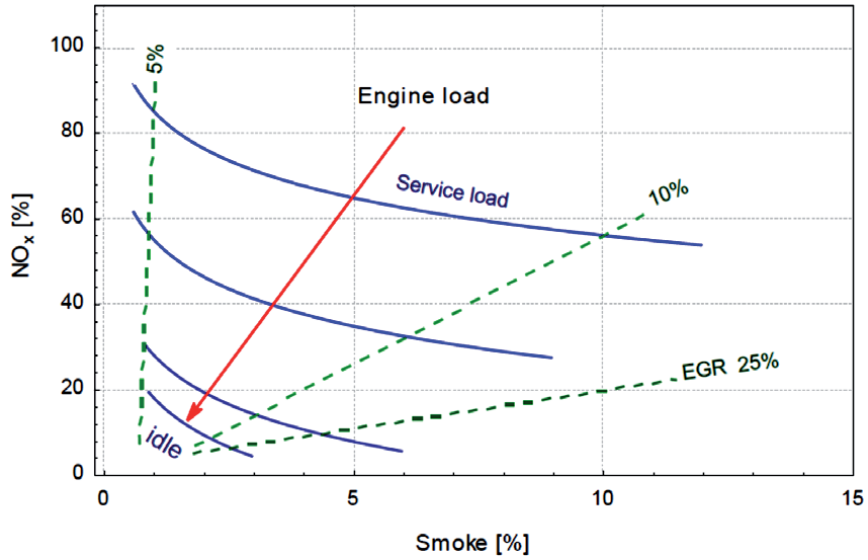


Fig. 8.38. $NO_x$ emission efficiency in relation to engine load and EGR level

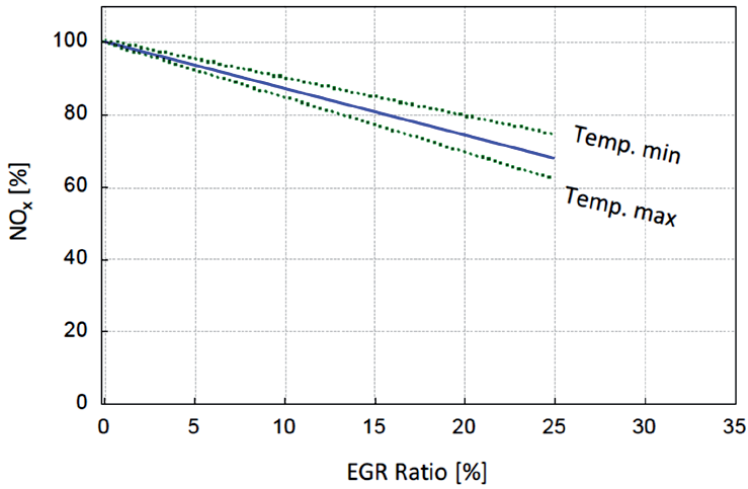


Fig. 8.39. Effect of EGR exhaust gas temperature on the $NO_x$ reduction ratio

of $NO_x$ at each engine load point 25, 50, 75 and 100% was proven during the test. The results are shown in Fig. 8.41.

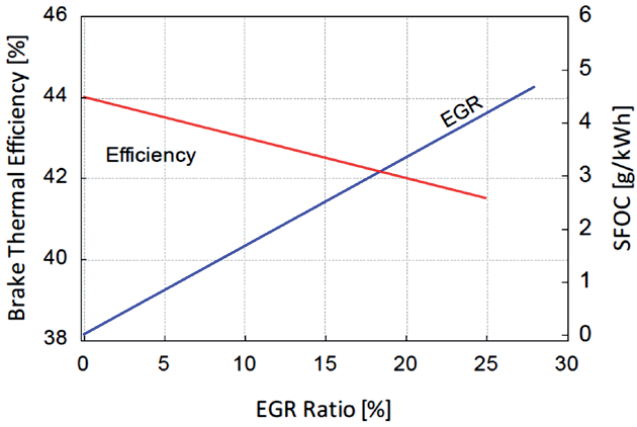


Fig. 8.40. Changes in engine efficiency and SFOC under the influence of EGR

Conclusion: EGR can be used to meet the strict standard of IMO and it can assist other technologies. However, the high level of recirculation may result in increased CO and particulate emissions, which may be controlled using additional techniques such as water in fuel to achieve an optimum balance between $NO_x$, CO and PM. Due to the nature of EGR systems' primary engine controls, system malfunction or deviations from the normal operation can significantly reduce engine efficiency and increase CO and PM. There is also a risk of greatly accelerated engine wear and increased maintenance requirements if the scrubber does not clean and cool the exhaust gas to the required levels.

*Non-thermal plasma*: Non-thermal plasma has been introduced as a promising method for $NO_x$ as well as PM removal. This system represents gas, which has been ionized into a mixture of highly reactive molecules. Plasma is created by means of high-voltage discharges. It is generated using an alternating high voltage to break-down the gas flowing between two electrodes. The region between two electrodes is filled with a material resulting in voltage breakdowns in the

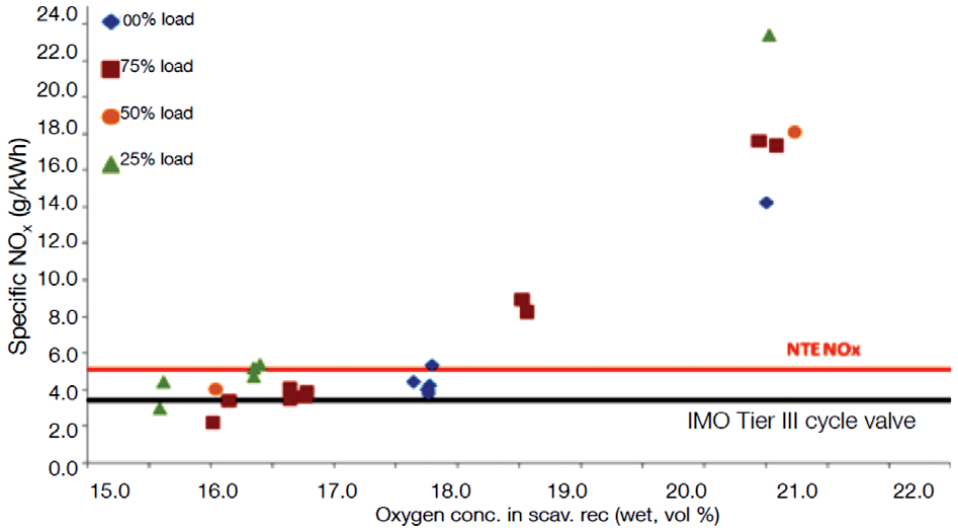


Fig. 8.41. $NO_x$ emission at different engine loads as a function of oxygen content in the scavenge air [21]

voids between the materials. The duration of the voltage breakdowns lies in the range of few nanoseconds. The system is compact and very flexible in terms of size and shape. The generated electric field produces free electrons, which travel through the gas creating O• and OH• radicals and they are effective in oxidizing exhaust gas emission compounds and therefore in reducing of harmful components.

In general, NTP can be generated in several ways, such as through electrical corona discharges, radio-frequency discharges, microwave discharges, dielectric barrier discharges and electron beams. To date, in connection with marine diesel engines exhausts, the dielectric barrier discharger (DBD) was commonly used [34-36].

As mentioned before, the $NO_x$ in engine exhausts is composed primarily of NO. Consequently, after-treatment schemes have focused on the reduction of NO. NTP is able to convert NO to $NO_2$ by the oxygen radicals. It is also possible in the presence of water, oxygen and hydrocarbon, while only partially oxidizing the hydrocarbons. The non-thermal plasma module for marine use requires robust design, low voltage, minimum maintenance, and low energy consumption with easily scalable efficiency, as the rate of $NO_x$ emission varies with engine load and external ship conditions.

An example of plasma operation process on engine exhaust gas is presented in Fig. 8.42. It can be observed that when the power supply of plasma reactor is turned off, the NO and $NO_2$ outlet concentration in the gas passing through the reactor correlates to the total $NO_x$ level recorded at the reactor inlet. When plasma reactor is under operation, NO oxidation to $NO_2$ proves to be quite stable and efficient [34].

Combination of NTP reactor and other post-treatment methods can also be implemented. Novel techniques for cleaning the exhaust gases is non-thermal plasma are currently investigated: NTP reactor in presence of catalyst plasma-based catalytic treatment (PBCT) or $NO_x$ reduction by non-thermal plasma and temperature swing adsorption (TSA). NTP assembly can be also combined with a diesel particulate filter (DPF). Hybrid methods are presented in Figs. 8.43-8.45.

Conclusion: NTP do not generate any additional wastes (wastewater) and it is also not consisted of many different parts (no additional tanks, storage installations). If necessary, this technology may not use the catalyst, urea or other reducing agent and the operating temperature can be lower than 150°C. Main disadvantages of NTP technology are high energy consumption and expensive price [38] and it will have a low treatment efficiency in the condition of excess $O_2$. While generating NTP through the electrical corona discharge, the electron energy is below

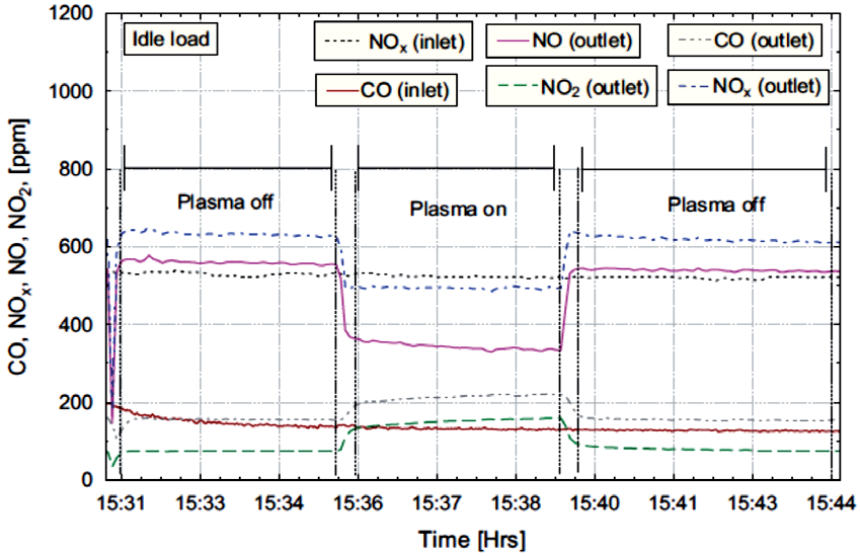


Fig. 8.42. An example of NTP reactor operation [34]

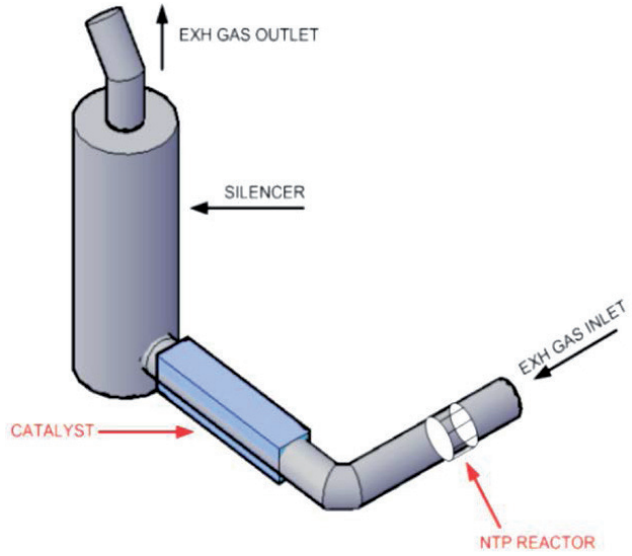


Fig. 8.43. Installation for $NO_x$ plasma-based catalytic treatment [37]

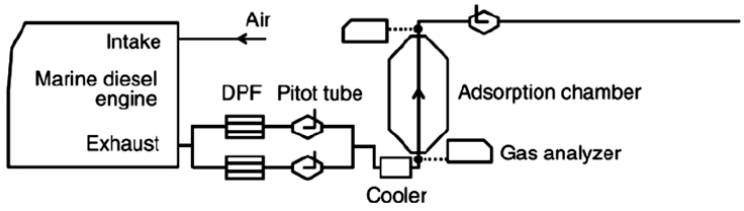


Fig. 8.44. Marine diesel engine exhaust using NTP treatment process – adsorption [31]

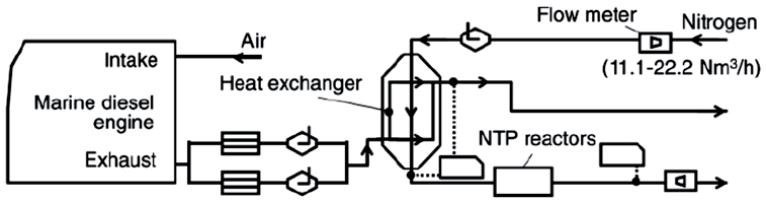


Fig. 8.45. Marine diesel engine exhaust using NTP treatment process – desorption [31]

10 eV, which results in an increase in gas temperature. While using the electron beam technology, accelerators cause ionization of the gas and thereafter formation of free radicals. Therefore, in the corona discharge for one NO atom (oxidation) about 50 eV is required whereas for electron beam technology it is 18 eV.

**Cost analysis**

As the high efficient $SO_x$ removal techniques are well known for many years, the main problem is an initial and running cost of an appropriate $NO_x$ removal method. As shown in Table 8.25, there are many technologies for $NO_x$ reduction. Tier II is responded by internal engine tuning including fuel injection timing retard, the arrangement of fuel valve injecting holes, and the optimization of the scavenging and exhaust systems. However, internal engine tuning cannot meet the requirements of Tier III, where a significant $NO_x$ reduction is required. There are two main types of measures for Tier III.

Table 8.25. The cost of different $NO_x$ reduction techniques [39]

| Item | $NO_x$ reduction rate (vs. Tier I) | Decrease of fuel efficiency | Technology | Initial cost | Running cost |
|---|---|---|---|---|---|
| Engine specification optimization (mechanical type engine) | Δ20% | +2~+3% | existing | small | small |
| Electronic control engine | Δ20% | 0~+1% | developed | middle | small |
| Water injection | water emulsified fuel: Δ50% | +2~+3% | developed | middle | middle |
| | independent water injection: Δ80% | +7~+10% | developed | middle | middle |
| | stratified fuel water injection: Δ80% (For restriction of fuel pump capacity etc., actual reduction rate will be at the Δ40% level) | approx. +10% | developed | middle | middle |
| EGR with scrubber | Δ80% | +1~+3% | developed (basic tests complete) | large | middle |
| SCR | Δ80%~90% | 0~+1% | developed (onboard test carried out) | large | large |

To date, the only proven technique, which is surely able to meet the strict IMO Tier III limits is the combination of SCR + low sulphur marine diesel oil (MDO) or SCR + seawater for wet scrubbing system (SWS).

For an exemplary single trip, emission quantity ($m_{e,trip}$) can be calculated for standby (sb), manoeuvring (m) and cruise (c) modes of the ship as follows [40]:

$$m_{e,trip} = m_{e,sb} + m_{e,m} + m_{e,c}$$

Two different methods can be used to estimate ship emissions. They are based either on fuel consumption or engine power. When fuel consumption for each phase of the trip is known, $m_{e,\,trip}$ can be computed by:

$$m_{e,trip} = \Sigma_{Ph}\,(m_{f,i,j} \times EF_{i,j} \times ER)$$

where: $m_f$ is the fuel consumption, EF is the fuel emission factor in kg/kg$_f$, i is the pollutant type, j is the fuel type and Ph is the phase of the trip. It includes cruise, manoeuvring, and standby with engine load of 80, 20, and 5%, respectively. ER is emissions reduction percentage in case of using emission control method.

When running time (T), power (P), load (L), and emission factor (E) in kg/kWh of an engine for a specific trip is known, $m_{e,trip}$ can be calculated using another equation:

$$m_{e,trip} = \Sigma_{Ph}\,(T \times P_{i,j} \times L_{i,j} \times E_{i,j} \times ER)$$

Diesel engine emission factors at low loads increase as the load decreases because of the increased specific fuel consumption and consequently the reduced efficiency. The exemplary values of medium-speed diesel engine emission factors (with MDO 1.0% of S, the speed of the main engine – 750 rpm) can be shown in Table 8.26.

Table 8.26. Medium-speed diesel engine emission factors [40]

| Fuel type | Emission factor [g/kWh] | $NO_x$ | $SO_x$ | PM | $CO_2$ | CO | HC |
|---|---|---|---|---|---|---|---|
| MDO (1.0% S) | at cruise | 13.2 | 3.97 | 0.47 | 646.08 | 1.1 | 0.5 |
| | at manoeuvering | 11.85 | 6.079 | 0.3211 | 869.1 | 4.344 | 1.132 |

Emission factors are increased in manoeuvring modes as engine load decreases. This trend results because at low loads specific fuel consumption of diesel engines is increased with reduced engine power and efficiency. Thus, mass emissions (in g/h) will be decreased at low loads while emission factor (in g/kW) will be increased.

*Economic analysis for emission control methods*: The annualized capital cost recovery (ACC) due to applying emission control method (ECM) depends on the capital cost value (CC), the average expected ship age after conversion (n), and the interest rate (r). ACC can be calculated as:

$$ACC = CC \times \frac{r(1+r)^2}{r(1+r)^n - 1}$$

Economically, applying either SCR or SWS systems will add extra annual installation costs (AIS) for the ship. These costs include ACC, annual maintenance and running costs (MC), fuel cost increment (ΔMGO) in case of using marine gas oil instead of SWS for $SO_x$ reduction. AIS can be calculated as:

$$AIS = \sum\nolimits_{ECM} ACC + \sum\nolimits_{ECM} MC + \Delta MGO$$

Finally, annual cost-effectiveness for each ECM ($ACE_{ECM}$) can be calculated separately for each pollutant. This involves calculating ACC, annual operating and maintenance costs (MC) and annual emission reduction (AR) in tons/year. $ACE_{ECM}$ can be calculated as:

$$ACE = \frac{ACC + MC}{AR}$$

The aim of SCR and SWS is to reduce exhaust gases emissions especially $SO_x$, $NO_x$ and PM emissions. SCR reduces $NO_x$ emissions by 90%, which would comply with required IMO emission levels. It depends on injecting urea solution into the exhaust gas stream in combination with catalyst housing in the exhaust channel. Compact SCR system consists of a reactor, which contains several catalyst layers, a treating and storage system for the reagent, and a control system. It has an average volume of 1.0 m$^3$/MW and a weight of 1.0 kg/kW, including urea storage tanks, pumps, injection and control system. Urea consumption rate for SCR system is

0.025 $m^3$/MWh onboard ships. On the other hand, both SWS and MGO reduce $SO_x$ emissions. The use of SWS system will reduce $SO_x$ and PM emissions by 98% and 70%, respectively, while the use of MGO (0.1% sulphur) will reduce sulphur emission rates from 3.97 g/kWh to 0.4 g/kWh with a reduction of 90%. In addition, PM emissions will be changed from 0.47 g/kWh to 0.19 g/kWh with a reduction of 60%. Nitrogen oxides and $CO_2$ emissions are unchanged. In order to reduce both $NO_x$ and $SO_x$ emissions, a combined system of SCR, SWS and MGO can be used as shown in Fig. 8.46. MGO is mainly used to reduce $SO_x$ emissions.

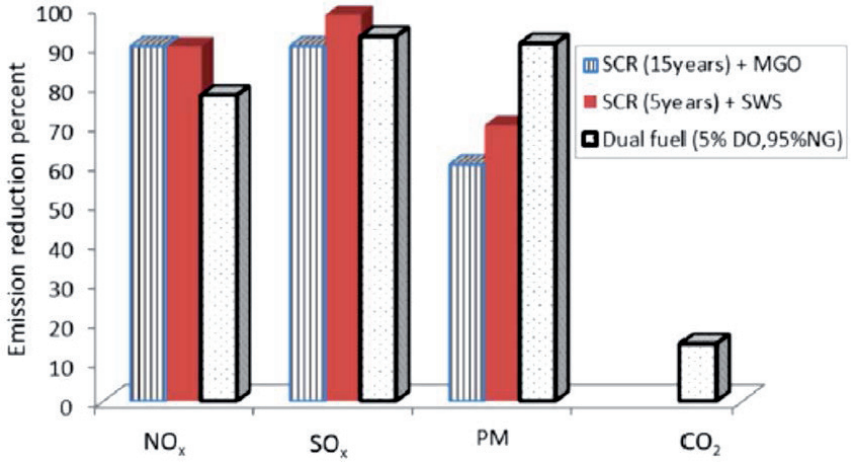


Fig. 8.46. Ship emission reduction with various strategies [40]

The yearly diesel engine $NO_x$, $SO_x$, $CO_2$, and PM emissions are 223.8, 68.31, 11.086 and 7.926 tons/year, respectively. A combined system of SCR and MGO leads to a reduction of $NO_x$, $SO_x$ and PM emissions with percentages of 90, 90 and 60%, respectively. These emissions can be reduced using SCR and SWS systems by 90, 98, and 70%, respectively. Dual-fuel engine with 5% diesel oil and 95% natural gas can be compared with other ECMs. The highest $CO_2$ emission reduction is achieved by dual-fuel engines. This is due to lower carbon content in natural gas compared with diesel oil. Economically, the ECM can be judged from average installation cost per kW of engine power, annual cost for capital cost recovery and annual cost-effectiveness for ECM. For this study, fuel costs were examined in terms of their cost efficiency. According to local prices, MGO cost is 193.5 \$/$m^3$ at the end of the year 2016. The capital cost of installing SWS onboard ship is 160 \$/kW with operating costs about 3% from this [40]. In addition, initial SCR investment cost rate is 50 000 \$/MW with 3.75 \$/MWh and 0.9 \$/MWh for running and maintenance costs, respectively. According to the literature, the main SCR component, the catalyst, requires rebuilding depending on the sulphur content (in %) by weight in fuel during operation. The reactor requires rebuilding in 15-20 years for $S < 0.2$ and in 5 years for $0.2 < S \leq 1.5$. For the case study, catalyst reactor has to be rebuilt every five years when used in SCR + SWS system where MDO contains 1.0% of sulphur. It needs rebuilding after 15 years when MGO with 0.1% of sulphur content is used. Figure 8.47 shows the annual and average installation costs for ECMs.

The installation costs for SCR and SWS are 175 895 \$/year and 244 358 \$/year, respectively with average engine output power cost of 20.35 \$/kW and 28.28 \$/kW, respectively. In addition, applying combined SCR + SWS and SCR + MGO will increase the ship annual operating costs by 420 252 \$/year and 384 453 \$/year, respectively, with average installation costs of 48.6 \$/kW and 44.5 \$/kW, respectively. In addition, the total installation and maintenance costs for the dual-fuel engine is 258 030 \$/year with 29.9 \$/kW average cost per output power. Annualized cost-effectiveness of each ERM can be used for choosing the suitable method for emission reduction. It compares the total annual capital and maintenance costs with the

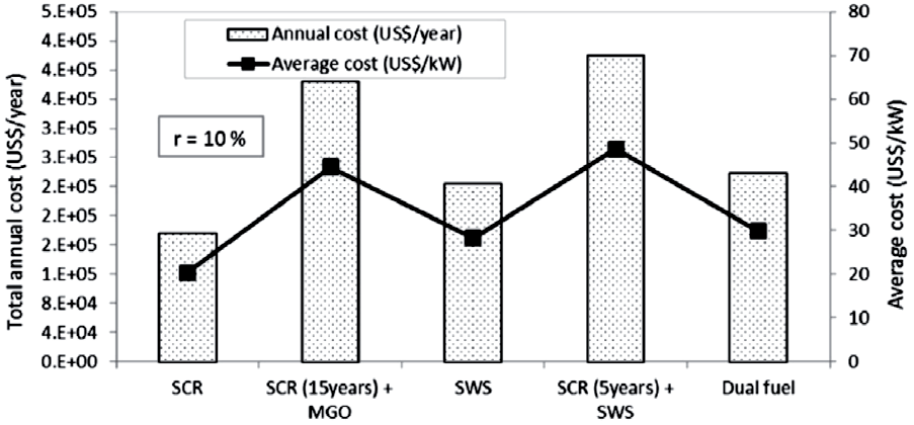


Fig. 8.47. Average and annual costs for applying different ECMs [40]

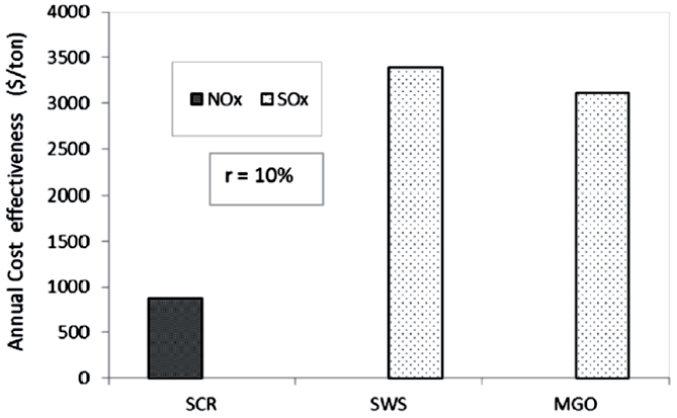


Fig. 8.48. Annual cost-effectiveness for $NO_x$ and $SO_x$ emission reduction measures [40]

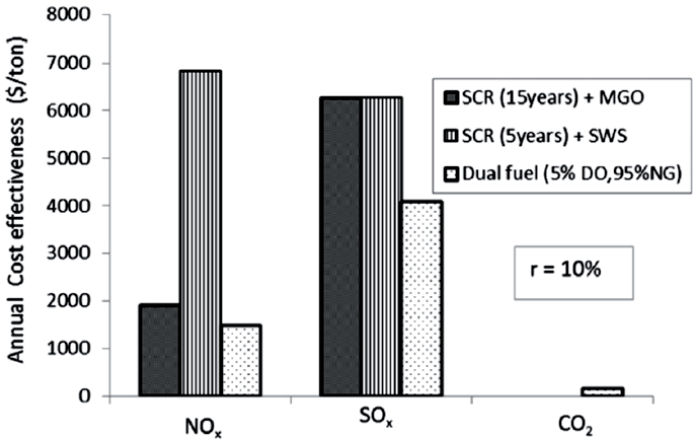


Fig. 8.49. Annual cost-effectiveness [40]

amount of emission reduction after applying exhaust reduction method. Figure 8.48 shows the cost-effectiveness for the reduction of $NO_x$ and $SO_x$ emissions using SCR, SWS and MGO.

The cost-effectiveness for reducing $NO_x$ emissions using SCR is 873.5 $/ton for the reduced 201.4 tons annually. $SO_x$ emissions can be reduced by 61.48 tons/year and 66.94 tons/year with the cost-effectiveness of 3392 $/ton and 3115 $/ton using MGO and SWS, respectively. In addition, combined systems of SCR, SWS and MGO can be used to reduce exhaust gas emissions in order to comply with new IMO regulations. Figure 8.49 shows the proposed two combined system compared with dual-fuel engines.

Using SCR + MGO system would reduce $NO_x$ and $SO_x$ for the case study with the cost--effectiveness of 1909 $/ton and 6254 $/ton, respectively. The reduction of these emissions can be achieved using (SCR + SWS) with the cost-effectiveness of 6836 $/ton and 6278 $/ton, respectively. The more economical option for reducing $NO_x$, $SO_x$ and $CO_2$ emissions is using the dual-fuel engine with the cost-effectiveness of 1486, 4084 and 160.8 $/ton, respectively.

**Simultaneous removal of $NO_x$ and $SO_x$**

Currently, many ship emission control techniques have been developed. However, most of these technically available technologies are applied to remove $NO_x$ or $SO_2$ separately. Few studies have been reported concentrating on the simultaneous removal of $NO_x$ and $SO_2$ in one process, but to date, there is no established technology opted for simultaneous removal of multi--gas pollutants for ocean-going vessels.

There was a proposition of an integrated system, which consisted of a monolithic $Pt/Al_2O_3$ oxidation catalyst and a seawater scrubber [41]. It managed to achieve a single compact device for simultaneous abatement of multi-gas pollutants. However, due to the limited sulphur resistance of the catalyst, this system could only be used with fuel sulphur content of up to 0.4%.

Another research project developed a hybrid process of electron beam irradiation plus seawater scrubbing to clean flue gas from marine diesel engines [42]. The active species formed in the plasma reaction converted NO into $NO_2$, which favoured seawater absorption. From the viewpoint of industrial application, this kind of integrated process for multi-gas pollutants removal may be especially suitable for ocean-going ships. It shows a great potential to reduce the equipment footprint and complexity of the system. Nonetheless, high $SO_2$ removal up to 99% and $NO_x$ up to 51% were obtained for exhaust gases with 1700 ppmv of $NO_x$ concentration even if high irradiation doses were applied. As the $NO_x$ removal is far below the 80-90%, this method cannot compliance with IMO Tier III regulations.

$NO_x$ removal by wet scrubbing methods has not been adopted on ships because of the low solubility of NO (accounting for more than 90% of $NO_x$) [39]. However, many wet scrubbing systems for $SO_x$ removal using seawater have been successfully used on ships. In addition, various chemical oxidants have been introduced in wet scrubbing technology for $NO_x$ removal [43]. In general, oxidizing agents, such as sodium chlorite, potassium permanganate, chlorine dioxide or hydrogen peroxide, are added to the scrubbing medium to convert insoluble NO to soluble $NO_2$ [44-49]. These oxidants achieved satisfying removal efficiencies in lab-scale and pilot-scale experiments. There have been many reports on the enhancement of wet scrubbers' performances. For $NO_x$ gases removing, $HNO_3$ and Ag(I) mixture in an integrated wet scrubber electrochemical system was investigated [50]. $NO_x$ was removed from the gas stream with 75% efficiency when the liquid/gas flow rate was 400 $L/m^3$. Another study has shown, that it is possible to use a sieve tray wet scrubber for removing NO gas. $NaClO_2$ was used as the scrubber medium to convert insoluble NO to soluble $NO_2$, which could then be removed by alkaline solution. This system could remove $NO_x$ from the flue gas stream with 51.5% efficiency using a liquid/gas flow rate of 7 $L/m^3$ [46]. In another case, aqueous chlorine dioxide was used as the scrubbing solution in a bubbling reactor to remove $NO_x$ from flue gas. Using a liquid/gas flow rate of 44 $L/m^3$, it was possible to remove $NO_x$ with 60% efficiency [51]. Because wet scrubbers use mostly high liquid/gas flow rates, it is very common to have water pollution problems. High concentrations of absorbents are also used to improve removal efficiency in wet scrubbers, which not only causes environmental problems but also leads to significant corrosion problems inside and outside the nozzles, tubes, and walls of scrubbers. There was a work, where 100% $SO_2$ removal, 100% NO oxidation, and 81% $NO_x$ removal efficiency were attained in a novel

swirl scrubber using $NaClO_2$ as the scrubber medium [43]. The $NO_x$ removal efficiency increased mainly with decreasing solution pH value. Increasing the initial $SO_2$ concentration enhanced the $NO_x$ removal efficiency, and this enhancement was more intense at higher pH values. A higher removal efficiency was obtained with increasing sodium chlorite concentration, but a supply of sodium chlorite above 0.2 M did not improve the removal efficiency considerably. The swirl scrubber of this study produced very large gas-liquid interfacial areas, and therefore, high removal efficiencies were observed using a low concentration of scrubbing medium and a low L/G ratio. Another promising $NO_x$ and $SO_2$ removal method for ship emissions based on seawater electrolysis technology was proposed and investigated in the semi-batch process [10]. Results of $NO_x$ removal by electrolysed seawater showed that $NO_x$ removal efficiencies increased with increasing active chlorine concentration of electrolysed seawater and $O_2$ concentration, but decreased with increasing gas flow rate. Relatively high removal efficiencies of NO and $NO_x$ were possible to reach when the initial pH was in a range of 4-6. $NO_x$ removal efficiencies were less sensitive to the change of NO inlet concentration, $CO_2$ concentration, and reaction temperature. For simultaneous removal of $NO_x$ and $SO_2$ from simulated ship emissions ($NO_x$ – 1000 ppm, $O_2$ – 15% $CO_2$ – 5%, $SO_2$ – 0-751 ppm), $NO_x$ removal efficiencies in single stage and two-stage experiments were more than 60% and 90%, respectively, under conditions of gas flow rate 1.26 L/min, absorbent volume 750 mL per stage, active chlorine concentration 1500 mg/L $Cl_2$, pH 7, and reaction temperature 20ºC.

### 8.1.5. Electron beam

**Introduction**

To date, only several studies concentrating on the simultaneous removal of $NO_x$ and $SO_2$ in one process (using electrolysis or electromagnetic techniques) have been carried out [3, 10, 46, 49]. To accomplish major reductions in $SO_x$ and $NO_x$ emissions, a new onboard installation of exhaust emission control is required and it may be an EBFGT process, which is one of the most effective methods of removing $SO_2$ and $NO_x$ from industrial flue gases.

Electron accelerators are reliable and durable electrically sourced equipment that can produce ionizing radiation when it is needed for a particular commercial use. There are a large number of electron accelerators being used worldwide in industrial applications, most of which involve polymer processing. Nowadays, there are over 1700 electron beam units, providing an estimated added value to numerous products, amounting to 100 billion $ or more [52]. High-current electron accelerators are used in diverse industries to enhance the physical and chemical properties of materials and to reduce undesirable contaminants such as pathogens, toxic by-products, or emissions. Over the past few decades, electron beam technologies have been developed aimed at ensuring the safety of gaseous and liquid effluents discharged to the environment. It has been demonstrated that electron beam technologies for flue gas treatment ($SO_x$ and $NO_x$ removal), wastewater purification, and sludge hygienization can be effectively deployed to mitigate environmental degradation. Recently, extensive work has been carried out on the use of electron beam for environmental remediation, which also includes the removal of emerging contaminants such as VOCs, endocrine disrupting chemicals (EDCs), and potential EDCs [53].

EBFGT is still a relatively new approach that was presented for the first time in Japan in the 1970s for the removal of $SO_2$ from exhaust gases [54]. However, this technology has been already successfully implemented on an industrial scale at coal-fired power plants in China (Chengdu and Hangzhou) [42] as well as in Poland (Szczecin 'Pomorzany'). The main parameters of these three industrial electron beam plants are presented in Table 8.27.

The process applied onboard is quite a different system from reported above. All of these installations were dry ammonia processes, using ammonia as the reagent. The system consisted of the following equipment in line: dry ESP (fly ash removal), humidification tower, accelerator driven process vessel, product collector – dry ESP, product granulation and packing installation as well as the ammonia storage and injection system. This type of technology, unit operation

Table 8.27. Main parameters of three industrial electron beam plants [42]

| Parameters | Unit | Chengdu TPP China | Hangzhou TPP China | Pomorzany EPS Poland |
|---|---|---|---|---|
| Nominal flue gas flow rate | $Nm^3/h$ | 300 000 | 305 400 | 270 000 |
| Inlet gas temperature | °C | 150 | 145 | 140 |
| Inlet $SO_2$ concentration | ppmv | 1 800 | 970 | 700 |
| Inlet $NO_x$ concentration | ppmv | 400 | 200 | 295 |
| $SO_2$ removal efficiency | % | 80 | 85 | 95 |
| $NO_x$ removal efficiency | % | 18 | 55 | 70 |
| Electron beam parameters | keV<br>mA | 800<br>2 × 400 | 800<br>2 × 400 | 700<br>4 × 375 |

and process equipment are not feasible for maritime applications. Moreover, while thinking about this technology in relation to the newest strict IMO Tier III regulation, the efficiency of $NO_x$ removal is insufficient (removal of 80% of $NO_x$ outside the ECA and removal of 90% of $NO_x$ inside the ECA are required). The other type of accelerators (low energy self-shielded units < 300 keV) have to be applied. For comparison, in the case of classical TV tube energy of the beam is equal to ca. 20 keV. Having considered that matter, the Institute of Nuclear Chemistry and Technology (Poland) undertook the study about complete, reliable and compact technology for gaseous pollutants removal that would meet Tier III standards and would be a real alternative for currently available onboard hazardous gas removal systems.

**Process key parameters**

In the electron beam technology, electrons are accelerated by a high voltage in a vacuum region before being injected through thin foil windows to the flue gases at the atmospheric--pressure processing chamber (plasma reactor). The energetic electrons collide with exhaust gas molecules and produce reactive free radicals, atoms, ions and secondary electrons that decompose the pollutants molecules in the irradiated flue gases. During this process, pollutants such as $SO_2$ and $NO_x$ are oxidized to higher oxides which then react with the water vapour present in the flue gases, resulting in the formation of $H_2SO_4$ and $HNO_3$ [54].

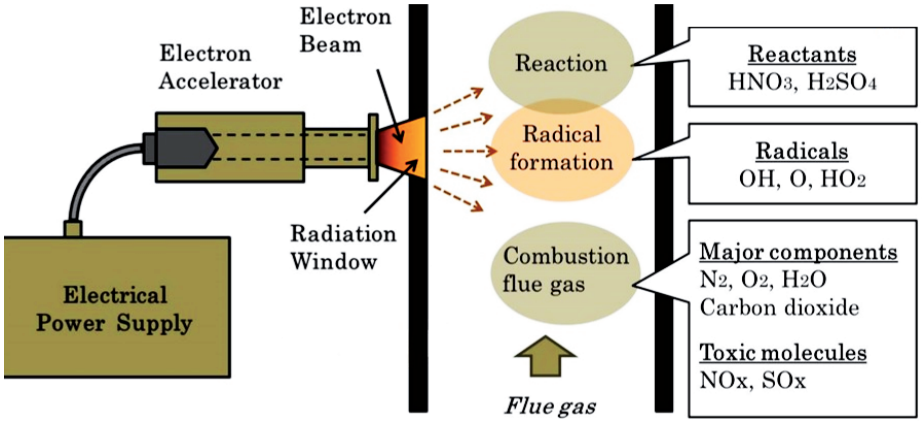


Fig. 8.50. The general scheme of the electron beam interaction with the flue gas

$NO + O(^3P) + M \rightarrow NO_2 + M$ (M is a third inert body in the reaction system) (8.21)
$O(^3P) + O_2 + M \rightarrow O_3 + M$ (8.22)
$NO + HO_2\bullet + M \rightarrow NO_2 + \bullet OH + M$ (8.24)
$SO_2 + \bullet OH + M \rightarrow \bullet HSO_3 + M$ (8.25)
$\bullet HSO_3 + O_2 \rightarrow SO_3 + HO_2\bullet$ (8.26)
$NO_2 + \bullet OH + M \rightarrow HNO_3 + M$ (8.27)
$SO_3 + H_2O \rightarrow H_2SO_4$ (8.28)

The general scheme of the electron beam interaction with the flue gas is given in Fig. 8.50.

There are different key parameters, which have a significant influence on process effectiveness [42, 52-54]:

- inlet $NO_x$ and $SO_2$ concentrations,
- irradiation dose,
- $SO_2/NO_x$ inlet concentration ratio,
- temperature.

To date, in order to investigate such parameters influence on electron beam exhaust gas treatment system, a number of tests have been carried out. The studies of this process can be divided into three parts:

- irradiation by electron beam ($NO_x$ and $SO_2$ removal),
- irradiation by electron beam + wet scrubber ($NO_x$ and $SO_2$ removal),
- irradiation by electron beam + wet scrubber + $NaClO_2$ ($NO_x$ removal).

*Irradiation by electron beam*: The influence of the inlet NO concentration on the efficiency of $NO_x$ removal was firstly examined (no reagents, no scrubbing). Results indicated that increasing the NO inlet concentration from 200 ppm to 1000 ppm in such a case caused a significant decrease in the removal efficiency of $NO_x$. It can be explained that with the inlet NO concentration increase, more oxidant species, e.g. OH and $O_3$, are used to oxidize NO into $NO_2$ which is still present in the gas phase. To increase $NO_x$ removal efficiency, more oxidant species are needed, e.g. OH, to oxidize $NO_2$ into $HNO_3$ which can be removed from the gas phase. However the water concentration in the gas mixture is constant in the experimental conditions and •OH radicals generated from water radiolysis mainly depends on the absorbed dose, the ratio between concentration of •OH radicals to total concentration of NO and $NO_2$ decreases with increasing inlet concentration of NO, thus the $NO_x$ ($NO + NO_2$) removal efficiency decreases significantly during the concentration range of 200 ppm to 1000 ppm. This led to the conclusion that when exhaust gases contain high concentrations of NO, increasing the dose is not a sufficient or cost-effective method and an alternative solution has to be considered. $SO_2$ influence on $NO_x$ removal efficiency was studied for the high and low inlet concentration of NO. In the low inlet concentration of NO (200 ppm), a relatively high removal efficiency of NO was obtained. By increasing the $SO_2$ inlet concentration, the removal efficiency of NO increased noticeably, especially at a higher irradiation dose.

The effect of the presence of $SO_2$ in enhancing $NO_x$ removal efficiency can be explained by the chain of reactions (8.25, 8.26, 8.24, 8.27). Radicals $HO_2\bullet$, which are produced during reactions with $SO_2$ (reactions (8.25) and (8.26)), react with NO and oxidize them into $NO_2$ (reaction (8.24)). This is later converted to $HNO_3$ (reaction (8.27)). When the NO inlet concentration is high, this synergistic effect is more advantageous at high concentrations of $SO_2$. When the $NO_x$ inlet concentration was low or high, an increase in temperature increased the $NO_x$ removal efficiency. The temperature did not have a significant impact on $NO_x$ removal efficiency at a high NO inlet concentration (1000 ppm). Similarly to NO, when the $SO_2$ inlet concentration increases, the efficiency of its removal decreases. This effect is less significant compared to that of NO.

In contrast to the analogous dependence study on $NO_x$ removal efficiency, a higher NO inlet concentration resulted in lower $SO_2$ removal efficiency. The explanation of this phenomenon is based on competing reactions. $SO_2$, as well as $NO_2$, uses •OH radicals during the oxidation to the higher oxides. However, the reaction between $NO_2$ and •OH (reaction (8.27)) has a higher rate constant than the reaction between $SO_2$ and •OH (reaction (8.25)), which results in the predominance of $NO_x$ removal over that of $SO_2$.

Temperature influence on $SO_2$ removal efficiency was also studied. The removal efficiency of $SO_2$, in contrast to that of $NO_x$, was higher when the temperature was lower. 90°C was chosen as an optimal temperature at which reasonably high removal efficiencies of $SO_2$ and $NO_x$ were obtained.

*Irradiation by electron beam + wet $SO_x$ scrubber*: In the second part of the experiments electron beam technology was coupled with the wet scrubbing method. The purpose of the hybrid technology was to enhance the removal efficiency of $NO_x$ and $SO_2$, especially when the inlet concentration of pollutants in exhaust gases is high. In the experiment, outlet gas was bubbled through simulated seawater filled glass probe. This arrangement corresponds to the single scrubber plate (in a high ship scrubber there are a number of plates). Comparisons of $NO_x$ removal efficiency were made under two experimental conditions: the sole use of the electron beam, and the use of wet scrubber after electron beam.

In both cases, the removal efficiency of $NO_x$ increased significantly when the hybrid technology was used. The relatively high removal efficiency of $NO_x$ was obtained at a lower absorbed dose, thus reducing energy consumption for $NO_x$ removal, especially for high inlet concentrations of NO. $NO_x$ consists mainly of NO and $NO_2$. Under electron beam irradiation, NO is first oxidized to $NO_2$. When seawater was used as a wet scrubbing solution, $NO_2$ was removed from the gas stream due to its high solubility in seawater; thus $NO_x$ removal efficiency increased.

When hybrid technology was used, the tendency was the same as when the sole electron beam was applied; higher NO inlet concentration resulted in lower $NO_x$ removal efficiency. However, the effect was not as significant as when electron beam technology only was used. The influence of $SO_2$ inlet concentration on $NO_x$ removal efficiency was also studied in the hybrid process of electron beam coupled with a wet scrubber. An increase of $SO_2$ inlet concentration resulted in an increase in $NO_x$ removal efficiency, a similar phenomenon was observed for the electron beam process. However, the effect in the hybrid process was less significant than that in the electron beam process. The $SO_2$ removal efficiency was also examined after hybrid technology treatment and compared with the results achieved with electron beam technology. Experiments showed that removal efficiency of $SO_2$ was much higher when hybrid technology was applied. Efficiencies as high as 93% were obtained for high doses (21.8 kGy and 32.7 kGy). When lower doses were applied the removal efficiency was near or above 80%.

*Irradiation by electron beam + wet scrubber + $NaClO_2$*: The main problem during the third part of the study was to accomplish the $NO_x$ removal efficiency, which should meet IMO Tier III standards inside the ECA. The block diagram of EB + SWS + $NaClO_2$ process is presented in Fig. 8.51.

During the third part of the study, 25 mM of $NaClO_2$ and the appropriate amount of Michaelis buffer, maintaining the water pH at 6.25 were added to the seawater. The gas flow was around 5 $m^3/h$ and inlet concentrations of $NO_x$ and $SO_2$ were equal to 1000 ppmv and 700 ppmv, respectively. The inlet temperature of the gases varies between 350°C and 400°C.

The irradiated waste gases are introduced from the bottom of the column and flow countercurrently to the sprayed process water. There is a direct gas-liquid interaction. $NaClO_2$ oxidizes the remaining after the irradiation NO and thereafter, at the appropriate pH 6-7 of the solution, it absorbs $NO_2$ with simultaneous production of nitric and hydrochloric acids. Both acids are neutralized by components of high alkalinity of process water. The post-reaction water flows down the column, where it is discharged to the purification set.

As explained in detail in section titled '$SO_2$ pollution control', the efficiency of $NO_x$ removal in the wet scrubber depends on the efficiency of gas-liquid interactions. The study has shown that significantly higher effectiveness of gas purification can be achieved while using a wet barbotage tower scrubber, where the interfacial area is considerably greater. However, the basic obstacles in using it are due to the dustiness of the exhaust gases and the permissible pressure drop in the scrubber. With high dustiness of the waste gases, exhaust gases may be clogged by a sieve flow gas distribution system at the inlet to the bubble scrubber. To avoid this, flue gases need to be deducted. The block diagram of EB + SWS + $NaClO_2$ process with wet barbotage tower scrubber is presented in Fig. 8.52.

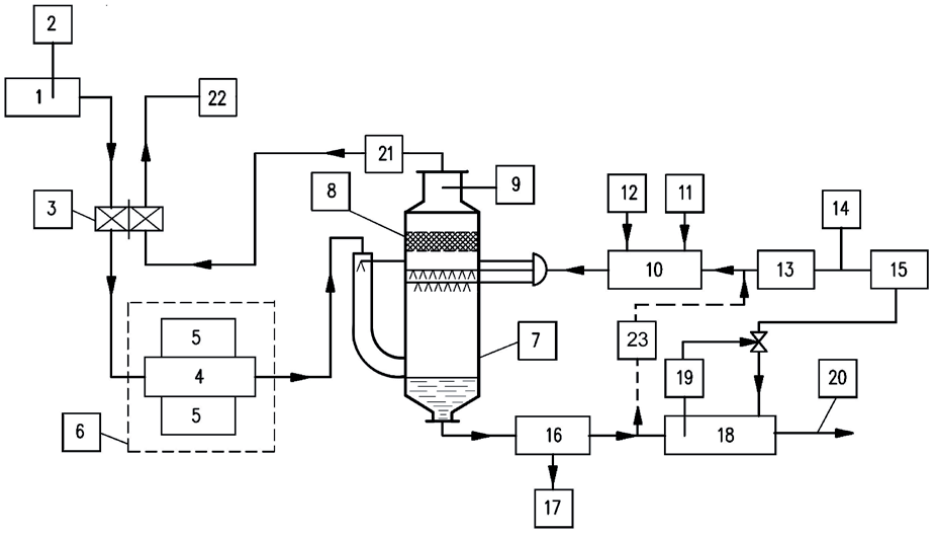


Fig. 8.51. E + SWS + $NaClO_2$ block diagram: 1 – inlet to the installation, 2 – inlet gas parameters, 3 – heat exchanger (outlet temperature 70-90ºC), 4 – process chamber, 5 – accelerator, 6 – accelerator's shelter, 7 – wet simple spray tower scrubber, 8 – demister, 9 – outlet gas parameters (of scrubber), 10 – process water (fresh), 11 – $NaClO_2$, 12 – Michaelis buffer $Na_2HPO_4$ and $KH_2PO_4$, 13 – seawater, 14 – NaCl solution, 15 – fresh water, 16 – centrifugal separator, 17 – sludge tank, 18 – post-reaction water tank, 19 – monitoring system of post-reaction water, 20 – sewage or sea, 21 – exhaust fan, 22 – stack, 23 – re-circulation (optional)

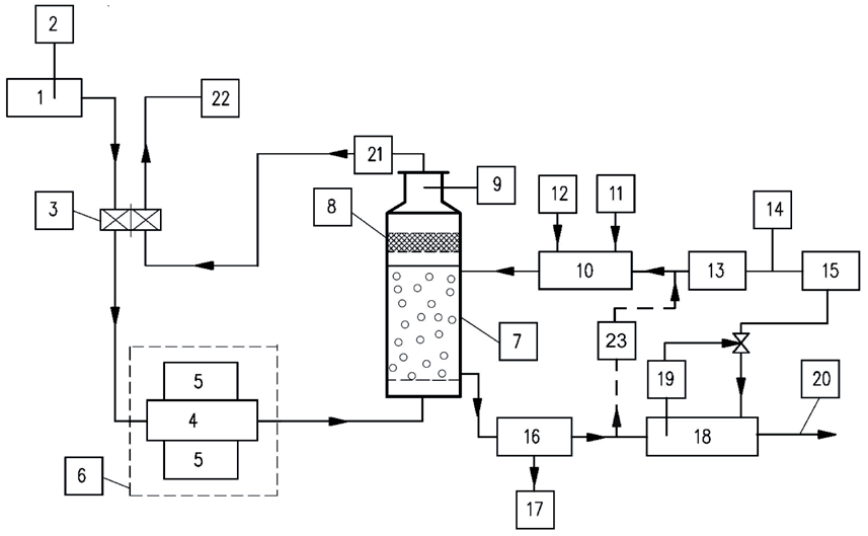


Fig. 8.52. E + SWS + $NaClO_2$ flowchart: 1 – inlet to the installation, 2 – inlet gas parameters, 3 – heat exchanger (outlet temperature 70-90℃), 4 – process chamber, 5 – accelerator, 6 – accelerator's shelter, 7 – wet barbotage tower scrubber, 8 – demister, 9 – outlet gas parameters (of scrubber), 10 – process water (fresh), 11 – $NaClO_2$, 12 – Michaelis buffer $Na_2HPO_4$ and $KH_2PO_4$, 13 – seawater, 14 – NaCl solution, 15 – fresh water, 16 – centrifugal separator, 17 – sludge tank, 18 – post-reaction water tank, 19 – monitoring system of post-reaction water, 20 – sewage or sea, 21 – exhaust fan, 22 – stack, 23 – re-circulation (optional)

The obtained $NO_x$ removal efficiency in comparison to the previous study is shown in Fig. 8.53. In this version of tests, $NO_x$ removal is above 90% and thus meeting Tier III requirements was obtained.

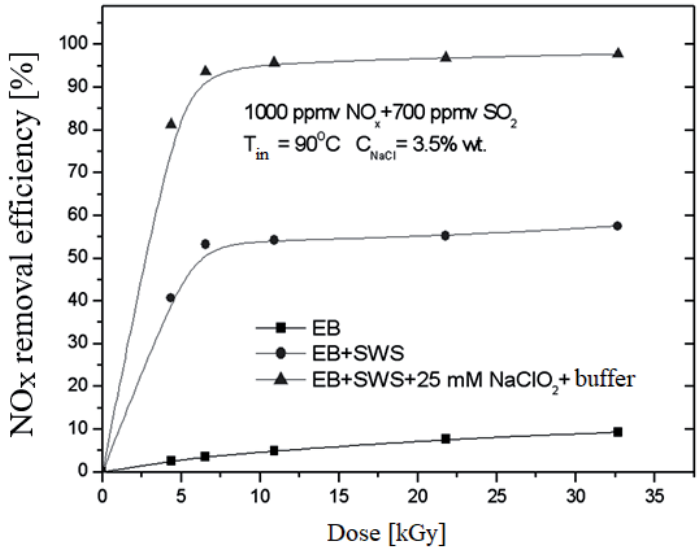


Fig. 8.53. The comparison of the $NO_x$ removal efficiency between technology using electron beam only, hybrid technology, where electron beam was coupled with wet scrubber, and hybrid technology, where electron beam was coupled with wet scrubber as well as with $NaClO_2$ and buffer (the inlet $SO_2$ concentration was 700 ppm and NO was 1000 ppm). EB – irradiation of gases with the electron beam from the accelerator, SWS – seawater scrubber, buffer – Michaelis buffer

The removal efficiency of $SO_2$, in a similar way as in classic scrubbers depends on the scrubber height (number of theoretical absorption plates), liquid/gas ratio and solution alkalinity. Therefore, if over 50% can be achieved in a single step which corresponds roughly to one theoretic plate, it is possible to reduce the height of the absorber.

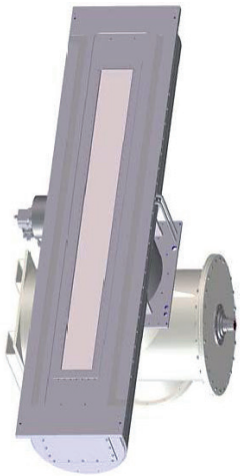

Fig. 8.54. Electron accelerator with the linear cathode

Table 8.28. Main parameters of the accelerator

| Parameter | Value |
|---|---|
| Accelerator voltage | 75-250 kV |
| Electron beam current | 0-2000 mV |
| Working length | 400-3000 mm |
| Throughput | 14 000 kGy m/min |
| Distribution of dosage over the working length | < +/- 10% |
| No cooling of the electron exit window necessary (at room temperature) | |

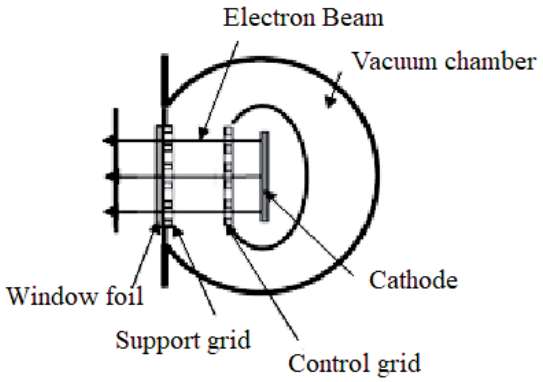


Fig. 8.55. Accelerator with multiple linear cathodes

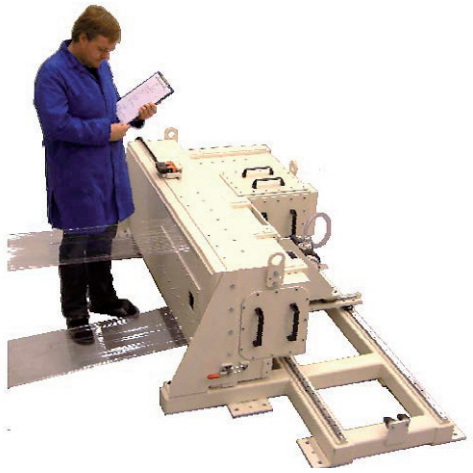

Fig. 8.56. Accelerator with the linear cathode and its operator

**Accelerators for onboard applications**

As it was stated before, the accelerators to be applied on the ship are different type units in comparison with those applied in power industry for coal-fired boiler flue gas treatment. An example of the accelerator which may be applied to the discussed technology is presented in Fig. 8.54 and main parameters are given in Table 8.28.
If the shorter length is needed, the multicathode system has to be applied (Fig. 8.55).
The size of the units in comparison with the operator is presented in Fig. 8.56.

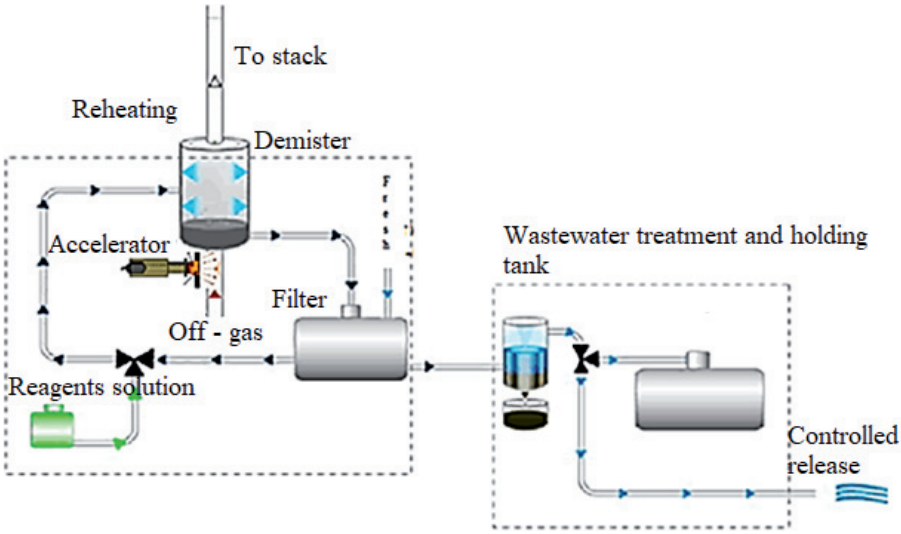


Fig. 8.57. Conceptual scheme of the installation using electron beam technology for $SO_x$ and $NO_x$ removal as applied onboard, water closed or hybrid system

The scheme of planned system installation for simultaneous $SO_x$ and $NO_x$ removal is presented in Fig. 8.57.

Table 8.29. Steps for a new de$SO_x$ and de$NO_x$ installations onboard applications [55]

| | |
|---|---|
| Initial phase | R&D works: process chemistry, process optimization, unit operations, equipment selection |
| Feasibility/conception engineering | Ship requirements, equipment configuration, conception/GA interfacing verifications, feasibility report, capex/opex estimates, project outline |
| Basic engineering, projects planning, contractors' selection | Basic engineering, preliminary approvals, final project plan, sub-contractors, selection, firm offer and contract for turnkey delivery |
| Detailed engineering and procurement | Completion of basic engineering, detailed engineering, procurement, drawings approvals from class, installation preparations |
| Construction and installation | Equipment delivery for prefabrication/installation, prefabrication, installation works and site management |
| Approvals and commissioning | Tests, approvals from flag/class, commissioning, crew training, hand over, start of lifecycle support |

The further R&D tests are being carried out for the process optimization, process engineering and will lead to the techno-economical assumptions elaboration. The closed or hybrid circulation system has to be developed during these experiments to ensure the standard composition of effluents to be discharged to the sea. The works will be performed in a laboratory leading to onshore test installation construction. The further implementation steps leading to pilot plant construction onboard are presented in Table 8.29.

**Conclusions and recommendations**

In order to protect human health and the environment, significant additional cuts in air pollutants emissions in accordance with IMO MARPOL Annex VI are necessary. Currently, several commercial technologies have been implemented onboard to reduce the level of $SO_x$ and $NO_x$ from marine diesel engines. Though these technologies can remove 99% of $SO_2$ and 90% of $NO_x$, they possess a number of important drawbacks. More often than not, two separate technologies for removal of $NO_x$ and $SO_x$ are necessary, which results in high installation cost. However, especially problematic is nitrogen monoxide (95% of all nitrogen oxides) due to its non-reactivity and insolubility. The most well-known $NO_x$ removal system, SCR, is best suited for steady high-load conditions, i.e. SCR is less suited for low load operation and manoeuvring in coastal and harbour areas. The sensitivity of the chemistry between the cylinder and fuel oil also shows limitations for marine operation. This is further emphasized by the need to fit the SCR reactor before the turbocharger due to the required temperature regime. As already mentioned, above 90% of $NO_x$ can be removed, however, some complications and limitations make it more difficult to apply SCR on marine vessels in service. This makes it unfeasible to remove more than 90-95% $NO_x$ due to the risk of ammonia slip (ammonia passing through the SCR unreacted). If we compare the SCR installation on new ships to a retrofitted SCR system it becomes obvious that it is far more complicated to retrofit the installation than to integrate SCR as the ship is being built.

First of all, to find the required space for the catalyst, piping, support, auxiliary equipment, and $NO_x$, $O_2$, and $NH_3$ measuring devices is a challenge and the number of SCR systems installed on two-stroke diesel engines is still limited. Therefore, today an SCR system is specially designed for each main engine. Retrofitting is complicated and not recommendable if the vessel has not been prepared for later SCR installation. To avoid chemical compositions blocking the SCR, the sulphur content in the fuel oil used on engines with SCR is important as is, in particular, the lower exhaust gas temperature limit at the inlet engine. Furthermore, some $SO_x$ will be converted to $SO_3$ in the SCR catalyst and thus create visible smoke. When installing the SCR catalyst, it is important to compensate the exhaust pipe and the component support for vibrations and temperature changes.

Taking everything into consideration, SCR is most common and well-known $NO_x$ removal system on stationary outposts, but it is not the best solution for marine vessels, due to numbers of limits and disadvantages, such as high installation cost, significant dimensions or necessity of catalyst removal as well as inconvenient process conditions.

Different other solutions, like humid air motor, exhaust gas recirculation or some simultaneous $SO_2$ and $NO_x$ removal systems have been also investigated in relation to the new MARPOL Annex VI limits, but, to date, they are insufficient or they were not tested enough to be successfully implemented onboard and to meet Tier III strict regulations. Hence, to accomplish major reductions in both $SO_x$ and $NO_x$ emissions, a new onboard installation of exhaust emission control is required and it may be an electron beam flue gas treatment process, which is one of the most effective methods of removing $SO_2$ and $NO_x$ from industrial flue gases.

The study was performed in the laboratory plant with $NO_x$ concentration up to 1700 ppmv and $SO_2$ concentration up to 1000 ppmv. Such high $NO_x$ and $SO_2$ concentrations were observed in the exhaust gases from marine high-power diesel engines fuelled with different heavy fuel oils. In the first part of the study, the simulated exhaust gases were irradiated by the electron beam from the accelerator. The simultaneous removal of $SO_2$ and $NO_x$ were obtained and their removal efficiencies strongly depend on irradiation dose and inlet $NO_x$ concentration. For $NO_x$ concentrations above 800 ppmv, low removal efficiencies were obtained even if applied high doses. In the second part of the study, the irradiated gases were directed to the seawater scrubber

for further purification. The scrubbing process enhances removal efficiencies of both pollutants. The $SO_2$ removal efficiencies above 98.5% were obtained with irradiation dose greater than 5.3 kGy (in one theoretical plate scrubber only). For inlet $NO_x$ concentrations of 1700 ppmv the $NO_x$ removal efficiency about 51% was obtained with the dose greater than 8.8 kGy. In the third part of the study, 25 mM $NaClO_2$ and the appropriate amount of Michaelis buffer, maintaining the water pH at 6.25 were added to the seawater. The exhaust gas was first irradiated with the electron beam technology to reduce the NO, in the dose range of 10-12 kGy with a temperature of the exhaust gas not exceeding 90°C and then followed by a wet scrubber method with appropriately prepared process water, with an addition of the strong oxidant $NaClO_2$. Further research on closed loop applications is needed. In this version of tests, $NO_x$ removal was above 90% and thus meeting Tier III requirements was obtained.

The results of this study indicate that electron beam combined with wet scrubbing and $NaClO_2$ oxidant is a very promising technology to be applied in the simultaneous reduction of high concentrations of $NO_x$ and $SO_2$ emitted from diesel engines on ships, which are the main sources of $SO_2$ and $NO_x$ pollution along their navigation routes. No solid state catalyst is required and reactor cross-section is free of any packing. It is now required, to execute the full material and energy balance as well as the equipment cost analysis and thereafter realization of the first test onboard. These data will be obtained when planned R&D programme will be concluded. The steps to be carried out before pilot plant onboard installation was presented at the end of the paper.

*This work is financed by the National Centre for Research and Development (Poland) project Tango 2 'Plasma technology for high $NO_x$ treatment on off-gases'.*

## 8.2. BALLAST WATER TREATMENT

Discharge of sea water used for ballasting ships poses a threat to coastal ecosystems. Introduction of alien species as a result of ballast water exchange may lead to excessive development of these organisms in the new environment and cause a threat to native plant and animal communities. Low salinity is the basic natural factor shaping the biodiversity of the Baltic Sea and results in a small, in comparison with other seas, species diversity. Therefore, brackish seas, such as the Baltic Sea, are particularly sensitive to newly introduced species because they are poor in native species.

In 2004, the International Maritime Organization developed the International Convention for the Control and Management of Ships' Ballast Water and Sediments (BWM Convention). The BWM Convention entered into force globally on 8 September 2017. It provides a uniform legal regulation of the ballast water handling in order to prevent the spread of potentially harmful aquatic organisms and pathogens around the world.

There are two ballast water management standards (D-1 and D-2). From the date of entry into force of the BWM Convention, all ships must conform to at least the D-1 standard, and all new ships – to the D-2 standard. The D-1 standard requires ships to exchange their ballast water in open seas, away from coastal areas. The D-2 standard specifies the maximum amount of viable organisms allowed to be discharged, including specified indicator microbes harmful to human health. The D-2 standard specifies that ships can only discharge ballast water that meets the following criteria:

- less than 10 viable organisms per cubic metre which are greater than or equal to 50 μm in minimum dimension,
- less than 10 viable organisms per millilitre which are between 10 μm and 50 μm in minimum dimension.

Amount of the harmful microorganisms present in the discharged ballast water should be:

- less than 1 colony-forming unit (cfu) per 100 ml of toxicogenic *Vibrio cholerae*,

- less than 250 cfu per 100 ml of *Escherichia coli*,
- less than 100 cfu per 100 ml of intestinal *Enterococci*.

Several ballast water treatment technologies have been certified according to the IMO guidelines, however further evaluation is necessary with regards to new marine organisms with emphasis on higher organisms, development of new processes at lab, pilot and full-scale, as well as studying the environmental implications of these technologies.

There are two main categories of ballast water treatment methods: primary and secondary separation techniques. Primary separation includes physical methods of separation such as filtration and hydrocyclones. Secondary separation includes a wide range of mechanical and chemical methods or a combination of them applied to ballast tanks. The most common mechanical methods include ultraviolet (UV) radiation, thermal, ultrasound (US), magnetic and electrical treatment. Chemical methods include the use of biocides, chlorine, ozone, hydrogen peroxide, chlorine dioxide and others [56]. Very strict requirements regarding ballast water and sediments discharged to the environment together with limitations of the technologies currently used for the ballast water treatment motivates to the implementation of the new solutions, which can ensure the high effectiveness of the microbiological decontamination of the ballast water and sediments simultaneously being friendly for the environment.

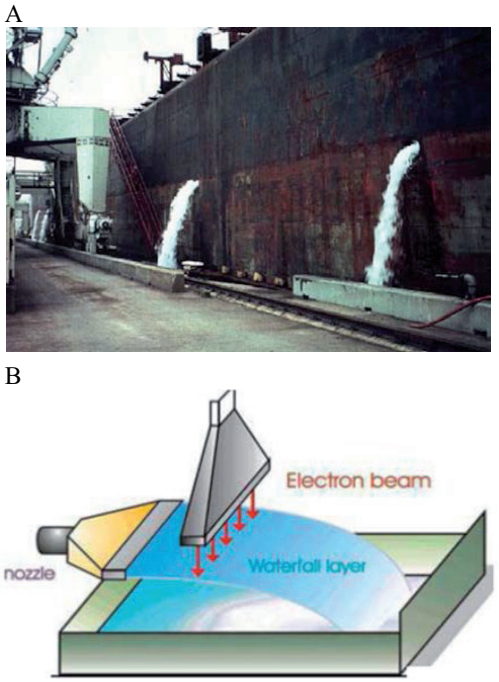


Fig. 8.58. Discharge of ballast water from a ship in dry dock (A) and conception of wastewater treatment (B)

The ship before entering shipyard has to replace the ballast water (with its antibiological treatment) at open sea waters. However, some water still remains together with solid state sediment containing biological contamination. When ship is placed in the dry dock for she's maintenance, repair, painting, etc., this ballast water has to be discharged (Fig. 8.58) and ship water sanitization units based on UV or chemical method applications are not effective.

Therefore the best solution can be based on application of ionizing radiation, used widely for sterilization. Application of low-energy electron beam accelerator for the ballast water and sediments management can be very promising alternative to currently used systems. Electrons

are an effective agent for irradiation because they are not strongly scattered by turbidity, can penetrate deeply into organic materials, and are more ionizing than ultraviolet light [57, 58]. The primary advantages of this technology are as follows: there is no need to add any chemicals to the water supply, no by-products are created, and has no specialized storage requirements. The radiation sensitivity of a microorganism generally depends on the amount of DNA in the nucleus. The lethal dose depends on how well the organism is protected from electron penetration.

The $D_{10}$ values, which are defined as the incremental doses that are required to reduce the surviving number of microorganisms by a factor of ten, or one log, for the microorganisms included in the BWM Convention are known from the literature and are really low.
$D_{10}$ dose [kGy] resulting in a tenfold reduction in the population is [59-61]:

– *Vibrio cholerae*, *Vibrio parahaemolyticus*, *Vibrio vulnificus*: 0.1 kGy;
– *Escherichia coli*: 0.5 kGy;
– *Enterococci*: 0.6 kGy.

This suggests that irradiation doses required for the microbiological decontamination of the ballast water and sediments even with the high bioburden level will be low, what have positive impact on the cost-effectiveness of the process.

The most feasible for this application is self-shielded electron accelerator. An important additional effect of the re-dithering process is the degradation of a number of harmful compounds, like organic compounds. Additionally the use of radiation treatment allows for the complete elimination of nematodes and parasitic eggs (*Ascaris sp., Trichuris sp., Toxocara sp., ATT*) and the practical elimination of pathogens, such as contagious bacterial contamination and *Coliform* titer (decrease by three orders of magnitude for a dose of 1 kGy), *Clostridium perfrigenes* titer (decrease by five orders of magnitude for a dose of 1 kGy).

Sediment from the bottom of ballast tanks, due to their consistency, requires the development of special treatment methods. It is necessary to perform dosimetric tests allowing to determine the depth of penetration of the electron beam inside the material being processed. Construction of the irradiation chamber is also very important issue to resolve. The process of optimizing the construction of a sludge irradiation chamber should include testing the method of forming a product stream with process parameters appropriate for the process (geometric dimensions, flow velocity) associated with the energy of the electron beam and the dose.

The selection of an accelerator for a radiation installation requires taking into account a number of technical and economic factors and is made after a detailed analysis of a number of factors. The most important are: appropriate range of energy and power of the average beam of accelerated electrons, knowledge of the technology used by the manufacturer and positive feedback from users of accelerators. These parameters should be verified in detail based on the offer data and the implementation of specific construction and installation conceptions. Estimated capital costs related to the purchase price of the electron accelerator are the following:

- shielding and ventilation: 15%,
- building with fittings: 30%,
- technological equipment: 20%,
- process control system: 5%,
- technical design and permits: 10%,
- installation and validation: 10-20%,
- depreciation (10 years): 10%,
- cost of service work (fixed/variable): 3-5%.

When designing a ballast water treatment installation, the key information, besides the content of organic pathogens, is their physical and chemical composition. The process streams may contain solid impurities from more than a few centimetres to suspensions with a micron particle size, oil fractions, silica, abrasive residues, dissolved substances, metal ions such as iron, copper, zinc, chromium, nickel, other heavy metals, chlorides and sulphates. After preliminary separation of large diameter solid particulates, processes such as sedimentation, flocculation, coagulation, flotation, neutralization, separation, extraction, sorption, electrolysis and many

others can be used to remove other pollutants. Depending on the composition of the ballast water, it is possible to purify the ballast water stream using one or more of these methods.

## 8.3. 'ZERO ENERGY' TECHNOLOGY FOR SLUDGE HYGIENIZATION

Waste management originated from wastewater treatment plants (WWPs) is a worldwide growing problem. Nowadays domestic sewage is being cleaned mostly with the use of the method of activated sludge. Further utilization of excess sludge is regulated by the EU directives:

- Council Directive 86/278/EEC on the protection of the environment, and in particular of the soil, when sewage sludge is used in agriculture;
- Water Framework Directive 2000/60/EC on water protection;
- Directive 91/271/EEC on urban waste water treatment;
- Directive 96/61/EC concerning integrated pollution prevention and control;
- Directive 99/31/EC on the landfill of waste;
- Waste Framework Directive 2008/98/EC protection of the environment, pollution control, water protection and landfill of wastes.

According to current regulations sludge arising from wastewater treatment can be used but only after elimination of threat for human health and environment. Waste Framework Directive 2008/98/EC lays down some basic waste management principles: it requires that waste must be managed without endangering human health and harming the environment, and in particular without risk to water, air, soil, plants or animals, without causing a nuisance through noise or odours, and without adversely affecting the countryside or places of special interest.

Excess of activated sludge has high organic matter content and can be utilized in thermal processes, in anaerobic digestion (AD) process to produce biogas or be used in agriculture. Thermal process including drying and burning, is not an environmentally friendly method due to greenhouse gas and dioxins emissions. The energy yield of this method which uses a burning process is reduced due to high levels of hydration of the biomass, which requires the moisture to be evaporated unproductively. Thus the preferred method is methane fermentation whereby biogas is produced. Anaerobic digestion is a technology which allows generation of renewable energy. During AD, microorganisms break down the organic matter contained in the sludge and convert it into biogas. Biogas, which contains mainly methane, can be used for simultaneous electricity and heat production. During such a process, mineralization of the sludge takes place which leads to reduction of its mass, but remaining digestate needs to be disposed of. The digestate thus processed constitutes a valuable fertilizer, especially if enriched with additional mineral components. However, as tests show, the process of fermentation does not eliminate microbiological contamination completely. The main problem for agriculture application is contamination by human and animal parasites, their eggs, and also pathogenic bacteria. Therefore an additional process of hygienization is required to make it safe. One of the methods for sludge treatment consists in drying and burning, which is not an environmentally friendly method due to greenhouse gas and dioxins emissions. The energy yield of this method which uses a burning process is reduced due to high levels of hydration of the biomass, which requires the moisture to be evaporated unproductively. Thus the preferred method is methane fermentation whereby biogas is produced. Excess sludges from municipal sewage treatment plants contain organic and inorganic components valuable as soil fertilizer, so if disinfected they can be beneficial recycled in agriculture instead of being burdensome waste. The control of microbiological contamination of the sludge include following methods:

- feedstock control to exclude hazardous biomass from anaerobic digestion,
- feedstock pasteurization,
- pressure hygienization,
- radiation hygienization.

Table 8.30. Bacteria and their spore radiosensitivity

| Bacteria | Bacteria content/index | | | |
|---|---|---|---|---|
| | 0 | 5,0 | 7,5 | 10,0 |
| Spore forming bacteria in 1 ml | $8.4 \cdot 10^4$ | $2.5 \cdot 10^3$ | $2.1 \cdot 10^3$ | $2.0 \cdot 10^2$ |
| *Coliform* counts | $10^{-7}$ | $10^{-5}$ | $10^{-4}$ | $10^{-4}$ |
| *Clostridium perfringens* counts | $10^{-6}$ | $10^{-5}$ | $10^{-4}$ | $10^{-1}$ |

Radiation technologies have been commercially applied for wastewater and sludge treatment [62]. It has been demonstrated that ionizing radiation destroys microorganisms and it can eliminate even resistant spore forming bacteria [63]. Effective reduction in number of bacteria and parasite eggs can be achieved applying doses up to 7 kGy [64]. Regarding radiation hygienization experiments have been performed at the INCT to test influence of 10 MeV electron beam on bacteria, parasites and parasite eggs content in municipal sewage sludges from different locations in Poland. Double-begged samples of sludges (I kg weight and 2.5-3 cm thick) were irradiated with the doses of 5-7 kGy with the use of Russian electron accelerator LAE 13/9 type. Total bacteria content, spore-forming bacteria content, *Coliform* counts and *Clostridium perfringens* counts (Table 8.30), as well as the number of parasites and their eggs (Table 8.31) were determined.

Table 8.31. Adult parasites and their eggs radiosensitivity

| Dose [kGy] | Nematodes | | | |
|---|---|---|---|---|
| | Adults | Eggs [pcs/kg dry mass] | | |
| | | *Ascaris sp.* | *Trichuris sp.* | *Toxocara sp.* |
| 0 | many living | 480 | 320 | 320 |
| 5.0 | 0 | 0 | 0 | 0 |
| 7.5 | 0 | 0 | 0 | 0 |
| 10.0 | 0 | 0 | 0 | 0 |

The dose of 6 kGy kills all parasite eggs and decreases total bacteria content by 3 logs, spore-forming bacteria and *Coliform* counts by 2 logs and *Clostridium perfringens* counts by 1 log. It should be added that all adult parasites are killed, too, as they are much more radiosensitive than their eggs. On the basis of experiments the conception of installation has been designed for disinfection of dewatered sewage sludges (Fig. 8.59).

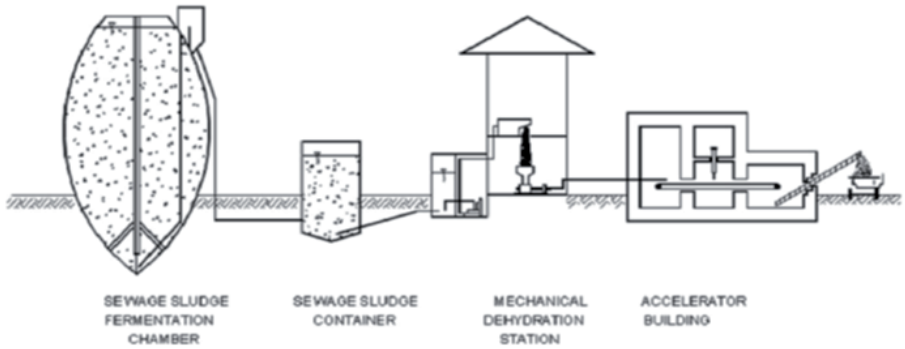


Fig. 8.59. Conception of sludge hygienization plant with 10 MeV, 10 kW accelerator

A typical electron beam sludge treatment plant consists of sludge feeding system, electron accelerator with shield structure. Dewatered sludge is spread through a flat wide nozzle onto a stainless steel conveyor belt and fed past the electron beam in an 8-40 mm thick layer at a rate that provides an absorbed dose of 5-10 kGy; the maximum feed rate is 3 ton/h. The thickness of sludge depends on the energy of electron beam. After irradiation, the sludge is moved to a conveyor belt where it is composted under conditions of controlled aeration and frequent mixing. The irradiated sludge, being pathogen free, can be beneficially used as manure in agricultural fields, as it is rich in required soil nutrients.

One of the methods for sludge treatment consists in drying and burning, which is not an environmentally friendly method due to greenhouse gas and dioxins emissions. The energy yield of this method which uses a burning process is reduced due to high levels of hydration of the biomass, which requires the moisture to be evaporated unproductively. Thus the preferred method is methane fermentation whereby biogas is produced. Recently the INCT has developed a new technology regarding biogas two-stage plant engineering and two 1.2 MW units have been constructed.

On the basis of this developments a new conception of 'zero energy' sludge hygienization technology was elaborated. The use of electron accelerators as ionizing radiation source creates new opportunities for the irradiation technology, both environmental and economic justification of usage. An electron accelerator can be powered with energy provided by a cogenerator fuelled by biogas produced in the process of sludge methane fermentation. Such solution, described in patent application P-419131 [65] can be defined as 'zero energy' method of sludge treatment. According to the invention, biomass originating from waste prior to its fermentation or digestate derived in the process of methane fermentation is irradiated with electron beams that use energies from 1 MeV to 10 MeV, preferably 1-3 MeV. For a digestate derived in the process of fermenting biomass originating from waste and having a liquid form with the content of dry matter less than 5%, the radiation dose is from 1 kGy to 5 kGy, whereas for a digestate from which the aqueous phase has been filtered out and which has a dry matter content up to 30%, the radiation dose is from 5 kGy to 20 kGy.

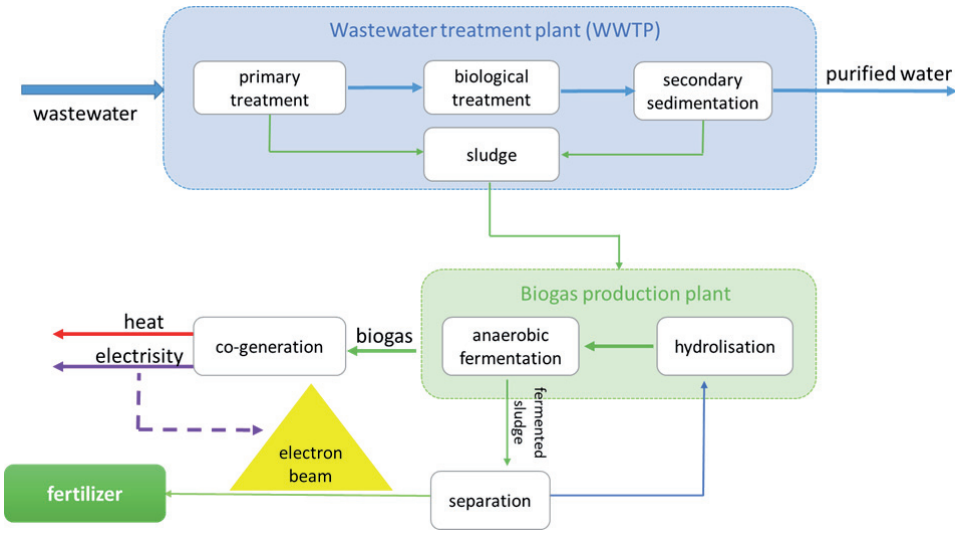


Fig. 8.60. 'Zero energy' sludge hygienization technology principle

An electron accelerator is favourably powered with energy provided by a cogenerator fuelled by biogas produced in the process of methane fermentation (Fig. 8.60).

According to conception of 'zero energy' technology for sludge hygenization, presented in Fig. 8.60, biomass originating from wastewater treatment plant after its fermentation in the process of anaerobic digestion and separation is irradiated with electron beams. The advantage of the method consists in the fact that the energy is generated from renewable waste material which is widely available. It does not require energy from external sources and, thanks to the fact that irradiated digestate is utilized as a fertilizer, does not generate wastes. The method allows pathogens to be eliminated from sludge and does not have a negative impact on the environment.

## References


[1]. Nunes, R.A.O., Alvim-Ferraz, M.C.M., Martins, F.G., & Sousa, S.I.V. (2017). The activity-based methodology to asses ship emissions – A review. *Environ. Pollut.*, *231*, 87-103.

[2]. Petranović, Z., Besenić, T., Vujanović, M., & Duić, N. (2017). Modelling pollutant emissions in diesel engines, influence of biofuel on pollutant formation. *J. Environ. Manage.*, *203*, 1038-1046.

[3]. Lloyd's Register. (2012). *Understanding exhaust gas treatment systems. Guidance for shipowners and operators*. London.

[4]. Viana, M., Hammingh, P., Colette, A., Querol, X., Degraeuwe, B., Vlieger, I., & Aardenne, J. (2014). Impact of maritime transport emissions on coastal air quality in Europe. *Atmos. Environ.*, *90*, 96-105.

[5]. European Environment Agency. (2013). *The impact of international shipping on European air quality and climate forcing*. EEA Technical report No 4/2013.

[6]. Winnes, H., & Fridell, E. (2010). Emission of $NO_x$ and particles from manoeuvring ships. *Transport. Res. Part D*, *15*, 204-211.

[7]. International Maritime Organization. (2017). *IMO what it is*. London.

[8]. International Maritime Organization. (2017). *List of conventions, other multilateral instruments and amendments in respect of which the organization performs depositary and other functions*.

[9]. International Maritime Organization. (2005). International Convention for the Prevention of Marine Pollution from Ships, 1973, as modified by the Protocol of 1978 relating thereto (MARPOL 73/78). Annex VI: Prevention of Air Pollution from Ships.

[10]. Shaolong, Y., Xinxiang, P., Zhitao, H., Dongsheng, Z., Bojun, L., Dekang, Z., & Zhijun, Y. (2018). Removal of $NO_x$ and $SO_2$ from simulated ship emissions using wet scrubbing based on seawater electrolysis technology. *Chem. Eng. J.*, *331*, 1, 8-15.

[11]. Giernalczyk, M. (2014). Analiza możliwości redukcji emisji związków toksycznych oraz $CO_2$ poprzez ograniczenie zużycia paliwa przez statki morskie. *Zeszyty Naukowe Akademii Morskiej w Gdyni*, 83, 53-65.

[12]. Talebizadeh, P., Babaie, M., Brown, R., Rahimzadeh, H., Ristovski, Z., & Arai, M. (2014). The role of non-thermal plasma technique in $NO_x$ treatment: A review. *Renew. Sust. Energy Rev.*, *40*, 886-901.

[13]. Stratakis, G.A. (2004). *Experimental investigation of catalytic soot oxidation and pressure drop characteristics in wall-flow diesel particulate filters*. Doctoral dissertation, University of Thessaly, Greece. PhD Thesis UTh/MIE No. (11).

[14]. Pauleta, S.R, Dell'Acqua, S., & Moura, I. (2013). Nitrous oxide reductase. *Coord. Chem. Rev.*, *257*, 332-49.

[15]. National Aeronautics and Space Administration. (2011). *4 Stroke Internal Combustion Engine*. Received May 25, 2018, from https://www.grc.nasa.gov/WWW/K-12/airplane/engopt.html.

[16]. Cengel, Y.A., & Boles, M.A. (2014). *Thermodynamics: An engineering approach* (8th edition). McGraw Hill Education.

[17]. MAN Diesel & Turbo. (2017). *Emission control. MAN B&W Two-Stroke Diesel Engines*. Denmark.

[18]. Rajput, R.K. (2017). *A textbook of automobile engineering*. Delhi: Laxmi Publications.

[19]. MAN Diesel & Turbo. (2017). *Marine Engine IMO Tier II and Tier III Programme*. Denamark.

[20]. Austin, C., Macdonald, F., & Rojon, I. (2015). *Marine scrubbers: The guide 2015*. Fathom.

[21]. MAN Diesel & Turbo. (2012). *Tier III two-stroke technology*. Denmark.

[22]. Warych, J. (1999). *Procesy oczyszczania gazów. Problemy projektowo-obliczeniowe*. Warszawa: Oficyna Wydawnicza Politechniki Warszawskiej.
[23]. Treybal, R.E. (1981). *Mass-transfer operations* (3rd edition). New York: McGraw-Hill Book Company.
[24]. Warych, J. (1996). *Aparatura chemiczna i procesowa*. Warszawa: Oficyna Wydawnicza Politechniki Warszawskiej.
[25]. Baukal, Jr., E.C. (2003). *Industrial combustion pollution and control*. Boca Raton: CRC Press.
[26]. Ruthven, D.M. (1984). *Principles of adsorption and adsorption processes*. John Wiley & Sons.
[27]. Knaebel, K.S. (2018). *A "How To" Guide for Adsorber Design*. Retrived May 205, 2018, from http://www.adsorption.com/wp-content/uploads/2016/04/AdsorberDes2.pdf.
[28]. Chen, X. (2015). Modelling of experimental adsorption isotherm data. *Information*, *6*, 14-22.
[29]. Raptotasios, S.I., Sakellaridis, N.F., Papagiannakis, R.G., & Hountalas, D.T. (2015). Application of a multi-zone combustion model to investigate the $NO_x$ reduction potential of two-stroke marine diesel engines using EGR. *Appl. Energy*, *157*, 814-823.
[30]. European Environmental Bureau (EEB), European Federation for Transport and Environment (T&E), Seas At Risk (SAR), Swedish NGO Secretariat on Acid Rain. (2004). *Air pollution from ships*. Retrieved March 15, 2018, from http://www.airclim.org/sites/default/files/documents/shipbriefing_nov04.pdf.
[31]. Guo, M., Fu, Z., Ma, D., Ji, N., Song, C., & Liu, Q. (2015). A short review of treatment methods of marine diesel engine exhaust gases. *Procedia Eng.*, *121*, 938-943.
[32]. Yara Marine Technologies. (2017). *$NO_x$ cleaning technology*. Retrieved March 15, 2016, from https://yaramarine.com/nox-cleaning-technology/.
[33]. Wang, Z., Zhou, S., Feng, Y., & Zhu, Y. (2017). Research of $NO_x$ reduction on a low-speed two--stroke marine diesel engine by using EGR (exhaust gas recirculation) - CB (cylinder bypass) and EGB (exhaust gas bypass). *Int. J. Hydrogen Energy*, *42*, 19337-19345.
[34]. Borkowski, T., Myśków, J., Hołub, M., & Kalisiak, S. (2007). Development of the low temperature plasma $NO_x$ control system for the marine diesel engine. *Journal of KONES Powertrain and Transport*, *14*, 3, 91-99.
[35]. Jolibois, J., Takashima, K., & Mizuno, A. (2012). Application of a non-thermal surface plasma discharge in wet condition for gas exhaust treatment: $NO_x$ removal. *J. Electrostat.*, *70*, 300-308.
[36]. Reddy, P.M.K., Raju, P.R., Karuppiah, J., Reddy, E.L., & Subrahmanyam, C. (2013). Degradation and mineralization of methylene blue by dielectric barrier discharge non-thermal plasma reactor. *Chem. Eng. J.*, *217*, 41-47.
[37]. Myśków, J., Borkowski, T. Bludszuweit, M., & Fröhlingsdorf, W. (2011). Marine exhaust gas emission after treatment system concept. *Journal of KONES Powertrain and Transport*, *18*, 4.
[38]. Deng, Z.P. (2013). *An experimental study to reduce $NO_x$ of the marine diesel engine by SCR*. Beijing University of Technology, China.
[39]. Clean Air Technology Center. (1999). *Nitrogen oxides ($NO_x$), why and how they are controlled*. Technical Bulletin EPA-456/F-99-006R.
[40]. Ammar, N.R., & Seddiek, I.S. (2017). Eco-environmental analysis of ship emission control methods: Case study RO-RO cargo vessel. *Ocean Eng.*, *137*, 166-173.
[41]. Boscarato, I, Hickey, N., Kašpar, J., Prati, M.V, & Mariani, A. (2015). Green shipping: marine engine pollution abatement using a combined catalyst/seawater scrubber system. 1. Effect of catalyst. *J. Catal.*, *328*, 248-257.
[42]. Licki, J., Pawelec, A., Zimek, Z., & Witman-Zając, S. (2015). Electron beam treatment of simulated marine diesel exhaust gases. *Nukleonika*, *60*(3), 689-695.
[43]. Pourmohammadbagher, A., Jamshidi, E., Ale-Ebrahim, H., & Dabir, S. (2011). Study on simultaneous removal of $NO_x$ and $SO_2$ with $NaClO_2$ in a novel swirl wet system. *Ind. Eng. Chem. Res.*, *50*(13), 8278-8284.
[44]. Sada, E., Kumazawa, H., Yamanka, Y., Kudo, I., & Kondo, T. (1978). Kinetics of absorption of sulfur dioxide and nitric oxide in aqueous mixed solutions of sodium chlorite and sodium hydroxide. *J. Chem. Eng. Jpn.*, *11*, 276.
[45]. Yang, C.L., & Shaw, H. (1998). Aqueous absorption of $NO_x$ induced by sodium chlorite oxidation in the presence of sulfur dioxide. *Environ. Prog.*, *17*, 80.

[46]. Chien, T.W., & Chu, H. (2000). Removal of $SO_2$ and NO from flue gas by wet scrubbing using an aqueous $NaClO_2$ solution. *J. Hazard. Mater.*, *80*, 43.
[47]. Chien, T.W., Chu, H., & Hsueh, H.T. (2003). Kinetic study on absorption of $SO_2$ and $NO_X$ with acidic $NaClO_2$ solutions using the spraying column. *J. Environ. Eng.*, *129*, 967.
[48]. Chu, H., Chien, T.W., & Li, S.Y. (2001). Simultaneous absorption of $SO_2$ and NO from flue gas with $KMnO_4$/NaOH solutions. *Sci. Total Environ.*, *275*, 127.
[49]. Jin, D.S., Deshwal, B.R., Park, Y.S., & Lee, H.K. (2006). Simultaneous removal of $SO_2$ and NO by wet scrubbing using aqueous chlorine dioxide solution. *J. Hazard. Mater.*, *135*, 412.
[50]. Chandrasekara, P.K., Chung, S.J., Raju, T., & & Moon, I.S. Experimental aspects of combined $NO_X$ and $SO_2$ removal from flue-gas mixture in an integrated wet scrubber-electrochemical cell system. *Chemosphere*, *76*, 657.
[51]. Deshwal, B.R., Jin, D.S., Lee, S.H., Moon, S.H., Jung, J.H., & Lee, H.K. (2008). Removal of NO from flue gas by aqueous chlorine-dioxide scrubbing solution in a lab-scale bubbling reactor. *J. Hazard. Mater.*, *150*, 649.
[52]. Frank, W.N. (1995). Economics of the electron beam process. *Radiat. Phys. Chem.*, *45*, 6, 1017-1019.
[53]. Chmielewski, A.G., & Han, B. (2017). Electron beam technology for environmental pollution control. In M. Venturi, M. D'Angelantonio (Eds.), *Applications of radiation chemistry in the fields of industry, biotechnology and environment* (pp. 37-66). Springer. Series: Topics in Current Chemistry Collections.
[54]. Chmielewski, A.G. Zwolińska, E., Licki, J., Sun, Y., Zimek, Z., & Bułka, S. (2018). A hybrid plasma-chemical system for high-$NO_x$ flue gas treatment. *Radiat. Phys. Chem.*, *144*, 1-7.
[55]. Wärtsilä Corporation. (2013). *Environmental Solution: Retrofit Solutions*. Retrieved May 25, 2018, from http://cdn.wartsila.com/docs/default-source/product-files/egc/brochure-o-env-retrofit-solutions.pdf?sfvrsn=18.
[56]. Tsolaki, E., & Diamadopoulos, E. (2010). Technologies for ballast water treatment: a review. *J. Chem. Technol. Biotechnol*., *85*, 19-32. DOI: 10.1002/jctb.2276.
[57]. Fisch, M. (2010). Study of electron beam mitigation of ballast water. In *Proposal to the US PA*.
[58]. Maruthi, Y.A., Das, N.L., Hossain, K., Sarma, K.S.S., Rawat, K.P., & Sabharwal, S. (2011). Disinfection and reduction of organic load of sewage water by electron beam radiation. *Appl. Water Sci*., *1*, 49-56. DOI 10.1007/s13201-011-0008-z.
[59]. Mallett, J.C., Beghian, L.E., Metcalf, T.G., & Kaylor, J.D. (1991). Potential of irradiation technology for improved shellfish sanitation. *J. Food Safety*, *11*, 231-245. DOI: 10.1111/j.1745-4565.1991.tb00055.x.
[60]. Kong, Q., Wu, A., Qi, W., Qi, R., Carter, J.M., Rasooly, R., & He, X. (2014). Effects of electron--beam irradiation on blueberries inoculated with *Escherichia coli* and their nutritional quality and shelf life. *Postharvest Biol. Technol.*, *95*, 28-35. DOI: 10.1016/j.postharvbio.2014.04.004.
[61]. Aguirre, J.S., Rodríguez, M.R., & García de Fernando, G.D. (2011). Effects of electron beam irradiation on the variability in survivor number and duration of lag phase of four food-borne organisms. *Int. J. Food Microbiol.*, *149*, 236-246. DOI: 10.1016/j.ijfoodmicro.2011.07.003.
[62]. Chmielewski, A.G. (2011). Electron accelerators for environmental protection. *Reviews of Accelerator Science and Technology*, 4, 147-159.
[63]. Skowron, K., Paluszak, Z., Olszewska, H., Wieczorek, M., Zimek, Z., & Śrutek, M. (2014). Effectiveness of high energy electron beam against spore bacteria and viruses in slurry. *Radiat. Phys. Chem.*, *101*, 36-40.
[64]. Chmielewski, A.G., Zimek, Z., Bryl-Sandelewska, T., & Kosmal, W. (1995). Disinfection of municipal sewage sludges in installation equipped with electron accelerator. *Radiat. Phys. Chem.*, *46*(4-6), 1071-1074.
[65]. Chmielewski, A.G., Palige, J., Roubinek, O., Zimek, Z., Gryczka, U., Usidus, J., Pietrzak, K., & Edgecock, R. (2016). *Sposób higienizacji osadów ściekowych* (Method for hygienization of sewage sludge). Patent application P-419131.

[#] Section 8.1 of this chapter was published as the INCT report – *Raporty IChTJ. Seria B nr 2/2018* and is available on the INCT website: http://www.ichtj.waw.pl/ichtj/publ/b_report/b2018_02.htm.

## Chapter 9

# SUMMARY

This book is a result of work carried out under the Horizon 2020 project "Accelerator research and innovation for European science and society" (ARIES) and concerns the development of new technologies to ensure that future accelerators will be more affordable, reliable, sustainable and more effective. Considerations include energy efficiency, new accelerator conceptions, new high-temperature superconductors, new superconducting coatings and new materials for thermal management. The examples presented in the book are a good basis for planning such a development. The present state of technologies based on electron accelerators implemented by the Institute of Nuclear Chemistry and Technology (INCT) with discussion of the advantages and disadvantages of machines is a good platform to plan future actions to ensure that achievements of WP 3 "Industrial and societal applications (ISA)" will be widely adopted in the industrial world.

Knowledge-based economy is one of the important attributes of a modern state. Radiation technology is a modern, important from the point of view of the development of research and practical applications, area belonging to the high-tech. It is opening an opportunity to create innovative industries. The INCT launched a major European and world research potential and application in the field of electron accelerators, which enabled the implementation of many radiation technologies such as radiation sterilization of disposable medical equipment and transplantation grafts (INCT), production of heat-shrinkable tubes (RADPOL, Człuchów licensed by the INCT and some foreign institutions), modification of semiconductor devices (Lamina, Piaseczno licensed by the INCT), food irradiation (INCT), radiation removal of $SO_2$ and $NO_x$ from flue gas (Pomorzany Power Station, Szczecin licensed by the INCT and tested in Bulgaria and Saudi Arabia), as well as the use of ionizing radiation for conservation of cultural heritage objects, environment protection and other practical applications.

Activities in the field of chemistry and radiation technology based on the use of electron accelerator began in Poland, when the first accelerator (electron energy: 5-13 MeV, average beam power: 9 kW) was put into operation in the INCT in 1971. For many years, the LAE 13/9 accelerator was the only source of ionizing radiation in the form of electron beam available in the country. The installation of low energy electron accelerator ILU 6 type with energy of 0.5-2 MeV and beam power of up to 20 kW was another technical challenge. The investment was closely related to the developed technologies for obtaining heat-shrinkable tubes and tapes. Both of these technologies were implemented using the ILU 6 accelerator applied at the pilot polymer radiation processing plant. In addition, the ILU 6 accelerator was used in laboratory installations to remove $SO_2$ and $NO_x$ from flue gases. These study had a significant impact on the launch of the pilot plant at Kawęczyn Power Station (two accelerators with an electron energy of 0.7 keV and beam power of 50 kW each). A significant breakthrough occurred in the removal of $SO_2$ and $NO_x$ from flue gases with the use of electron beam when the industrial installation at the Pomorzany Power Station was built and commissioned. This installation with four accelerators with an electron energy of 0.8 MeV and a beam power of 300 kW each was intended for the purification of flue gas stream with a volume flow of 270 000 $Nm^3/h$. Operation of the pilot plant developed in cooperation with EB Tech (Republic of Korea) in Saudi Arabia has proved that this technology can also be used for the purification of flue gases from heavy oil fired boilers.

The development of the accelerator base at the INCT, intended for the radiation sterilization of disposable medical devices, was particularly important. It was an installation of a dedicated linear accelerator (1993) with a nominal energy of 10 MeV and a beam power of 10 kW, and an accelerator built and running at its own with an energy of 10 MeV and a beam power of 15 kW. The base is supplemented with a linear accelerator (10 MeV, 10 kW) designed

for hygienization of agricultural products, an effective method of food preservation and sanitization, consisting in elimination or reduction of pathogenic microorganisms in food to a level that ensures its safe consumption and food spoilage.

The development of scientific research in the field of radiation chemistry required the extension of the accelerator base designed to carry out experimental work. The need to obtain specific time parameters of the electron beam, appropriate to the requirements of dynamically developing kinetic studies, caused that decision was made to build a research installation equipped with LAE 10 accelerator for kinetic studies using nanosecond pulse radiolysis method. The greatest achievement of radiation chemistry was the discovery of a hydrated electron, which is crucial for the course of transient processes and understanding the mechanisms of radical reactions.

Progress in the development of radiation technologies creates opportunities for their various industrial applications, especially in the field of materials engineering, medicine and agriculture or in environmental protection. A diversified base of accelerators allows the implementation of new techniques of radiation technologies. The new challenges, including application of chemical and radiation techniques in the development of new pharmaceuticals, tissue and biomedical engineering, implants for reconstructive and surgical surgery, tissue banks and for the production of composite materials, nanomaterials, semiconductor products, issues related to nuclear energy and environmental protection were undertaken thanks to these possibilities.

The implementation of new technologies including radiation technologies in Polish and worldwide conditions is still a particularly difficult task. Additional criteria should be added to the criteria set for basic research, the fulfillment of which will enable the chosen technology to achieve commercial success, namely the right time and place for implementation. These conditions are related to the demand for a given technology, which is determined not only by technical development, but also by expectations and social needs in a given country.

Sewage treatment and the hygienization of sewage sludge from municipal wastewater treatment plants using electron beam have been the subject of intense study and laboratory experiments for many years. Interest in the use of radiation technologies for this purpose results from the need to meet the growing requirements in the field of environmental protection. The lack of implementations was mainly caused by economic factors related to the need to process a large amount of sewage, high cost of accelerators and low technical level of technologies used in municipal wastewater treatment plants. Due to the huge technological leap that can currently be observed in the technology of wastewater treatment and the significant development of accelerator technologies, practical applications of radiation technology in this field are expected in the future.

The rationale for the above mentioned activities are not only literature reports and practical results achieved by specialized units in Western countries, but also the results of their own research and development works. It should be noted that there is currently no other radiation installation in Poland that would allow the undertaking of a research and implementation program and a service program on a sufficiently large scale and the directions of activities discussed above; such units are rare in other countries as well. On the other hand, starting the implementation and production activity will allow to apply for funding under the EU projects.

Intensive application research conducted at the INCT enabled the practical implementation of a number of radiation technologies (radiation sterilization, crosslinking of polyethylene for heat-shrinkable products, modification of semiconductor products), which contributed to the dynamic development of the accelerator base. As a result, it led to the construction and launch of a number of specialized accelerator installations. At present the INCT is one of the world's leading R&D units in the field of radiation technology operating four pilot stations based on the electron accelerator.

Implementation of the results of scientific research is an important measure of their importance and success of the team conducting this research. There are real possibilities to implement the results of research carried out with the use of radiation chemistry methods in the field of new materials processing and testing including those applied in the field of nuclear

energy. Significant opportunities for large-scale deployments in the protection of the natural environment can also be attributed to the radiation technology of removing off-gas pollution as well as the hygienization of municipal sludge.

All these applications are based on science developed in the universities and research centers and then transferred to industry to be used in a safe and proper manner. It is a joint contribution of scientists and professionals working in the field to the main EU Horizon 2020 objectives to fulfill the promises for more breakthroughs, discoveries and world-firsts by taking great ideas from the lab to the market and UN Millennium Goals of achieving a resource-efficient and climate-change-resilient economy and society, protecting and sustainably managing natural resources and ecosystems, and ensuring a sustainable supply and use of raw materials and other environmental resources. This universal humanistic role of science was articulated by Madame Curie, a lady, born 150 years ago in Warsaw as Maria Skłodowska. She developed a new innovative and effective tool – ionizing radiation, which broke new ground in physics and chemistry opening the door for advances in engineering, biology and medicine. The next generation including teams involved in the realization of the projects reported in the book continues this message by introducing to the practice the new types of ionizing radiation emitters – accelerators.

Recent projects reported in this book were partly co-financed by the Ministry of Science and Higher Education project 3697/H2020/2017/2.

# Editorial Series on ACCELERATOR SCIENCE

Vol. LI
Carlotta Accettura: Ultra-high Vacuum Characterization of Advanced Materials for Future Particle Accelerator

Vol. L
Federico Carra: Thermomechanical Response of Advanced Materials under Quasi-Instantaneous Heating

Vol. XLIX
Janne Ruuskanen: Predicting Heat Propagation in Roebel Cable Based Accelerator Magnet Prototype

Vol. XLVIII
Liangliang Shi: Higher-Order-Mode-based Beam Phase and Beam Position Measurements in Superconducting Accelerating Cavities at the European XFEL

Vol. XLVII
Raphael Kleindienst: Radio Frequency Characterization of Superconductors for Particle Accelerators

Vol. XLVI
Sebastian Keckert: Optimizing a Calorimetry Chamber for the RF Characterization of Superconductors

Vol. XLV
Maurizio Vretenar (Ed.): Final EuCARD-2 Project Report

Vol. XLIV
Frank Zimmermann (Ed.): Strategy for Future Extreme Beam Facilities

Vol. XLIII
Mike Seidel (Ed.): The Energy Efficiency of Proton Driver Accelerators

Vol. XLII
Andrzej Rychter: Measurement Based Characterisation and Modelling of Micropixel Avalanche Photodiodes

Vol. XLI
Rafał Graczyk: Reliability and Performance Modeling of Configurable Electronic Systems for Unmanned Spacecraft

Vol. XL
Maciej Lipiński: Methods to Increase Reliability and Ensure Determinism in a White Rabbit Network

Vol. XXXIX
Antonella Chiuchiolo: Cryogenic Fiber Optic Sensors for Superconducting Magnets and Power Transmission Lines in High Energy Physics Applications

Vol. XXXVIII
Oscar Frasciello: Wake Fields and Impedance Calculations of LHC Collimators' Real Structures

Vol. XXXVII
Sławomir Wronka: Interlaced Energy Linac with Smooth Energy Regulation

Vol. XXXVI
Lucas Nathan Brouwer: Canted-Cosine-Theta Superconducting Accelerator Magnets for High Energy Physics and Ion Beam Cancer Therapy

Vol. XXXV
Nicholas C. Shipman: Experimental Study of DC Vacuum Breakdown and Application to High-Gradient Accelerating Structures for CLIC

Vol. XXXIV
Tiina Salmi: Optimization of Quench Protection Heater Performance in High-Field Accelerator Magnets Through Computational and Experimental Analysis

Vol. XXXIII
Thomas Flisgen: Compact State-Space Models for Complex Superconducting Radio-Frequency Structures Based on Model Order Reduction and Concatenation Methods

Vol. XXXII
Marija Cauchi: Thermo-Mechanical Studies of Large Hadron Collider Collimators in Accident Scenarios

Vol. XXXI
Daniele Mirarchi: Crystal Collimation for LHC

Vol. XXX
Grzegorz Korcyl: A Novel Data Acquisition System Based on Fast Optical Links and Universal Readout Boards

Vol. XXIX
Marcello Spera: Pinning Mechanisms in YBCO Tapes

Vol. XXVIII
Adrian Fiergolski: Hardware Implementation of the Track Identification Algorithm in the Scalable Readout System for the TOTEM Experiment

Vol. XXVII
Bartłomiej Juszczyk, Grzegorz Kasprowicz: MicroTCA Based Platform for Advanced Particle Accelerators Diagnostics

Vol. XXVI
Michał Kozieł: Development of Radiation Hardened Pixel Sensors for Charged Particle Detection

Vol. XXV
Ben Hall: Designing the Four Rod Crab Cavity for the High-Luminosity LHC Upgrade

Vol. XXIV
José Luis Abelleira Fernández: Optics Designs of Final-Focus Systems for Future LHC Upgrades

Vol. XXIII
César Octavio Domínguez Sánchez de la Blanca: Electron Cloud Studies for the LHC and Future Proton Colliders

Vol. XXII
Jean-Pierre Koutchouk and Agnes Szeberenyi (Eds): EuCARD Final Project Report

Vol. XXI
Tomasz Pławski: Digital RF Control System for Superconducting Cavity with Large Lorentz Force Detuning Coefficient

Vol. XX
Maciej Kwiatkowski: Methods for the Application of Programmable Logic Devices in Electronic Protection Systems for High Energy Particle Accelerators

Vol. XIX
Gianluca Valentino: Fast Automatic Beam-Based Alignment of the LHC Collimator Jaws

Vol. XVIII
Krzysztof Czuba: RF Phase Reference Distribution System for TESLA Technology Based Projects

Vol. XVII
Anna Wysocka-Rabin: Advances in Conformal Radiotherapy. Using Monte Carlo Code to Design New IMRT and IORT Accelerators and Interpret CT Numbers

Vol. XVI
Pei Zhang: Beam Position Diagnostics with Higher Order Modes in Third Harmonic Superconducting Accelerating Cavities

Vol. XV
Tobias Junginger: Investigation of the Surface Resistance of Superconducting Materials

Vol. XIV
Michał Dziewiecki: Measurement-based Characterization of Multipixel Avalanche Photodiodes for Scintillating Detectors

Vol. XIII
Matthew Alexander Fraser: Beam Dynamics Studies of the ISOLDE Post-Accelerator for the High Intensity and Energy Upgrade

Vol. XII
Claire Antoine: Materials and Surface Aspects in the Development of SRF Niobium Cavities

Vol. XI
Grzegorz Kasprowicz: Determination of Beam Intensity and Position in a Particle Accelerator

Vol. X
Wolfgang Weingarten: European Infrastructures for R&D and Test of Superconducting Radio-Frequency Cavities and Cryo-Modules

Vol. IX
Vasim Khan: A Damped and Detuned Accelerating Structure for the Main Linacs of the Compact Linear Collider

Vol. VIII
Paweł Gryboś: Front-end Electronics for Multichannel Semiconductor Detector Systems

Vol. VII
Tomasz Czarski: Complex Envelope Control of Pulsed Accelerating Fields in Superconducting Cavities

Vol. VI
Guido Sterbini: An Early Separation Scheme for the LHC Luminosity Upgrade

Vol. V
Helmut Mais: Some Topics in Beam Dynamics of Storage Rings

Vol. IV
Roy Aleksan and Olivier Napoly (Eds): Coordinated Accelerator Research in Europe. Summary of Project Achievements

Vol. III
Zbigniew Szadkowski: Triggers for the Pierre Auger Observatory, the Current Status and Plans for the Future

Vol. II
Krzysztof Poźniak: Detektorowe systemy pomiarowe typu TRIDAQ w eksperymentach fizyki wysokich energii (TRIDAQ Detector Systems for High Energy Physics Experiments)

Vol. I
Jacek Sekutowicz: Multi-cell Superconducting Structures for High Energy $e^+$ $e^-$ Colliders and Free Electron Laser Linacs